Core conditions of Unit-1 to Unit-3 of the Fukushima Daiichi Nuclear Power Station

November 30, 2011

Tokyo Electric Power Company

Summary

Estimated core conditions of Unit-1 to Unit-3 of the Fukushima Daiichi Nuclear Power Station were disclosed on May 23, 2011, which explained that the cores of all units had been largely damaged, the molten fuel had been relocated to the lower plenum, and most of it had been cooled in the vicinity of the lower plenum, although a possibility of some molten fuel having been relocated to outside the reactor pressure vessel (RPV) could not be excluded. The disclosed estimation came from a comprehensive judgement based on the core conditions predicted by the MAAP analyses and the core conditions derived from the measured temperature behaviors at various locations in the containment vessels (PCVs) (see Figure 3.1-1).

Since the above estimation was made in May 2011, a number of new operational actions (see ① below, for instance), examinations and analyses have been attempted for investigation. These results have provided updated findings on estimations of the core conditions. These updated estimations include the following.

① It could be estimated from temperature behavior observed at various points when the water injection paths or amounts were changed, that: in Unit-1, little fuel debris was left in the RPV, because the RPV temperatures decreased largely; and at Unit-2 and Unit-3, some of the fuel debris was present in the RPV.

② It could be estimated from the results of water filling to the variable and reference legs of the reactor water level indicators and calibration of the water level indicators, that: in Unit-1 and Unit-2, the reactor water level was not in the original core region and the fuel was not present at its original position.

③ It could be estimated from Cs concentrations obtained in the nuclei analysis of gases in the PCVs of Unit-1 and Unit-2, that: in Unit-1 the amount of molten fuel was larger than that of Unit-2.

④ It could be estimated from the heat balance evaluation of decay heat and heat removal, i.e., the initial decay heat which could not be removed by the isolation condensers (ICs) or high pressure core injection (HPCI) systems, that: in Unit-1 core damage and RPV damage occurred earlier than in Unit-2 or Unit-3, and the initial decay heat of Unit-1 that could not be removed was about three times that of Unit-2 or Unit-3.

⑤ It could be estimated from the heat balance evaluation in the RPV, that: in Unit-2 and Unit-3, the fuel was mostly under water and the uncovered fuel was less than 3% as of October 10, 2011.

⑥ It could be estimated from the analysis of core-concrete reactions, that: even in Unit-1, which was considered to have the largest fraction of fuel being relocated to the PCV pedestal, the erosion depths of PCV pedestal concrete were not so deep as to be reaching the PCV inner wall.

Comprehensive analysis of the information thus obtained could update the estimated core conditions of May 2011. In Unit-1, almost all molten fuel in the accident progression was relocated to the reactor vessel lower plenum, leaving almost no fuel in the original core region. Most of the fuel debris in the lower plenum was considered to have been further relocated to the PCV pedestal, where the fuel debris caused core-concrete reactions, but as of November 2011 (the time of this report compilation) the core-concrete reactions were estimated to have ceased because the debris has been cooled by injected water and its decay heat has decreased. The debris was considered now (November 2011) to be cooling stably. In Unit-2 and Unit-3, the molten fuel was estimated to remain partly in the original core region, to have been relocated partly to the reactor lower plenum, and now (November 2011) to be cooling stably.

It should be noted that the conditions inside the RPV or the PCV have not been directly and visually observed, but indirectly estimated based on indirectly acquired information. Possibilities of direct visual observation will be pursued hereafter.

Table of contents

1. Introduction

The Tohoku District Off-Pacific Ocean Earthquake (Great East Japan Earthquake) which occurred on March 11, 2011 with its hypocenter off the Sanriku Coast, led to a series of events caused by the earthquake (tsunami, station blackout coupled with damage to emergency power generation equipment and subsequent loss of cooling equipment) in Unit-1 to Unit-3 of the Fukushima Daiichi Nuclear Power Station that caused a severe accident as the units remained in continued station blackout conditions. The accident far exceeded design basis accidents and even multiple accidents which had been assumed in developing the accident management procedures, i.e., all emergency core cooling systems could not function or stopped including those of adjacent units. It is very important to grasp both the accident progression after the earthquake and the current plant conditions for termination of the accident and for recovery activities hereafter.

In response to a request from the Nuclear and Industrial Safety Agency (NISA), the Ministry of Economy, Trade and Industry (METI) (*) received on April 25, 2011, plant data at the time of the earthquake were collected to the extent possible and were reported to METI (**) on May 16, 2011. The plant statuses were evaluated by the Modular Accident Analysis Program (hereafter called “MAAP”) by using the collected data. The results were submitted on May 23, 2011, as the Annex (***) to the data report above.

Work has been continued for recovery at Unit-1 to Unit-3 since the report was submitted. Consequently, temperatures and pressures in the RPV and PCV have decreased and stable cooling has become possible. During the 6 months after the report submission, new findings have been accumulated concerning the reactor behavior through the experienced changes of water injection methods to the reactor, changes of injection water amounts and changes of environmental conditions including natural phenomena. Among such new findings, some are not consistent with the past estimation of reactor conditions. Therefore, the accumulated findings were reviewed and the estimation of “Core conditions at Unit-1 to Unit-3 of the Fukushima Daiichi Nuclear Power Station” has been updated.

It should be noted that the results reported here were based on the limited information available at the time of this report compilation and some estimates and assumptions were made as needed for analyses. The uncertainties in the analysis results may be significant. The results therefore can be quite different from the results which will be obtained hereafter based on future investigations and evaluations.

(*) Request of reports pursuant to Clause 1, Article 67 of the Reactor Regulation Law (Law No. 67) (Notification Number: H23-04-24 Gen-1), April 25, 2011, NISA, METI

(**) Operation records, analyses of accident records and evaluation of their impacts at the Fukushima Daiichi Nuclear Power Station at the time of the Tohoku District Off-Pacific Ocean Earthquake, May 16, 2011, Tokyo Electric Power Company

(***) Estimated core conditions at Unit-1 to Unit-3 of the Fukushima Daiichi Nuclear Power Station, May 23, 2011, Tokyo Electric Power Company)

2 Findings from analyses

2.1 MAAP analysis

The MAAP analysis gave the following results. In Unit-1 the core was damaged at a fairly early stage leading to the RPV damage thereafter, if the isolation condensers (ICs) were assumed to have stopped after the station blackout due to the tsunami arrival. In addition, it has been found from the calibration of Unit-1 reactor water level indicators that the water level in the RPV was not in the core region, notwithstanding the readings of the water level indicators. On the other hand, in Unit-2 and Unit-3 the cores were damaged but eventually retained in the RPVs; the cores were damaged when the reactor water levels decreased after the reactor core isolation cooling (RCIC) systems or high pressure coolant injection (HPCI) systems had stopped, although reactor water injection could have been continued after the station blackout until the tsunami arrival; but the cores could have been eventually retained in the core region owing to the restarted reactor water injection. But it should be noted that the readings of water level indicators might be incorrect, because the water in the water level indicators might have evaporated. Assuming the lower actual reactor water level was lower than the indicated readings, cutting below the bottom of active fuel (BAF), MAAP predicted further advancing of the core damage, leading to the RPV damage thereafter.

Figure 2.1-1 illustrates the fuel distributions in the core of each unit at the time the analysis was terminated.

It was estimated that the fuel was being cooled after being relocated from the core region to the lower plenum, because the following data were measured in Unit-1 to Unit-3 at the time of this report on MAAP results (May 2011): temperatures in the RPV bottom, these would not have been measurable if the RPVs were significantly damaged; high temperatures, these would be likely when a heat source existed in the RPVs; and multiple temperature indicators had value changes at their measurement points consistent with the changes in the amounts of reactor water injection.

(Refer to Attachment-1 “Estimated core conditions disclosed in May 2011”)

2.2 Heat balance between decay heat and heat removal

Unit-1 to Unit-3 were in a situation that they were unable to remove their decay heat until water injection to the reactor could be started after heat removal by the ICs, RCIC or HPCI had stopped. Consequently, the fuel was overheated, and the core was damaged in each unit. The decay heat decreases rapidly as soon as the fission reactions cease due to the reactor scrams. Figure 2.2-1 compares decay heat not removed between the three units In Unit-1, the ICs stopped early, and more time was needed to start water injection to the reactor. The decay heat that had not been able to be removed was about three times that of Unit-2 or Unit-3. Figure 2.2-2 indicates the decay heat not removed from Unit-1 was bigger than the energy needed for melting fuel or structures, while it was less at Unit-2 and Unit-3. This was the main reason for the present MAAP results (Case 1): the core damage started earlier at Unit-1, and the RPV was damaged; on the other hand, early initiation of water injection could have retained fuel in the core region of Unit-2 or Unit-3. At Unit-2 and Unit-3, a sufficient amount of water injection was assumed to have been secured once injection had been started. If this assumption failed and the decay heat could not be adequately removed, the core damage would advance and the RPV would be damaged as predicted by MAAP (Case 2).

(Refer to Attachment-2 “Core conditions estimated from heat balance while water injection was being interrupted”)

3. Findings from observed results

3.1 Estimation from measured temperatures and pressures

Figure 3.1-1 shows temperature changes at typical points of Unit-1. Water was injected via the feedwater line which did not go through the core directly, but the measured temperatures cut below 100 deg C as of August 2011. It was considered, therefore, that the fuel was being sufficiently cooled in the RPV lower plenum or the PCV pedestal.

Figures 3.1-2 and 3.1-3 show temperature changes at typical points of Unit-2 and Unit-3, respectively. For Unit-2 and Unit-3, the temperature changes after the accident indicated that the temperatures remained higher at the RPV upper part than at the RPV lower part. Since the RPV water level was considered to have been below the core level, part of the fuel was considered to have been present in the gaseous phase in the core region, i.e., steam generated from the injected water in the RPV lower part was considered to have been heated up by the uncovered core fuel and that raised the temperatures at the RPV upper part. The uncovered fuel was considered to have remained in the core region, because the fuel in the outer core region had not melted due to lower power densities and therefore lower decay heat. Even if the cladding of uncovered fuel had kept its configuration when the water injection was initiated, its original configuration was likely to have been lost at the time of this report (November 2011), because it (the uncovered fuel) remained overheated and exposed to the steam environment over an extended time. Water injection from core spray (CS) lines immediately above the core region started on September 1 in Unit-2 and September 14 in Unit-3. Consequently, cooling of the uncovered fuel left in the core region could have started and temperatures at all measurement points could have significantly dropped. This estimation was consistent with the MAAP analysis results that the whole fuel of Unit-1 was relocated from the core region, while part of the fuel remained in the outer core region in Unit-2 and Unit-3.

(Refer to Attachment-3 "Core conditions estimated from the measured temperatures and pressures")

3.2 Heat balance in the RPV

The water injected into the reactor was discharged as liquid or steam after being heated by decay heat. By using this scenario, the decay heat energy consumption in the RPV (heat balance) was schematized in a model as indicated in Figure 3.2-1. Based on this model, possible core conditions were investigated which could reproduce measured temperature increases. Five forms of energy consumption were considered: ① water temperature increases; ② water evaporation; ③steam temperature increases; ④ fuel temperature increases; and ⑤ temperature increases of structural materials. For a given amount of water injection to the reactor and the decay heat, reactor conditions could be estimated, by using the assumed heat balance model, which can reproduce the measured parameters. The investigation predicted the fraction of uncovered fuel as of October 10, 2011, was about 3% or less for Unit-2 and Unit-3, the fuel being mostly covered by water. It should be noted that this type of investigation was not conducted for Unit-1, because the current heat balance model assumed energy transfer from fuel to structural materials by steam produced, and the situation of a small amount of steam production was not covered, while the temperatures around the RPV of Unit-1 were low (and steam production was limited).

(Refer to Attachment-4 "Core fuel temperatures estimated by the in-RPV temperature evaluation model")

3.3 Readings of reactor water level indicators

Figure 3.3-1 shows the reactor water level indicator configuration. As seen in the figure, the water level in the reference leg located outside the RPV is kept constant, and the pressure difference between the water head in the reference leg and the water head corresponding to the reactor water level (Hs – Hr) is converted to indicate the reactor water level. However, under accident conditions, the water in the instrumentation lines may evaporate. If the water in the reference leg evaporates, for instance, the reference water level lowers and the reactor water level will read higher (Figure 3.3-2).

On May 11 for Unit-1, reactor water level indicators were calibrated by installing a temporary differential pressure gauge, and filling water to the reference leg and instrumentation line. The reactor water level indicators showed that the reactor water level was below the top of active fuel (TAF), at minus 5 m or lower. For Unit-2, a differential pressure gauge was installed on June 22, and the reference leg and the variable leg were filled with water on June 22 and again on October 21. For Unit-2, calibration of the water level indicators could not be conducted because of the high radiation level, but the reactor water level was estimated to be 5 m below TAF-5m or lower from instantaneous readings of temporary differential pressure gauges installed after the accident. It should be noted that the water in both lines of the reference leg and the variable leg had been observed to evaporate within a short time after filling on June 22, and that the water in the variable leg had been observed to evaporate gradually after it was filled on October 21.

From these observations, the reactor water levels are considered (as of this report compilation) not yet to have reached the original fuel region in both Unit-1 and Unit-2, and the fuel was considered unlikely to have remained at its original position of the original configuration. In Unit-2, part of the fuel (acting as a heat source) might be present in the vicinity of the variable leg, because only the water in the variable leg evaporated in October when water was filled. In Unit-1, water evaporation was not observed in the variable leg.

In Unit-3, water level indicator calibration and water filling have not been conducted due to extremely high-level radiation near the instrumentation devices.

(Refer to Attachment-5 “Calibration of water level indicators”)

3.4 Nuclei analysis of in-PCV gases

Gamma rays from nuclei in the gases in the Unit-1 PCV and the Unit-2 PCV were analyzed. Table 3.4-1 shows the results. As summarized in the table, the Cs radioactivity concentration (corrected) in the Unit-1 PCV was about three times that in the Unit-2 PCV. The Cs discharge rate might depend on the gas fractions and temperatures in the PCV.

Therefore, direct comparisons were not possible, but Unit-1 shows the severest results. This was consistent with the results from other evaluations that the core damage of Unit-1 was the largest.

No gas sampling was conducted for Unit-3, because the radiation level was too high near the sampling lines.

(Refer to Attachment-6 “Radioactivity concentrations in the atmosphere of the containment vessel”)

3.5 Findings from other observed results

The following findings have been observed besides those in 3.1 to 3.4. Some of them are difficult to use for estimating the core conditions, and some others may be effectively used, but no conclusive knowledge has been derived yet. Analysis work and estimation will be continued.

① Condition checking of LPRM detectors (Unit-2, Unit-3)

TDR measurements (time-domain reflectometry: a measurement technique used to diagnose disconnection/insulation deterioration of electrical lines by observing reflected waveforms) were conducted on the LPRM detectors, which were one of the neutron monitors installed in the reactors. Attempts were made to estimate the reactor bottom conditions from the measurement results, but at the time of this report compilation, it has been found not to be easy to derive convincing clues.

② Condition checking of control rod position indicator probes (PIPs) (Unit-1, Unit-3)

Energization checks were conducted on the control rod position indicator probes (PIPs), which were in-core position monitors of control rods mounted on the control rod drive mechanism. Attempts were made to estimate the reactor bottom conditions from the measurement results, but at the time of this report compilation, it has been found not to be easy to derive convincing clues.

③ Recovery work of drywell (D/W) equipment sump thermometers (Unit-1, Unit-2, Unit-3)

In-service measurements by D/W equipment sump thermometers were attempted in order to get the PCV bottom temperatures. Temperatures were measured for Unit-1 and Unit-3, but the instrumentation line was found to be disconnected for Unit-2. Continued analysis is considered to be necessary, because these thermometers have not been in service for a long period and no definite trends have been observed yet.

④ Recovery work of the primary loop recirculation (PLR) pump inlet thermometers (Unit-1, Unit-2, Unit-3)

In-service measurements by the primary loop recirculation (PLR) pump inlet thermometers were attempted in order to get the PCV bottom temperatures. Temperatures were measured for all units. Continued analysis is considered to be necessary, because reliabilities of readings of these thermometers were still being analyzed at the time of this report compilation.

(Refer to Attachment-7 “Operability checks of local power range monitor (LPRM) detectors (Unit-2, Unit-3) (Attempt to estimate core conditions from LPRM data)”)

(Refer to Attachment-8 “Operability checks of control rod position indicator probes (PIPs) (Unit-1, Unit-3) (Attempt to estimate core conditions from control rod position indicator probe (PIP) data)”)

(Refer to Attachment-9 “Results of condition checks and behavior of drywell (D/W) sump thermometers”)

(Refer to Attachment-10 “Behavior of the primary loop recirculation (PLR) pump inlet thermometers”)

4. Impacts of core-concrete reactions on the containment vessels

4.1 Core-concrete reactions

Upon relocation of molten fuel to the PCV, it will spread on the pedestal floor if the fluidity is maintained, part of the molten fuel further will leak out through pedestal slits and solidify as flat lumps with a large surface (Figure 4.1-1). If there are openings on the pedestal floor, such as an equipment drain sump pit, the fuel debris may clog them heavily (Figure 4.1-2). If water is retained on the bottom of the PCV, the molten fuel will solidify, being cooled upon contact with water, into many small lumps. Thus, there are large uncertainties in shapes and distributions of fuel debris, once the molten fuel drops to the PCV. Large uncertainties also exist in heat transfer from the fuel debris to water, since the fuel debris can contact water in many diverse configurations. If the heat of fuel debris in the PCV cannot be sufficiently removed, core-concrete reactions occur, in which the concrete is heated to above its melting temperature, and the concrete is thermally decomposed and eroded. The erosion ends when the decay heat decreases and water injection to the reactor is resumed. The erosion depths vary greatly depending upon conditions assumed, for instance, uncertain geometrical configurations (an easily heat-removable flat shape or a hard to remove pit-type shape) or heat transfers.

4.2 Reactor building closed cooling water system (RCW) of Unit-1

Radiation distributions measured in the Unit-1 reactor building (R/B) showed high dose rates on the RCW system lines (Figure 4.2-1). The RCW is a closed loop for cooling auxiliary equipment and it is unlikely to be contaminated as high as several hundreds of mSv/h in normal situations. But the RCW lines were laid widely in the R/B and they cooled the equipment in the PCV, too. As seen in Figure 4.2-2, the RCW line for drain cooling was laid in the equipment drain pit in the lower part of the PCV. Therefore, it was highly possible in Unit-1 that the molten fuel was relocated to the equipment drain pit and damaged the RCW piping and this caused the high RCW line contamination. It was considered that, upon damage to piping, high dose steam or water was transferred to the RCW secondary lines and radioactive materials were simultaneously transferred. On the other hand, if the RCW lines had been damaged by the relocated fuel debris, water from the RCW secondary lines might have flowed to the PCV and contributed to the fuel debris cooling.

No such high dose rates have been recognized for Unit-2 and Unit-3.

(Refer to Attachment-11 “Contamination of the reactor building closed cooling water (RCW) system”)

4.3 Evaluation results of core-concrete reactions

MAAP has a module which can evaluate core-concrete reactions, too, not only the module to evaluate fuel behavior in the RPV. This module for core-concrete reactions was used to analyze the Unit-1 core-concrete reactions. Unit-1 was thought to have the largest fraction of relocated fuel debris to the PCV. Big uncertainties in the initial conditions and given analytical conditions might cause big uncertainties in the results as well. Realistic conditions shown in Table 4.3-1 were used in the evaluation and the results are shown in Figure 4.3-1. The results indicated that the concrete was eroded but the fuel debris could remain in the PCV.

A seismic evaluation was also conducted when the pedestal floor concrete had been eroded by core-concrete reactions. No seismic concerns were identified.

(Refer to Attachment-12 “Impacts of core-concrete reactions on the reactor containment vessel”)

(Refer to Attachment-13 “Estimation of the conditions of structural materials in the Unit-1 containment vessel”)

4.4 PCV gas analyses

Gas samples used for nuclei analysis in 3.4 were also provided for gas composition analysis. It was long after the core-concrete reactions were thought to have ceased, and putting aside the question of whether or not they had occurred, that gas sampling from the PCV became possible. Therefore, even if hydrogen, carbon monoxide or carbon dioxide had been generated in the core-concrete reactions, they would be unlikely to have remained in the sampled gas at the time of gas sampling, since they were diluted with steam, nitrogen gas and others. Table 4.4-1 shows the results of gas analysis. In all samples, the concentration of carbon dioxide was limited to the level which would be anticipated when carbon dioxide contained in the reactor water was separated and transferred to the gaseous phase, while the concentrations of hydrogen and carbon monoxide were at the level of the detection limit. This means that no core-concrete reactions were occurring at the time of this report compilation.

(Refer to Attachment-14 “Results of in-containment gas composition analysis”)

(Refer to Attachment-15 “Gas residues from the early phase of core-concrete reactions”)

5. Cooling situations of each unit

5.1 Cooling situations of Unit-1

The RPV temperatures of Unit-1 were lowered to about 40 deg C as of November 21, 2011, as seen in Figure 5.1-1. No symptoms of superheated steam production were recognizable in the core region where injected water could not reach.

Steam blowout from the Floor 1 penetration observed on June 3, 2011, was not recognizable on October 13, 2011 (Figure 5.1-2 and Figure 5.1-3). It was concluded that cooling was being continued with decreasing decay heat. Another point to be noted was that the RPV temperatures and D/W temperatures decreased, and that the suppression chamber (S/C) pool temperatures slightly increased when the amount of water injection was increased from October 28, 2011 (Figure 5.1-4). This might indicate the following scenario: steam was being produced in the PCV but it was condensed before leaking out to the R/B until the injected water amount was increased; and more decay heat was consumed for increasing water temperature, steam production decreased, more hot water flowed into the S/C, and the S/C temperature increased. The targeted increase of injected water amount was the flow rate that could remove decay heat only by water temperature increases without steam production. The temperature behavior anticipated as its consequence was actually observed, and therefore, well-controlled cooling was being implemented.

Figure 5.1-5 shows the changes of D/W pressure and nitrogen gas filling pressure, which were recorded for monitoring the nitrogen gas injection conditions. The nitrogen gas filling pressure should behave as the D/W pressure if the injection nozzle is in the gaseous phase, because the pressures in the D/W should be uniform, but if the injection nozzle is covered with water, the filling pressure should be higher than the D/W pressure, because the filling pressure must be higher than the D/W gaseous pressure plus the water head. Figure 5.1-5 shows that, after the amount of injected water to Unit-1 was increased on October 28, 2011, the nitrogen gas filing pressure and the D/W pressure started to move away from each other from around November 1, 2011. Thereafter, both pressures reached the same level, despite no changes in the amount of injected water. The elevation of the nitrogen gas filling nozzle was OP6700mm, while the bottom end of the vent tube, which is the theoretical minimum water level from structural constraints, was OP6600mm. Therefore, the current PCV water level was considered to be between these two levels, but there was no way to determine the definite water level at the time of report compilation.

5.2 Cooling situations of Unit-2

The Unit-2 RPV temperatures were lowered to about 80 deg C as of November 21, 2011, as shown in Figure 5.2-1. This temperature decrease was considered to be due to the water injection via the CS system from September 14, 2011. The water from the CS could cool the fuel debris left in the core region, which was in the water injection path of the CS.

Steam blowout from the R/B Floor 5 just above the reactor that was observed on September 17, 2011 was not recognizable on October 20, 2011 (Figure 5.2-2 and Figure 5.2-3). It could be concluded that cooling was being continued owing to the increased water injection from October 4, 2011. In the photo of October 20, 2011, significant deterioration of coatings on the ceiling crane was recognized. The coatings were considered to have lost adhesiveness by absorbing moisture and they were stripped off due to increased internal stresses caused by dehydration. This observation also indicated that steam release from immediately above the reactor had ceased.

It was attempted to estimate the PCV water level, as was done for Unit-1, by comparing the D/W pressures with the pressures at the nitrogen gas discharge nozzle, which were considered to include the water head above the nozzle. It was not possible, though, because no appropriate discharge nozzle was located. The fuel in the PCV was judged probably to be under water, because the amount of relocated fuel of Unit-2 was considered limited, sufficient water was now being injected for removing decay heat only by sensible heat, and no unusual hot spots were observed in the PCV atmospheric temperature measurements.

(Refer to Attachment-16 “Paint stripping-off incidents of Unit-2 reactor building ceiling cranes”)

5.3 Cooling situations of Unit-3

The Unit-3 RPV temperatures were lowered to about 70 deg C as of November 21, 2011, as shown in Figure 5.3-1. This temperature decrease was considered to be due to the water injection via the CS system from September 1, 2011. The water from the CS could cool the fuel debris left in the core region, which was in the water injection path of the CS.

The temperature increase observed around the shield plug probably was caused by the steam blowout on March 20, 2011. As of October 20, 2011, the number of high temperature spots had decreased, and the scale became smaller (Figure 5.3-2 and Figure 5.3-3). It could be concluded that cooling was being continued with decreasing decay heat.

Figure 5.3-4 compares the D/W pressure and S/C pressure. If the S/C nitrogen gas discharge nozzle is not under water, the S/C pressure should behave as the D/W pressure, but if the discharge nozzle is covered by water, the S/C pressure should exceed the D/W pressure in order to withstand the D/W pressure plus the water head. Figure 5.3-4 shows that the S/C pressure was constantly higher than the D/W pressure from October 1, 2011. The pressure difference between the two indicated that the current PCV water level was at a level between OP12,000 and OP13,000. The fuel in the PCV would probably be under water, because the amount of relocated fuel of Unit-3 was considered limited, sufficient water was now being injected for removing decay heat only by sensible heat, and no unusual hot spots were observed in the PCV atmospheric temperature measurements.

6. Estimation of core conditions

6.1 Core conditions of Unit-1

At Unit-1, water was being injected via the feedwater system (FWS), as seen in Figure 6.1-1, and the water injected to the RPV was flowing down outside the shroud and reaching the lower plenum. The reactor water level indicator calibration (3.3) showed that the RPV water level was below TAF-5m, namely, the water level was not in the core region.

Based on such findings and the evaluation results in 5.1 and other places, the Unit-1 core conditions could be estimated as shown in Figure 6.1-1: almost all the molten fuel in the accident progression was relocated to the RPV lower plenum, leaving almost no fuel in the original core region. Most of the fuel debris in the lower plenum was considered to have been further relocated to the PCV pedestal. The fuel debris caused core-concrete reactions, but by November 2011, the time of this report compilation, the core-concrete reactions were estimated to have ceased because the debris was being cooled by injected water and its decay heat decreased, and the debris was considered to remain in the PCV.

6.2 Core conditions of Unit-2

At Unit-2, water was being injected via the CS and the FWS, as seen in Figure 6.2-1. The water injected from the CS to the RPV flowed down inside the shroud, while the water from the FWS flowed down outside the shroud, and both reached the lower plenum. The results of water filling to the water level indicators (described in 3.3) indicated the RPV water level was below TAF-5m, and no water level was considered to be present in the core region.

Based on such findings and the evaluation results in 5.2 and other places, the Unit-2 core conditions could be estimated as shown in Figure 6.2-1: part of the molten fuel in the accident progression was relocated to the RPV lower plenum or PCV pedestal, leaving part of the fuel in the original core region.

6.3 Core conditions of Unit-3

At Unit-3, water was being injected via the CS and the FWS, as seen in Figure 6.3-1. The water injected from the CS to the RPV flowed down inside the shroud, while the water from the FWS flowed down outside the shroud, and both reached the lower plenum. The Unit-3 RPV temperatures were lowered to about 70 deg C as of November 21, 2011. This temperature decrease was considered to be due to the water injection via the CS system from September 1, 2011. The water from the CS could cool the fuel debris left in the core region, which was in the water injection path of the CS.

Based on such findings and the evaluation results of 5.3, the Unit-3 core conditions could be estimated as shown in Figure 6.3-1: part of the molten fuel in the accident progression was relocated to the RPV lower plenum or PCV pedestal, leaving part of the fuel in the original core region.

End

Table 3.4.1　Estimated concentrations in PCV gases

Nuclei	Radioactivity concentrations (Bq/cm^3)	
	Unit-1 (Sampled on 9/14/2011)	Unit-2 (Sampled on 8/9/2011)
Cs-134	1.6×10^{0}	4.4×10^{-1}
Cs-137	2.0×10^{0}	4.6×10^{-1}
Steam fraction	About 46%	About 100%

Table 4.3-1　Conditions for core-concrete reaction analysis

	Conditions
Initial amount of fuel debris	Unit-1: Full core (100%)
Decay heat source	ORIGEN2 data with fuel burnup history being considered
Depletion of volatile FP decay heat	20% depletion assumed
Fine grain formation of fuel debris by water originally present in the pedestal	Not considered
Fuel debris sedimentation	Inflow conditions to sump pits: P/D uniform sedimentation on the floor D/W partial outflow from the floor 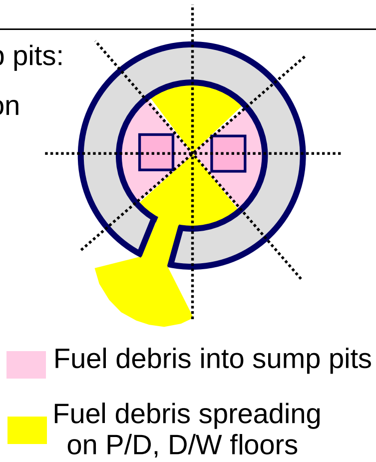
Fuel debris sedimentation thickness	In sumps: 0.81m (P/D, D/W floors: 0.35m)

Table 4.4-1 Concentrations (%) of hydrogen, carbon monoxide, carbon dioxide in PCVs

	H	CO	CO_2
Unit-2 (August 2011) Sample ①	0.558	0.016	0.152
Unit-2 (August 2011) Sample ②	1.062	0.017	0.150
Unit-2 (August 2011) Sample ③	<0.001	<0.01	0.152
Unit-1 (September 2011) Sample ①	0.154	<0.01	0.118
Unit-1 (September 2011) Sample ②	0.101	<0.01	0.201
Unit-1 (September 2011) Sample ③	0.079	<0.01	0.129

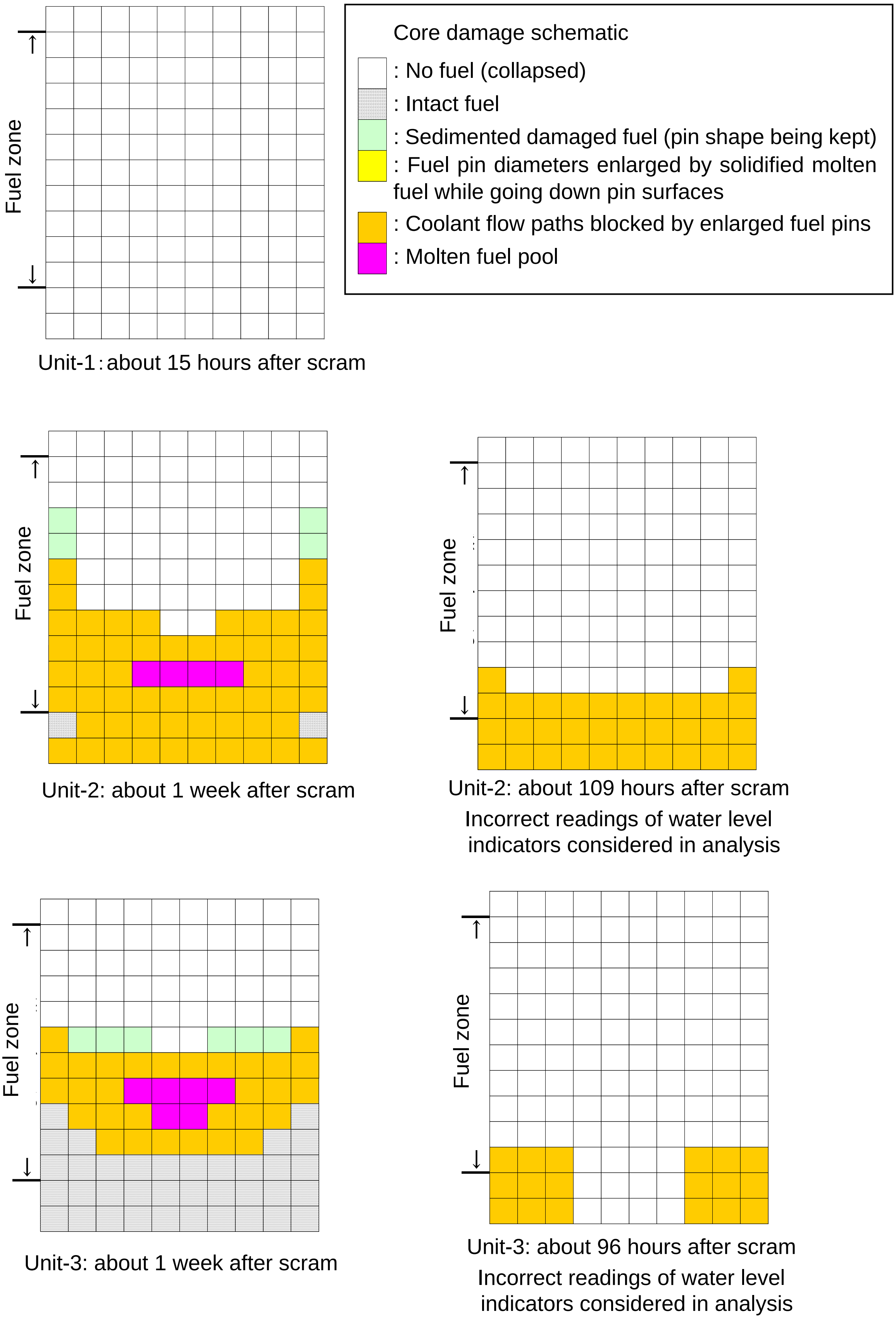

Figure 2.1-1 Analysis results by MAAP (core conditions)

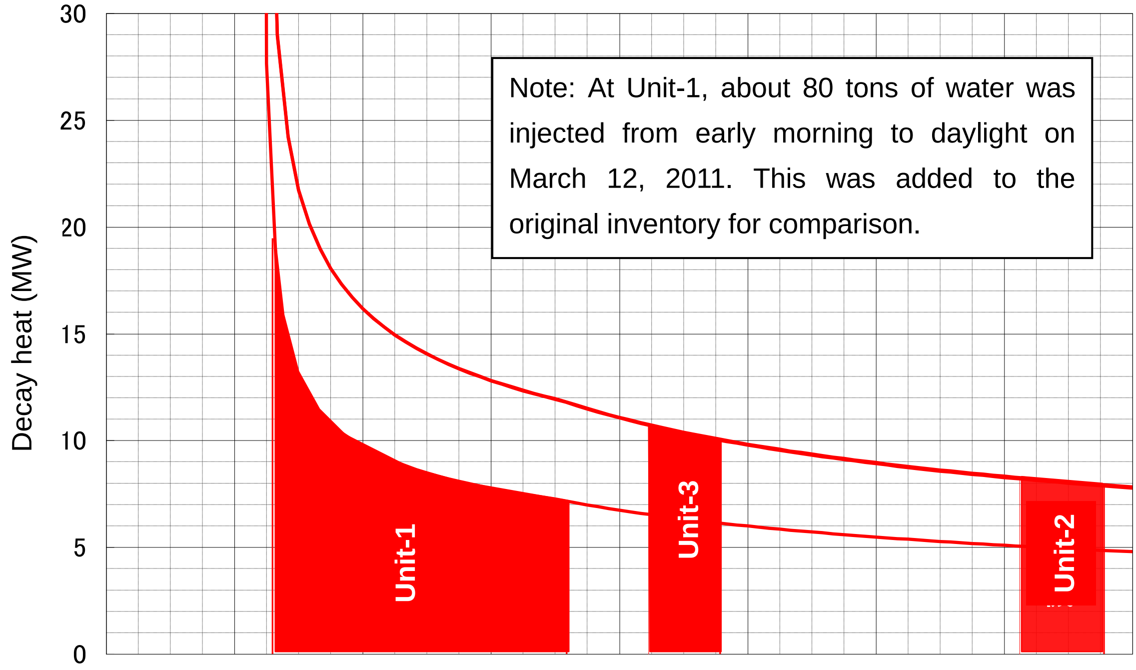

Figure 2.2-1 Decay heat changes and timings of no water injection at each unit

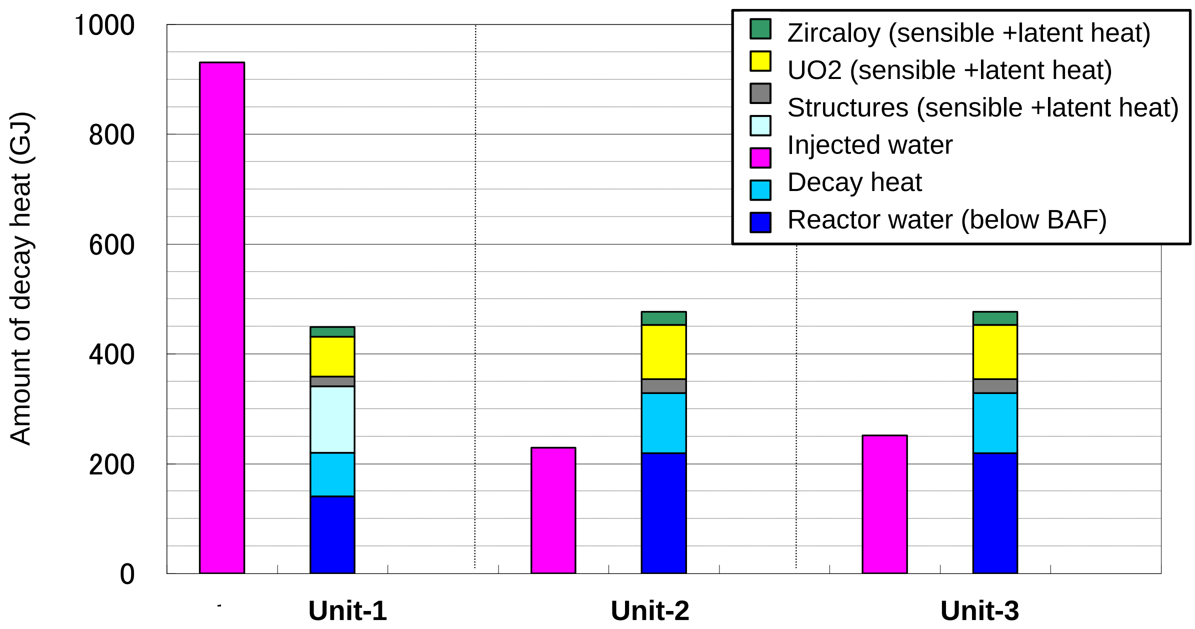

Figure 2.2-2 Comparison of decay heat and heat removal capacities

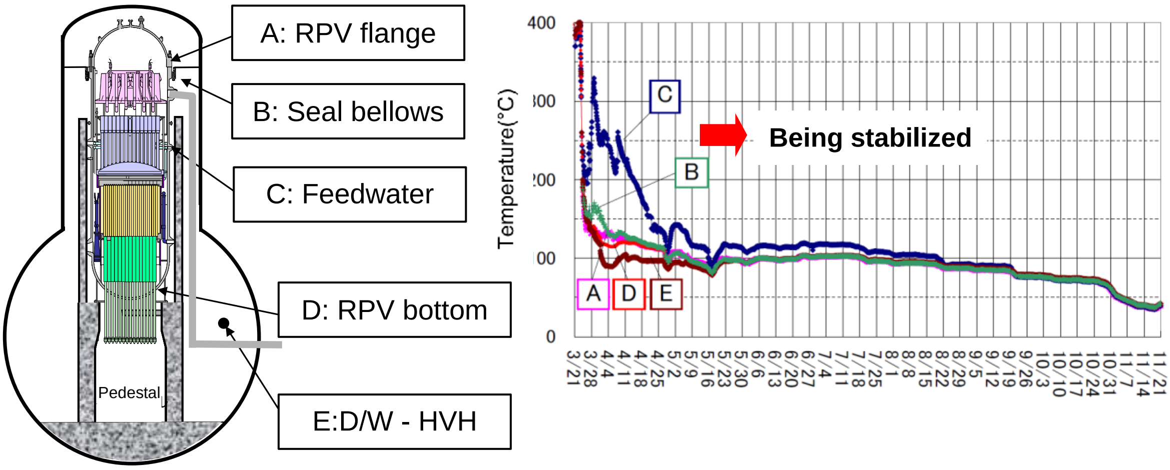

Figure 3.1-1　Temperature changes of Unit-1

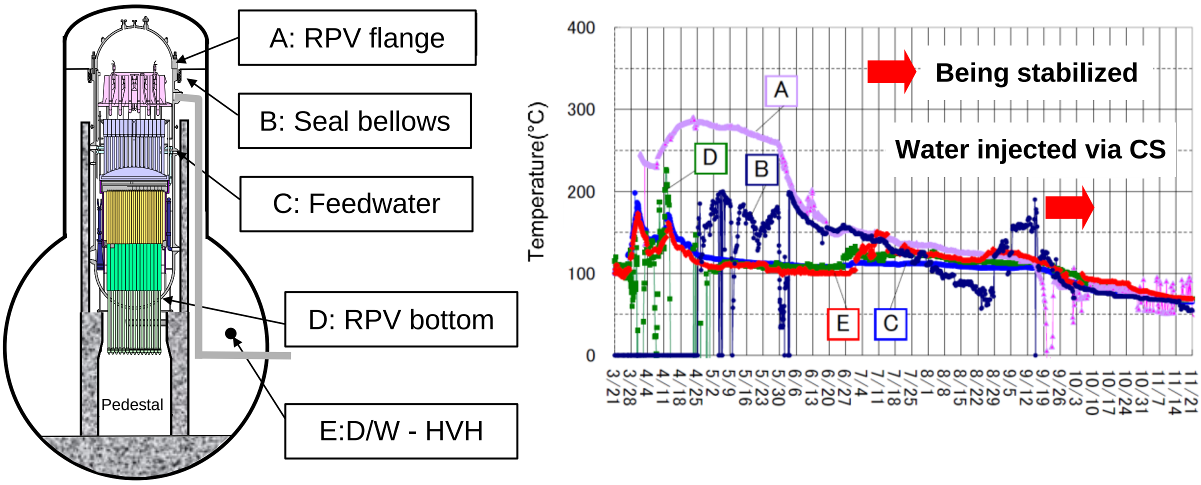

Figure 3.1-2　Temperature changes of Unit-2

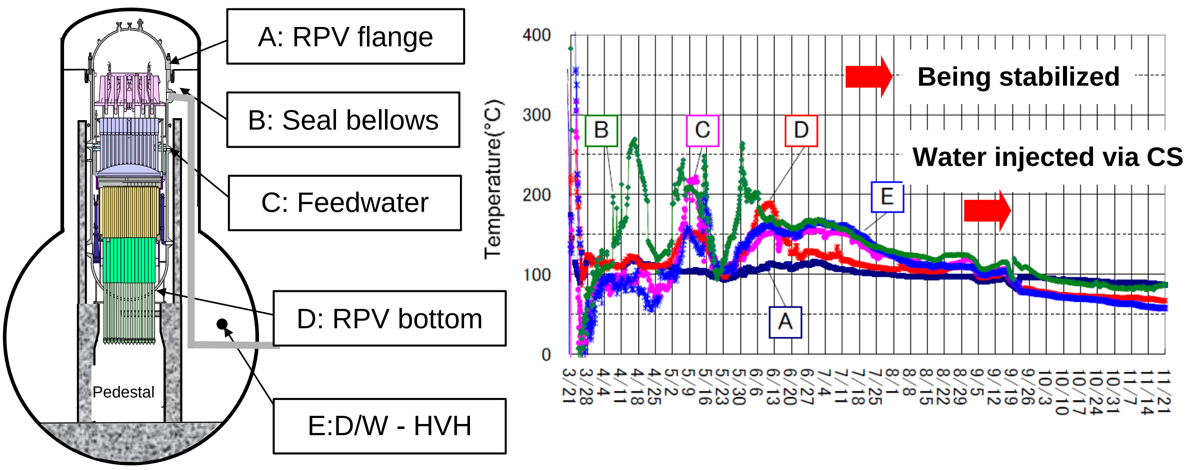

Figure 3.1-3　Temperature changes of Unit-3

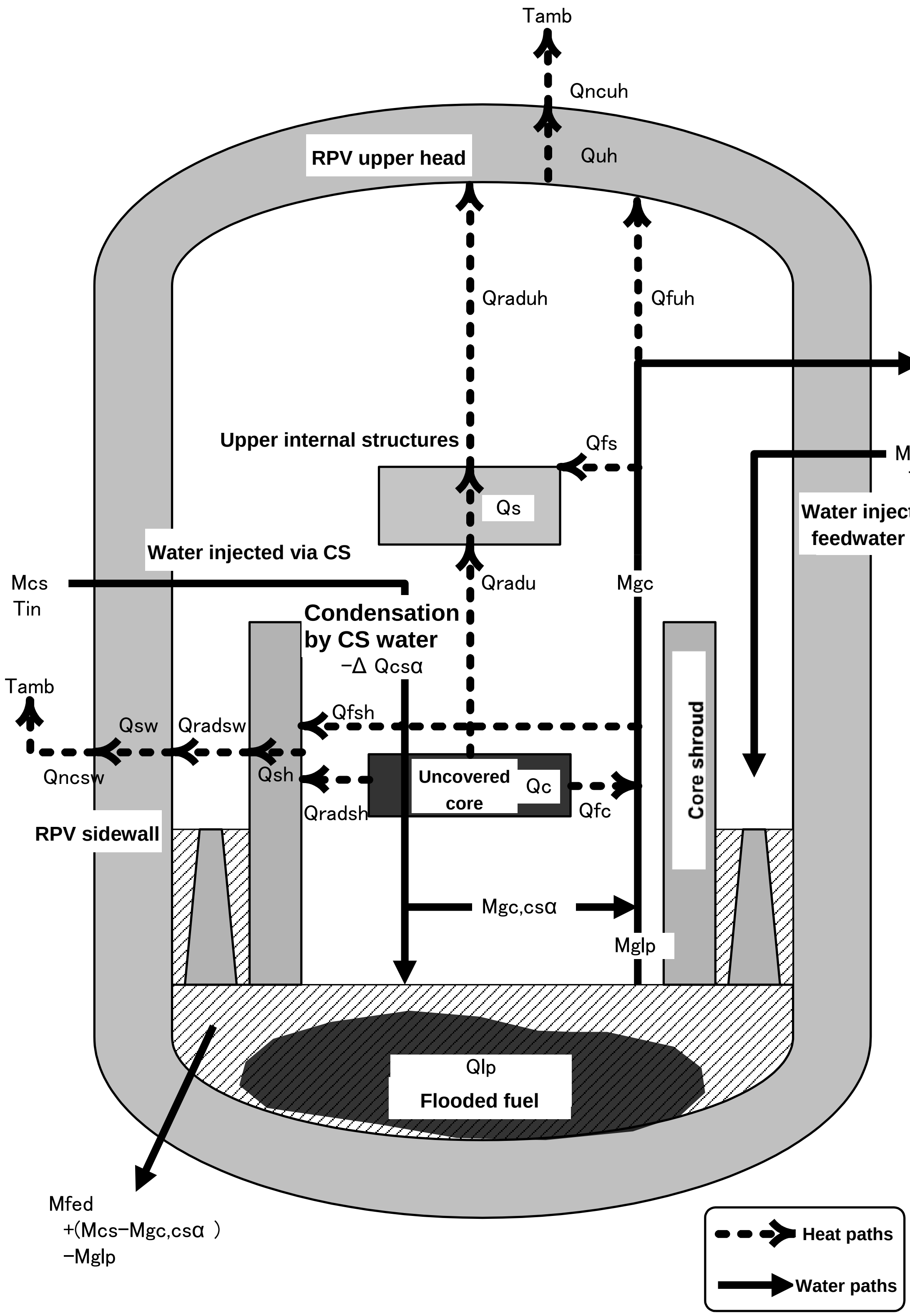

See Attachment-4 or variables in the figure.

Figure 3.2-1 Heat balance model

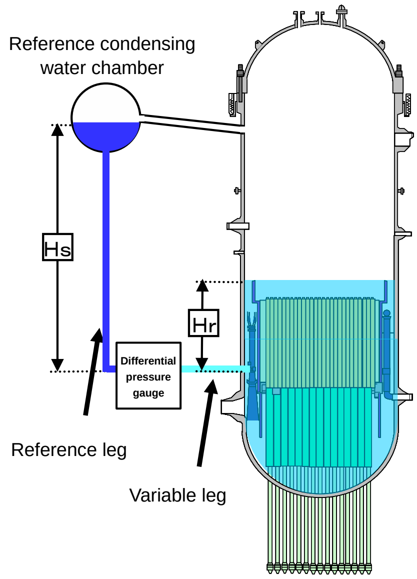

Figure 3.3-1 Schematic illustration of a reactor water level indicator

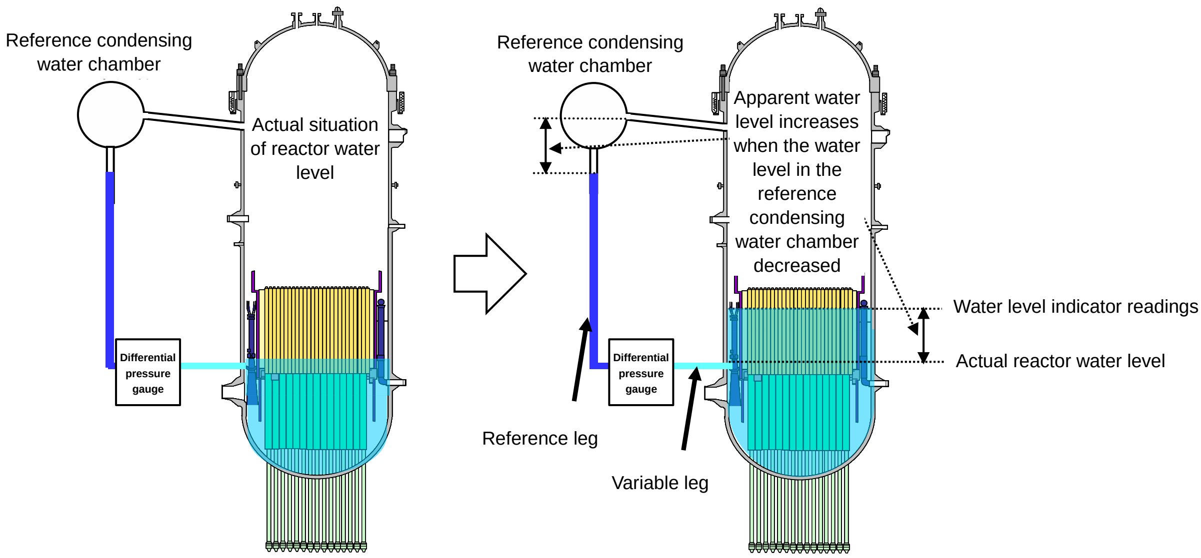

Figure 3.3-2 Reactor water level indicator readings when the water level in the instrumentation line dropped

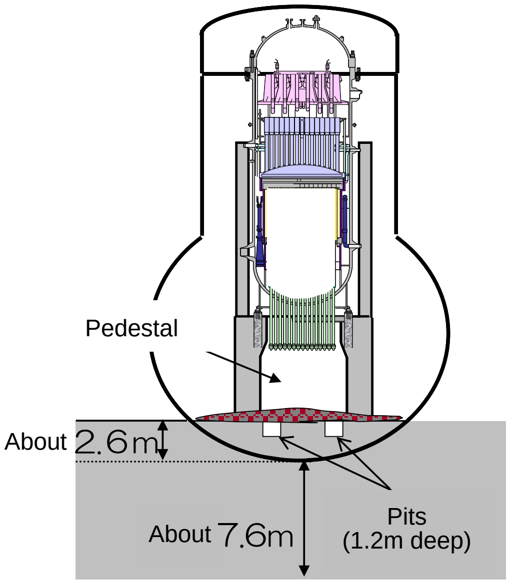

Figure 4.1-1　Estimated fuel debris configuration when relocated to the PCV pedestal (fuel debris remained fluid and spread widely)

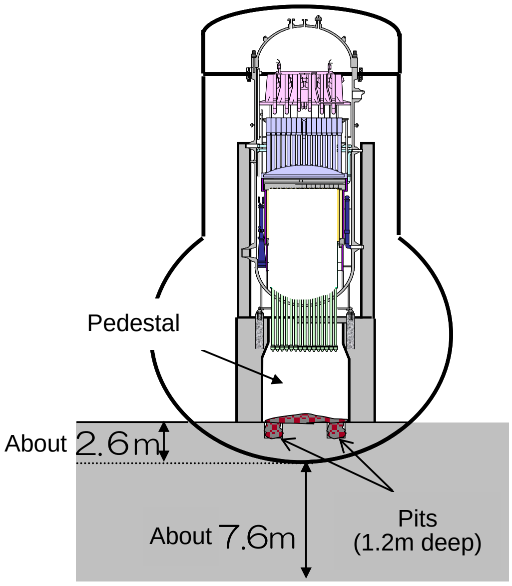

Figure 4.1-2　Estimated fuel debris configuration when relocated to the PCV pedestal (fuel debris clogged the pits)

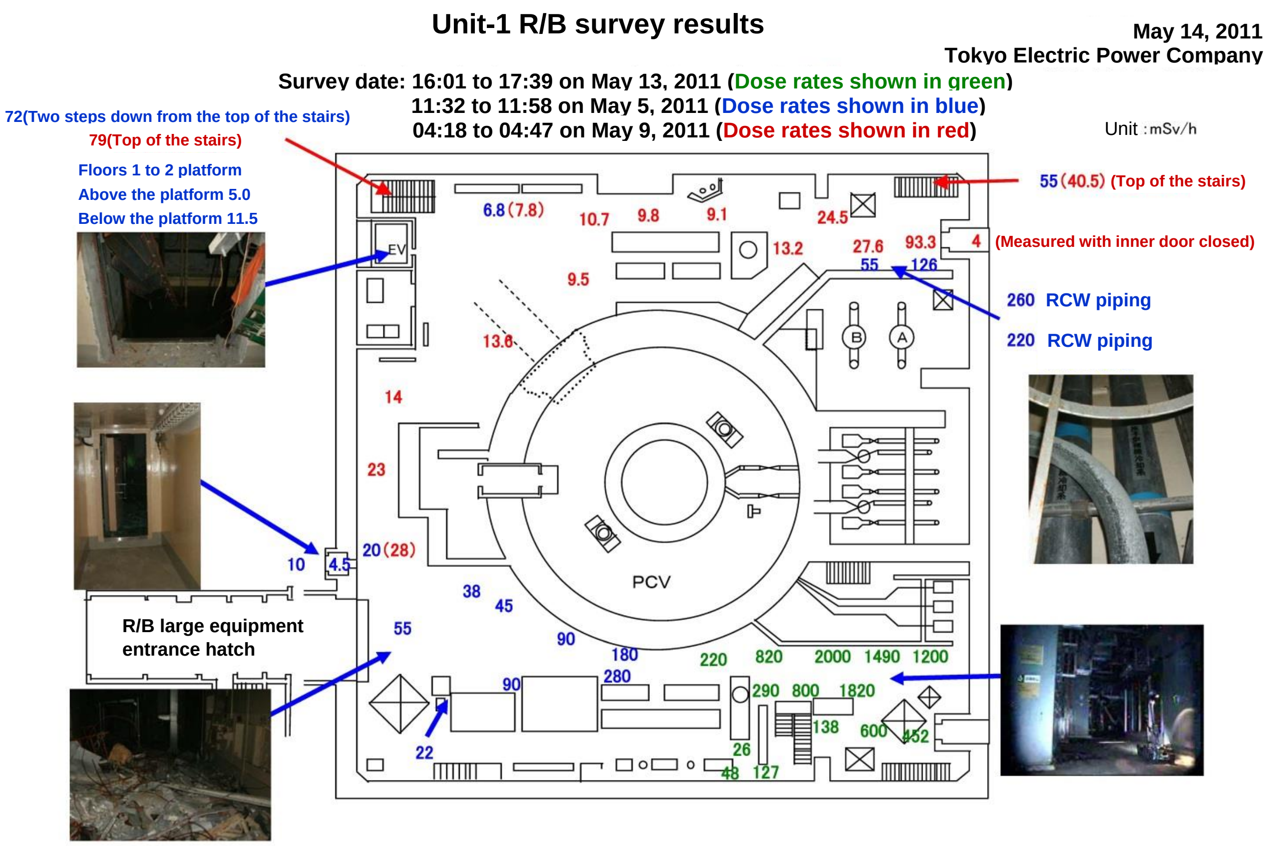

Figure 4.2-1　Unit-1 R/B dose rate survey results

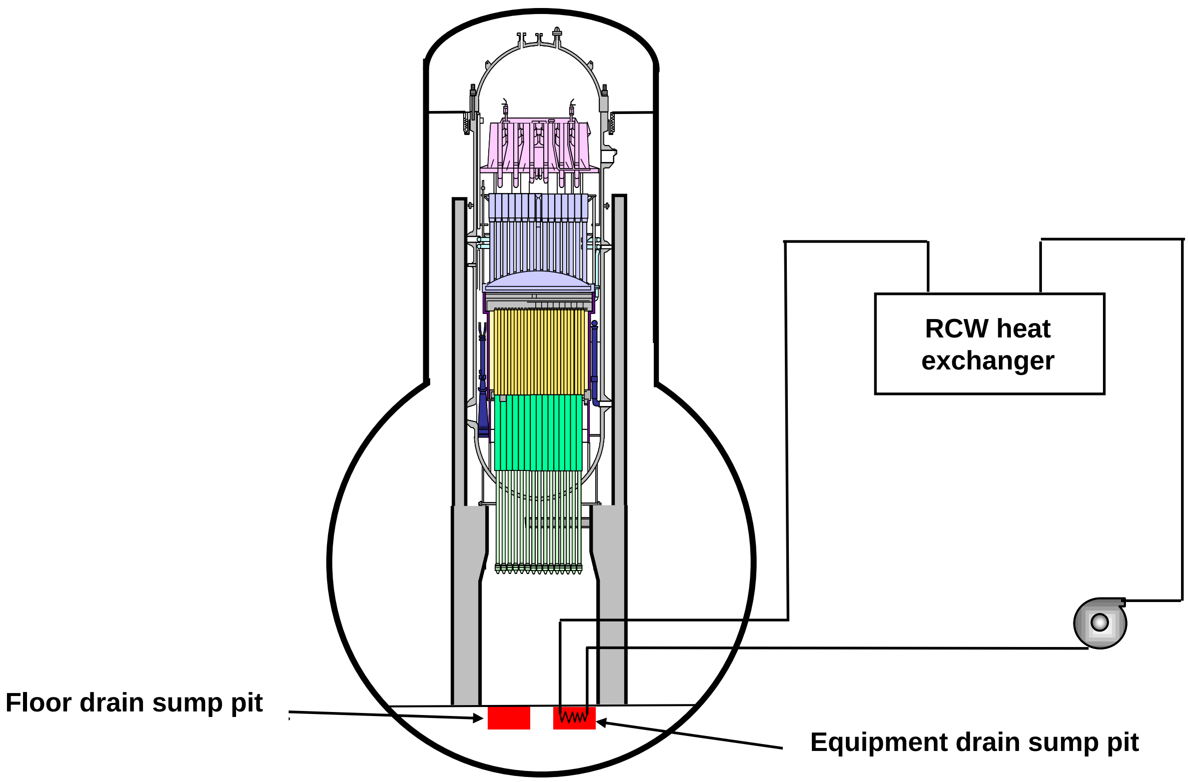

Figure 4.2-2　Schematic of interface between RCW and equipment drain pit

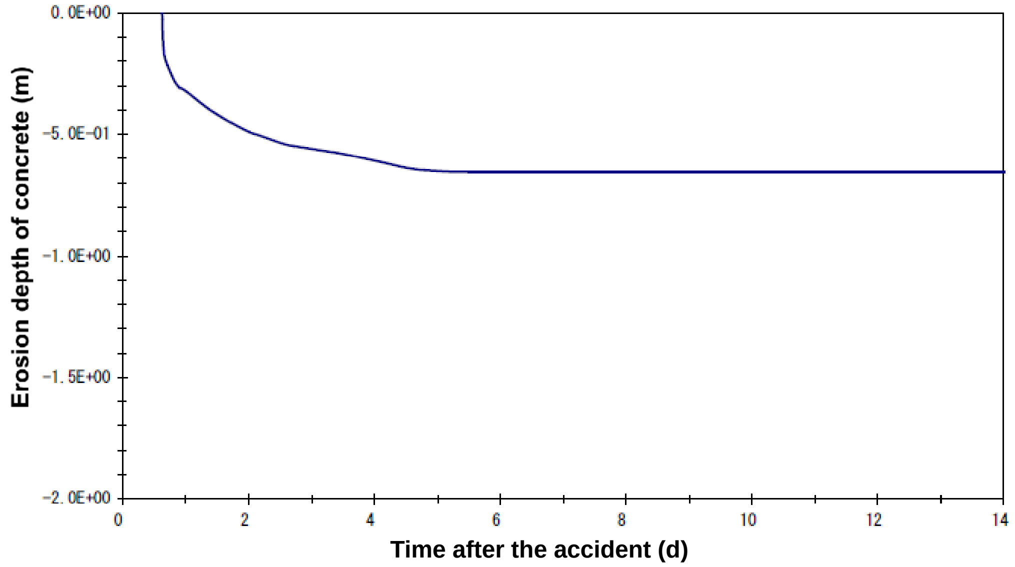

Figure 4.3-1 Evaluation of concrete erosion depth due to fuel debris relocated to the PCV

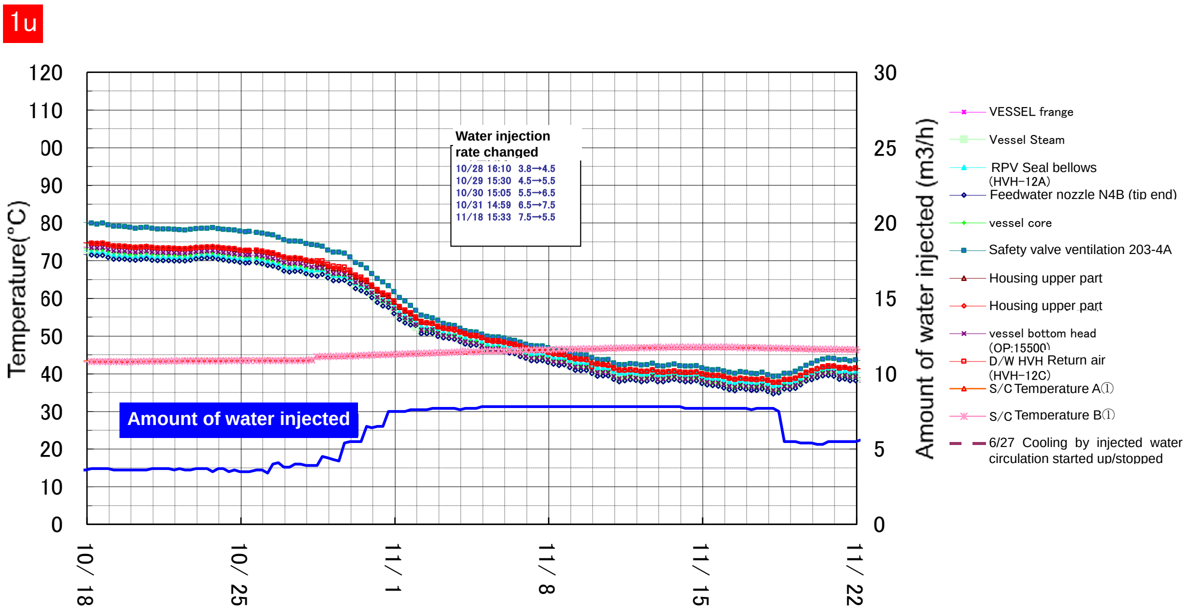

Figure 5.1-1 Latest temperature changes of Unit-1 (October 18 to November 22, 2011)

Figure 5.1-2　Steam blowout from floor penetration on Floor 1 filmed on June 3, 2011

Figure 5.1-3　No steam blowout from floor penetration on Floor 1 filmed on October 13, 2011

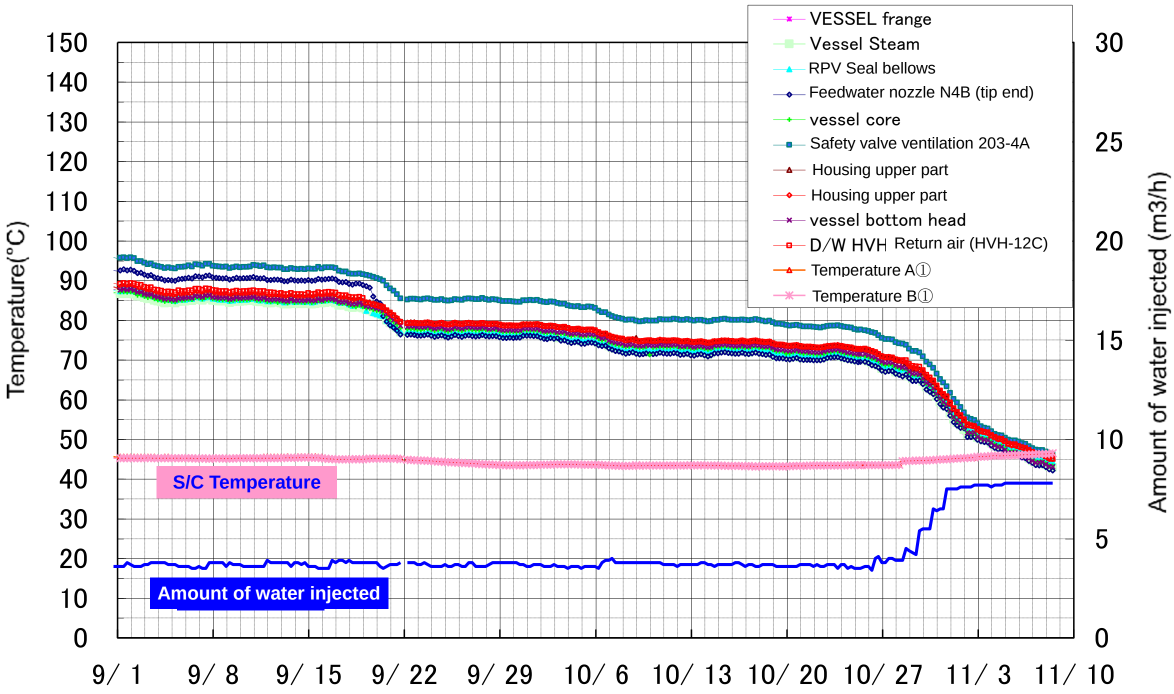

Figure 5.1-4　Temperature changes after increased water injection

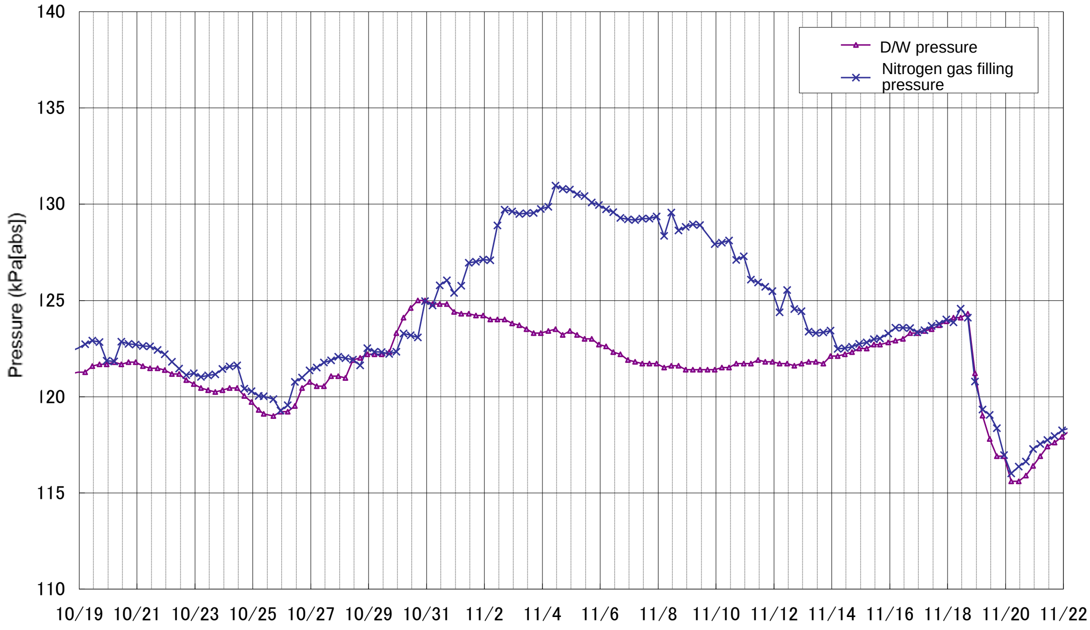

Figure 5.1-5　Changes of D/W pressure and nitrogen gas filling pressure

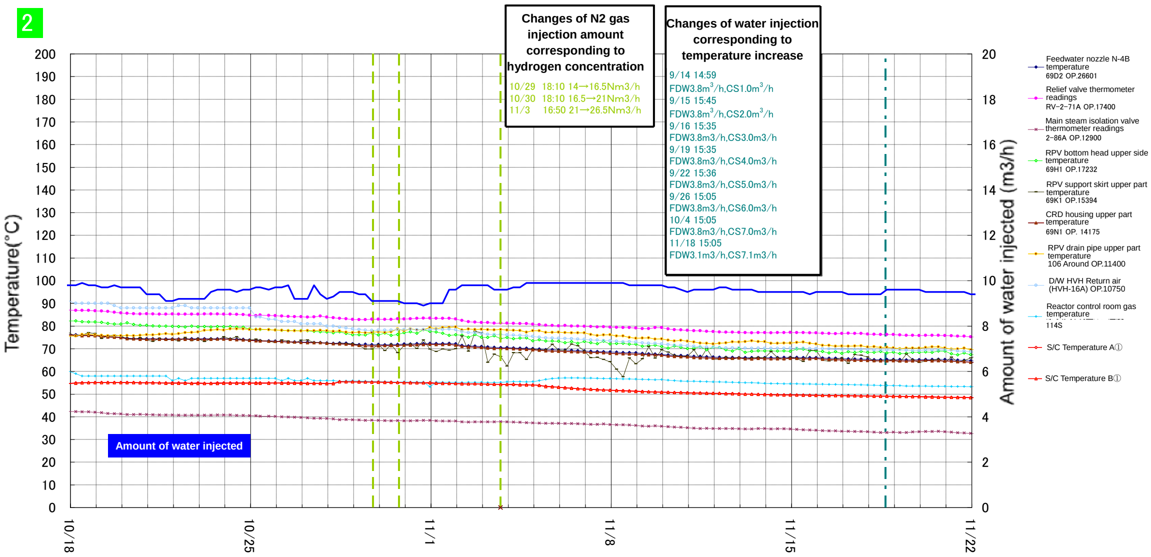

Figure 5.2-1　Latest temperature changes of Unit-2 (October 18 to November 22, 2011)

Figure 5.2-2 Steam blowout from immediately above the reactor on Floor 5 filmed on September 17, 2011

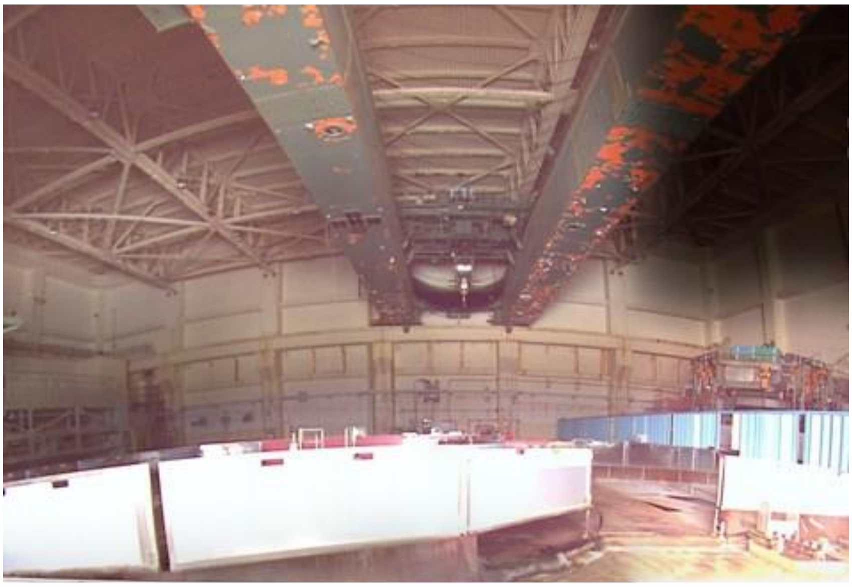

Figure 5.2-3　No steam blowout from immediately above the reactor on Floor 5 filmed on October 20, 2011

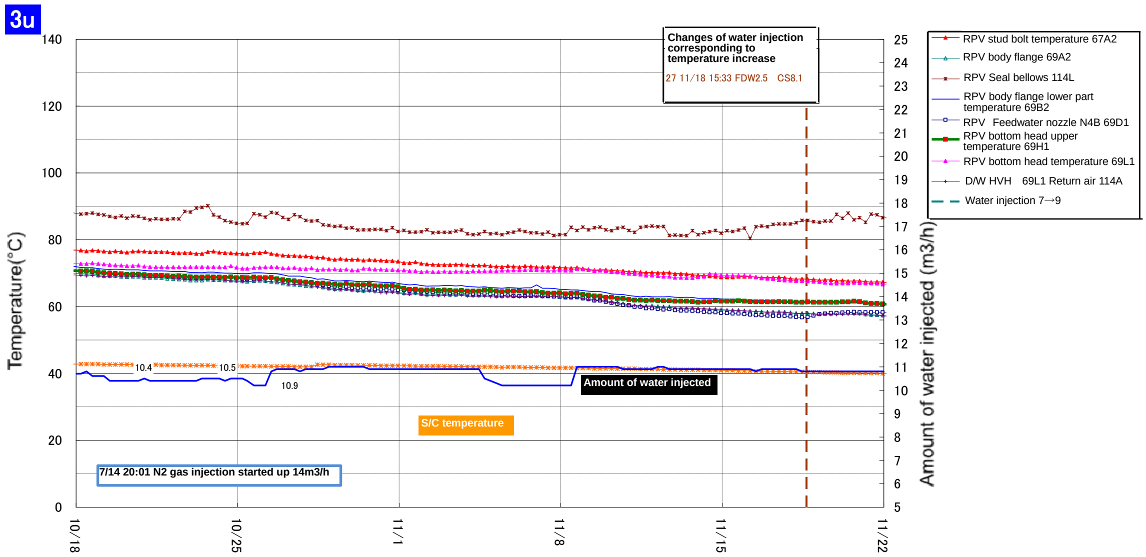

Figure 5.3-1 Latest temperature changes of Unit-3 (October 18 to November 22, 2011)

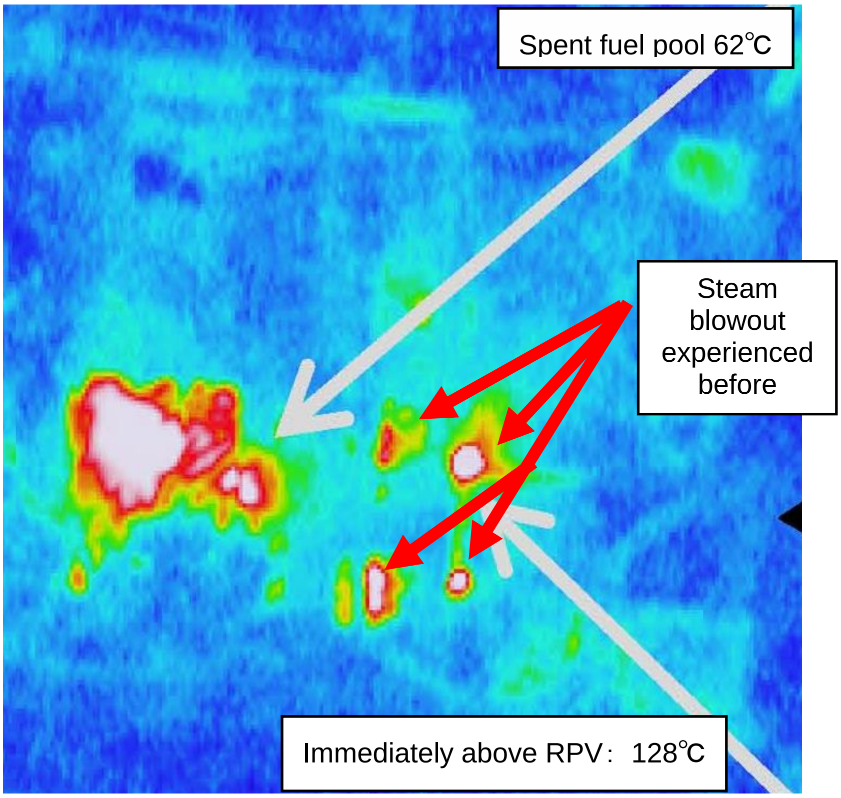

Figure 5.3-2　Temperature distribution of Unit-3 R/B filmed on March 20, 2011 (by the SDF)

Figure 5.3-3　Temperature distribution of Unit-3 R/B filmed on October 14, 2011

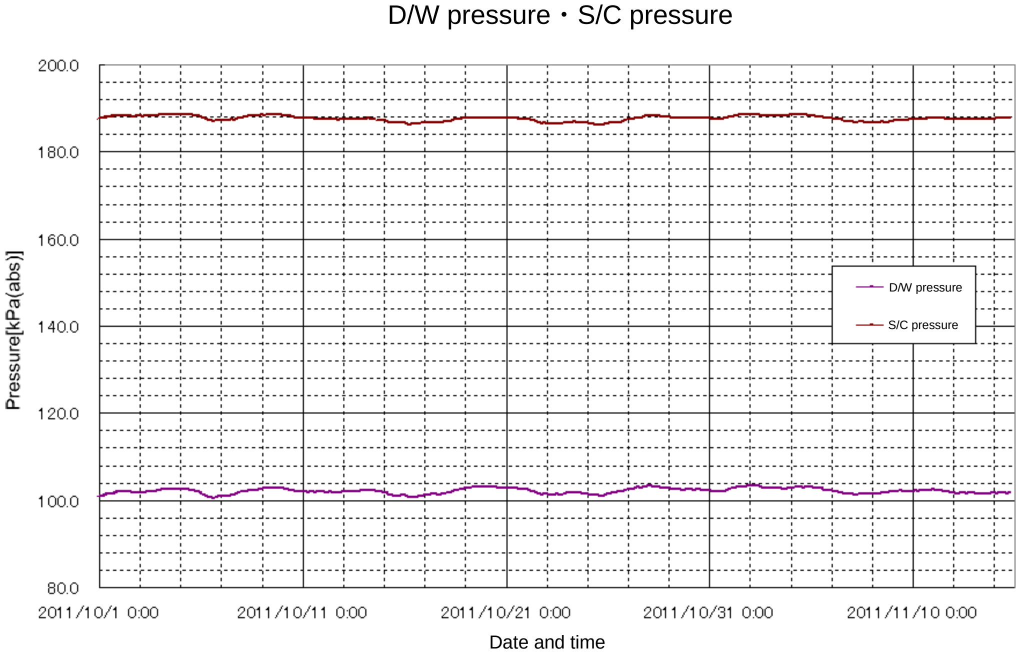

Figure 5.3-4 Changes of D/W pressure and S/C pressure

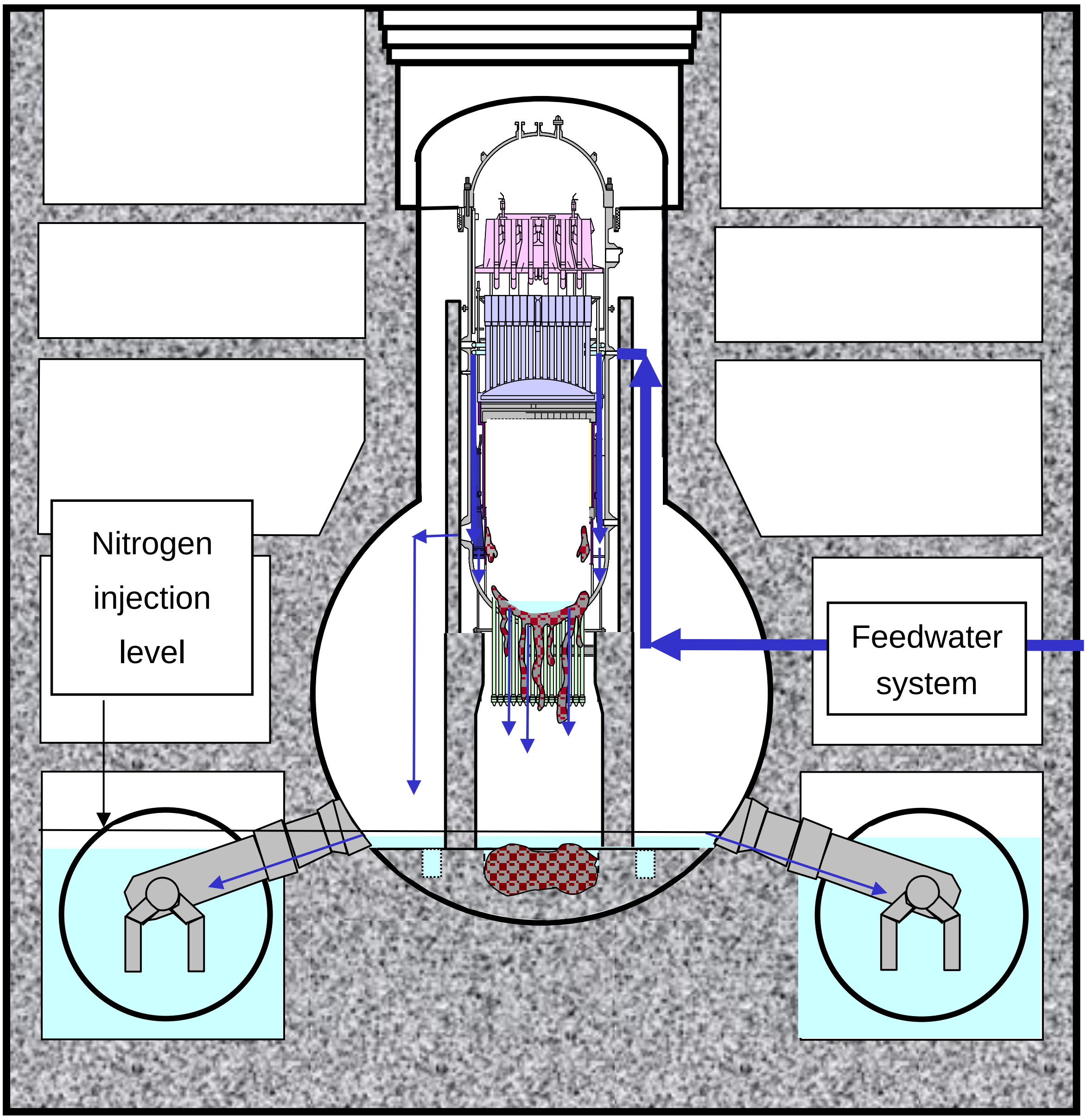

Figure 6.1-1　Estimated conditions of the Unit-1 core

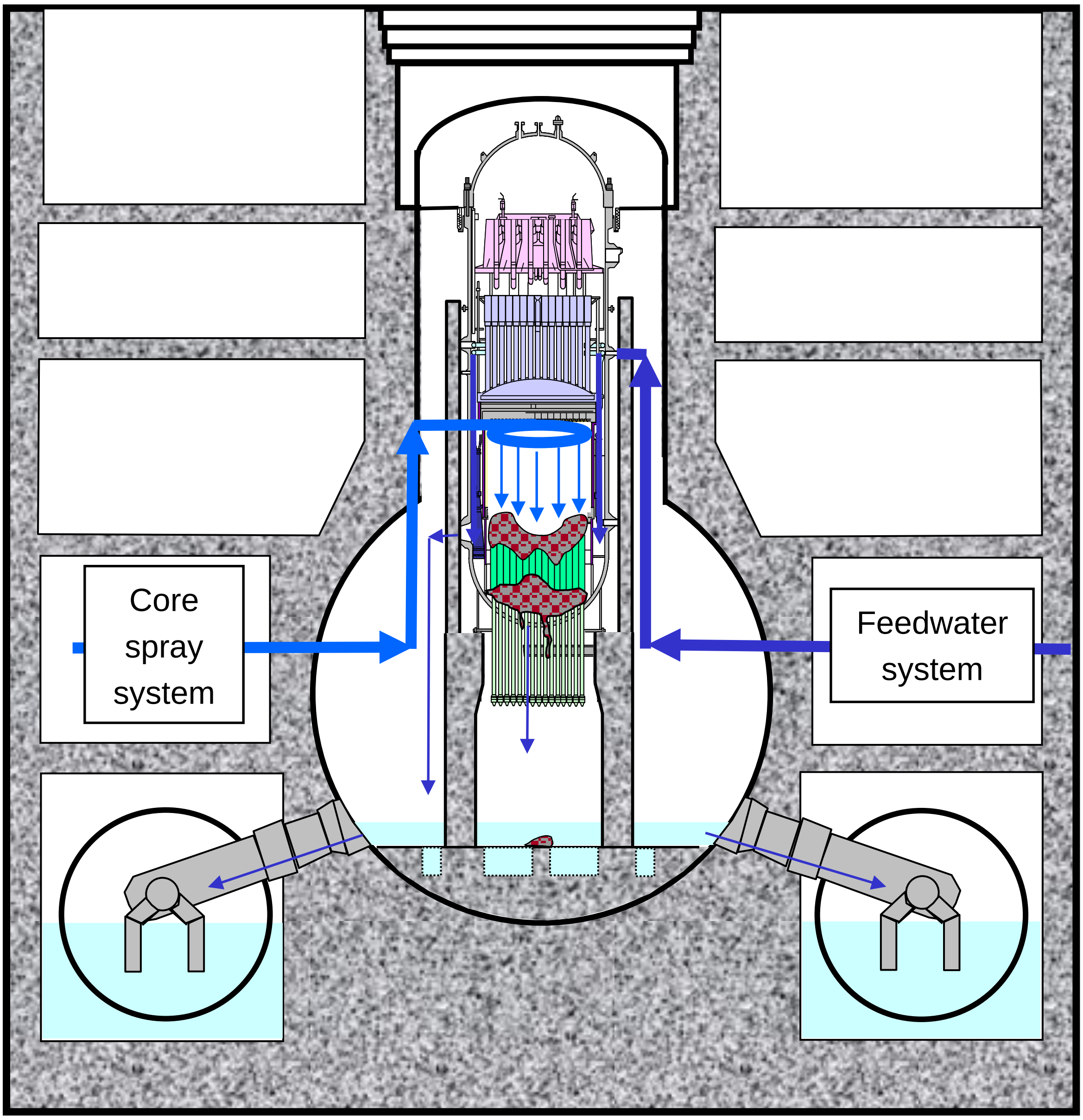

Figure 6.2-1 Estimated conditions of the Unit-2 core

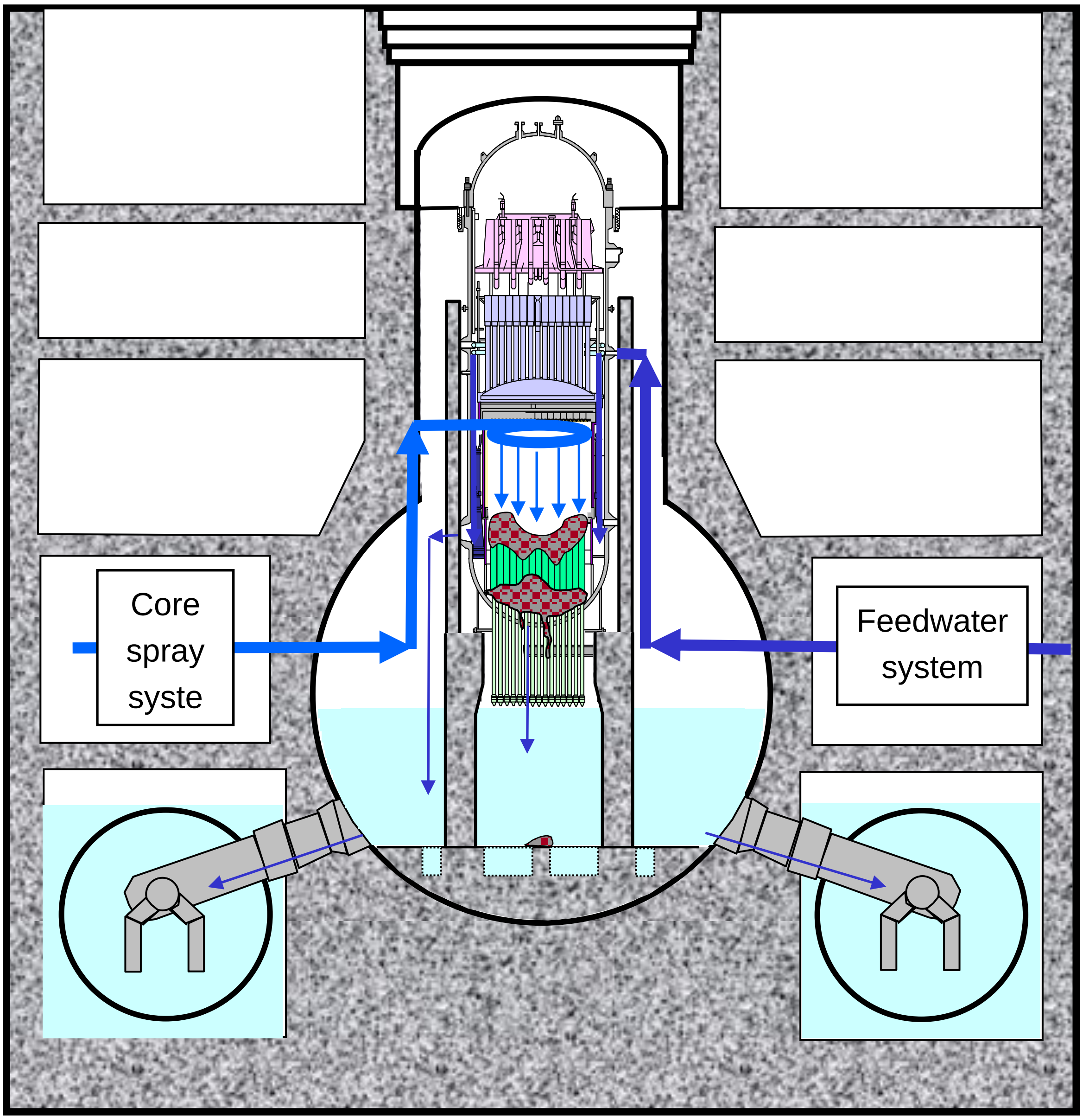

Figure 6.3-1 Estimated conditions of the Unit-3 core

Attachments

Attachments

Attachment-1

Estimated core conditions disclosed in May 2011

1. Introduction

The Tohoku District Off-Pacific Ocean Earthquake (Great East Japan Earthquake) which occurred on March 11, 2011 with its hypocenter off the Sanriku Coast, led to a series of events in Unit-1 to Unit-3 of the Fukushima Daiichi Nuclear Power Station that caused a severe accident as the units remained in continued station blackout conditions. The accident far exceeded design basis accidents and even multiple accidents which had been assumed in developing the accident management procedures, i.e., all emergency core cooling systems could not function or were stopped including those of adjacent units.

In response to the request from the Nuclear and Industrial Safety Agency (NISA), the Ministry of Economy, Trade and Industry (METI) (*) received on April 25, 2011, plant data at the time of the earthquake were collected to the extent possible and were reported to METI on May 16, 2011. The Modular Accident Analysis Program (hereafter referred to as “MAAP”) was applied to the system conditions, operation procedures and other parameters at the time of the early stage of earthquake and evaluated plant conditions. The data acquired were analyzed and the results were disclosed on May 23, 2011.

It should be noted, however, that the results disclosed had been based on the information available at that time as well as the estimations and assumptions for the analysis. The uncertainties of the results were quite large. The plant conditions could have turned out significantly different from the analysis results with the progress of investigations thereafter.

Estimated core conditions disclosed on May 23, 2011, were based on a comprehensive judgement derived from core conditions predicted by the MAAP analysis as well as from temperature behavior observed. Core conditions of Unit-1 to Unit-3 estimated and disclosed on May 23, 2011, are summarized below.

(*) Request of reports pursuant to Clause 1, Article 67 of the Reactor Regulation Law (Law No. 67) (Notification Number: H23-04-24 Gen-1), April 25, 2011, NISA, METI

2. Unit-1, Fukushima Daiichi Nuclear Power Station

2.1. MAAP analysis conditions

Table 1 gives key plant conditions for the analysis and Table 2 describes key event sequences.

The following assumptions were made in the analysis, concerning the isolation condensers (IC) and leaks from the containment vessel (PCV).

① Leaks from the PCV

Leaks from the PCV, specifically the drywell (D/W)), gaseous phase (about φ 3cm) were assumed at about 18 hours after the earthquake. This assumption was made to simulate the PCV pressure behavior actually measured. Enlarged leaks (about φ 7cm) were also assumed at about 50 hours after the earthquake.

It should be noted that these assumptions were purely for analysis. It was not known then (in May 2011) whether leaks from the PCV (D/W) had actually occurred, or whether there had been inconsistencies between measured values and analysis due to problems of measurement devices.

② Operability conditions of isolation condensers

Operability of isolation condensers (ICs) was not assumed in the analysis, since their operability was not certain yet, after the unit had entered the station blackout (*). But another situation was also analyzed, as a sensitivity analysis, in which the IC operability was assumed for a limited time after the station blackout had started.

It should be mentioned that, in this sensitivity analysis, one IC sub-system was assumed to have been operated intermittently during the time after the station blackout, on the grounds that the reactor pressures before the station blackout had been changing below the safety relief valve (SRV) actuation pressure (about 7.4MPa[abs]).

(*) When the local water level indicators in the IC shell side were checked on October 18, 2011, the readings were 65% in Sub-system A and 85% in Sub-system B (normal level 80%).

According to the records on the IC coolant temperature chart, the temperature of the Sub-system B stopped increasing at about 70 deg C. Coolant evaporation, which causes coolant water level changes, is considered to have been limited. The temperatures of Sub-system A increased to about 100 deg C, saturation temperature, at around the time when tsunami arrived at the unit. The coolant water level decrease of Sub-system A is considered to have been mainly due to heat exchange after the tsunami arrival.

It should be noted, however, that it is unknown, from the following reasons, to what extent Sub-system A was operable and how long it was actually functioning after the tsunami arrival: ① the isolation valve aperture inside the PCV is unknown; ② the IC heat removal performance deteriorates by accumulation of non-condensable hydrogen gas generated in water-zirconium reactions due to overheated fuel; and ③ the IC heat removal performance also deteriorates by the decreased amount of steam inflow to the IC from the reactor, because the reactor pressure dropped at the latest by 03:00 on March 12, 2011, and this caused the decrease of steam inflow to the IC.

In conclusion, the assumption in May 2011 of no IC operability after the station blackout is considered to have been appropriate.

Table 1 Unit-1 key plant conditions

Item	Condition
Initial reactor power	1380MWt (rated)
Initial reactor pressure	7.03MPa[abs] (normal operating pressure)
Initial reactor water level	Normal level
Nodalization in RPV core	See Figure 4 in the reference (Outline of MAAP at the end of this document)
Effective core nodalization	Radial: 5 nodes Axial: 10 nodes
Cladding damage temperature	1000K
Core node melting point	2500K
PCV model	See Figure 5 in the reference (Outline of MAAP)
PCV free volume	D/W: 3410m^3 S/C: 2620m^3
Water volume in S/C pool	1750m^3
Decay heat	Model ANSI/ANS5.1-1979 (Parameters adjusted to simulate the ORIGEN2 decay heat with fuel burnup considered)

Attachment 1-4

Table 2　Unit-1 event sequence

Note　○: Recorded　△: Estimated from records　□: Assumed in analysis

Conditions for analysis				Type	Remarks	
No	Day & Time		Events to analyze			○: Where records to refer to can be found △ or □: Grounds for estimation or assumption
1	3/11	14:46	Earthquake	○	－	
2		14:46	Reactor scrammed	○	4. Operation sheets, Supervisor shift transfer records in the 5/16 Report (*4)	
3		14:47	MSIV closed	○	4. Operation sheets, Supervisor shift transfer records in the 5/16 Report	
4		14:52	IC(A) (B) automatic start-up	○	3. Alarm records by alarm loggers in the 5/16 Report	
5		About 15:03	IC(A) stopped	△	6. IC assumed closed from data recorded in the transient recorder in the 5/16 Report	
6		About 15:03	IC(B) stopped	△	6. IC assumed closed from data recorded in the transient recorder in the 5/16 Report	
7		15:17	IC(A) restarted	△	IC operation estimated from reactor pressure changes (2. Chart records in the 5/16 Report) *1	
8		15:19	IC(A) stopped	△	IC operation estimated from reactor pressure changes (2. Chart records in the 5/16 Report) *1	
9		15:24	IC(A) restarted	△	IC operation estimated from reactor pressure changes (2. Chart records in the 5/16 Report) *1	
10		15:26	IC(A) stopped	△	IC operation estimated from reactor pressure changes (2. Chart records in the 5/16 Report) *1	

Attachment 1-5

11		15:32	IC(A) restarted	△	IC operation estimated from reactor pressure changes (2. Chart records in the 5/16 Report) *1
12		15:34	IC(A) stopped	△	IC operation estimated from reactor pressure changes (2. Chart records in the 5/16 Report) *1
13		15:37	Station blackout	○	4. Operation sheets, Supervisor shift transfer records in the 5/16 Report
14		18:10	IC(A) Valve-2A and 3A opened/Steam generation confirmed	□	IC functions assumed lost after station blackout, although this part is mentioned in 7. Operational procedure records in the 5/16 Report *2
15		18:25	IC(A) Valve-3A closed	□	IC functions assumed lost after station blackout, although this part is mentioned in 7. Operational procedure records in the 5/16 Report *2
16		21:19	IC connected to diesel-driven fire pump (D/D-FP)	□	IC functions assumed lost after station blackout, although this part is mentioned in 7. Operational procedure records in the 5/16 Report *2
17		21:30	IC Valve-3A opened	□	IC functions assumed lost after station blackout, although this part is mentioned in 7. Operational procedure records in the 5/16 Report *2
18		21:35	IC in service by D/D-FP input	□	IC functions assumed lost after station blackout, although this part is mentioned in 7. Operational procedure records in the 5/16 Report *2
20		05:46	Freshwater injection started by fire engines	○	7. Operational procedure records in the 5/16 Report *3
21		14:30	PCV pressure decrease confirmed by actuating AO valve on suppression chamber (S/C) side at 10:17 (PCV venting)	△	7. Operational procedure records in the 5/16 Report, PCV venting assumed done at 14:30 when the PCV pressure decrease was confirmed

22		14:49	PCV vent valve closed	△	PCV vent valve closure assumed from PCV pressure increase
23		14:53	Freshwater injection ended	○	7. Operational procedure records in the 5/16 Report
24		15:36	Explosion at Unit-1 reactor building	○	7. Operational procedure records in the 5/16 Report
25		20:20	Seawater injection started	○	7. Operational procedure records in the 5/16 Report *3

*1 The IC operability prior to the station blackout was not well known, but in the analysis one of two sub-systems was assumed to have been in operation intermittently, because the reactor pressures were changing between about 6.2 to 7.2MPa[abs], according to the records on the charts (Item 2 in the May 16 Report), while the preset actuation pressure for relief functions of SRV No. 1 was about 7.4MPa[abs] and that for stopping the blow-out was about 6.9MPa[abs].

*2 The IC operability after the station blackout started was not well known, either. In the analysis, the ICs were assumed to have lost their functions, because the records of IC operation were insufficient.

*3 Timings of changing the water injection flow rates and their amounts were set so as not to exceed the daily average flow rates and the total injection amount, based on the day-to-day records of injection amount to the reactor (Item 7. Compilation of operational procedures in the May 16 Report).

*4 Operation records, analyses of accident records and evaluation of their impacts at the Fukushima Daiichi Nuclear Power Station at the time of Tohoku District Off-Pacific Ocean Earthquake, May 16, 2011, Tokyo Electric Power Company

2.2. Results of MAAP analysis

Table 3 summarizes the analysis results.

Table 3 Summary of Unit-1 analysis results

Item	Results
Timing of core starting to be uncovered	About 3 hours after the earthquake
Timing of core starting to be damaged	About 4 hours after the earthquake
Timing of RPV being damaged	About 15 hours after the earthquake

Details of the results follow.

The reactor water level decreased to the level of top of active fuel (TAF) in about 2 hours after the IC was assumed to have stopped its functions after the tsunami arrival and thereafter, the core was damaged (Figure 1).

The reactor water level actually measured changed in the core region after the earthquake. This was quite different from the analysis results. In the analysis, the water level could not be maintained in the reactor pressure vessel (RPV) and the RPV was damaged. It is possible that the water in the water level indicators evaporated due to elevated PCV temperatures and the water level indicator readings were not correct. As a matter of fact, water level indicators of Unit-1 were calibrated at a later date by water filling and the reactor water level was found to have been below the core.

The RPV pressure increase after IC shutdown was assumed but this was maintained at about 8MPa by the SRV functions. After the core damage, fuel debris was relocated to the lower plenum, and about 15 hours after the earthquake the RPV was damaged and the reactor pressure quickly dropped (Figure 2).

The PCV pressures increased temporarily due to the steam and hydrogen gas (generated by the water-zirconium reactions in the core) discharged from the RPV but then decreased due to the leaks assumed from the PCV and later on March 12, 2011, they sharply dropped due to venting (Figure 3).

Water injection to the reactor started about 14 hours after the IC shutdown was assumed. By that time, the fuel was molten due to the decay heat, had relocated to the lower plenum, and the RPV was damaged about 15 hours after the earthquake (Figure 4).

2.3. Estimation of Unit-1 core conditions

The core conditions were estimated as follows, by comprehensively considering the information available including the core conditions being estimated from the temperature behavior actually measured.

The analysis gave the results that the core damage had started relatively early after the unit had entered station blackout and that the RPV damage had followed. The results were considered to have predicted the accident progression as being severer than the actual progression, when the plant conditions, estimated from the following temperatures at various points of the reactor and other information, were considered.

When temperatures became measurable at various points of the reactor, the RPV temperatures were above 400 deg C at multiple measurement points. At that timing, the core was considered to have been under insufficiently cooled situations. But, as soon as water injection to the reactor was certainly ensured by using the feedwater (FW) line, the RPV temperatures decreased quickly. The core was considered then to have been undergoing cooling sufficiently.

Most fuel was considered as being cooled in the RPV from the following observations (Figure 5): temperatures under the RPV, e.g., those of CRD housings, had been measurable but they would not have been measurable if the RPV had been broken; the RPV steel temperatures were changing in the region of 100 to 120 deg C, and at multiple measurement points the temperatures responded in a consistent manner to the changing amount of water injection; and the temperatures in the upper part of the RPV were in higher trends at multiple points, indicating the heat source was present in the RPV. When the analysis was made, MAAP was considered to have predicted the severer accident progression than the reality, on the grounds that the ICs were known to have been out of service at the time of tsunami arrival, but the detailed operation conditions were unclear.

Consequently, based on the analysis results and plant parameters (temperatures around the RPV), the core was considered to have been significantly damaged and relocated to a location lower than the original position (lower plenum), and it was being cooled there in a stable manner.

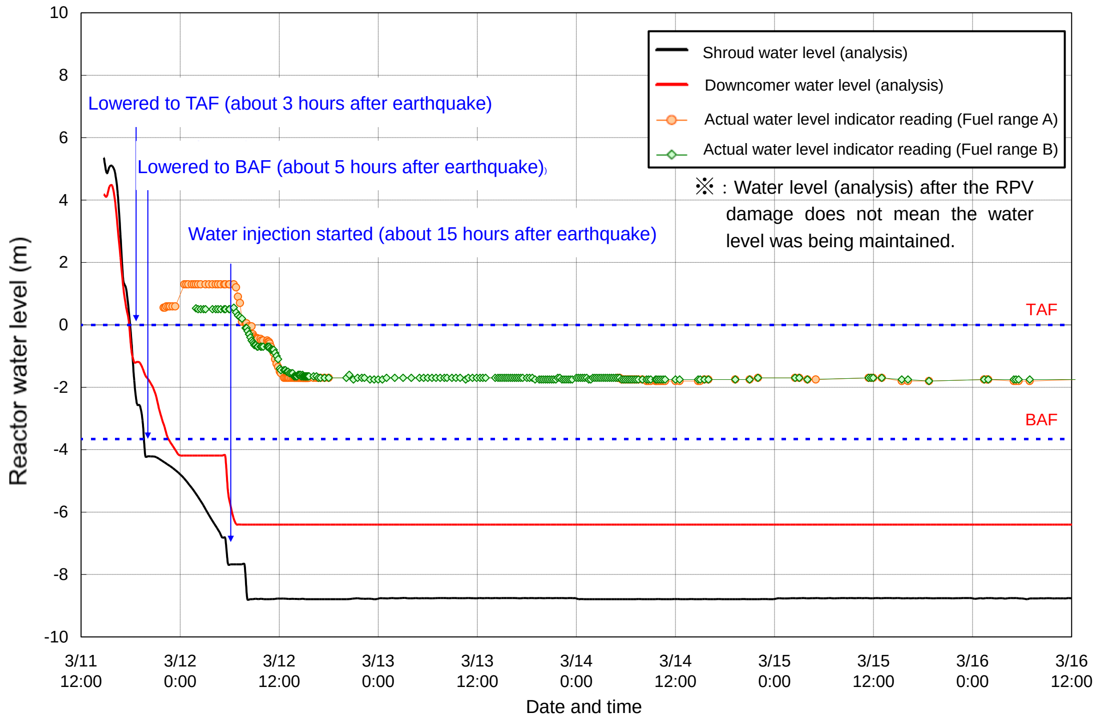

Figure 1　Unit-1 reactor water level changes

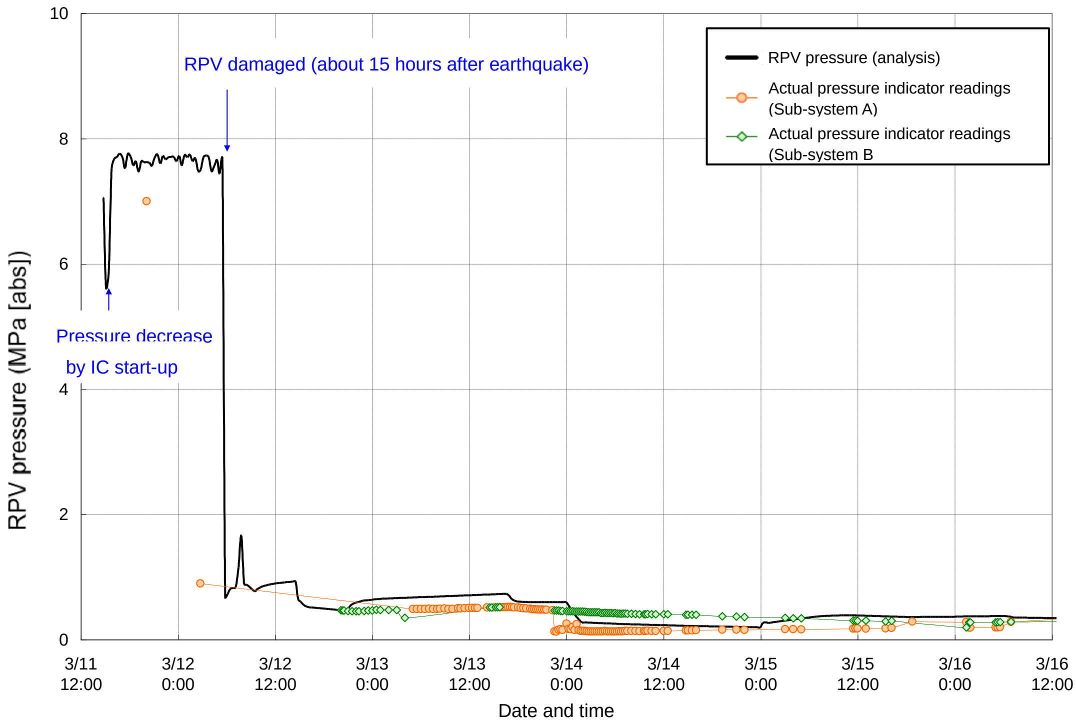

Figure 2　Unit-1 RPV pressure changes

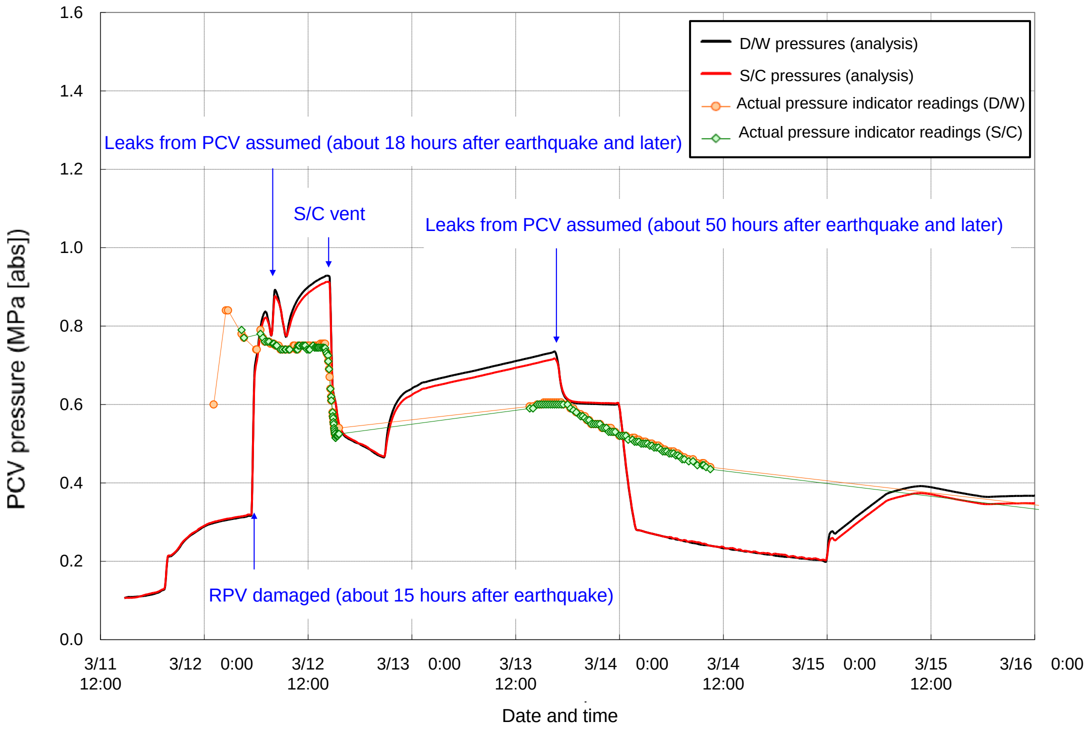

Figure 3 Unit-1 PCV pressure changes

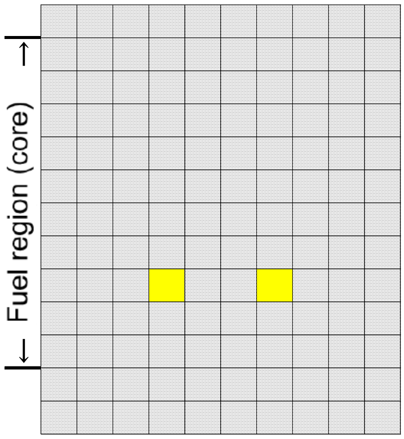

About 4.7 hours after scram

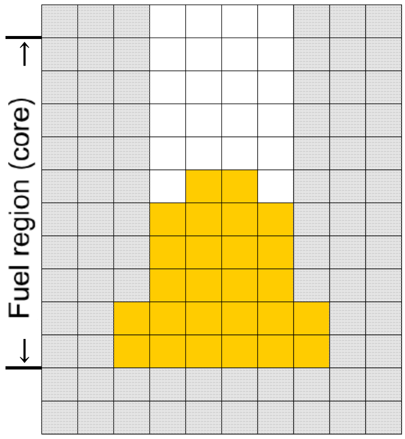

About 5.3 hours after scram

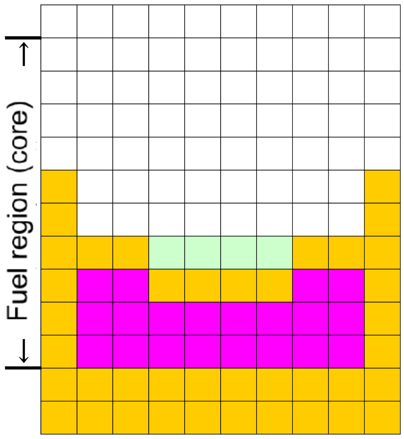

About 15 hours after scram

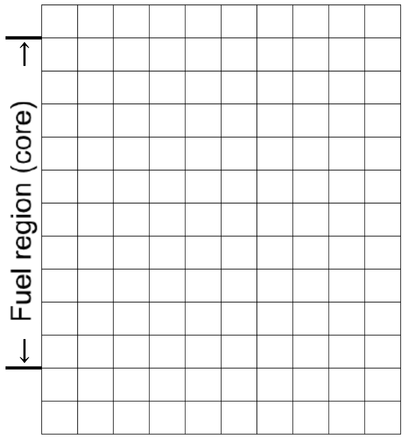

About 14.3 hours after scram

Core damage schematic
: No fuel (collapsed)
: Intact fuel
: Sedimented damaged fuel (pin shape was kept)
: Fuel pin diameters enlarged by solidified molten fuel while going down pin surfaces
: Coolant flow paths blocked by enlarged fuel pins
: Molten fuel pool

Figure 4 Unit-1 estimated core conditions

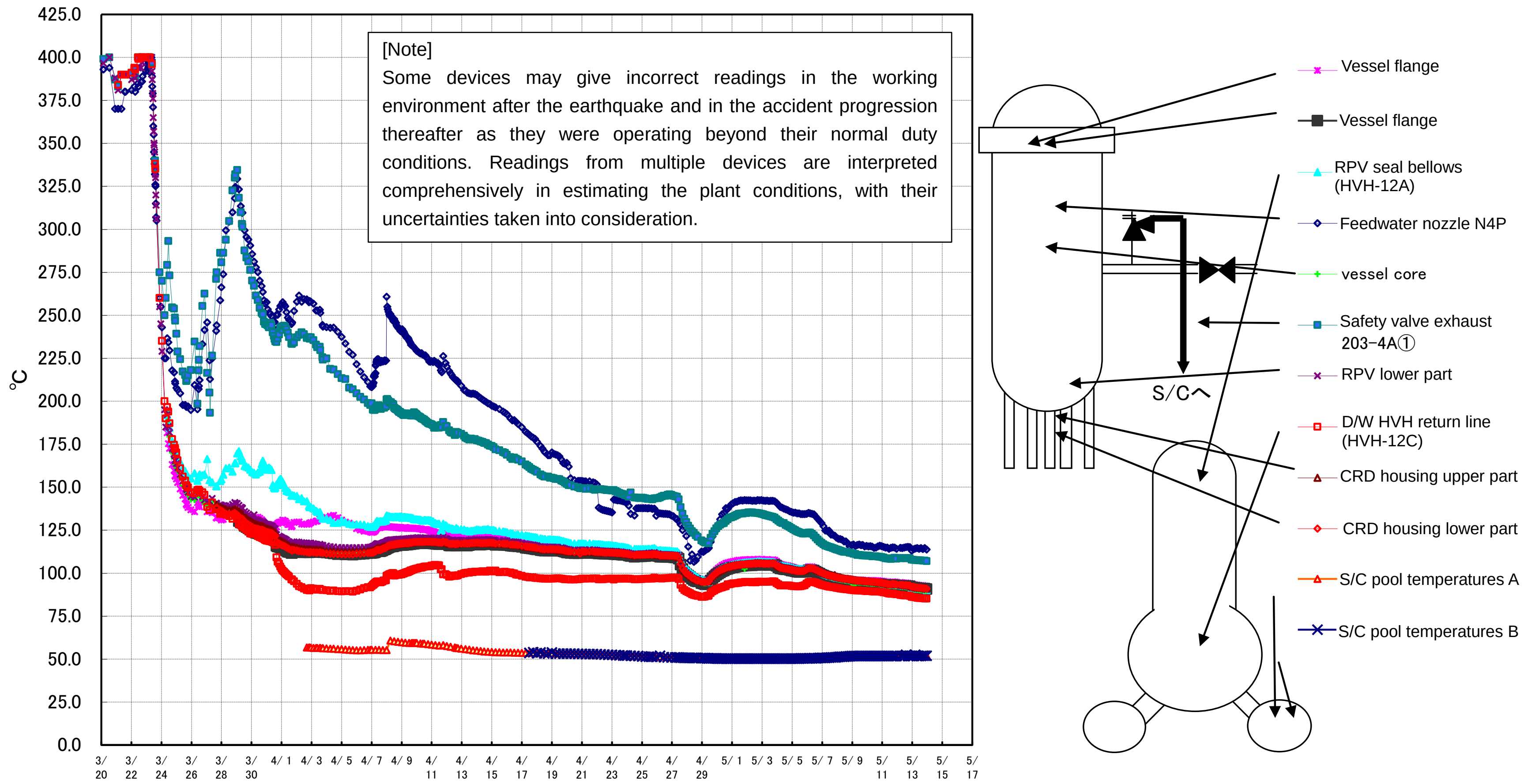

Figure 5 Unit-1 temperature changes at typical points (May 2011 when disclosed)

3. Unit-2, Fukushima Daiichi Nuclear Power Station

3.1. MAAP analysis conditions

Table 4 gives key plant conditions for the analysis and Table 5 describes key event sequences.

The following two cases were analyzed, and the following assumptions were made concerning the leaks from the PCV.

① Two cases analyzed

At Unit-2, seawater injection started at 19:54 on March 14, 2011, as seen in Table 5. The following two cases were analyzed concerning the amount of seawater injection thereafter.

Case 1: The reactor water level actually measured (at around the core center) was simulated by setting the amount of water injected to the reactor in the analysis at lower values than those measured at the fire engine discharge point.

Case 2: The amount of water injected to the reactor in the analysis was set at a lower value than those measured at the fire engine discharge point so that the reactor water level in the analysis could maintain the level approximately below the core level in the reactor. This case was chosen, because the reactor water level indicators might have failed to give correct readings, as had been experienced at Unit-1, and the reactor water level might not have been maintained in the core region.

② Leaks from the PCV

Leaks from the PCV, specifically the D/W, gaseous phase (about φ 10cm) were assumed at about 21 hours after the earthquake. This assumption was made to simulate the PCV pressure behavior actually measured. In addition, leaks from the PCV, specifically the S/C), gaseous phase (about φ 10cm) were assumed at the timing when unusual sounds around the S/C had been noticed on March 15, 2011.

It should be noted that these assumptions were purely for analysis. It was not known by then (May 23, 2011) whether leaks from the PCV (D/W) had actually occurred, or whether there had been inconsistencies between measured values and analysis due to problems of measurement devices.

Table 4　Unit-2 key plant conditions

Item	Condition
Initial reactor power	2381MWt (rated)
Initial reactor pressure	7.03MPa[abs] (normal operating pressure)
Initial reactor water level	Normal level
Node division in RPV core	See Figure 6 in the reference (Outline of MAAP)
Effective core node divisions	Radial: 5 nodes Axial: 10 nodes
Cladding damage temperature	1000K
Core node melting point	2500K
PCV model	See Figure 7 in the reference (Outline of MAAP)
PCV open volume	D/W: 4240m^3 S/C: 3160m^3
Water volume in S/C pool	2980m^3
Decay heat	Model ANSI/ANS5.1-1979 (Burnup at the end of equilibrium core assumed)

Table 5　Unit-2 event sequence

Note　○: Recorded　△: Estimated from records　□: Assumed in analysis

Conditions for analysis				Type	Remarks	
No	Day & Time		Events to analyze			○: Where records to refer to can be found △ or □: Grounds for estimation or assumption
1	3/11	14:46	Earthquake	○	—	
2		14:47	Reactor scrammed	○	4. Operation sheets, shift supervisor logbooks in the 5/16 Report	
3		15:02	RCIC manually started up	○	7. Operational procedure records in the 5/16 Report	
4		15:28	RCIC tripped (L-8)	○	7. Operational procedure records in the 5/16 Report	
5		15:41	Station blackout	○	4. Operation sheets, shift supervisor logbooks in the 5/16 Report	
6	3/12	04:20 to 05:00	RCIC water source switched from condensate storage tank to S/C	○	7. Operational procedure records in the 5/16 Report	
7	3/14	13:25	RCIC stopped	○	7. Operational procedure records in the 5/16 Report	
8		16:34	RPV depressurization operation started (opening SRV1)	○	7. Operational procedure records in the 5/16 Report	
		16:34	Seawater injection started via fire engine water lines	○	7. Operational procedure records in the 5/16 Report *1	
9		About 18:00	RPV pressure decrease confirmed	○	7. Operational procedure records in the 5/16 Report	
10		19:20	Fire engines stopped pumping (out of fuel)	○	7. Operational procedure records in the 5/16 Report *1	
11		19:54	First fire engine started pumping	○	7. Operational procedure records in the 5/16 Report *1, *2	

		19:57	Second fire engine started pumping	○	7. Operational procedure records in the 5/16 Report *1
12		21:20	RPV depressurized by opening SRV2 and reactor water level recovered	○	7. Operational procedure records in the 5/16 Report *1
13		About 23:00	SRV1 closure assumed	□	SRV1 closure assumed, as the RPV increased at this timing at about 23:00.
14	3/15	About 06:14	Unusual sounds near the S/C, followed by pressure decrease in the chamber	○	Press release (TEPCO HP (http://www.tepco.co.jp/index-j.html)

*1 The seawater injection was assumed to have started at 19:54 on March 14, 2011, when the reactor water level increase had been confirmed. There is an earlier record at 19:20 on March 14, 2011, “fire engines stopped,” which means that some amount of seawater may have been injected till then after 16:34 on March 14, 2011, but the effect of this temporary water injection was ignored in the analysis.

*2 Timings of changing the water injection flow rates and their amount were set so as not to exceed the daily average flow rates and the total injection amount, based on the day-to-day records of injection amount to the reactor (Item 7. Compilation of operational procedures in the May 16 Report).

3.2. Results of MAAP analysis

3.2.1. Results of Case 1 analysis

Table 6 summarizes the analysis results.

Table 6 Summary of Unit-2 analysis results Case 1

Item	Results
Timing of core starting to be uncovered	About 75 hours after the earthquake
Timing of core starting to be damaged	About 77 hours after the earthquake
Timing of RPV being damaged	No RVP damage occurred in this analysis

Details of the Case 1 analysis results follow.

The reactor water level gradually decreased after the RCIC had stopped, the core started to be uncovered, the core became totally uncovered by the SRV actuation, and the core started being damaged (Figure 6). Almost at the same time, water injection was started, but the amount of water injected had been adjusted to simulate the reactor water level indicated by the indicator readings. The amount was insufficient and the water level just deep enough to cover only about half of the core could be maintained. The core became damaged.

The RPV pressures were kept high at around the SRV actuation pressure until the RCIC was shut down. Upon SRV actuation after the RCIC shutdown, the reactor was rapidly depressurized and pressure gradually decreased to around the atmospheric pressure.

While the RCIC was functioning, the measured reactor pressures changed at a lower level than the analyzed pressure. There is a possibility that a leak path from the PCV to S/C via the SRVs was formed, but it was not known then (May 2011) whether there were actual leaks or whether there were simply instrumentation system problems. After SRV actuations, the reactor pressures changed roughly in a consistent manner in measurement and analysis (Figure 7).

The PCV pressures increased following the S/C pool temperature increase, but the D/W pressure increasing rate after the earthquake until just before the assumed leaks slowed down, consistent with the measurement, since leaks from the PCV (D/W) had been assumed. Upon SRV actuation on March 14, 2011, the PCV pressures showed a temporary increase. Measured PCV pressures began to decrease thereafter. In the analysis, too, leaks from the S/C gaseous phase were assumed to have occurred when unusual sounds were noticed in the vicinity of the S/C on March 15, 2011 (Figure 8).

The Unit-2 core was concluded to have remained in the core region, although part of the molten fuel remained as a pool, and the RPV was concluded not to have been damaged. This was considered to have been feasible because, water injection via the RCIC at an early stage could have been implemented fairly continuously, and the time delay from the RCIC shutdown to water injection initiation could have been shorter than at Unit-1 (Figure 9).

3.2.2. Results of Case 2 analysis

Table 6 summarizes the analysis results.

Table 7 Summary of Unit-2 analysis results Case 2

Item	Results
Timing of core starting to be uncovered	About 75 hours after the earthquake
Timing of core starting to be damaged	About 77 hours after the earthquake
Timing of RPV being damaged	About 109 hours after the earthquake

Details of the Case 2 analysis results follow.

The reactor water level gradually decreased after the RCIC had stopped, the core started to be uncovered, the core became totally uncovered by the SRV actuation, and the core started being damaged. Almost at the same time, water injection was started, but the amount of water injected had been adjusted as insufficient to maintain the reactor water level above the bottom of active fuel (Figure 10).

The RPV pressures showed a temporary increase after depressurization by the SRV actuation. This was due to the steam produced when part of the molten fuel was relocated to the lower plenum. But the overall behavior (Figure 11) other than this point was similar to the behavior in Case 1.

The PCV pressures showed a temporary increase, as in the case of reactor pressures, due to the steam produced when part of molten fuel was relocated to the lower plenum. But the overall behavior (Figure 12) other than this point was similar to the behavior in Case 1.

Part of the molten fuel remained in the RPV, but the RPV was damaged. The amount of water injected had been set at a lower value than that in Case 1 and this caused the core damage to be advanced (Figure 13).

3.3. Estimation of Unit-2 core conditions

The core conditions are estimated as follows, by comprehensively considering the information available including the core conditions being estimated from the temperature behavior actually measured.

The analysis of Case 1 gave the results that the fuel in the core had been molten but remained in the core region, although part of the molten fuel had remained as a pool, and that the RPV had not been damaged. The analysis of Case 2 gave the results that part of molten fuel had remained in the RPV, but the RPV had been damaged.

Most of the fuel was considered to have been undergoing cooling in the RPV from the following plant parameters observed: the RPV bottom temperatures were changing at around 100 to 120 deg C and at more than one measurement points the temperatures responded in a consistent manner to the changing amount of water injected; and the heat source was considered to be in the RPV, because the RPV upper part gave higher temperatures (Figure 14).

Consequently, based on the analysis results and plant parameters, the core was considered to have been significantly damaged and relocated to a location lower than its original position (lower plenum), and it was mostly being cooled there in a stable manner.

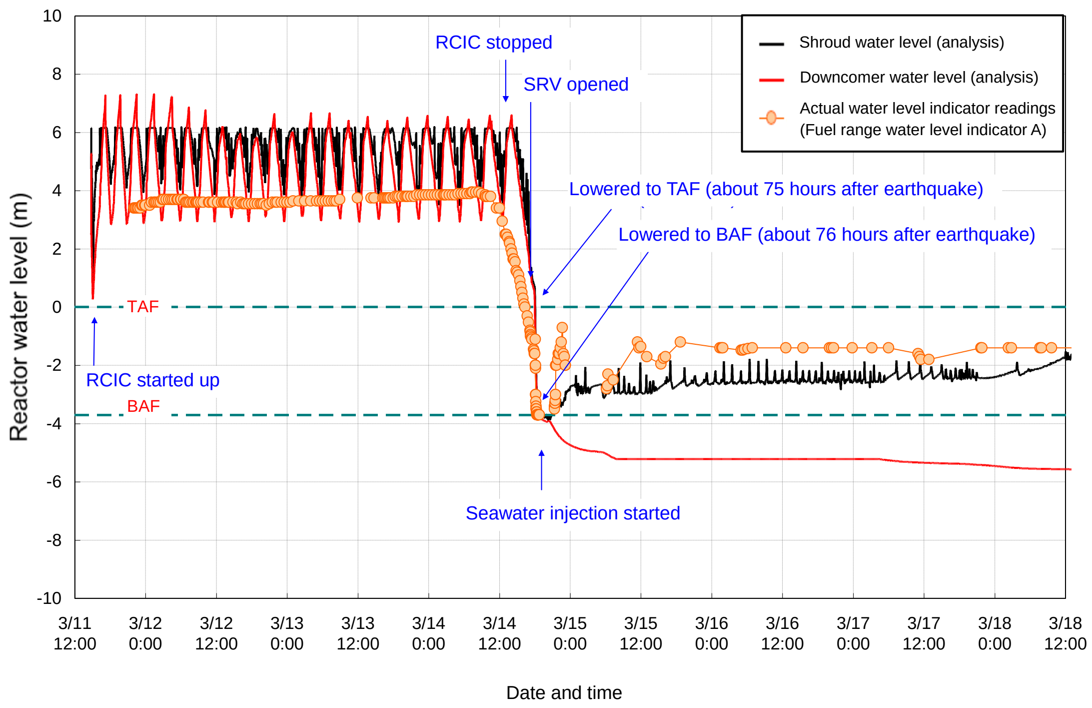

Figure 6　Unit-2 reactor water level changes Case 1

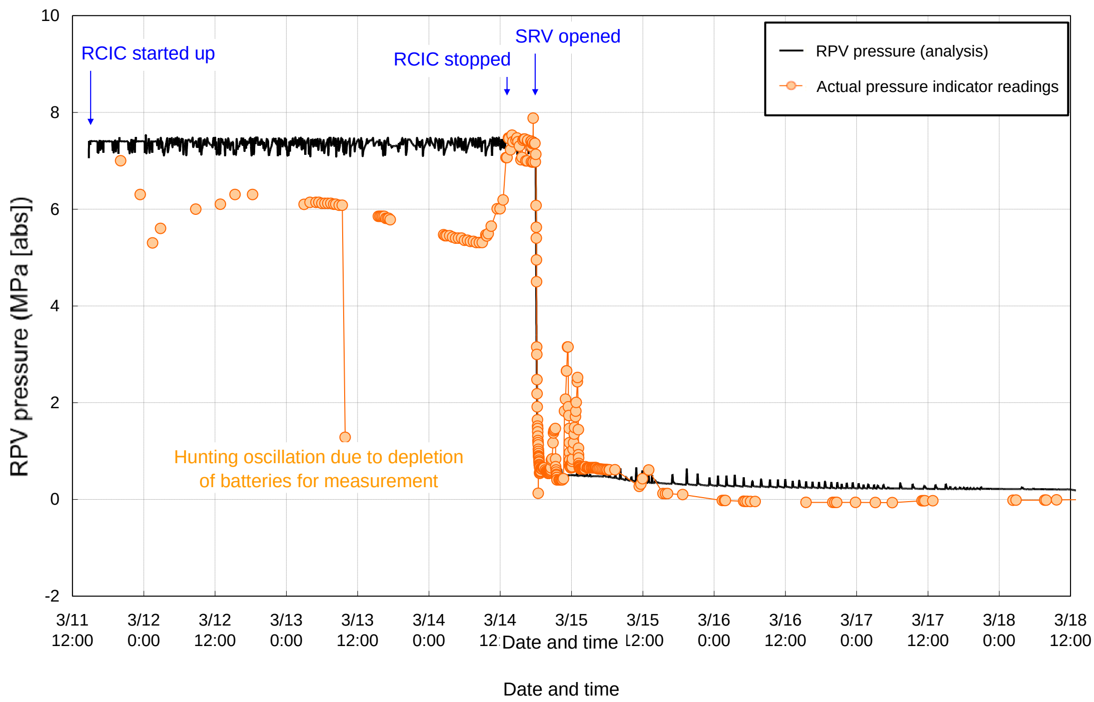

Figure 7　Unit-2 RPV pressure changes Case 1

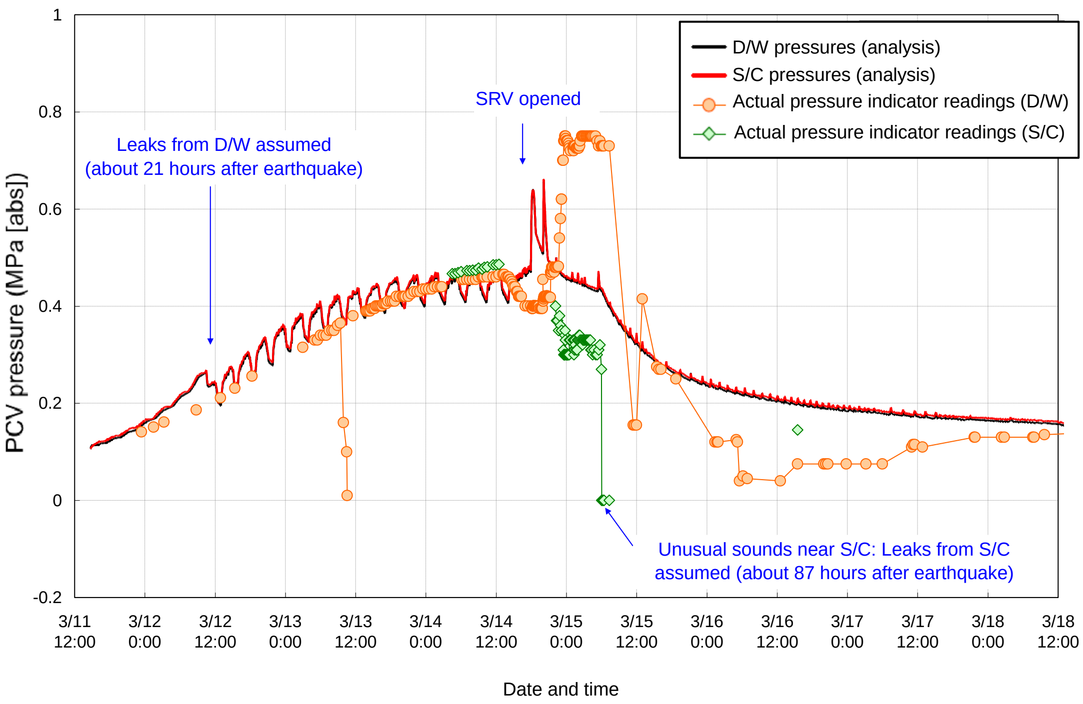

Figure 8　Unit-2 PCV pressure changes Case 1

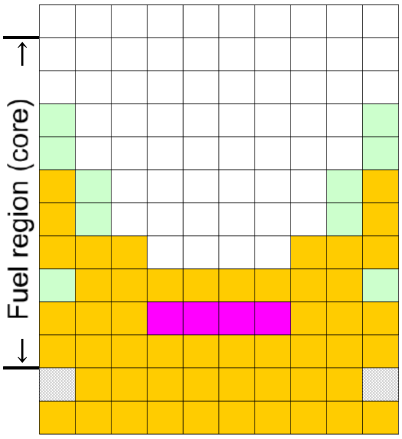

About 87 hours after scram

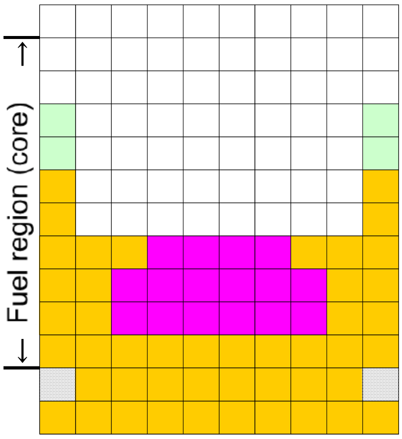

About 96 hours after scram

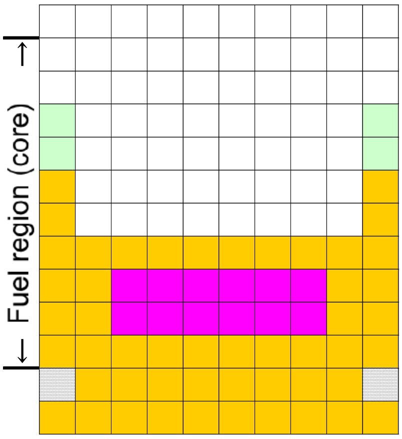

About 120 hours after scram

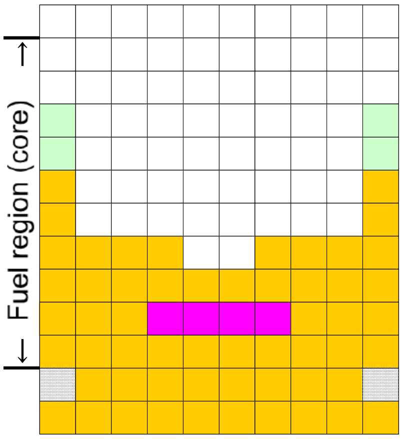

About 1 week after scram

Core damage schematic
: No fuel (collapsed)
: Intact fuel
: Sedimented damaged fuel (pin shape was kept)
: Fuel pin diameters enlarged by solidified molten fuel while going down pin surfaces
: Coolant flow paths blocked by enlarged fuel pins
: Molten fuel pool

Figure 9 Unit-2 core conditions Case 1

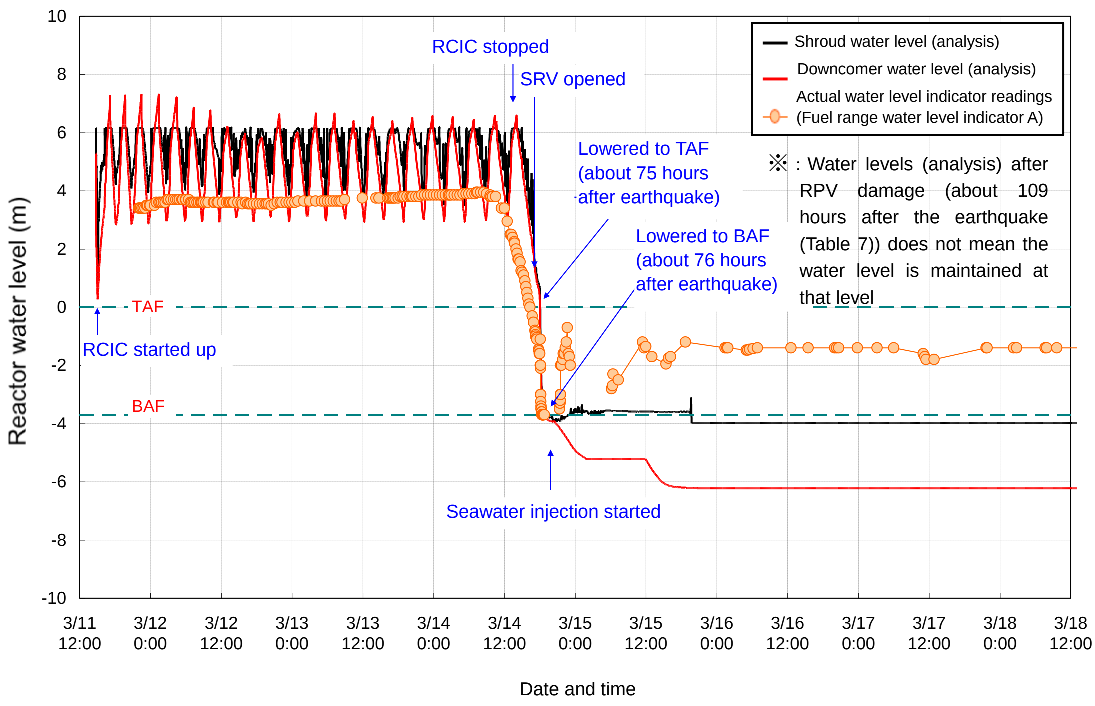

Figure 10　Unit-2 reactor water level changes Case 2

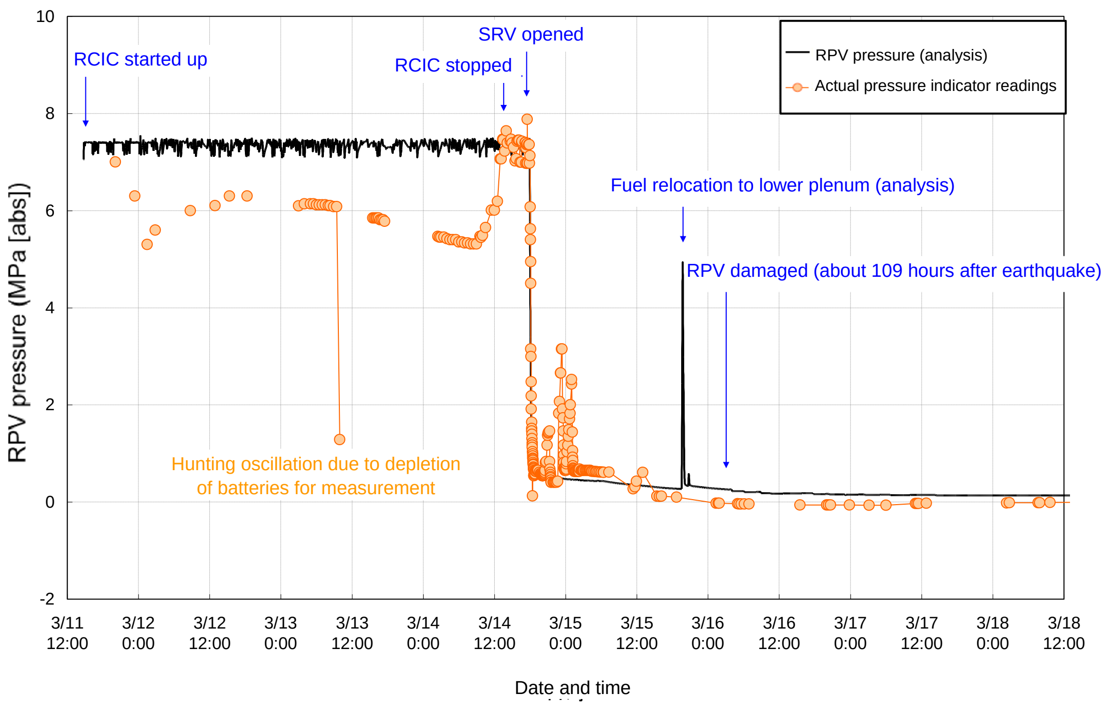

Figure 11　Unit-2 RPV pressure changes Case 2

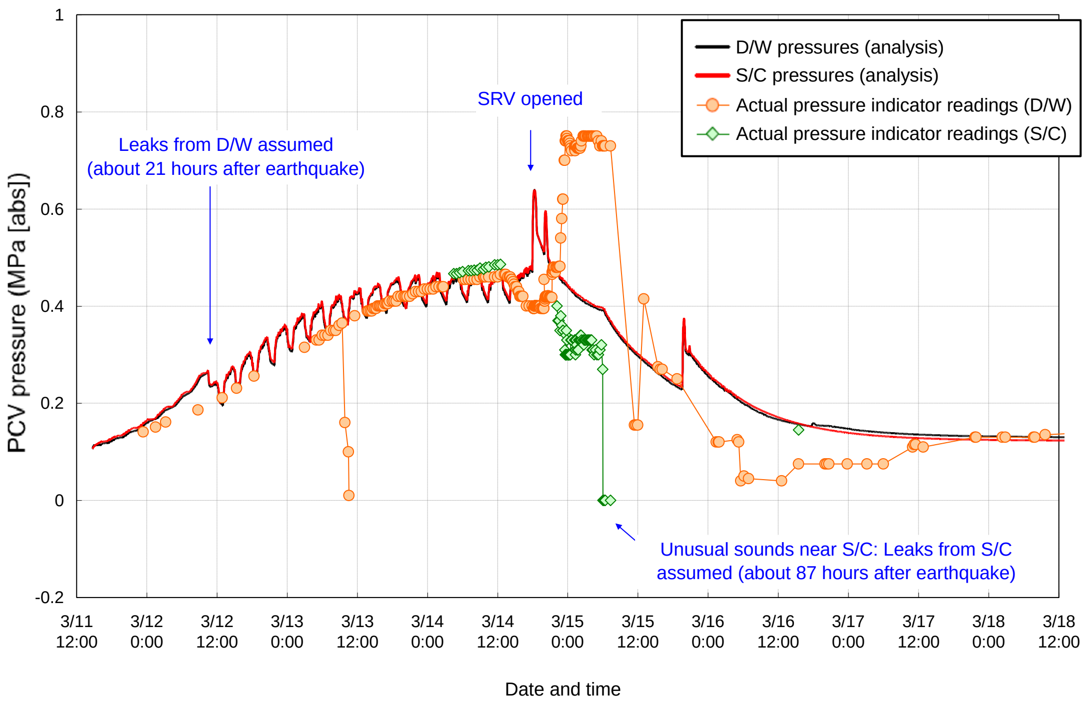

Figure 12 Unit-2 PCV pressure changes Case 2

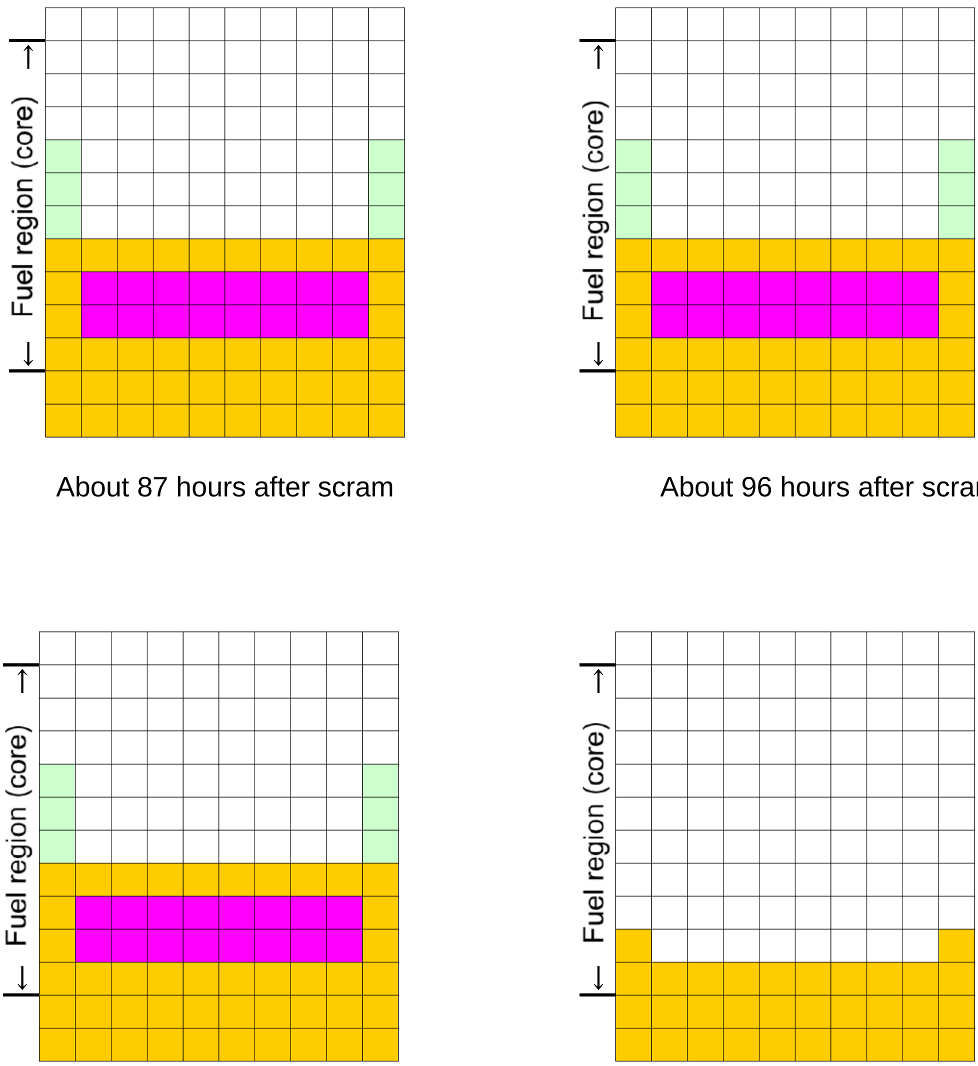

About 87 hours after scram

About 96 hours after scram

About 100 hours after scram

About 109 hours after scram

Core damage schematic
: No fuel (collapsed)
: Intact fuel
: Sedimented damaged fuel (pin shape was kept)
: Fuel pin diameters enlarged by solidified molten fuel while going down pin surfaces
: Coolant flow paths blocked by enlarged fuel pins
: Molten fuel pool

Figure 13 Unit-2 core conditions Case 2

Attachment 1-26

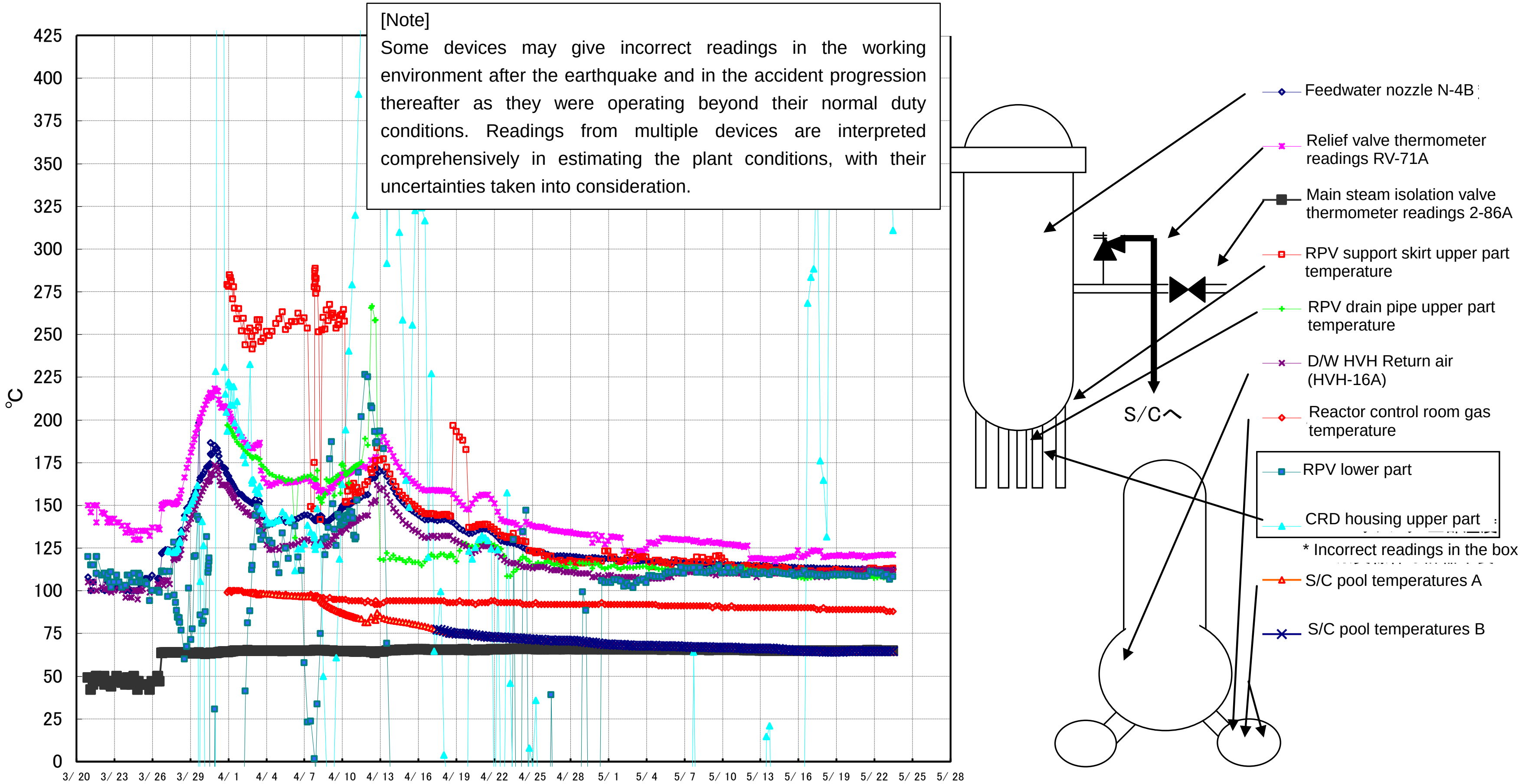

Figure 14 Unit-2 temperature changes at typical points (May 2011 when disclosed)

4. Unit-3, Fukushima Daiichi Nuclear Power Station

4.1. MAAP analysis conditions

Table 8 gives key plant conditions for the analysis and Table 9 describes key event sequences.

The following two cases were analyzed.

At Unit-3, fresh water injection started at 09:25 on March 13, 2011, as Table 9 shows. The following two cases of water injection amount thereafter were analyzed.

Case 1: The reactor water levels actually measured (at around the core center) were simulated by setting the amount of water injected to the reactor in the analysis at the lower values than those measured at the fire engine discharge point.

Case 2: The amount of water injected to the reactor in the analysis was set at lower values than those measured at the fire engine discharge point so that the reactor water level in the analysis could maintain the level approximately below the core level in the reactor. This case was chosen, because the reactor water level indicators might have failed to give correct readings, as had been experienced at Unit-1, and the reactor water level might not have been maintained in the core region.

Table 8 Unit-3 key plant conditions

Item	Condition
Initial reactor power	2381MWt (rated)
Initial reactor pressure	7.03MPa[abs] (normal operating pressure)
Initial reactor water level	Normal level
Node division in RPV core	See Figure 6 in the reference (Outline of MAAP)
Effective core node divisions	Radial: 5 nodes Axial: 10 nodes
Cladding damage temperature	1000K
Core node melting point	2500K
PCV model	See Figure 7 in the reference (Outline of MAAP)
PCV open volume	D/W: 4240m^3 S/C: 3160m^3
Water volume in S/C pool	2980m^3
Decay heat	Model ANSI/ANS5.1-1979 (Burnup at the end of equilibrium core assumed)

Table 9 Unit-3 event sequences

Note ○: Recorded △: Estimated from records □: Assumed in analysis

Conditions for analysis				Type	Remarks	○: Where records to refer to can be found △ or □: Grounds for estimation or assumption
No	Day & Time		Events to analyze			
1	3/11	14:46	Earthquake	○	—	
2		14:47	Reactor scrammed	○	4. Operation sheets, shift supervisor logbooks in the 5/16 Report	
3		15:06	RCIC manually started up	○	7. Operational procedure records in the 5/16 Report	
4		15:25	RCIC tripped (L-8)	○	7. Operational procedure records in the 5/16 Report	
5		15:38	Station blackout	○	4. Operation sheets, shift supervisor logbooks in the 5/16 Report	
6		16:03	RCIC manually started up	○	7. Operational procedure records in the 5/16 Report	
7	3/12	11:36	RCIC tripped	○	7. Operational procedure records in the 5/16 Report	
8		12:35	HPCI started up (L-2)	○	7. Operational procedure records in the 5/16 Report	
9	3/13	02:42	HPCI stopped	○	7. Operational procedure records in the 5/16 Report	
10		About 09:08	RPV depressurization operation by SRVs	○	7. Operational procedure records in the 5/16 Report	
11		09:20	PCV pressure decrease by PCV venting confirmed	○	PCV venting assumed to have started at this timing 09:20, when PCV pressure decrease was confirmed, although the vent line configuration is recorded to have been completed at 08:41 by actuating the S/C side AO valve in 7. Operational procedure records in the 5/16 Report	

12		09:25	Freshwater injection started	○	7. Operational procedure records in the 5/16 Report *1
13		11:17	AO valve closure on the PCV vent line confirmed due to pressure loss for driving air cylinder	○	7. Operational procedure records in the 5/16 Report
14		12:30	Valve actuated on the PCV vent line	○	7. Operational procedure records in the 5/16 Report
15		13:12	Freshwater injection switched to seawater injection	○	7. Operational procedure records in the 5/16 Report *1
16		14:10	Valve closure assumed on the PCV vent line	△	PCV venting, which started at 12:30 on 3/13 (No.14), assumed to have ended at this timing 14:10 from D/W pressure increase. Note: 7. Records of operational procedures in the 5/16 Report records the valve closure was confirmed at 16:00 on 3/15.
17	3/14	01:10	Water injection halted to allow filling for the water source pit	○	7. Operational procedure records in the 5/16 Report
18		03:20	Water source pit filled, reactor water injection restarted	○	7. Operational procedure records in the 5/16 Report *1
19		05:20	S/C side AO valve actuated for PCV venting	○	7. Operational procedure records in the 5/16 Report
20		12:00	S/C side valve closure assumed for PCV venting	△	PCV venting, which started at 05:20 on 3/14 (No.19), assumed to have ended at this timing 12:00 from D/W pressure increase. Note: 7. Operational procedure records in the 5/16 Report records the valve closure was confirmed at 16:00 on 3/15
21		16:00	S/C side valve actuation assumed for	△	PCV venting assumed at this timing from D/W pressure decrease

			PCV venting		
22		21:04	S/C side valve closure operation assumed for PCV venting	△	PCV venting assumed to have ended at this timing from D/W pressure increase
23	3/15	16:05	S/C side valve actuated for PCV venting	○	7. Operational procedure records in the 5/16 Report
24	3/16	01:55	S/C side valve actuation for PCV venting recorded, but assumed not to have been actuated	△	No venting assumed, because no D/W pressure changes confirmed, although 7. Records of operational procedures in the 5/16 Report says the PCV was being vented at this timing.
25	3/17	21:00	S/C side valve closure confirmed for PCV venting	△	S/C side valve assumed not to have been closed, because of the D/W pressure changes, although 7. Operational procedure records in the 5/16 Report says the valve had been closed to end the PCV venting at 16:05 on 3/15 (No.23).
26		21:30	S/C side valve actuated for PCV venting	△	The valve assumed not to have been opened because of the D/W pressure changes, although 7. Records of operational procedures in the 5/16 Report says the valve had been actuated.
27	3/18	05:30	S/C side valve closure confirmed for PCV venting	—	Outside the time span of the current analysis, although 7. Operational procedure records in the 5/16 Report t mentions the PCV venting.
28		About 05:30	S/C side valve actuated for PCV venting	—	Outside the time span of the current analysis, although 7. Operational procedure records in the 5/16 Report mentions the PCV venting.
29	3/19	11:30	S/C side valve closure confirmed for PCV venting	—	Outside the time span of the current analysis, although 7. Operational procedure records in the 5/16 Report mentions the PCV venting.
30	3/20	About 11:25	S/C side valve actuated for PCV venting	—	Outside the time span of the current analysis, although 7. Operational procedure records in the 5/16 Report mentions the PCV venting.

*1 Timings of changing the water injection flow rates and their amounts were set so as not to exceed the daily average flow rates and the total injection amount, based on the day-to-day records of injection amount to the reactor (Item 7. Compilation of operational procedures in the May 16 Report).

4.2. Results of MAAP analysis

4.2.1. Results of Case 1 analysis

Table 10 summarizes the analysis results for Case 1.

Table 10 Summary of Unit-3 analysis results Case 1

Item	Results
Timing of core starting to be uncovered	About 40 hours after the earthquake
Timing of core starting to be damaged	About 42 hours after the earthquake
Timing of RPV being damaged	No RVP damage occurred in this analysis

Details of the Case 1 analysis results follow.

The reactor water levels gradually decreased after the high-pressure coolant injection (HPCI) had stopped, the core started to be uncovered, the core became totally uncovered by the SRV actuation, and the core started to be damaged (Figure 15). Water injection started, but the amount of water injected had been adjusted to simulate the reactor water levels measured; this amount was insufficient and was at the level to cover only about half of the core. Consequently, the core became damaged.

The RPV pressures remained high at around the SRV actuation pressure until the RCIC and the HPCI stopped. Upon SRV actuation after HPCI shutdown, the RPV pressures dropped quickly and then decreased to the atmospheric pressure (Figure 16).

Concerning the PCV pressures, the D/W pressures and S/C pressures continued to increase, because the steam produced in the reactor was discharged to the S/C. They increased sharply for a while upon SRV actuation, but they decreased upon the S/C venting. The PCV pressures repeated ups and downs, thereafter, responding to the venting operations (Figure 17).

The Unit-3 core was concluded to have remained in the core region, although part of the molten fuel remained as a pool, and the RPV was concluded not to have been damaged (Figure 18). This was considered to have been feasible because, water injection via the RCIC and HPCI could have been implemented fairly continuously, and the time delay from the HPCI shutdown to water injection initiation could have been shorter than at Unit-1.

It should be noted that the RPV pressures showed a decreasing trend while the HPCI was in service. In the analysis reported in May 2011, steam leaks to outside the D/W had been assumed via HPCI piping to simulate the RPV pressure changes and D/W pressure changes. Investigations thereafter, however, showed that leak paths on the HPCI line were thought to be very unlikely to have formed on the following grounds: if steam had leaked from the HPCI piping, the R/B would have been at too high temperatures or in too high temperature steam atmospheres including the HPCI cell for anybody to access, but actually some operational staff did access the HPCI cell after the HPCI had stopped on March 13; the HPCI steam piping was found not to have been damaged by the earthquake from the results of a seismic evaluation. The RPV pressure changes can be considered to be due to continued steam consumption by the HPCI continued operation.

4.2.2. Results of Case 2 analysis

Table 11 summarizes the analysis results of Case 2.

Table 11 Summary of Unit-3 analysis results Case 2

Item	Results
Timing of core starting to be uncovered	About 40 hours after the earthquake
Timing of core starting to be damaged	About 42 hours after the earthquake
Timing of RPV being damaged	About 66 hours after the earthquake

Details of the Case 2 analysis results follow.

The reactor water level gradually decreased after the HPCI had stopped, the core started to be uncovered, the core became totally uncovered by the SRV actuation, and the core started to be damaged (Figure 19). Water injection was started, but as an insufficient amount of injected water had been assumed, the reactor water level did not reach above the bottom of active fuel, and this caused the core damage to be more advanced than in Case 1.

The RPV pressures showed a temporary increase after depressurization by the SRV actuation. This was due to the steam produced when part of the molten fuel was relocated to the lower plenum. But the overall behavior (Figure 20) other than this point was similar to the behavior in Case 1.

The PCV pressures showed a temporary increase, as in the case of RPV pressures, due to the steam produced when part of the molten fuel was relocated to the lower plenum. But the overall behavior (Figure 21) other than this point was similar to the behavior in Case 1.

Part of the molten fuel remained in the RPV, but the RPV was damaged. The amount of water injected at the beginning had been set at a lower value than that in Case 1 and this caused the core damage to be more advanced (Figure 22).

4.3. Estimation of Unit-3 core conditions

The core conditions were estimated as follows, by comprehensively considering the information available including the core conditions having been estimated from the temperature behavior actually measured.

The analysis of Case 1 gave the results that the fuel in the Unit-3 core had been molten but remained in the core region, although part of the molten fuel had remained as a pool, and that the RPV had not been damaged. The analysis of Case 2 gave the results that part of the molten fuel had remained in the RPV, but the RPV had been damaged.

On the other hand, observed plant parameters seemed to have indicated that most of the fuel was being cooled in the RPV based on the following grounds: the RPV steel temperatures were changing at around 100 to 120 deg C and at more than one measurement point the temperatures responded in a consistent manner to the changing amount of water injected; the heat source could be considered to be in the RPV, because temperatures at several points showed an increase in May 2011; and the RPV bottom temperatures changed at around 100 to 170 deg C, the same levels as the temperatures at other locations around the RPV (Figure 23).

Consequently, based on the analysis results and plant parameters, the core was considered to have been significantly damaged and relocated to a location lower than its original position (lower plenum), and was being cooled there in a stable manner.

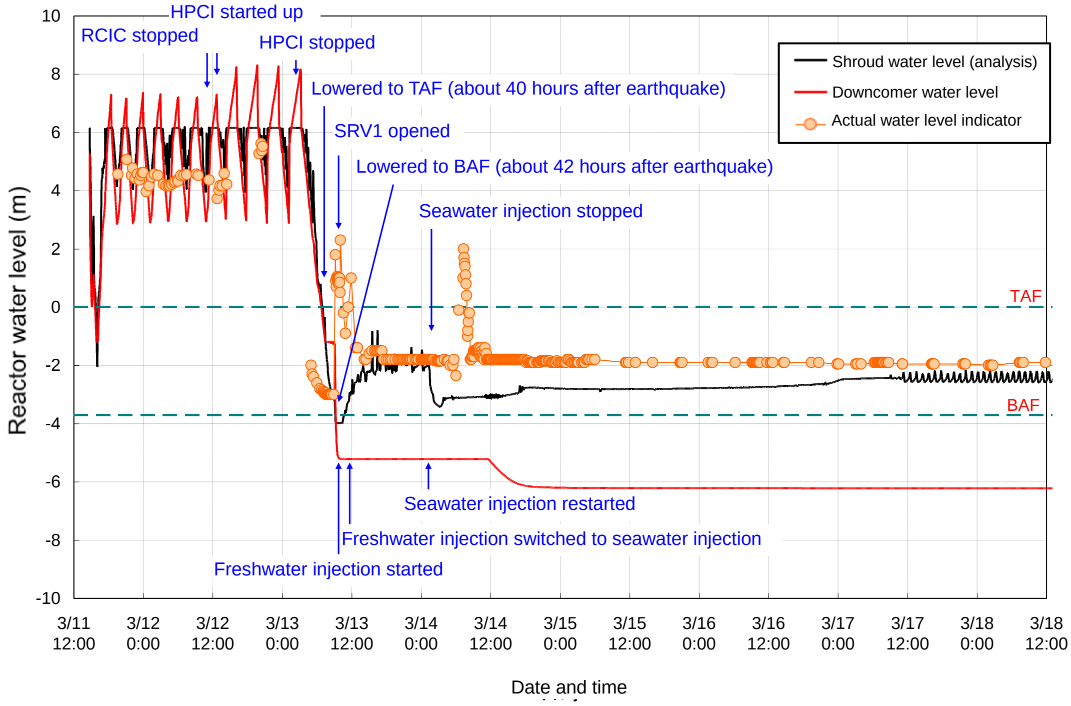

Figure 15　Unit-3 reactor water level changes Case 1

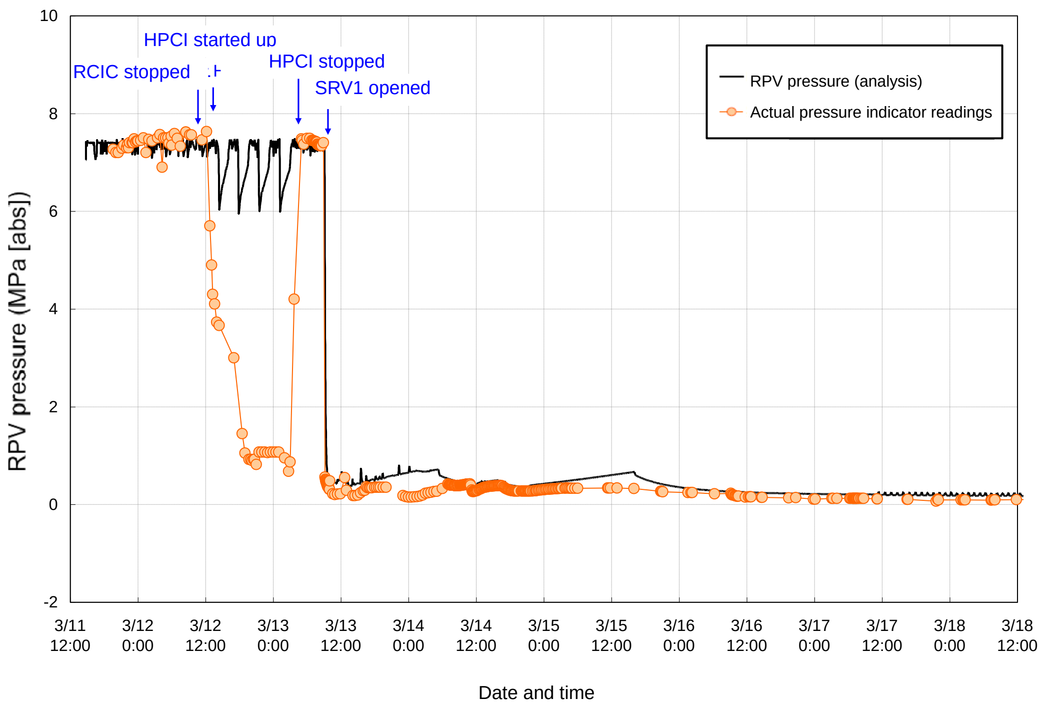

Figure 16　Unit-3 RPV pressure changes Case 1

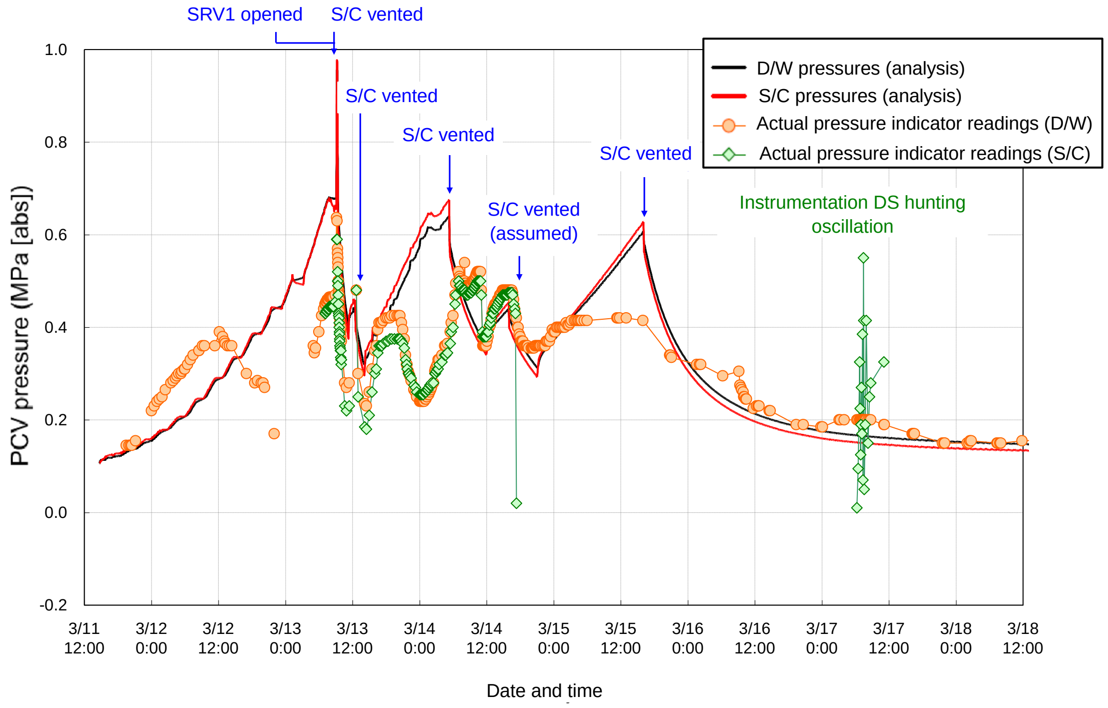

Figure 17　Unit-3 PCV pressure changes Case 1

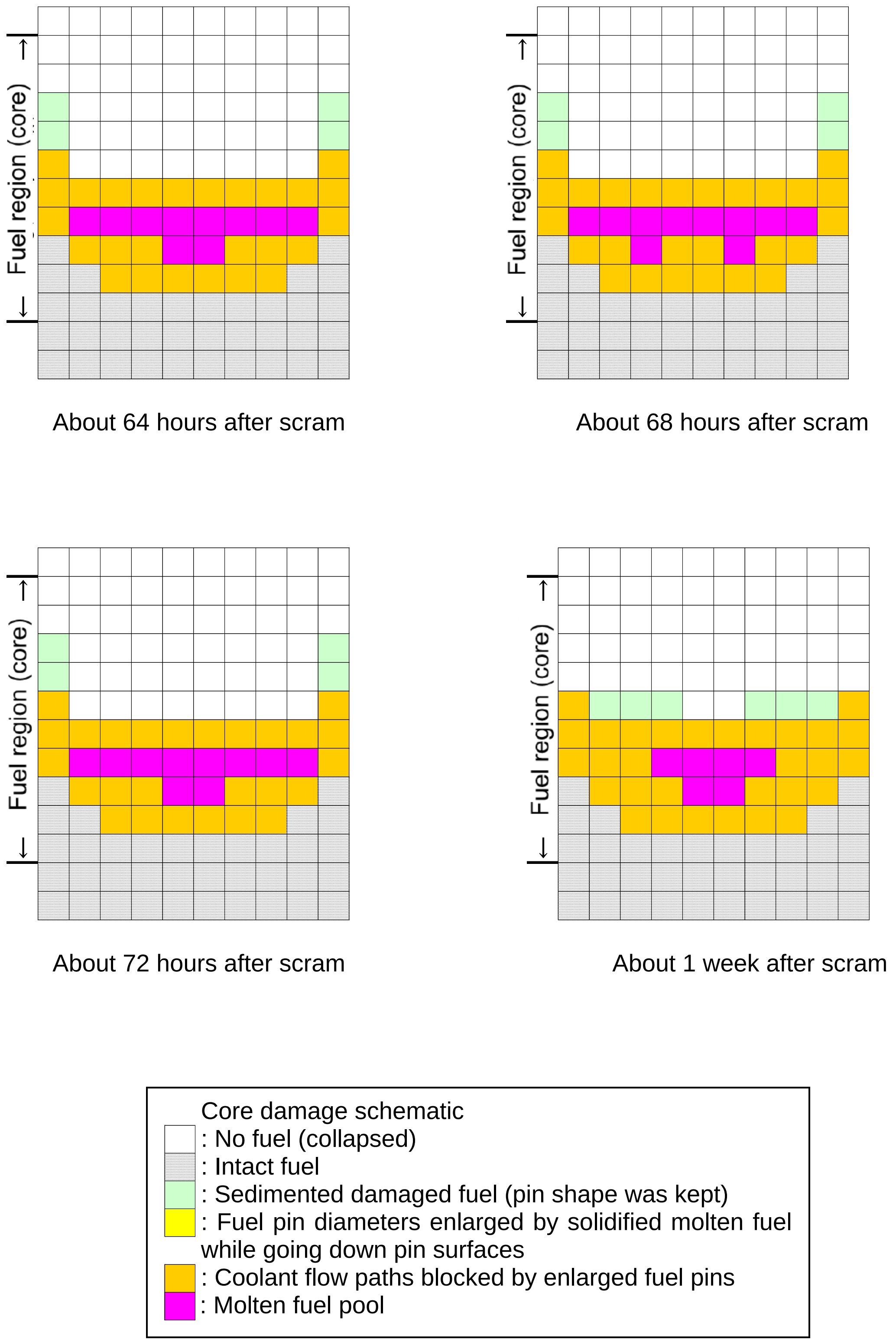

Figure 18 Unit-3 core conditions Case 1

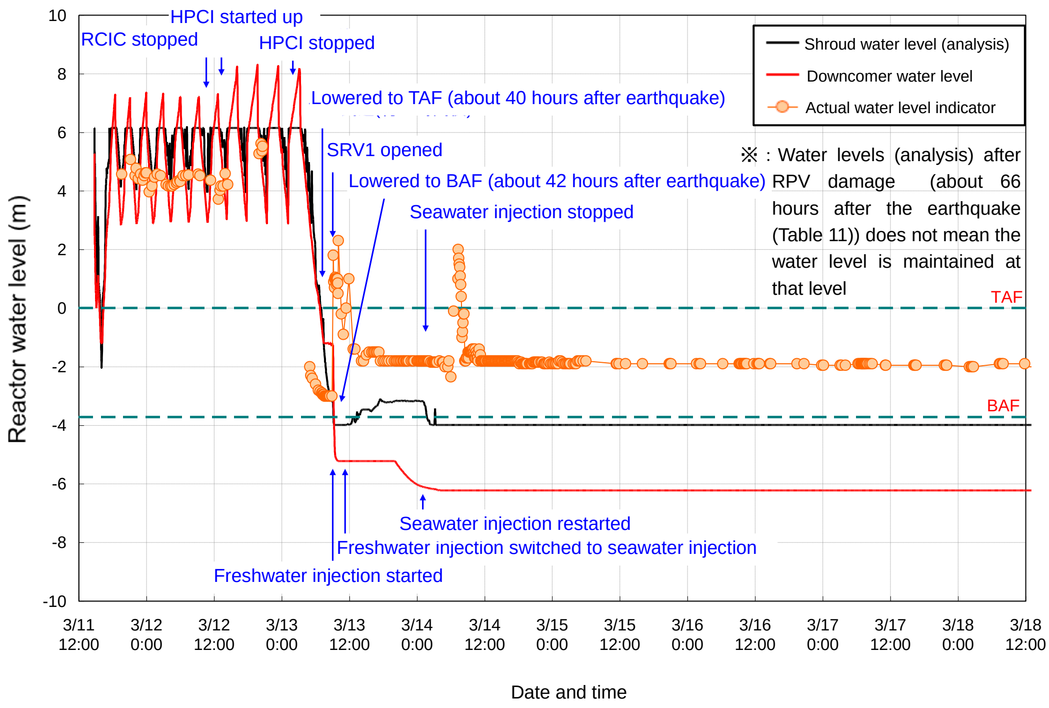

Figure 19　Unit-3 reactor water level changes Case 2

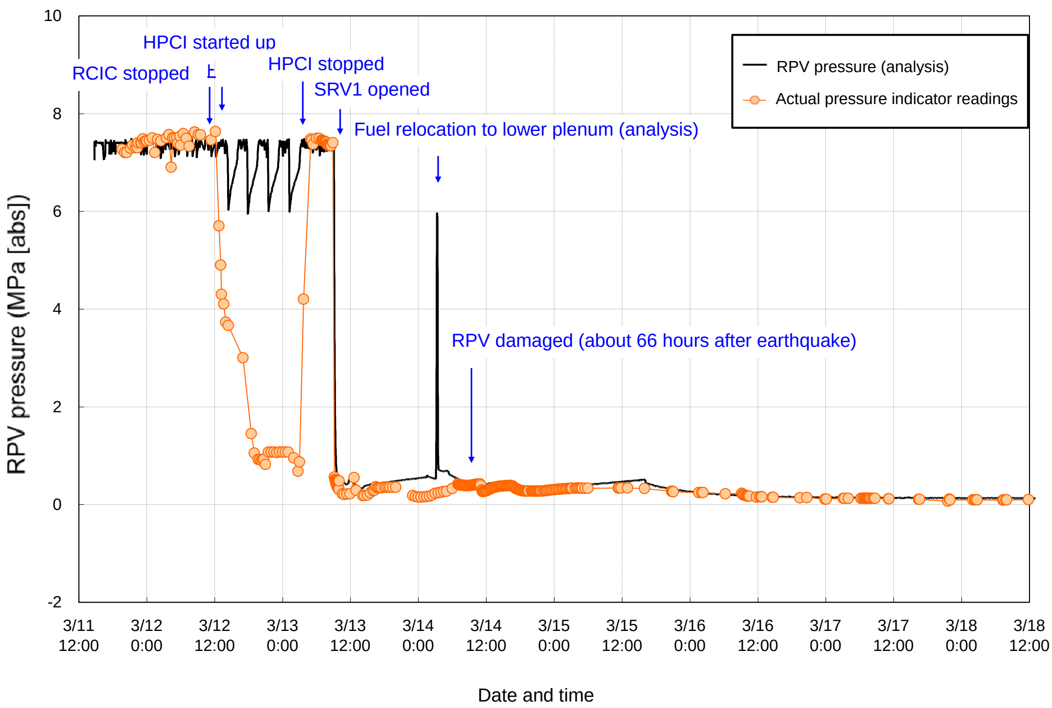

Figure 20　Unit-3 RPV pressure changes Case 2

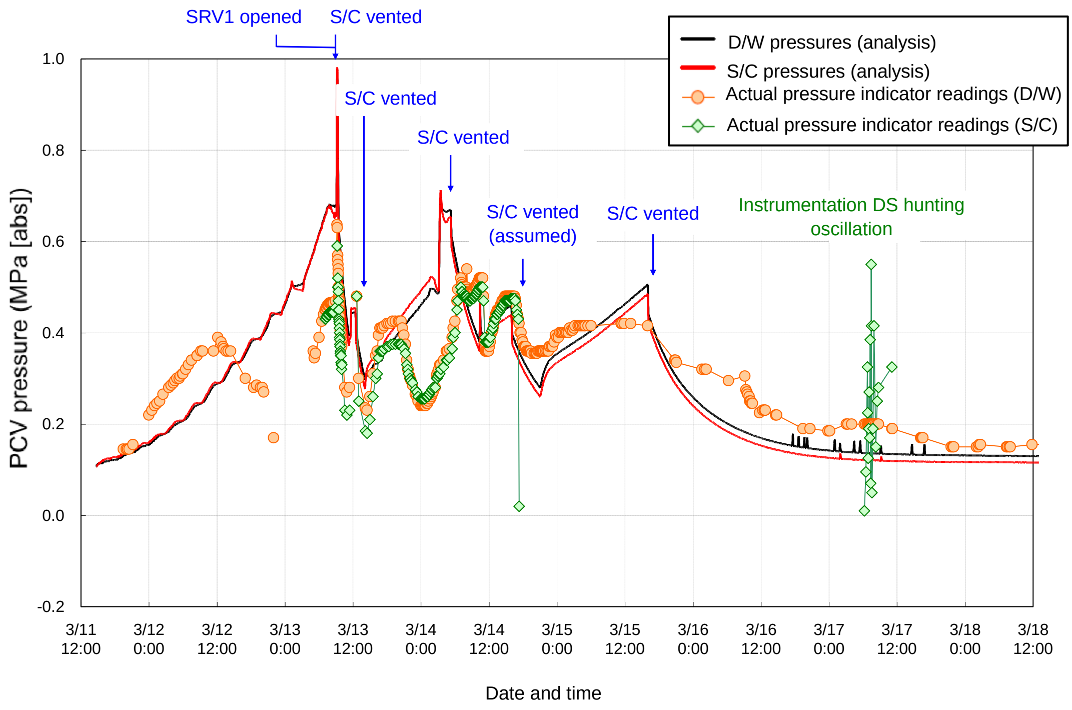

Figure 21 Unit-3 PCV pressure changes Case 2

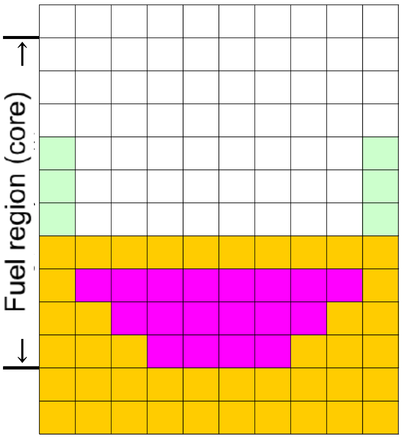

About 58 hours after scram

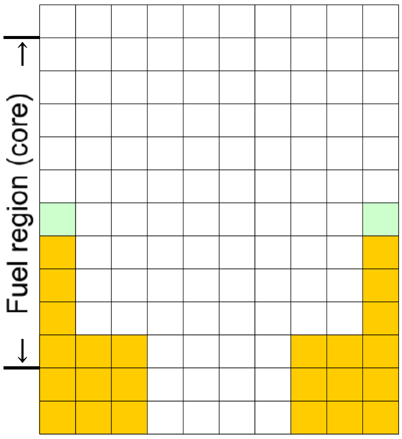

About 62 hours after scram

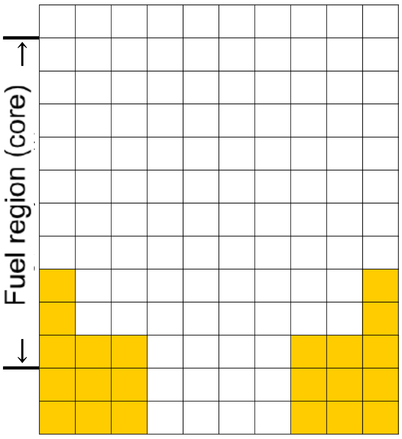

About 66 hours after scram

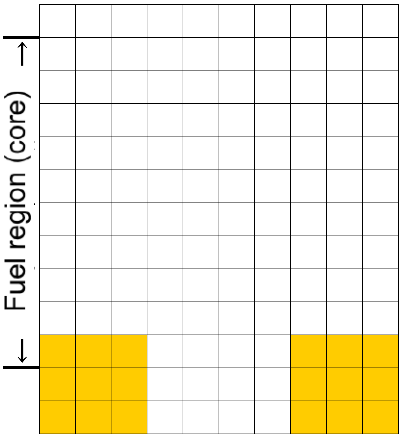

About 96 hours after scram

Core damage schematic
: No fuel (collapsed)
: Intact fuel
: Sedimented damaged fuel (pin shape being kept)
: Fuel pin diameters enlarged by solidified molten fuel while going down pin surfaces
: Coolant flow paths blocked by enlarged fuel pins
: Molten fuel pool

Figure 22 Unit-3 core conditions Case 2

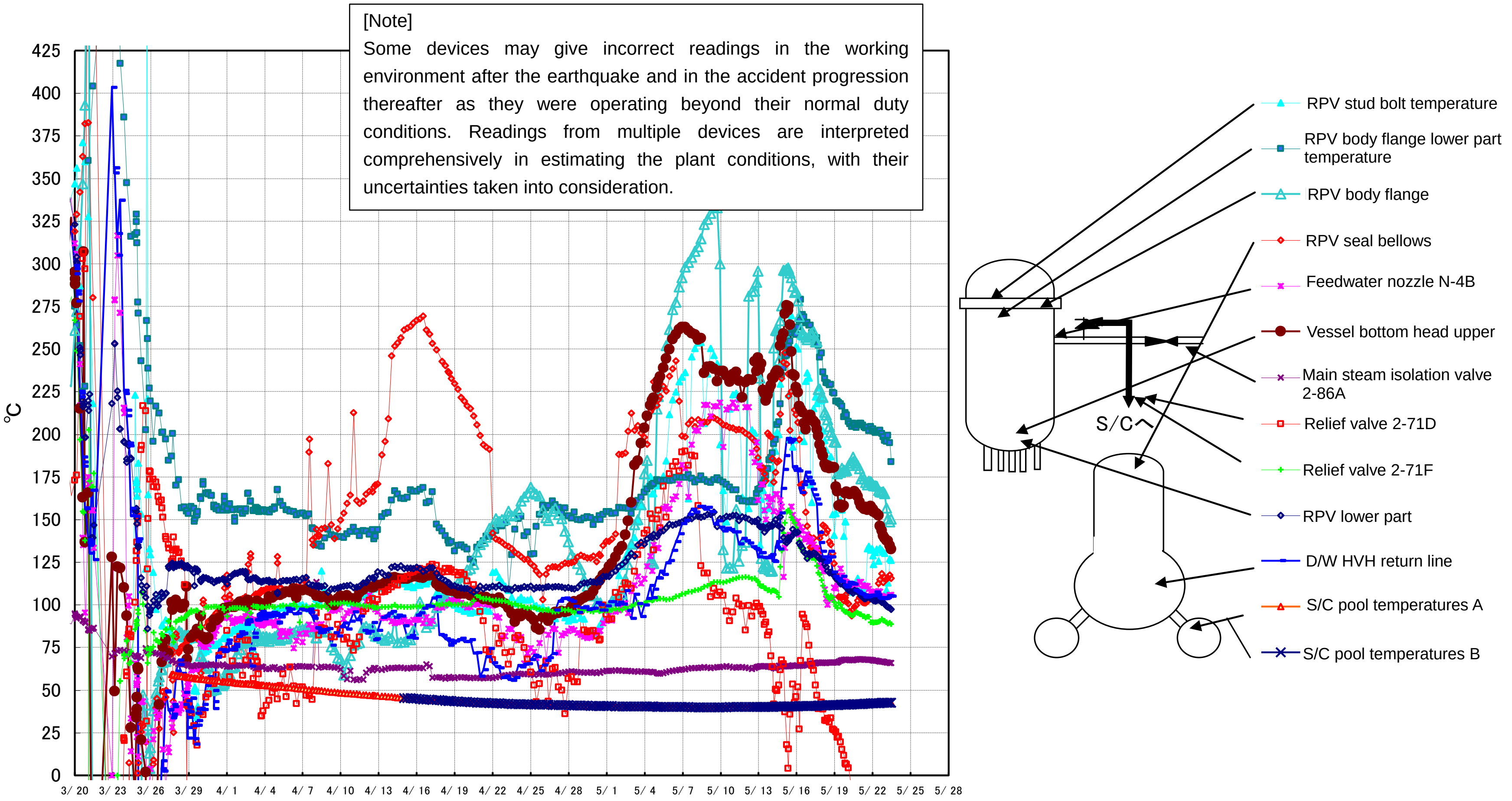

Figure 23 Unit-3 temperature changes at typical points (May 2011 when disclosed)

Core conditions estimated from heat balance while water injection was interrupted

The extent of core damage was estimated by comparing the decay heat during the period of no water injection after the accident, and the amount of coolant which had existed in the RPV at the beginning, or sensible and latent heat of fuel and in-core structural materials. Table 1 to Table 3 give event sequences and the time periods when water injection was halted at each unit. Figure 1 shows the decay heat during the time when water injection was halted, while Figure 2 compares the heat production and heat removal. Table 4 specifies weights of fuel, structural materials and other items used in the calculation. Decay heats used at each unit are given in Figure 3 to Figure 5.

At Unit-1, the decay heat released before the seawater injection was started at full capacity far exceeded the amount which could be absorbed by the water and other materials that had existed in the RPV. Consequently, the molten fuel that was at elevated temperatures was relocated to the RPV bottom, where it damaged the RPV and most of the molten fuel would have been relocated to the PCV.

At Unit-2 and Unit-3, the decay heat released while water injection was halted was at the same level as the amount which could be absorbed by the water and other materials that had existed in the RPV. Therefore, a certain amount of fuel might have been relocated to the RPV bottom after being molten, but the RPV would not have been so significantly damaged as to allow a big amount of fuel to be relocated to the PCV.

Table 1　Operation timeline of water injection to Unit-1 reactor

Day and time	Operation records
14:46 on March 11, 2011	Earthquake occurred
	Reactor scrammed
14;47	MSIV closed
14:52	IC(A) (B) started up automatically
15:03	IC(A) stopped
	IC(B) stopped
15:17	IC(A) restarted
15:19	IC(A) stopped
15:24	IC(A) restarted
15:26	IC(A) stopped
15:32	IC(A) restarted
15:34	IC(A) stopped
15:37	Station blackout
05:46 on March 12, 2011	Freshwater injection started by fire engines
14:55	Freshwater injection terminated
19:04	Seawater injection started

Time of event	Being cooled or water being injected
Time of event	No or little water injection

Table 2 Operation timeline of water injection to Unit-2 reactor

Day and time	Operation records
14:46 on March 11, 2011	Earthquake occurred
14:47	Reactor scrammed
15:02	Reactor Isolation Cooling System (RCIC) manually started up
15:28	RCIC tripped (L-4)
15:41	Station blackout
13:25 on March 14, 2011	RCIC stopped
16:34	RPV depressurization started (ARV1 valve opening)
	Seawater injection started via Fire Protection System
About 18:00	RPV pressure decrease confirmed
19:20	Fire engines stopped due to fuel shortage
19:54	First fire engine started pumping again
19:57	Second fire engine started pumping again
21:20	RPV depressurized by SRV2 opening, water level recovered

Time of event	Being cooled or water being injected
Time of event	No or little water injection

Table 3 Operation timeline of water injection to Unit-3 reactor

Day and time	Operation records
14:46 on March 11, 2011	Earthquake occurred
14:47	Reactor scrammed
15:06	RCIC manually started up
15:25	RCIC tripped (L-8)
15:38	Station blackout
16:03	RCIC manually started up
11:36 on March 12, 2011	RCIC tripped
12:35	HPCI started up (L-2)
02:42 on March 13, 2011	HPCI stopped
About 09:08	RPV depressurization operation by SRVs
09:20	PCV pressure decrease due to PCV venting confirmed
09:25	Freshwater injection started

Time of event	Being cooled or water being injected
Time of event	No or little water injection

Table 4 Weights used in the calculation (structures, fuel, water inventory)

	Unit-1		Unit-2, Unit-3	
CR guide tube	12.3	t	17.4	t
CRD housing (in the core)	4.6	t	6.5	t
In-core probe guide tube	0.8	t	1.1	t
In-core probe housing	0.2	t	0.3	t
In-core probe stabilizer (in the core)	0.1	t	0.1	t
Total core internals (Sum of the above) *	18	t	25	t
UO_2	79	t	107	t
Zircaloy	32	t	43	t
(Water inventory)				
Water below bottom of fuel	52.4	t	72.6	t
Water between fuel bottom and normal level)	93	t	145	t
Injected water	80	t	0	t

* Rounded off to the first number after the decimal point

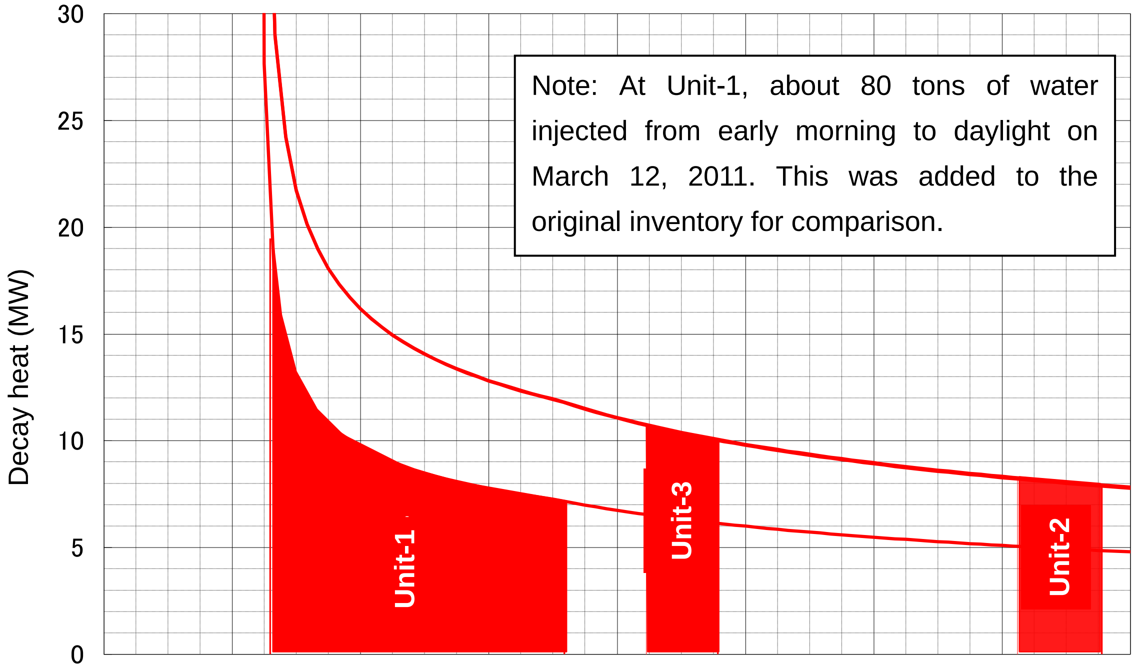

Figure 1 Decay heat changes and timings of no water injection at each unit

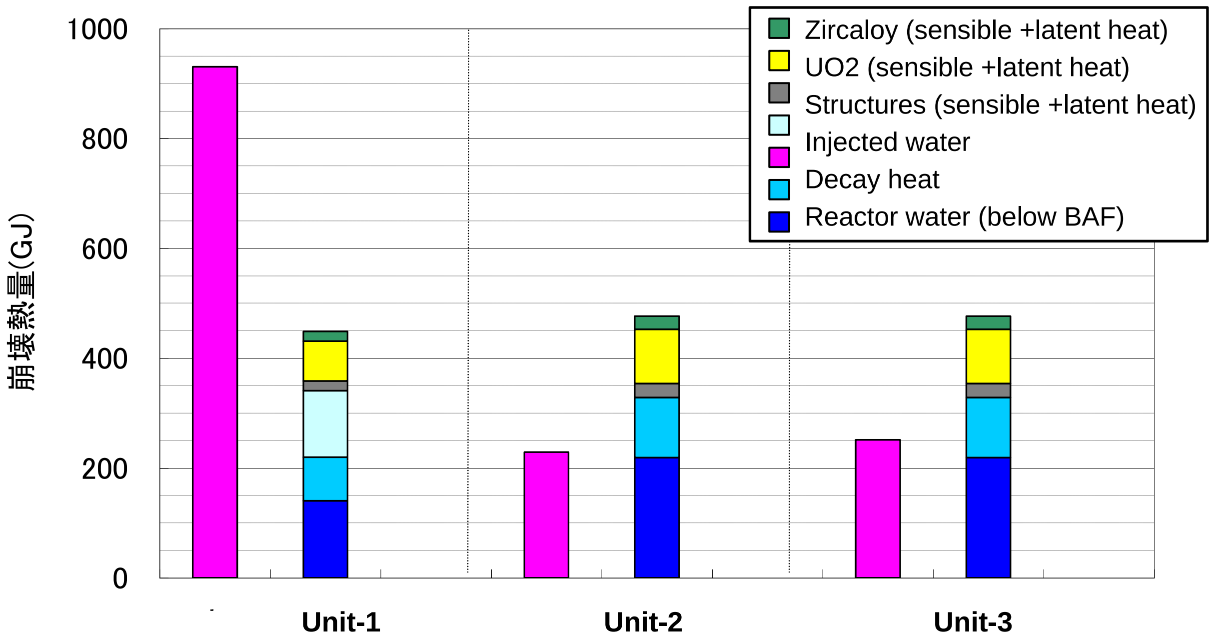

Figure 2 Comparison of decay heat and heat removal capacities

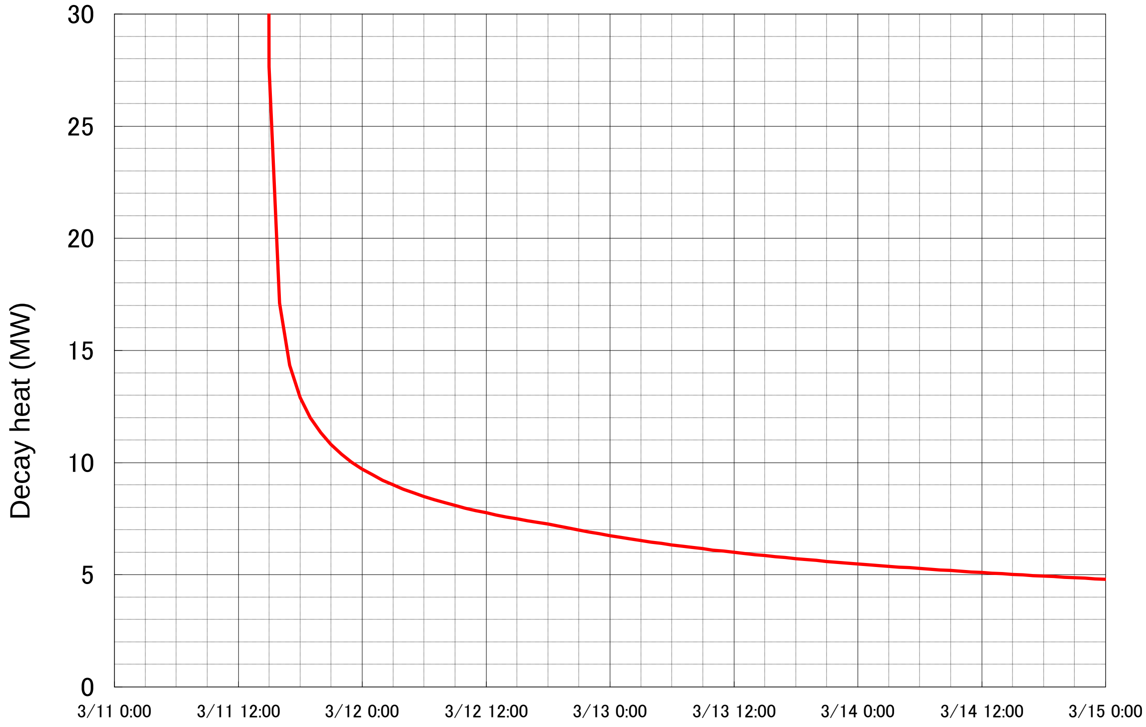

Figure 3 Unit-1 decay heat

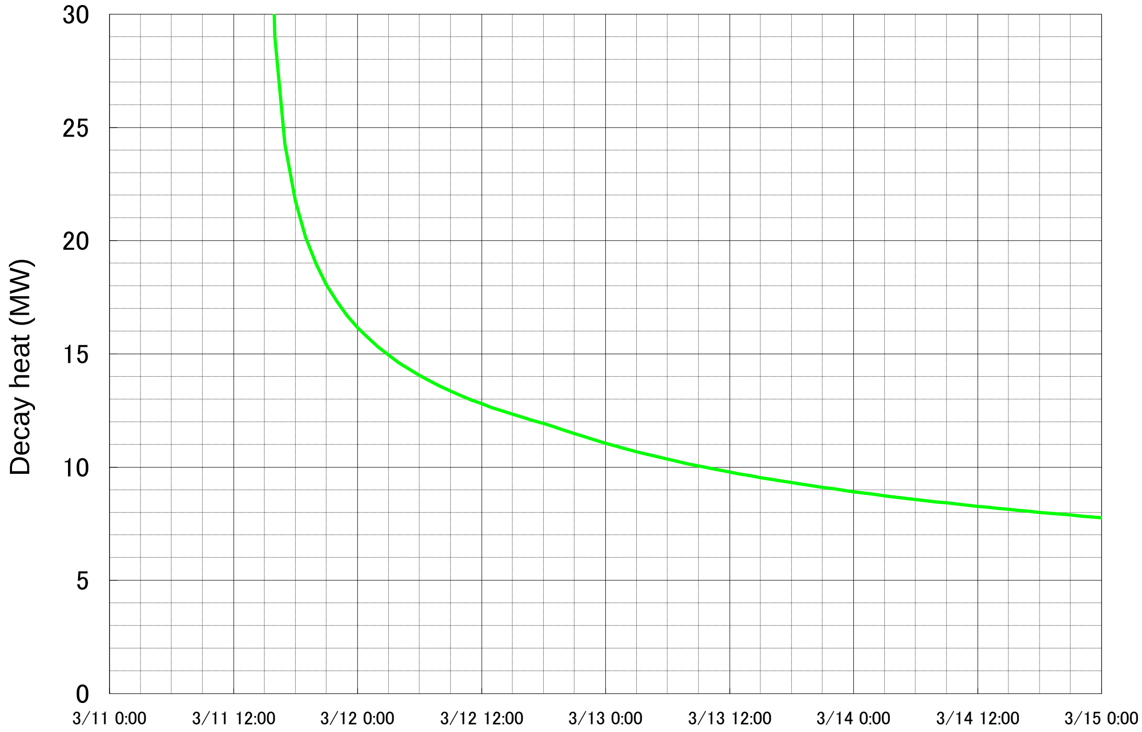

Figure 4 Unit-2 decay heat

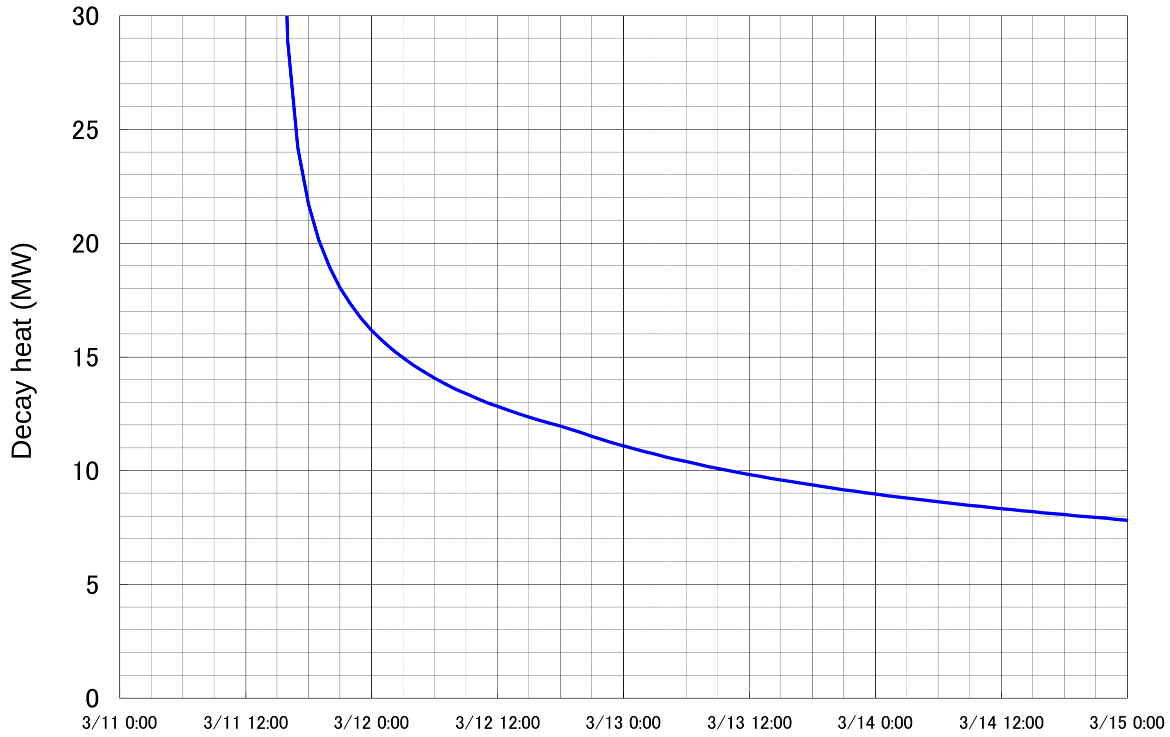

Figure 5 Unit-3 decay heat

This document includes some undisclosed data, not contained in the "Plant_data" of the TEPCO homepage.

Attachment-3

Core conditions estimated from the temperatures and pressures measured

1. Outline of reactor cooling conditions and temperature and pressure behaviors

At each unit, water injection started after the accident using the accident management (AM) lines and other paths, the drywell (D/W) pressure measurements started immediately after the accident, and the temperature measurements started from the second half of March 2011. Cooling conditions, and temperature and pressure behaviors at each unit are summarized below.

(1) Unit-1

At Unit-1, water injection started on the day after the earthquake (March 12, 2011) via the fire protection systems, followed by the injection via the feedwater system (FWS), which had been placed in service from March 23, 2011. Nitrogen injection to the D/W started on April 7, 2011.

In May 2011, the amount of water injection was temporarily increased to test for the possibility of flooding the containment vessel (PCV) with water. Thermometer readings responded roughly consistently to the changing amount of water being injected. The D/W pressure indicator readings responded clearly to the amount of water injected, i.e., the tendency of pressure decrease with increased water injection and pressure increase with reduced water injection was clearly recognized.

Thereafter, the amount of water injection was reduced, in response to the decreasing decay heat. This was necessary to cope with the concern that the amount of contaminated water retained on the site was increasing, and the amount of water injection was being optimized (3.5 to 4.0m^3/h was being maintained).

Since August 2011, water injection of 3.5 to 4.0m^3/h has been continued, and the overall temperatures, including those of the reactor vessel (RPV) and PCV cut below 100 deg C and have continued to decrease gradually.

In late October 2011, the water injection rate via the FWS was increased to 7.5m^3/h to ensure control of steam generation. The RPV and PCV temperatures decreased further accordingly.

The water injection rare was temporarily decreased to 5.5m^3/h in preparation for placing the core spray (CS) system in service. The RPV and PCV temperatures are currently (as of November 21, 2011) changing around 40 deg C.

Figure 1 shows the temperature trends at typical points of the RPV and PCV, while Figure 2 shows the D/W pressure trends.

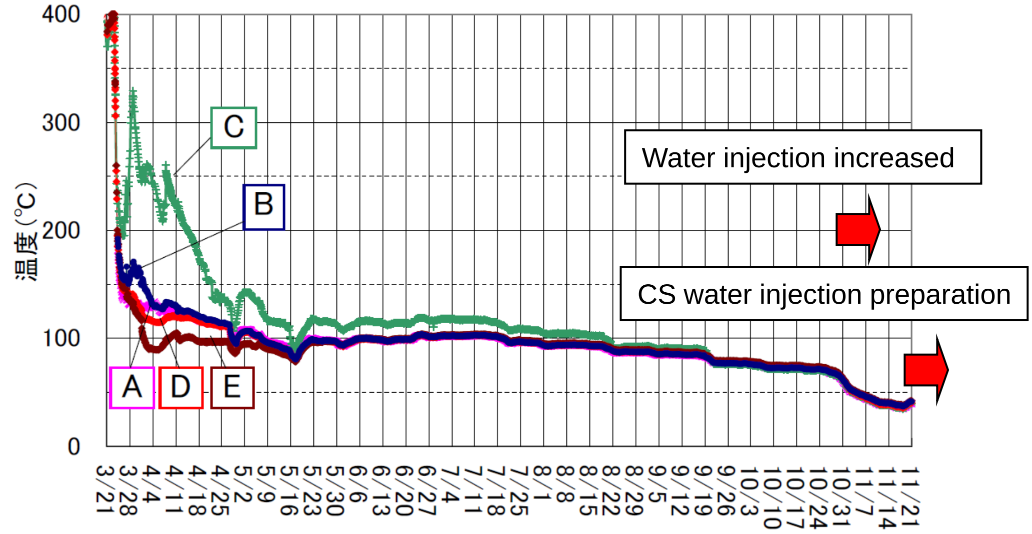

Figure 1　Unit-1 RPV and PCV temperature trends

(A: RPV flange, B: Seal bellows, C: Feedwater nozzle, D: RPV lower part, E: D/W-HVH)

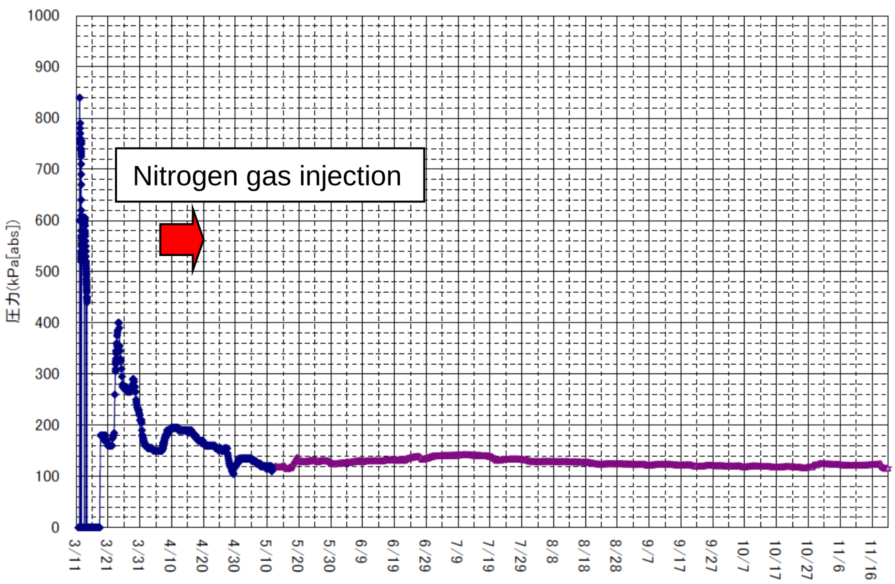

Figure 2　Unit-1 D/W pressure trends

(2)　Unit-2

At Unit-2, water injection started via the fire protection system 2 days after the earthquake. In late May 2011, the FWS was placed in service for water injection. The water injection continued by the FWS after switching from the fire protection system. After the FWS was placed in service for water injection, temperatures of the RPV bottom (upper face of the RPV bottom head) were changing around the saturation temperature, but at the RPV upper and middle parts temperature behavior indicated superheated conditions.

Thereafter, the amount of water injection was reduced, in response to the decreasing decay heat. This was necessary to cope with the concern that the amount of contaminated water retained on the site was increasing, and the amount of water injection was being optimized (3.5 to 4.0m^3/h was being maintained). On June 28, 2011, nitrogen gas injection started.

From the middle of September 2011, the CS system started water injection in parallel with the FWS, and this was intended to improve water injection efficiency. The water injection path from the CS system goes directly through the core region. The D/W pressures increased temporarily due to the water injection from the CS system. This is considered as being caused by the water injected from the CS system contacting the superheated structures in the RPV and mostly generating steam within a limited time. Thereafter, the D/W pressures began to decrease with the increasing amount of water being injected. In addition, the degree of superheating at the RPV upper part began to decrease as soon as the CS system had been placed in service for water injection.

In late September 2011, the amount of CS system water injection was increased in response to the improved service conditions of the contaminated water processing system. Since early October 2011, almost all RPV and PCV thermometers have been indicating lower temperatures than the D/W saturation temperature, with the exception of some thermometers outside the RPV indicating higher temperatures locally.

It is noted that the D/W pressures began a gradual increase in late September 2011. This is estimated to be due to nitrogen injection, when the overall temperature behavior is considered.

Figure 3 shows the temperature trends after March 2011 at some typical points of the RPV and PCV, while Figure 4 shows the D/W pressure trends.

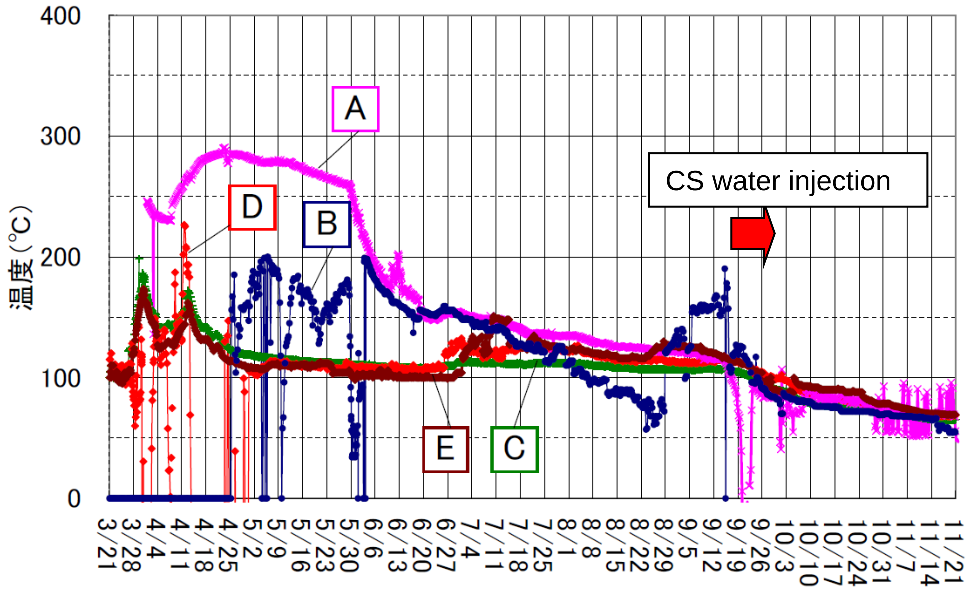

Figure 3　Unit-2 RPV and PCV temperature trends

(A: RPV flange, B: Seal bellows, C: Feedwater nozzle, D: RPV lower part, E: D/W-HVH)

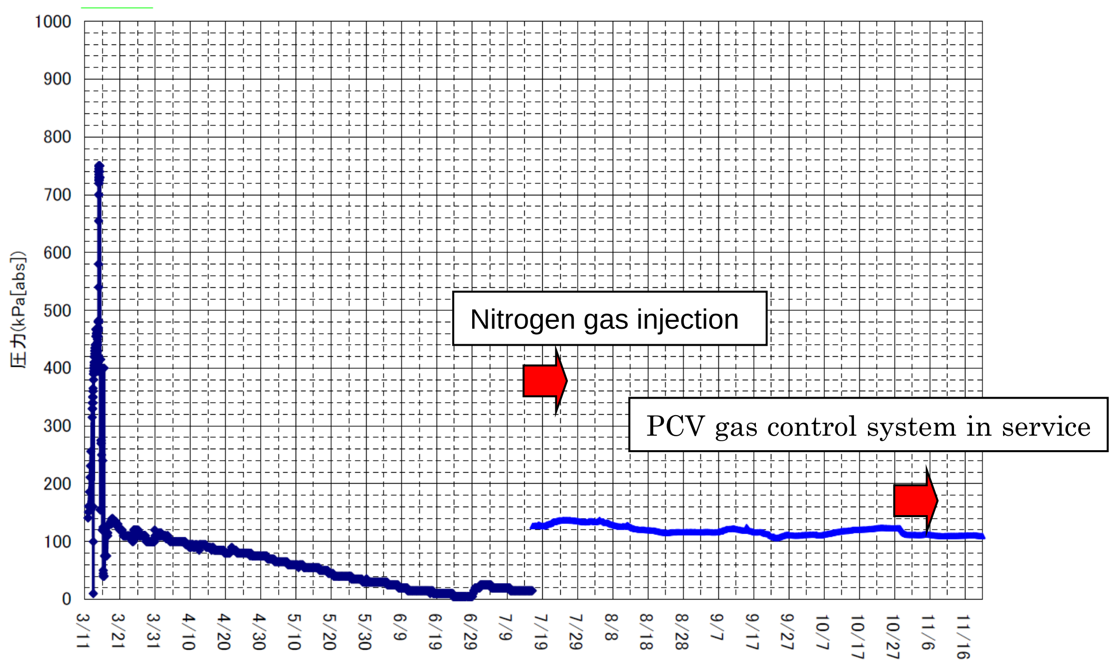

Figure 4　Unit-2 D/W pressure trends

(3)　Unit-3

At Unit-3, water injection started via the fire protection system 2 days after the earthquake. In the middle of May 2011, the FWS was placed in service for water injection. The water injection continued by the FWS after being switched from the fire protection system. After the FWS was placed in service for water injection, temperatures at various points of the RPV continued to indicate superheated conditions. The temperatures have been changing in a stable manner since June 2011 at a higher level.

Thereafter, the amount of water injection was reduced, in response to the decreasing decay heat. This was necessary to cope with the concern that the amount of contaminated water retained on the site was increasing, and the amount of water injection was being optimized (reduced from 13.5 m^3/h to 4.0 m^3/h with time). On July 14, 2011, nitrogen gas injection was started.

In early September 2011, the CS system started water injection in parallel with the FWS, and this was intended to improve water injection efficiency. The water injection path from the CS system goes directly through the core region. The degree of superheating over the whole RPV began to decrease as soon as the CS system had been placed in service for water injection.

In the middle of September 2011, the amount of CS system water injection was increased in response to the improved service conditions of the contaminated water processing system. Consequently, in late September 2011 most of the RPV thermometers including the one at the reactor bottom (bottom head) gave readings below 100 deg C. Until early October 2011, some thermometers outside the RPV indicated high temperatures locally, but now (November 2011) thermometers at all measurement points indicate readings below 100 deg C.

It is noted that the D/W pressures were changing at the level around the atmospheric pressure since March 2011, but that no change has been noticed although nitrogen gas injection started in July 2011 (the pressure indicator was switched over at the same time).

Figure 5 shows the temperature trends after March 2011 at some typical points of the RPV and PCV, while Figure 6 shows the D/W pressure trends.

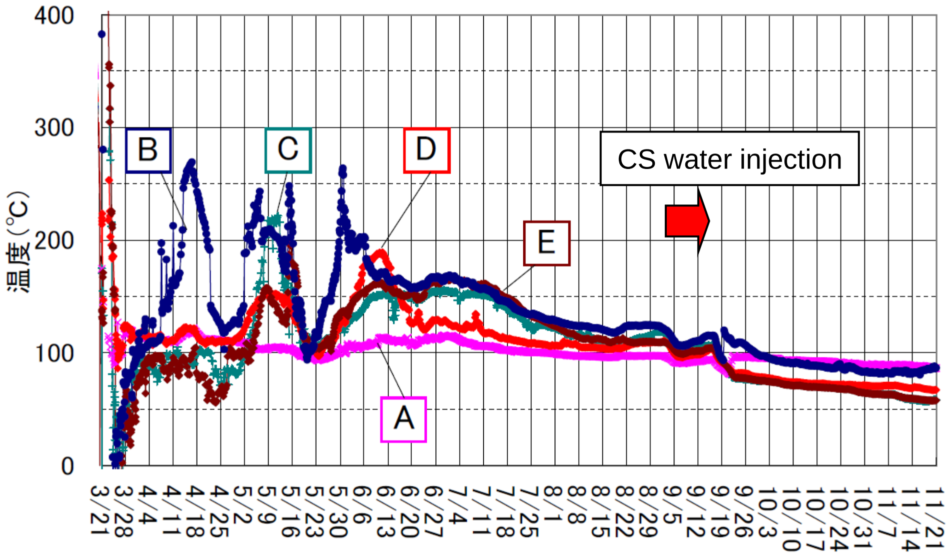

Figure 5　Unit-3 RPV and PCV temperature trends

(A: RPV flange, B: Seal bellows, C: Feedwater nozzle, D: RPV lower part, E: D/W-HVH)

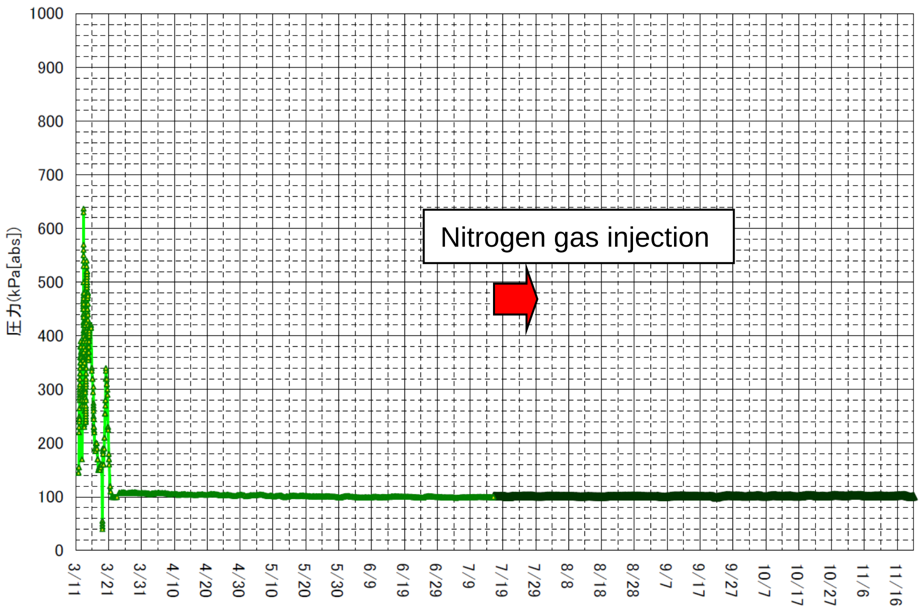

Figure 6　Unit-3 D/W pressure trends

2.　Analysis from temperature behavior

Cooling conditions discussed in the previous section and temperature and pressure behaviors have been analyzed. The results are summarized below.

(1) Unit-1

[Analysis of temperature behavior from March to May 2011]

When the capability to measure RPV temperatures was recovered in late March, the RPV temperatures were above 400 deg C at more than one point. At that time, the core is considered not to have been sufficiently cooled. But as soon as the water injection path to the reactor was changed to the FWS, the water was assured to reach the reactor and temperatures at various points decreased rapidly. The core was then considered to be being sufficiently cooled.

On the other hand, most of the fuel was considered to have been cooled in the RPV based on the following reasons: temperatures of CRD housings and other structures below the RPV were measurable, which would not be possible if the RPV had been damaged; the RPV steel temperatures were changing at the level around 100 to 120 deg and the temperatures at several points responded consistently to the changes of the amount of injected water; and the temperatures at the RPV upper part were higher at several points indicating the presence of the heat source in the RPV (Figure 7).

In conclusion, the core was considered, from plant parameters (temperatures around the RPV), to have been relocated from its original position to below (lower plenum) and mostly being cooled there in a stable manner, even if the core had been largely damaged.

It should be noted, however, that the temperature changes over an extended time till now (November 2011) indicated the rapid decrease of high temperatures observed at the RPV upper part in March and April 2011 being similar to the attenuation behavior of short half-life nuclides such as iodine-131 and others. This may mean that the high temperatures at the RPV upper part might have been caused by volatile radioactive materials that had deposited.

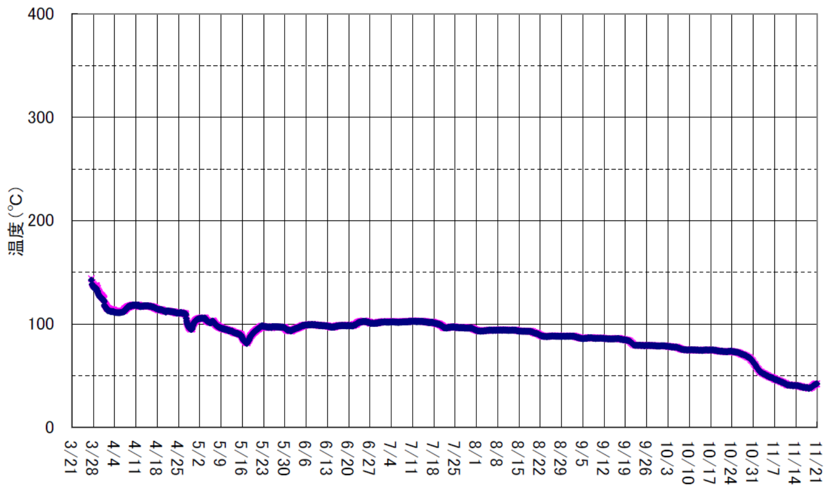

Figure 7　CRD housing temperature trends

[Analysis of temperature behavior from May to October 2011]

Temperatures of CRD housings and other structures below the RPV could be measured after May 2011, too. Measured temperatures at several points responded to the changes in the amount of injected water, as had been existing until May 2011. The following findings were newly obtained.

- The temperature difference between the RPV upper part and bottom decreased.
- The RPV bottom temperatures decreased to below the saturation temperature and have continued to decrease as of August 2011.

The fuel was considered not to be present in the core region, because the reduced temperature difference at the RPV upper and lower parts indicated that there is little uncovered fuel in the RPV, and also by considering the injected water path, which is not going through the core region, and the calibrated water level indicator readings. It should be noted in addition that the amount of water being injected was not sufficient to remove sensible heat, nevertheless the RPV bottom temperatures cut below the saturation temperature. Most of the fuel was considered not to be present in the RPV.

[Analysis of temperature behavior after October 2011]

The following findings were newly obtained by increasing the amount of water injection in late October.

- RPV and PCV temperatures rapidly decreased by cooling. Meanwhile, the suppression chamber (S/C) pool temperatures increased after the amount of injected water increased and the temperatures of the RPV and PCV and S/C pool were reversed (Figure 8).

If water flowed into the S/C from the RPV after heat exchange only in the RPV, the S/C temperatures should not exceed the RPV bottom temperatures, but actually the S/C temperatures exceeded the RPV bottom temperatures. This may indicate the possibility that a heat source existed in the PCV lower part (probably around the pedestal) and that the water flowed into the S/C through the vent tube after having contacted the heat source in the PCV. The S/C pool temperature increase is considered to have been caused by more hot water inflows to the S/C, when the water injection amount had been increased, carrying more energy equivalent to the decreased energy necessary for steam generation in the PCV.

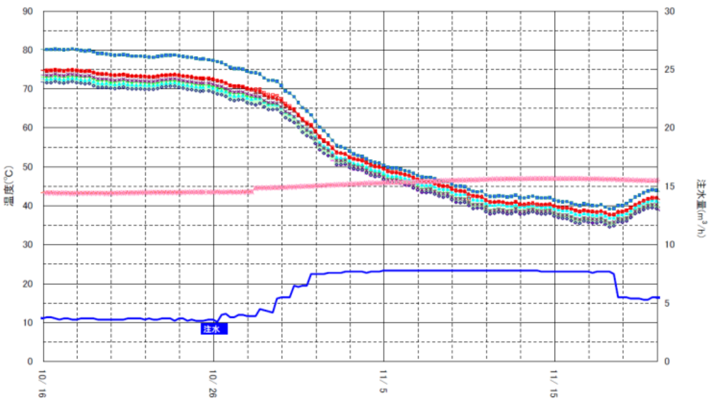

Figure 8 Relationships between RPV and PCV temperatures and S/C pool temperatures

(2) Unit-2

[Analysis of temperature behavior from March to May 2011]

Most of the fuel was considered to be being cooled in the RPV based on the following reasons: the RPV bottom temperatures were changing in the range of about 100 to 120 deg C and responded consistently at multiple points to the changing amount of injected water; and the temperatures at the RPV upper part were higher indicating the presence of a heat source in the RPV.

Consequently, the core was considered, from plant parameters, to have been relocated from its original position to below (lower plenum) and mostly being cooled there in a stable manner, even if the core had been largely damaged.

[Analysis of temperature behavior from May to September 2011]

The following findings were newly obtained from the RPV and PCV temperature behavior since May 2011.

- The RPV bottom temperatures indicated roughly readings around the saturation temperature since the water injection via the FWS started in May 2011, but the RPV upper and middle parts remained at higher temperatures.

From this observation, part of the uncovered fuel was considered to be present at the core region, overheating the RPV inside, although the cooling effect by the water from the FWS was confirmed.

[Analysis of temperature behavior from September 2011]

The following findings were newly obtained from the RPV and PCV temperature behavior since September 2011.

- Temperatures at the RPV upper part decreased due to the water directly passing through the core region from the CS system, and further decreased to below saturation temperature when the amount of water injection had been increased.

- Temperatures of the PCV atmosphere remain mostly below the saturation temperature, but very locally (CRD housings, SRVs and others) some thermometers still indicate high temperatures (above the saturation temperature).

From these observations, the following interpretations may be possible.

- Part of the fuel is present in the RPV core region, but most of the fuel is under water in the RPV lower part.
- Heat sources are present outside the RPV, too, but they are being cooled sufficiently. However, some fuel may be uncovered (around CRD housings) and some parts may be generating mild heat from the deposited volatile fission products and other species (around the SRVs) (Figure 9 and Figure 10).

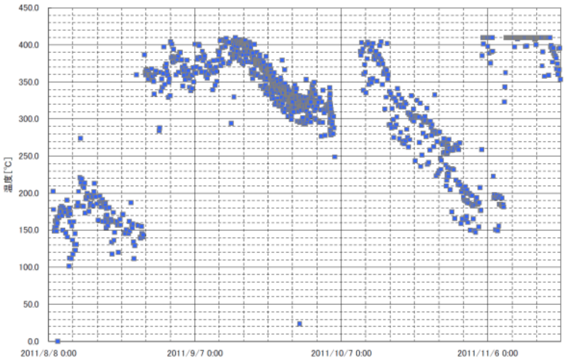

Figure 9　CRD housing temperature trends

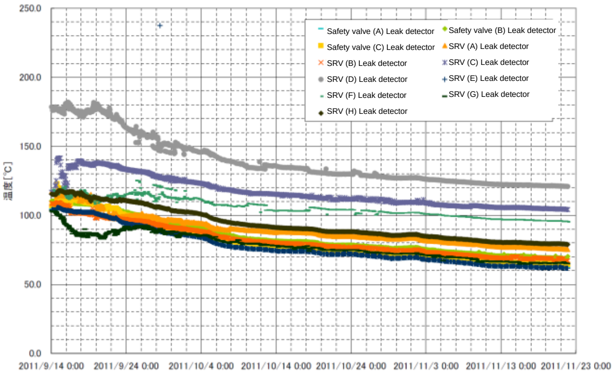

Figure 10　Safety valve and SRV leak detector temperature trends

(3) Unit-3

[Analysis of temperature behavior from March to May 2011]

Most of the fuel was considered to be being cooled in the RPV based on the following reasons: the RPV steel temperatures were changing in the range of about 100 to 200 deg C and responded consistently at multiple points to the changing amount of injected water; the heat source was estimated to be present in the RPV, because temperatures increased at multiple points in May 2011; and the temperatures at the RPV bottom were changing in the range of about 100 to 170 deg C, similar to the temperatures at other points around the RPV.

Consequently, the core was considered, from plant parameters, to have been largely damaged and relocated from its original position to below (lower plenum) and mostly being cooled there in a stable manner.

[Analysis of temperature behavior from May to August 2011]

The following findings were newly obtained from the RPV and PCV temperature behavior since May 2011.

- Overheated conditions of the RPV as a whole continued, although the water injection by FWS had been placed in service.
- The S/C temperatures increased when the amount of water injection was increased (Figure 11).

From these observations, part of the uncovered fuel was considered to be present in the core region, overheating the RPV inside, because no significant cooling effect was confirmed in the upper region of the core by the water from the FWS and some overheated parts remained in the RPV upper region of the RPV. Part of the fuel was considered to be present in the lower plenum as well as on the injected water path from the FWS, because the S/C temperatures increased.

[Analysis of temperature behavior from September 2011]

The following findings were newly obtained from the RPV and PCV temperature behavior since September 2011.

- Temperatures at the RPV upper part decreased due to the water directly passing through the core region from the CS, and further decreased to below 100 deg C in late September by increasing the amount of water injection
- Temperatures of the PCV atmosphere remained mostly below the saturation temperature, but for a while very locally (RPV seal bellows and SRVs) some thermometers still indicated high temperatures (above the saturation temperature)

even after the RPV temperatures were lowered below 100 deg C (Figure 12 and Figure 13).

From these observations, the following interpretations may be possible.

- Part of the fuel is present in the RPV core region, but most of the fuel is under water in the RPV lower part.
- Heat sources are present outside the RPV, too, but being cooled sufficiently. However, some fuel may be uncovered (around CRD housings) and some parts may be generating mild heat due to the deposited fission products (around the SRVs).

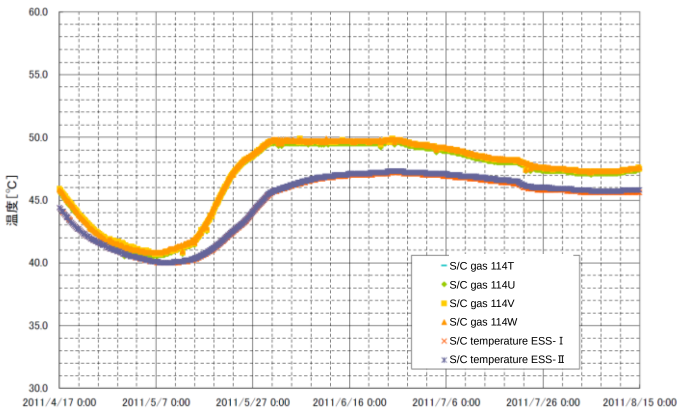

Figure 11　S/C temperature trends

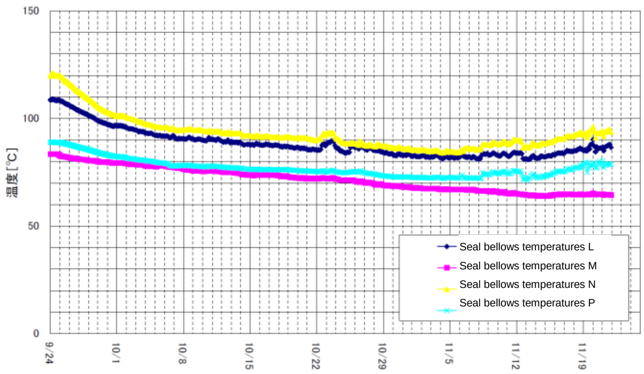

Figure 12　RPV seal bellows temperature trends

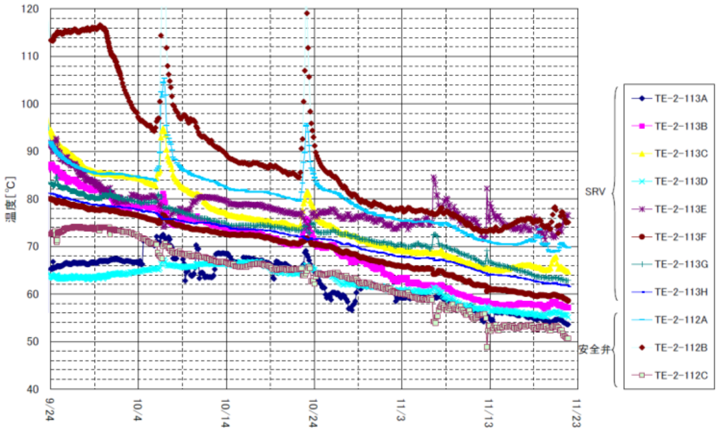

Figure 13　SRV leak detector temperature trends

3.　　Fuel locations estimated from temperature behavior

Summarized below are the fuel locations at each unit estimated from the analyses in this document.

(1) Unit-1

As of May 2011, most of the fuel was considered to have been being cooled in the RPV from the following reasons: temperatures of CRD housings and other structures below the RPV bottom were being measured; RPV steel temperatures were changing at high temperatures and responded at multiple points consistently to the changing amount of water injection; and heat sources were estimated to be present in the RPV, because temperatures at the RPV upper part were high at multiple points.

Therefore, the core was considered to have been relocated from its original location to below (lower plenum) and being cooled there in a stable manner, even if the core had been largely damaged.

However, the RPV bottom temperatures decreased to below the saturation temperature from May 2011, notwithstanding that the amount of water injection had been insufficient to remove sensible heat. Then part of the fuel was considered to be very likely not present in the RPV.

Furthermore, in October 2011, when the amount of water injection was increased, the S/C pool temperatures increased and exceeded the RPV and PCV temperatures. Presently (November 2011), the heat source is considered to be present in the lower part of the PCV (probably in the pedestal area).

(2) Unit-2

As of May 2011, most of the fuel was considered to have been being cooled in the RPV from the following reasons: temperatures of the RPV bottom were changing at the level of about 100 to 120 deg C and they responded at multiple points consistently to the changing amount of water injection; and the heat source was estimated to be present in the RPV, because temperatures at the RPV upper part were higher. Consequently, the core was considered to have been relocated from its original position to below (lower plenum) and being cooled there in a stable manner, even if the core had been largely damaged.

The RPV and PCV temperature behavior since September 2011 shows that the temperatures at the RPV upper part decreased due to the water injected by the CS system directly running through the core region and they cut below the saturation temperature, when the amount of water injection was increased. This also supports the estimation that most of the fuel is under water in the RPV lower part, although a limited amount of fuel is present at the RPV core region.

It should be noted that some heat source present outside the RPV is considered as being sufficiently cooled.

(3) Unit-3

As of May 2011, most fuel was considered to have been being cooled in the RPV from the following reasons: temperatures of the RPV bottom were changing at the level of about 100 to 200 deg C and they responded at multiple points consistently to the changing amount of water injection; and the heat source was estimated to be present in the RPV, because temperatures at the RPV upper part were higher. Consequently, the core was considered to have been relocated from its original position to below (lower plenum) and being cooled there in a stable manner, even if the core had been largely damaged.

The RPV and PCV temperature behavior since September 2011 shows that the temperatures at the RPV upper part decreased due to the water injected by the CS system directly running through the core region and cut below the saturation temperature when the amount of water injection was increased. This also supports the estimation that most fuel is under water in the RPV lower part, although a limited amount of fuel is present at the RPV core region.

It should be noted that some heat source present outside the RPV is considered as being sufficiently cooled.

End

Core fuel temperatures estimated by the in-RPV temperature evaluation model

1. Introduction

Temperatures of the core and structural materials in the reactor vessel (RPV) were estimated by evaluating the heat balance using an in-RPV temperature evaluation model. Uncertainties in the input data were considered by changing the data parametrically in a certain range and the measured values obtained to date were reviewed for evaluation.

This evaluation model is based on an energy transfer model in which the heat energy is transferred to each structural component by the steam produced. A case with little steam production is outside the scope of applicability. For this reason, Unit-1 was excluded from the evaluation, because the temperatures around the Unit-1 RPV were low. In-RPV temperatures of Unit-2 and Unit-3 were evaluated.

2. Temperature evaluation model in the RPV

2.1. Outline of the evaluation model

Figure 1 shows the configuration used in the model. Heat is generated by the fuel in the flooded and uncovered (unflooded) regions and transferred to the upper structures, core shroud, RPV upper wall and side walls. In the figure, coolant flows from the water injection lines are shown in solid lines, while broken lines show the heat flow from the fuel in the uncovered region.

In the model, heat is generated in the fuel in the RPV lower plenum (flooded), the fuel in the original core region (uncovered) and the fuel that had been relocated to the containment vessel (PCV). But the heat from the fuel in the PCV is assumed not to contribute to the steam production in the RPV. The fuel is cooled by the water injected from two systems, i.e., the feedwater system and the core spray (CS) system.

Water injected from the feedwater system goes through the lower plenum and becomes saturated steam while being heated in the flooded region, and further, becomes superheated steam at fuel surface temperatures by being heated in the uncovered region. On the other hand, water injected from the CS system (CS water) is considered to condense the superheated steam in the upper core region. In the model, the heat to be removed for condensation is considered as negative heat generation in the uncovered core region. Part of the water from the CS system becomes steam by being heated up in the uncovered core region and reaches the lower plenum, after transferring energy (heat) to the core shroud and upper structures, for steam production in the flooded region.

The uncovered core is cooled by the heat transfer to the saturated steam produced in the flooded core region and by the heat radiation transfer to the core shroud and upper structures. The heat transferred to the superheated steam and upper structures is further transferred to the RPV upper wall by natural convection heat transfer of single-phase steam or by heat radiation, and then removed to the drywell (D/W) by natural convection heat transfer via heat conduction in the RPV upper wall. The heat transferred to the core shroud is removed to the D/W by natural convection heat transfer via heat conduction in the core shroud, heat radiation transfer from the core shroud to the RPV side walls and heat conduction in the RPV side walls.

By solving the heat balance equation based on the scenario above, temperatures of the uncovered core and various points in the RPV can be calculated.

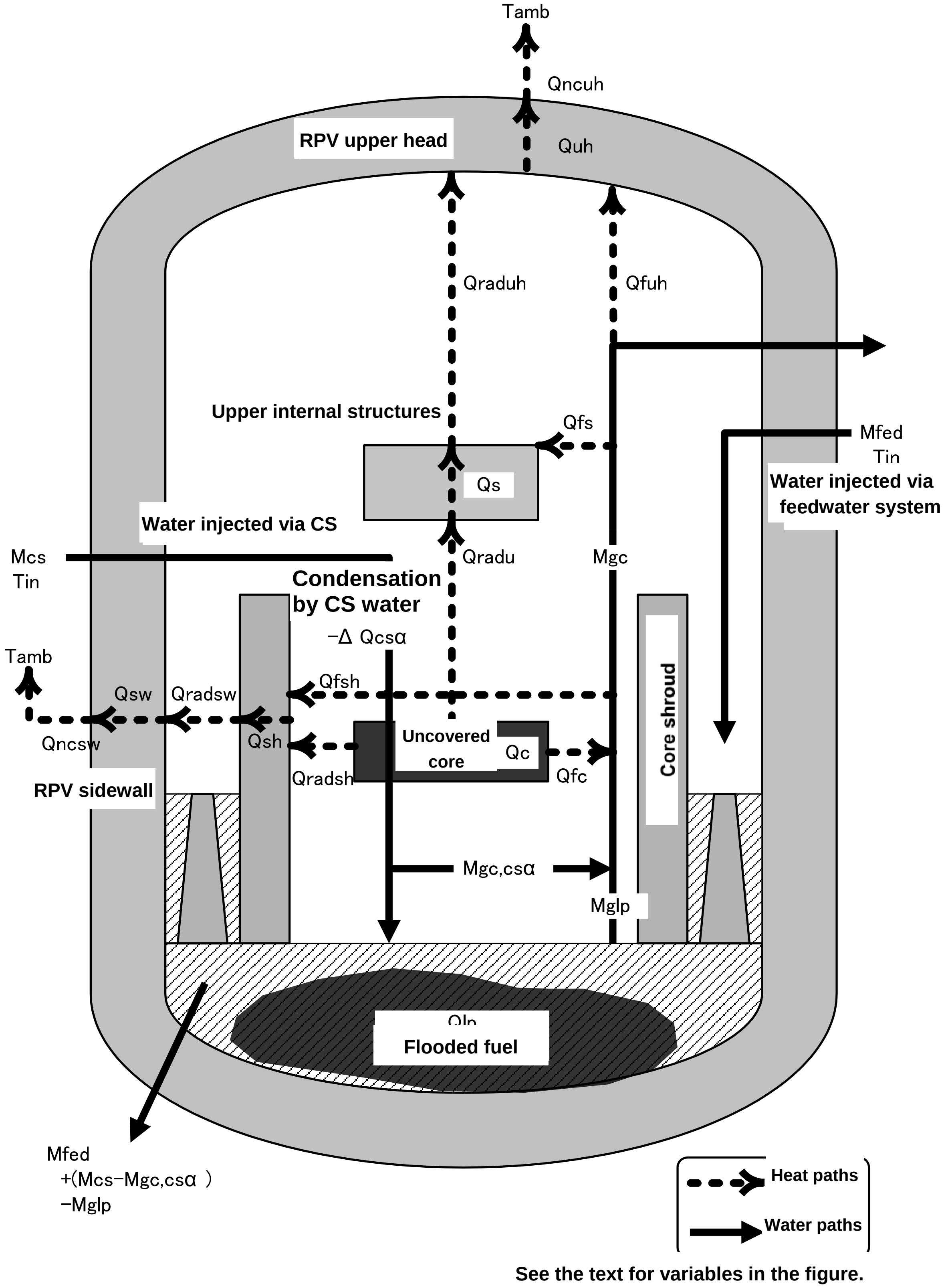

Figure 1　Schematic of in-RPV temperature evaluation model

2.2. Methods used for the temperature evaluation model in the RPV

2.2.1. Heat balance equations

The following heat balance equations are used in the evaluation.

Heat balance equation in the uncovered core

$$Q'_c = Q_{radsh} + Q_{radu} + Q_{fc} \quad \text{(Eq.1)}$$

Q'_c	Heat generated in the uncovered core (CS water considered)
Q_{radsh}	Heat radiation from the uncovered core to core shroud wall
Q_{radu}	Heat radiation from the uncovered core to the lower surface of upper structures
Q_{fc}	Heat received by steam passing through the uncovered core

Heat balance equation from the uncovered core to the RPV upper wall

$$Q_{ncuh} = Q_{uh} = Q_{raduh} + Q_{fuh} \quad \text{(Eq.2)}$$

$$Q_{raduh} = Q_s = Q_{radu} + Q_{fs} \quad \text{(Eq.3)}$$

Q_{ncuh}	Heat transfer from the RPV outer surface to D/W atmosphere
Q_{uh}	Heat conduction from the RPV upper wall inner surface to its outer surface
Q_{raduh}	Head radiation from upper structures to the RPV upper wall inner surface
Q_{fuh}	Heat transfer from steam running through upper structures to the RPV upper wall inner surface
Q_s	Heat conduction from the lower surface of upper structures to their upper surface
Q_{fs}	Heat transfer from steam running through the uncovered core to upper structures

Heat balance equation from the uncovered core to RPV side walls

$$Q_{ncsw} = Q_{sw} = Q_{radsw} = Q_{sh} = Q_{radsh} + Q_{fsh} \quad \text{(Eq.4)}$$

Q_{ncsw}	Heat transfer from the RPV side wall outer surface to D/W atmosphere
Q_{sw}	Heat transfer from the RPV side wall inner surface to its outer surface
Q_{radsw}	Heat radiation from the core shroud wall outer surface to the RPV side wall inner surface
Q_{sh}	Heat transfer from the core shroud wall inner surface to its outer surface

Q_{fsh}	Heat transfer from steam in the uncovered core to the core shroud wall

2.2.2. Amount of steam production and heat generated in the uncovered core region

In the current model, the heat is generated in the fuel in the RPV lower plenum (flooded), the fuel in the original core region (uncovered) and the fuel that had been relocated to the PCV. The heat from the fuel in the PCV is assumed not to contribute to the steam production in the RPV. Heat generation in each region is given by the following equations.

$$Q_d = Q_c + Q_{lp} + Q_{pcv} \quad \text{(Eq.5)}$$

$$Q_{lp} = X_f Q_d \quad \text{(Eq.6)}$$

$$Q_{pcv} = X_s Q_d \quad \text{(Eq.7)}$$

$$Q_c = (1 - X_f - X_s) Q_d \quad \text{(Eq.8)}$$

Q_d	Fuel decay heat
Q_c	Heat generation of uncovered fuel
Q_{lp}	Heat generation of flooded fuel
Q_{pcv}	Heat generation of relocated fuel to the PCV
X_f	Fraction of fuel in the flooded region
X_s	Fraction of fuel that had been relocated to the PCV (Fraction of relocated fuel to the PCV)

Water injected from the feedwater system and CS system is mixed, warmed and evaporated as steam in the flooded region in the lower plenum. The amount of steam produced in the lower plenum is given by the next equation.

$$M_{glp} = \frac{Q_{lp} - (1 - \chi_{wl})\{M_{fed} C_{pw} (T_{sat} - T_{in}) + \Delta Q_{lcs\alpha}\}}{\Delta h_{fg}} \quad \text{(Eq.9)}$$

M_{glp}	Steam production in the lower plenum
χ_{wl}	Fraction of injected water not contributing to cooling (Fraction of water leak)
M_{fed}	Amount of water injected from the feedwater system
C_{pw}	Specific heat of water
T_{sat}	Saturation temperature
T_{in}	Injected water temperatures
$\Delta Q_{lcs\alpha}$	Heat energy needed for CS water that had flowed into the lower plenum to become saturated water
Δh_{fg}	Latent heat

The amount of steam passing through the uncovered core is the sum of the amount of steam produced in the lower plenum and that produced in the uncovered core region from the water injected from the CS system.

$$M_{gc} = M_{glp} + M_{gc,cs\alpha} \qquad \text{(Eq.10)}$$

M_{gc} Amount of steam passing through the uncovered fuel region

$M_{gc,cs\alpha}$ Amount of CS water evaporation in the uncovered fuel region

Concerning the heat generation in the uncovered core fuel, part of the water injected from the CS system is considered to condense the superheated steam and that heat for condensation is, in the current model, regarded as negative heat generation in the uncovered fuel. The logical background of this model is the following.

The amount of heat generated by the uncovered fuel Q_c' is given by the following equation. When Q_1 is larger than Q_c, the whole uncovered fuel is being cooled by the water injected from the CS system.

$$Q_c' = \begin{cases} 0 & (Q_1 > Q_c) \\ Q_c - Q_1 & (Q_1 \le Q_c) \end{cases} \qquad \text{(Eq.11)}$$

$$Q_1 = \alpha M_{cs} \{\Delta h_{fg} + C_{pw}(T_{sat} - T_{in})\} \qquad \text{(Eq.12)}$$

Q_1 Heat energy needed for CS water contributing to cooling the unflooded fuel in the core region to become saturated steam

A Direct cooling rate of uncovered core by CS water (Fraction of effective CS contribution)

M_{cs} Amount of water injected from CS

Part of the CS injection water flows down to the lower plenum, after contributing to the condensation of the superheated steam. Its temperature is given by the following equation. It means that the CS water flows down to the lower plenum as saturated water if the heat energy Q_2 necessary for the CS water to reach the saturation temperature is less than the energy received by the CS water from the uncovered core, otherwise it exists as sub-cooled water.

$$T_{lcs} = \begin{cases} T_{sat} & (Q_c - Q_c' \ge Q_2) \\ T_{in} + \dfrac{\Delta Q_{cs\alpha}}{\alpha M_{cs} C_{pw}} & (Q_c - Q_c' < Q_2) \end{cases} \qquad \text{(Eq.13)}$$

$$Q_2 = \alpha M_{cs} C_{pw}(T_{sat} - T_{in}) \qquad \text{(Eq.14)}$$

T_{lcs} Temperature of CS water flowing to the lower plenum

Q_2 Heat energy needed for CS water to become saturated water

The amount of steam produced by heat removal from the uncovered core by the CS water can be expressed in the following form.

$$M_{gc,cs\alpha} = \frac{(Q_c - Q_c') - \alpha M_{cs} C_{pw} (T_{lcs} - T_{in})}{\Delta h_{fg}} \quad \text{(Eq.15)}$$

The amount of CS water flowing down to the lower plenum is the sum of the water which has contributed to the cooling of the uncovered core (minus the amount evaporated as steam) and the water which has not contributed. The heat energy necessary for this water (the sum) to become saturated water is given by the next expression.

$$\Delta Q_{lcs\alpha} = (\alpha M_{cs} - M_{gc,cs\alpha}) C_{pw} (T_{sat} - T_{lcs}) + (1-\alpha) M_{cs} C_{pw} (T_{sat} - T_{in}) \quad \text{(Eq.16)}$$

2.2.3. Heat transfer from the uncovered core to RPV upper wall

The heat generated in the uncovered core and the heat transferred to the steam Q_R passing through the core have the following relationship.

$$Q_{fc} = M_{gc} C_{pg} (T_c - T_{sat}) \quad \text{(Eq.17)}$$

C_{pg} Specific heat of steam

T_c Steam temperatures heated up in the uncovered core (fuel surface temperatures in the uncovered core)

Heat transfer from the superheated steam heated in the uncovered core to the upper structures is expressed in the following equation.

$$Q_{fs} = M_{gc} C_{pg} (T_{co} - T_{st}) \quad \text{(Eq.18)}$$

T_{co} Steam temperature in the uncovered core with consideration of heat transfer to the core shroud walls

T_{st} Temperature on the upper surface of upper structures

The amount of heat radiation transfer Q_{radu} from the uncovered core to upper structures and the amount of heat conduction Q_S from the lower surface to upper surface of upper structures are expressed in the following equations.

$$Q_{radu} = A_{ct} \frac{1}{\frac{1}{\varepsilon_c} + \frac{1}{\varepsilon_s} - 1} \sigma (T_c^4 - T_{sb}^4) \quad \text{(Eq.19)}$$

$$Q_s = A_s \lambda_s \frac{T_{sb} - T_{st}}{\delta_s} \quad \text{(Eq.20)}$$

A_{ct}	Upward projection area of the uncovered core
ε_c	Emissivity of the core
ε_s	Emissivity of upper structures
σ	Stefan-Boltzmann constant
T_{sb}	Temperature of upper structure lower surface
A_s	Heat transfer area of upper structures
λ_s	Heat conduction coefficient of upper structures
T_{st}	Temperature of upper structure upper surface
δ_s	Thickness of upper structures

In evaluating the heat transfer from the upper structures to the RPV upper wall, heat radiation from the upper structures and heat transfer by the steam passing through the upper structures are considered. The amount of heat transfer by heat radiation Q_{raduh} can be expressed by the next equation.

$$Q_{raduh} = A_s \frac{1}{\frac{1}{\varepsilon_s} + \frac{1}{\varepsilon_{uh}} - 1} \sigma\left(T_{st}^4 - T_{uhin}^4\right) \tag{Eq.21}$$

ε_{uh}	Emissivity of RPV upper wall
T_{uhin}	Temperature of RPV upper wall inner surface

Steam temperature $T_{uh,g}$ passing through upper structures can be obtained from the following two heat balance equations Q_{fuh}. One is the heat balance between the steam and RPV upper wall, and the other is the heat balance when the steam passes through the upper structures.

$$Q_{fuh} = A_{uh} h_{uhin}\left(T_{uh,g} - T_{uhin}\right) \tag{Eq.22}$$

$$Q_{fuh} = M_{gc} C_{pg}\left(T_{st} - T_{uh,g}\right) \tag{Eq.23}$$

A_{uh}	Heat transfer area of RPV upper wall
h_{uhin}	Heat transfer coefficient of RPV upper wall

Concerning the heat transfer from the RPV to the D/W atmosphere, heat conduction Q_{uh} from the RPV upper wall inner surface to outer surface, and heat transfer Q_{nuch} from the RPV upper wall outer surface to D/W atmosphere are considered.

$$Q_{uh} = A_{uh} \lambda_{uh} \frac{T_{uhin} - T_{uho}}{\delta_{uh}} \tag{Eq.24}$$

$$Q_{ncuh} = A_{uh} h_{nc}\left(T_{uho} - T_{amb}\right) \tag{Eq.25}$$

λ_{uh}	Heat conduction coefficient of RPV upper wall

T_{uho}	Temperatures of RPV upper wall outer surface
δ_{uho}	Thickness of RPV upper wall
h_{nc}	Heat transfer coefficient of natural convection
T_{amb}	D/W atmosphere temperatures

2.2.4. Heat transfer from the uncovered core to RPV side walls

Heat transfer from the uncovered core to the in-RPV steam and to the core shroud inner wall is obtained from the following heat balance equations. One is the heat balance between the in-RPV steam and core shroud inner wall, and the other is the heat balance when the in-RPV steam is cooled after having passed through the uncovered core.

$$Q_{fsh} = A_{sh} h_{shin} \left(T_{co} - T_{shin}\right) \qquad \text{(Eq.26)}$$

$$Q_{fsh} = M_{gc} C_{pg} \left(T_c - T_{co}\right) \qquad \text{(Eq.27)}$$

A_{sh}	Heat transfer area of the core shroud wall
h_{shin}	Heat transfer coefficient of the core shroud wall
T_{co}	In-RPV steam temperature
T_{shin}	Temperature of the core shroud wall inner surface

The amount of heat transfer Q_{radsh} by heat radiation from the uncovered core to the core shroud inner wall is given by the next equation.

$$Q_{radsh} = A_{cs} \frac{1}{\dfrac{1}{\varepsilon_c} + \dfrac{1}{\varepsilon_{sh}} - 1} \sigma \left(T_c^4 - T_{shin}^4\right) \qquad \text{(Eq.28)}$$

A_{cs}	Side wall area of the uncovered core
ε_{sh}	Emissivity of the core shroud wall

Four components are considered for the heat transfer from the core shroud inner wall to the D/W atmosphere: heat conduction from the core shroud inner surface to the outer surface Q_{sh}; heat radiation from the core shroud outer surface to the RPV side wall inner surface Q_{radsw}; heat conduction from the RPV inner surface to the outer surface Q_{sw}; and heat transfer from the RPV side wall outer surface to the D/W atmosphere Q_{ncsw}.

$$Q_{sh} = A_{sh} \lambda_{sh} \frac{T_{shin} - T_{sho}}{\delta_{sh}} \qquad \text{(Eq.29)}$$

$$Q_{radsw} = A_{sh} \frac{1}{\dfrac{1}{\varepsilon_{sh}} + \dfrac{1}{\varepsilon_{sw}} - 1} \sigma \left(T_{sho}^4 - T_{swin}^4\right) \qquad \text{(Eq.30)}$$

$$Q_{sw} = A_{sw}\lambda_{sw}\frac{T_{swin} - T_{swo}}{\delta_{sw}} \qquad \text{(Eq.31)}$$

$$Q_{ncsw} = A_{sw}h_{nc}\left(T_{swo} - T_{amb}\right) \qquad \text{(Eq.32)}$$

λ_{sh}	Heat conduction coefficient of the core shroud wall
T_{sho}	Temperature of the core shroud wall outer surface
δ_{sho}	Thickness of the core shroud wall
ε_{sw}	Emissivity of the RPV side wall
T_{swin}	Temperature of the RPV side wall inner surface
A_{sw}	Heat transfer area of the RPV side wall
λ_{sw}	Heat conduction coefficient of the RPV side wall
T_{swo}	Temperature of the RPV side wall outer surface
δ_{sw}	Thickness of the RPV side wall

3. Estimation of core fuel debris conditions

The in-RPV temperature evaluation model developed above (2.2) was applied to reproduce measured data to date, by which the debris distribution in the RPV was estimated. The estimated results were then used to evaluate the in-RPV temperature distributions as of October 10, 2011.

3.1. Selection of time points (date and time) and temperatures for evaluation

Time points for reproducing measured data were chosen from among possible points when plant parameters were not changing significantly due to the changing amount of water injection or other reasons. This is because the current evaluation model is based on the static heat balance model. Time points after the water injection via the CS started were also chosen so that the effect of water injection from the CS could be checked.

(1) Unit-2

By referring to temperature changes in Figure 2 (1), time points of August 12, 2011 and September 12, 2011 were chosen for measured data reproduction before the CS water injection was started, and September 26, 2001 was chosen for reproduction after the CS water injection was started.

The temperatures to be reproduced were set as follows. The thermometer at the feedwater nozzle was the only one available close to the RPV upper surface of interest in the current model. The temperatures at the feedwater nozzle of Unit-2 changed at a level lower than the temperatures at the RPV lower part over the whole period of interest for evaluation. For conservative evaluation, temperatures in the RPV upper part were set, by assuming higher temperatures present somewhere in the RPV upper part. From the temperature profile of Unit-3 (Figure 2 (2)), the temperature difference between the RPV shell flange and feedwater nozzle of Unit-3 was taken and added to the Unit-2 feedwater nozzle temperatures.

As the temperatures of the D/W atmosphere, the temperatures of the D/W HVH return line were used, which showed stable changes.

(2) Unit-3

Based on the temperature changes in Figure 2 (2), August 12 and August 30, 2011 before the CS water injection were chosen as the time points for evaluation, and September 12, 2011 after the CS water injection was chosen.

As for the temperatures, temperatures of the RPV shell flange were used as the temperatures of the RPV upper surface (outer surface of the RPV upper wall) in evaluating reproducibility of measured data. The temperatures of the RPV shell flange showed the highest values around the RPV upper part in Figure 2 (2) from August to early September 2011. Higher RPV upper part temperatures predict the higher fraction of uncovered core and lead to a conservative conclusion.

As the temperatures of the D/W atmosphere, the temperatures of the D/W HVH return line were used, which showed stable changes.

3.2. Estimation of fractions of the uncovered core and the effective CS contribution

Results of sensitivity analysis are given below, concerning the impact of RPV upper surface temperatures against the fractions of molten fuel that had been relocated to the PCV and of uncovered core left at the original position. The water leak fraction (not contributing to cooling) of CS water was set as 20%, 40% or 60%. The results correspond to the fractions at time points before water injection from the CS started. The fraction of molten fuel relocated to the PCV was set as 0%, 20%, 40% or 60%.

(1) Unit-2

Figure 3 (1) to Figure 3 (6) give the results of sensitivity analysis of the RPV upper surface temperatures against the fractions of relocated fuel to the PCV and uncovered core. From these figures, the fractions of uncovered core at the time point chosen to reproduce the measured RPV upper surface temperatures are obtained as 0.001 to 0.031 on August 12, 2011 and 0.008 to 0.027 on September 12, 2011.

By using the parameters obtained above (the fraction of water leaks, the fraction of relocated fuel to the PCV, the fraction of uncovered core), the fraction of effective cooling by

CS water (the uncovered core direct cooling rate by CS water) was estimated which could reproduce the RPV upper surface temperatures on September 26, 2011. The results range from 0.001 to 0.007.

The table below summarizes the results.

<table>
<tr><td colspan="2" rowspan="3">Parameters and their value ranges</td><td colspan="3">Results</td></tr>
<tr><td colspan="2">Fraction of uncovered core</td><td>Fraction of effective CS contribution</td></tr>
<tr><td>Aug. 12, 2011</td><td>Sept. 12, 2011</td><td>Sept. 26, 2011</td></tr>
<tr><td>Water leaks</td><td>20 to 60%</td><td rowspan="2">0.011 to 0.031</td><td rowspan="2">0.008 to 0.027</td><td rowspan="2">0.001 to 0.007</td></tr>
<tr><td>Relocation to PCV</td><td>0 to 60%</td></tr>
</table>

(2) Unit-3

Figure 3 (7) to Figure 3 (12) give the results of sensitivity analysis of the RPV upper surface temperatures against the fractions of relocated fuel to the PCV and uncovered core. From these figures, the fractions of uncovered core at the time point chosen to reproduce the measured RPV upper surface temperatures are obtained as 0.008 to 0.030 on August 12, 2011 and 0.009 to 0.031 on August 30, 2011.

By using the parameters obtained above (the fraction of water leaks, the fraction of relocated fuel to the PCV, the fraction of uncovered core), the fraction of effective cooling by CS water (the uncovered core direct cooling rate by CS water) was estimated which could reproduce the RPV upper surface temperatures on September 12, 2011. The results range from 0.002 to 0.011.

The table below summarizes the results.

<table>
<tr><td colspan="2" rowspan="3">Parameters and their value ranges</td><td colspan="3">Results</td></tr>
<tr><td colspan="2">Fraction of uncovered core</td><td>Fraction of effective CS contribution</td></tr>
<tr><td>Aug. 12, 2011</td><td>Aug. 30, 2011</td><td>Sept. 12, 2011</td></tr>
<tr><td>Water leaks</td><td>20 to 60%</td><td rowspan="2">0.008 to 0.030</td><td rowspan="2">0.009 to 0.031</td><td rowspan="2">0.002 to 0.011</td></tr>
<tr><td>Relocation to PCV</td><td>0 to 60%</td></tr>
</table>

3.3. Estimation of core conditions as of October 10, 2011

The RPV upper surface temperatures and uncovered core fuel surface temperatures as of October 10, 2011 were estimated, by using the parameters obtained in 3.2.

(1) Unit-2

The results are given in the table below. The RPV upper surface temperatures of 92.2 to 94.9 deg C are a little higher than the measured value of 78.6 deg C. The resulting uncovered core fuel surface temperatures are 92.7 to 99.3 deg C.

Parameters and their value ranges		Results		
		RPV upper surface temperatures	Uncovered core fuel surface temperatures	Upper structure temperatures
Water leaks	20 to 60%	92.1 to 94.9 deg C (measured: 78.6 deg C)	92.7 to 99.3 deg C	92.2 to 96.8 deg C
Relocation to PCV	0 to 60%			
Uncovered core (unflooded)	0.008 to 0.031			
Effective CS contribution	0.001 to 0.007			

(2) Unit-3

The results are given in the table below. The RPV upper surface temperatures of 71.2 to 81.8 deg C are roughly consistent with the measured value of 71.1 deg C. The resulting uncovered core fuel surface temperatures are 72.7 to 97.9 deg C.

Parameters and their value ranges		Results		
		RPV upper surface temperatures	Uncovered core fuel surface temperatures	Upper structure temperatures
Water leaks	20 to 60%	71.2 to 81.8 deg C (measured: 71.1 deg C)	72.7 to 97.9 deg C	71.4 to 89.0 deg C
Relocation to PCV	0 to 60%			
Uncovered core (unflooded)	0.008 to 0.031			
Effective CS contribution	0.002 to 0.011			

4. Conclusion

Heat balance in the RPV was evaluated using an in-RPV temperature evaluation model. The results show that the fractions of unflooded fuel (uncovered core) were less than about 3% in both Unit-2 and Unit-3, and the fuel surface temperatures in the unflooded region were below 100 deg C.

It can be estimated from the current (November 2011) temperature changes at various points of the RPV and PCV that the inside of the RPV and PCV are being sufficiently cooled and that uncovered overheated fuel is not present in significant quantities. The evaluation results of this report can be understood to support the estimation.

End

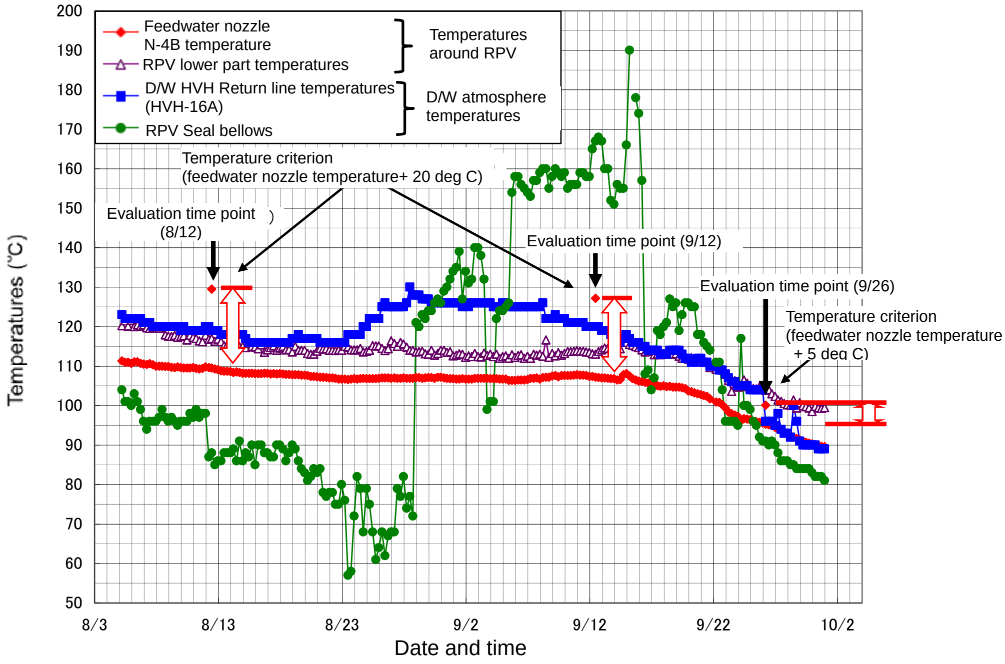

Figure 2 (1) Temperature changes around the RPV and D/W atmosphere (Unit-2)

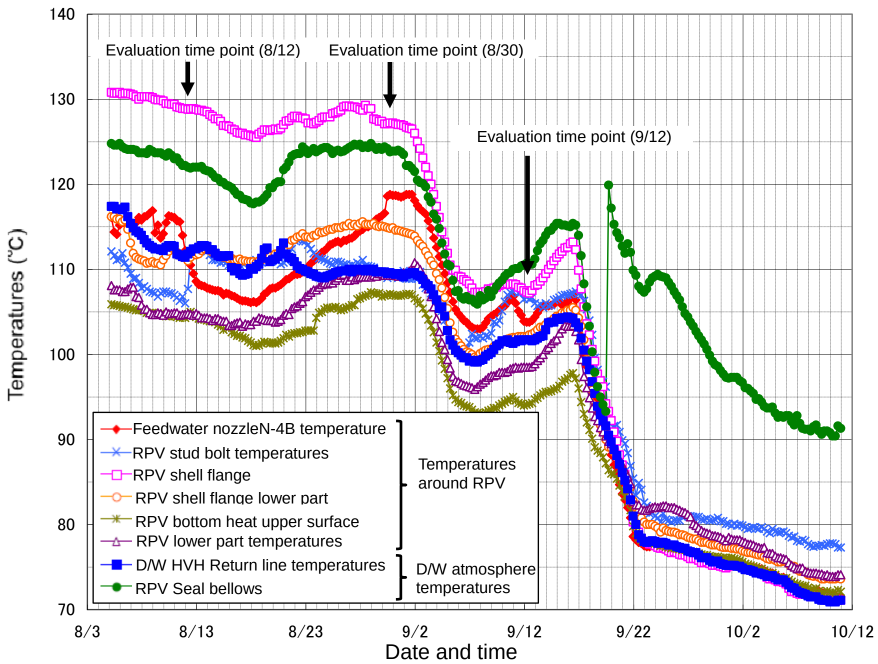

Figure 2 (2) Temperature changes around the RPV and D/W atmosphere (Unit-3)

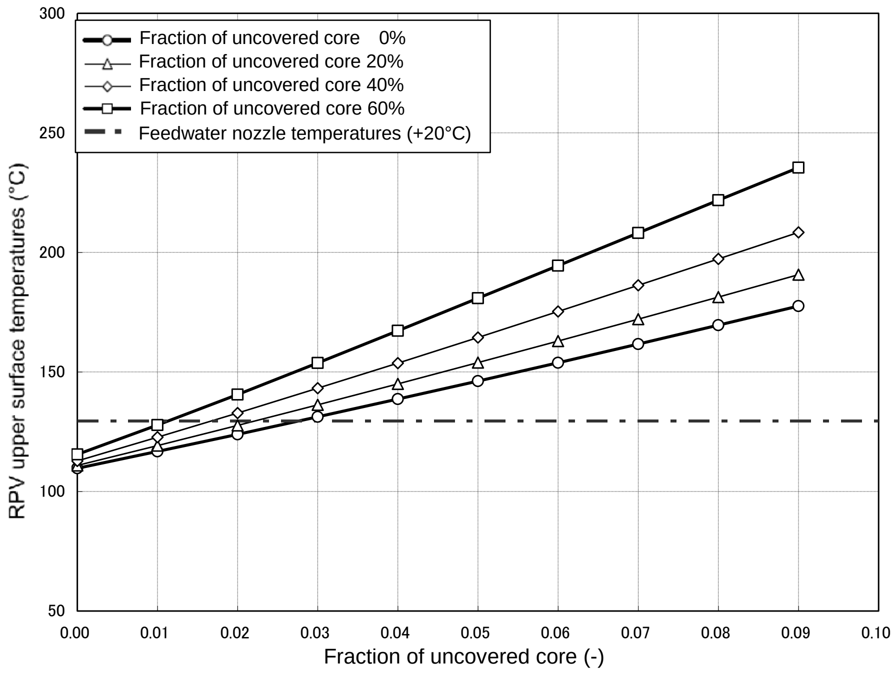

Figure 3 (1) Fractions of uncovered core and relocated fuel to the PCV, and RPV upper surface temperatures (Unit-2, August 12, 2011, water leak 20%)

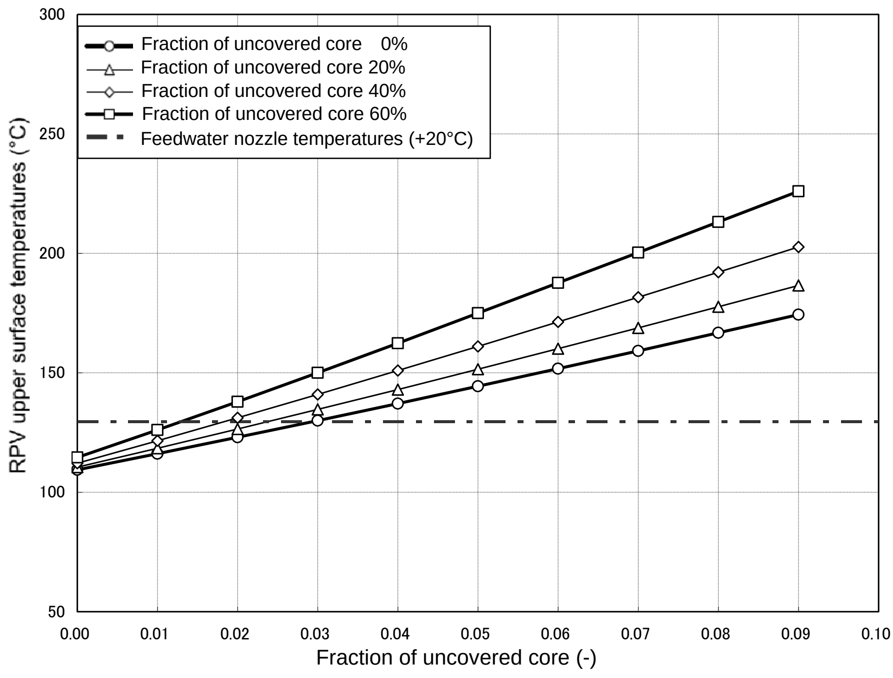

Figure 3 (2) Fractions of uncovered core and relocated fuel to the PCV, and RPV upper surface temperatures (Unit-2, August 12, 2011, water leak 40%)

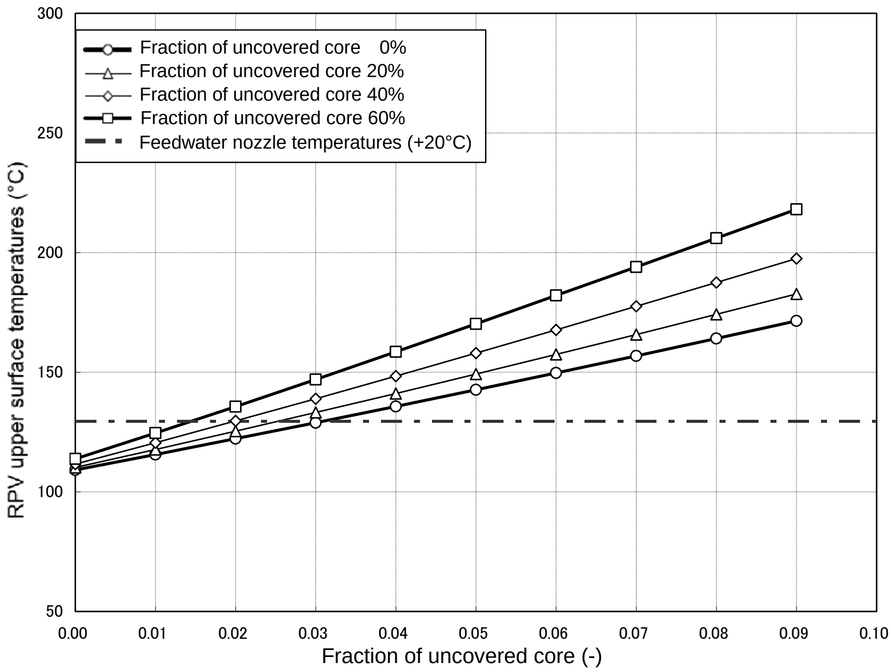

Figure 3 (3) Fractions of uncovered core and relocated fuel to the PCV, and RPV upper surface temperatures (Unit-2, August 12, 2011, water leak 60%)

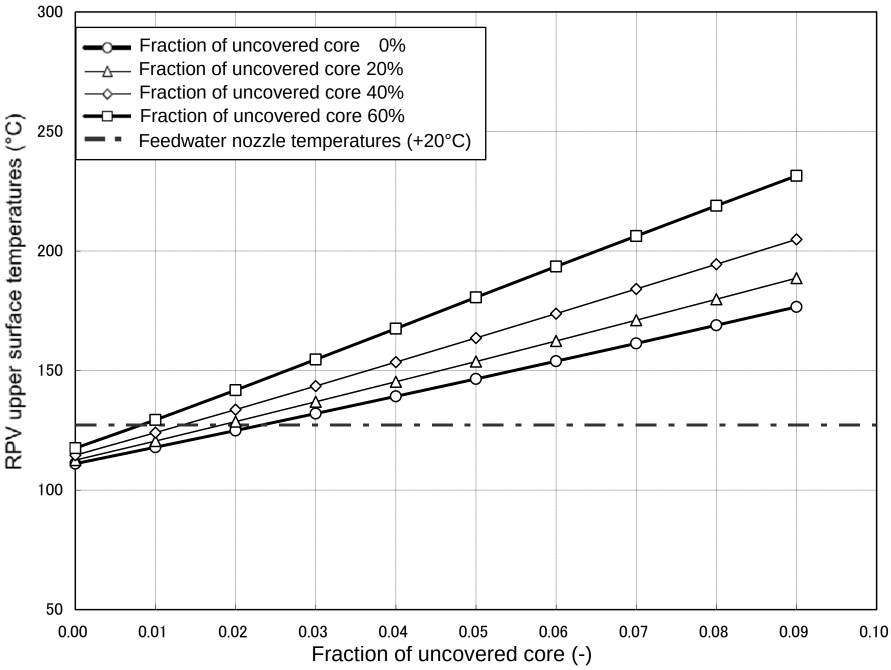

Figure 3 (4) Fractions of uncovered core and relocated fuel to the PCV, and RPV upper surface temperatures (Unit-2, September 12, 2011, water leak 20%)

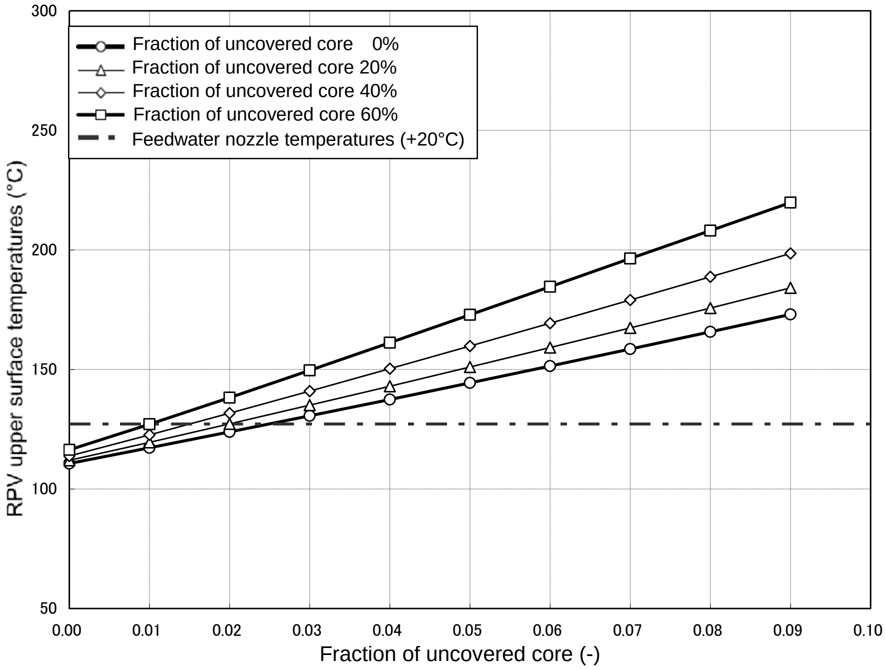

Figure 3 (5) Fractions of uncovered core and relocated fuel to the PCV, and RPV upper surface temperatures (Unit-2, September 12, 2011, water leak 40%)

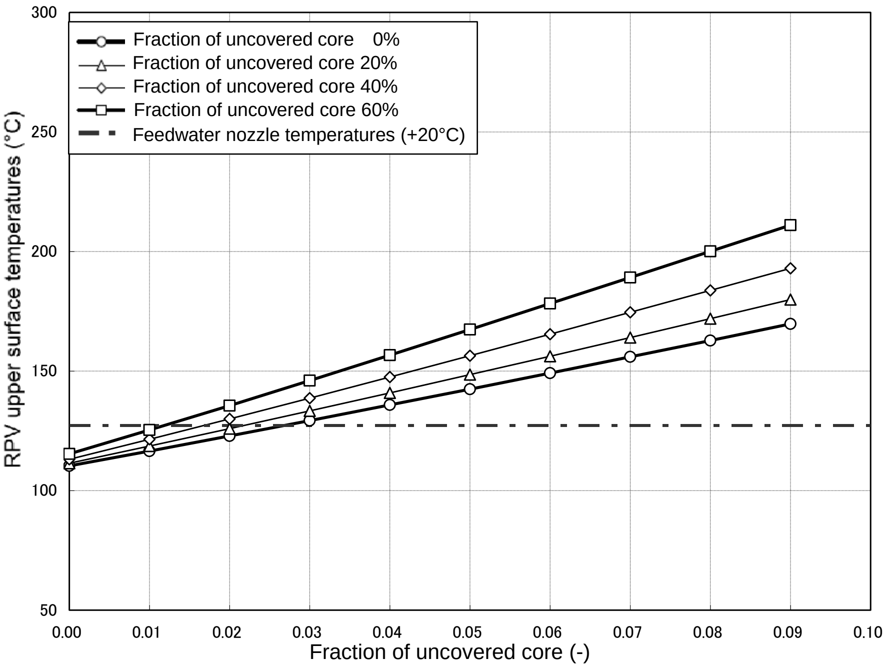

Figure 3 (6) Fractions of uncovered core and relocated fuel to the PCV, and RPV upper surface temperatures (Unit-2, September 12, 2011, water leak 60%)

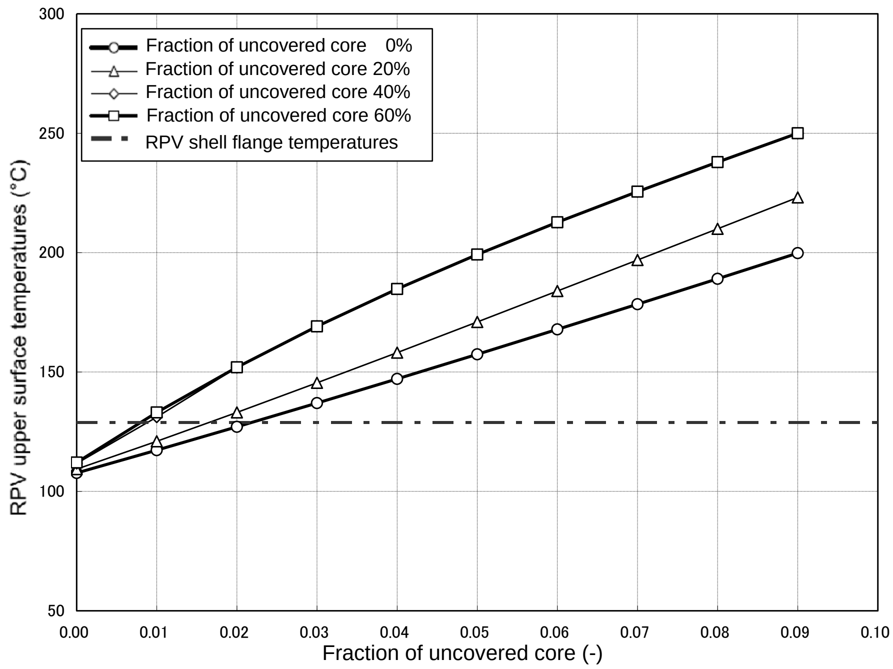

Figure 3 (7) Fractions of uncovered core and relocated fuel to the PCV, and RPV upper surface temperatures (Unit-3, August 12, 2011, water leak 20%)

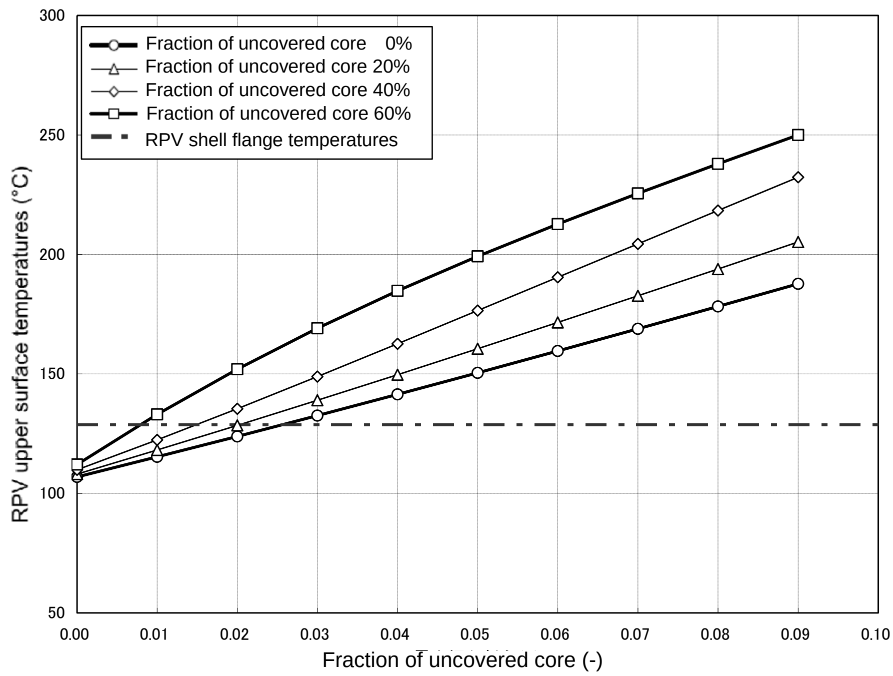

Figure 3 (8) Fractions of uncovered core and relocated fuel to the PCV, and RPV upper surface temperatures (Unit-3, August 12, 2011, water leak 40%)

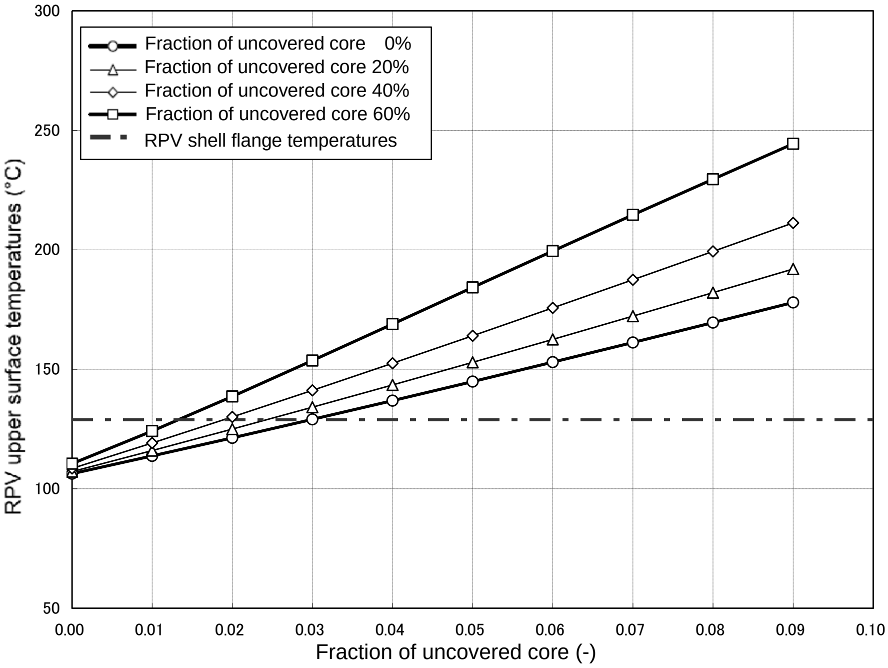

Figure 3 (9) Fractions of uncovered core and relocated fuel to the PCV, and RPV upper surface temperatures (Unit-3, August 12, 2011, water leak 60%)

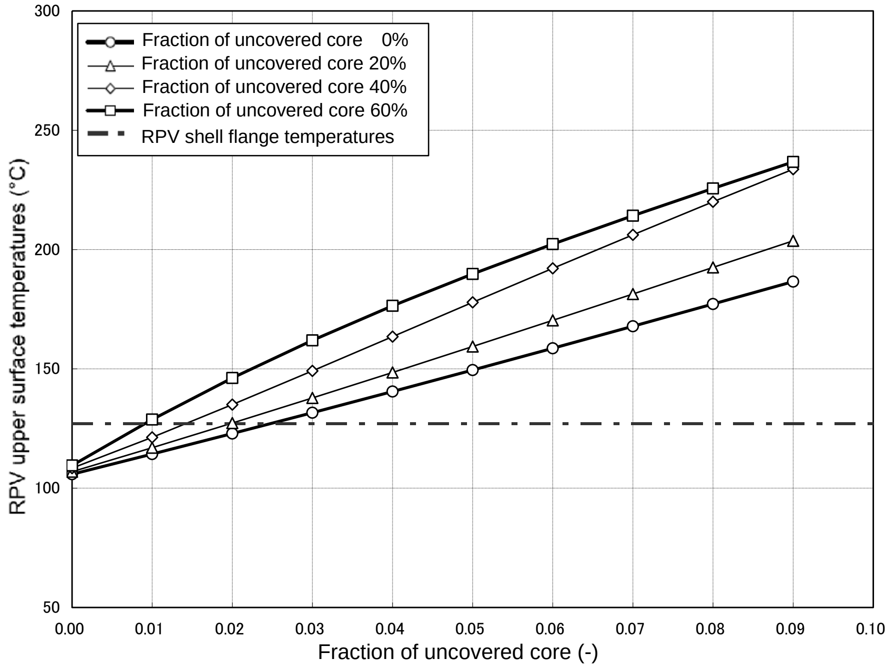

Figure 3 (10) Fractions of uncovered core and relocated fuel to the PCV, and RPV upper surface temperatures (Unit-3, August 30, 2011, water leak 20%)

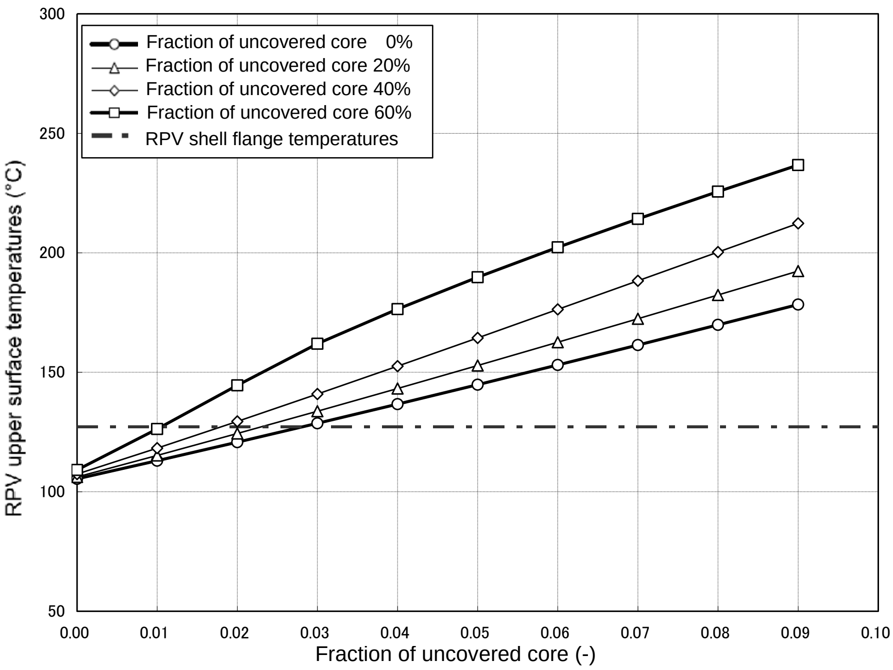

Figure 3 (11) Fractions of uncovered core and relocated fuel to the PCV, and RPV upper surface temperatures (Unit-3, August 30, 2011, water leak 40%)

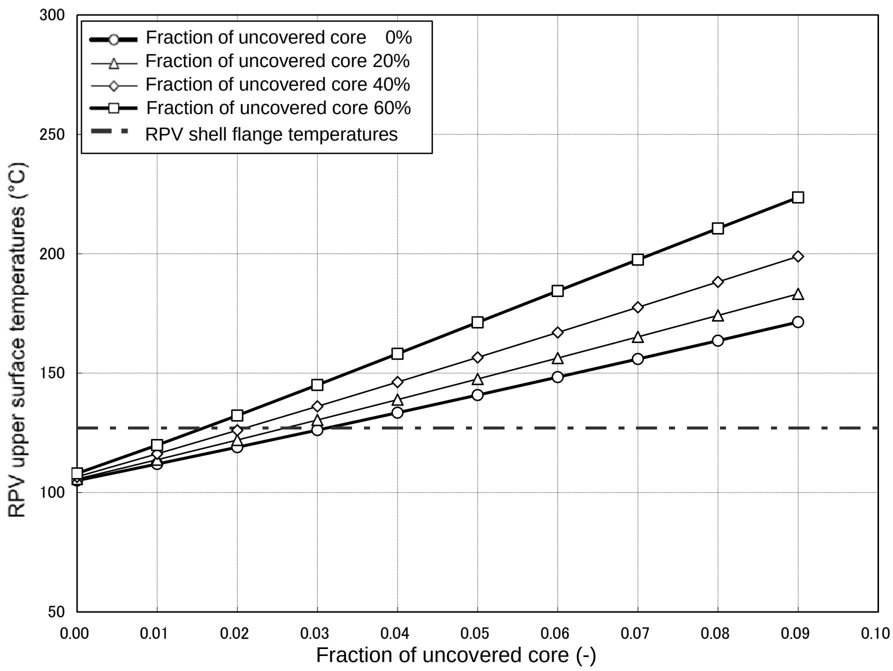

Figure 3 (12) Fractions of uncovered core and relocated fuel to the PCV, and RPV upper surface temperatures (Unit-3, August 30, 2011, water leak 60%)

Calibration of water level indicators

1. Principle of water level indicators

A typical fuel range water level indicator used in BWR plants is illustrated in Figure 1. It measures the reactor water level by measuring pressure difference (Hs – Hr) of two instrumentation piping systems (reference condensing water chamber side piping, hereafter described as the reference leg; and reactor side piping, hereafter variable leg) while keeping the water head Hs in the reference water head at a certain fixed value.

If the water level in the reference leg decreases due to evaporation or other reasons, the Hs, which should be constant, is reduced. But, since what is measured (or rather observed) is only the pressure difference, it cannot be distinguished whether Hs has decreased or Hr has increased. As a consequence, the apparent reactor water level seems to have increased (Figure 2).

2. Calibration of water level indicators of each unit

2.1. Unit-1

The Unit-1 reactor water level indicators were calibrated on May 11, 2011. The indicators themselves were confirmed to be functioning satisfactorily within the allowable errors. When the instrumentation lines and the reference condensing water chamber were filled with water thereafter before placing the water level indicators in service, the actual readings were checked. These readings were off the lower end of the scale.

The differential pressure gauge, temporarily installed after the accident to provide alternative measurements, was, in addition, off the upper end of the scale. The reactor water level was estimated to be below TAF-500 cm. Figure 3 shows the water level indicator calibration work.

- Calibration results of water level indicators

	Reactor water level reference (cm)	Input (kPa)	Output Voltage (mV)	Reactor water level converted (cm)	Error (%)	Allowable errors (%)
0%	−300	−78.53	40.7	−296.8	+0.4	±0.5
100%	500	−1.06	199.9	499.5	−0.1	

- Readings before and after water filling in the instrumentation lines

Monitoring device	Central monitor (LI-263-122A)	Remote monitor (LT-263-121A)	Temporary differential pressure gauge
Before filling	－170 cm	－1.67 m	－
After filling	Downscale *1	Downscale *1	Overscale *2

*1: Below -300 cm (below the lower limit of measurable range)

*2: The differential pressure gauge indicated “Off-scale (>100kPa).” This is equivalent in the water head to about TAF-500 cm or below (the reference value).

2.2. Unit-2

A temporary reading device was set on the normal water level indicator on June 22, 2011, and the instrumentation lines and the reference condensing water chamber were filled with water (Figure 4). After water filling, water in the instrumentation lines (reference leg, variable leg) in the PCV behaved as if it had evaporated. This is considered to be due to the atmospheric temperature in the instrumentation lines having been higher than the saturation temperature. Based on the instantaneous readings of the temporary device after water filling and the temperature changes thereafter, the reactor water level was estimated to be about TAF-500cm or below.

The instrumentation lines and the reference condensing water chamber were again filled with water on October 21, 2011. This was because the PCV temperatures were continuing to decrease and the temperatures in the PCV were lowered to about 85 deg C. The pressure difference immediately after water filling was off-scale and therefore, as in June 2011, the reactor water level was estimated to be below the instrumentation lines (approximately TAF-500cm or below). Concerning the variable leg, its pressure readings indicated a gradual decreasing trend as seen in Figure 5 and therefore the water in the variable leg is considered to have evaporated. This leads to an estimation that fuel (a heat source) is present near the variable leg.

Calibration of the normal water level indicator for Unit-2 is not possible yet, since the radiation level at its location is too high and for other reasons.

2.3. Unit-3

The reactor water level indicator calibration is not possible yet including water filling to instrumentation lines, since the radiation level at is location is too high and for other reasons.

End

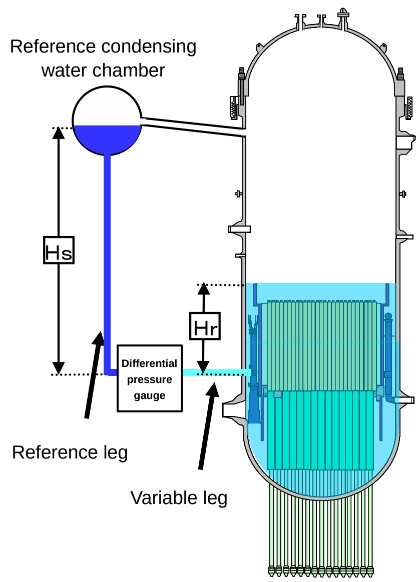

Figure 1　A schematic of reactor water level indicators

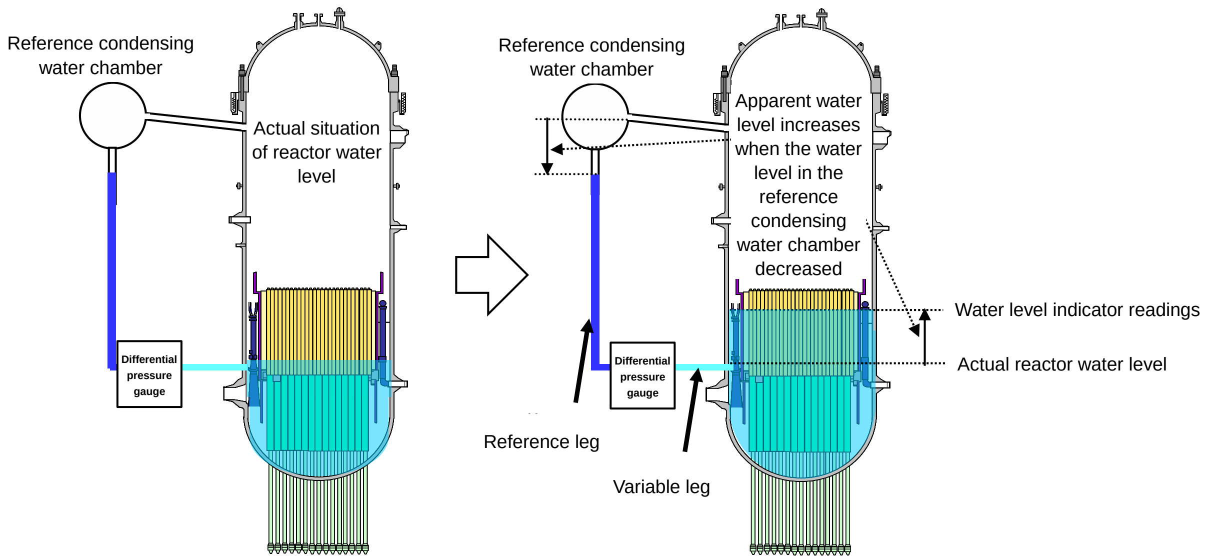

Figure 2　Reactor water level indicator readings upon the level decrease in the instrumentation lines

Figure 3　Calibration work on reactor water level indicators of Unit-1

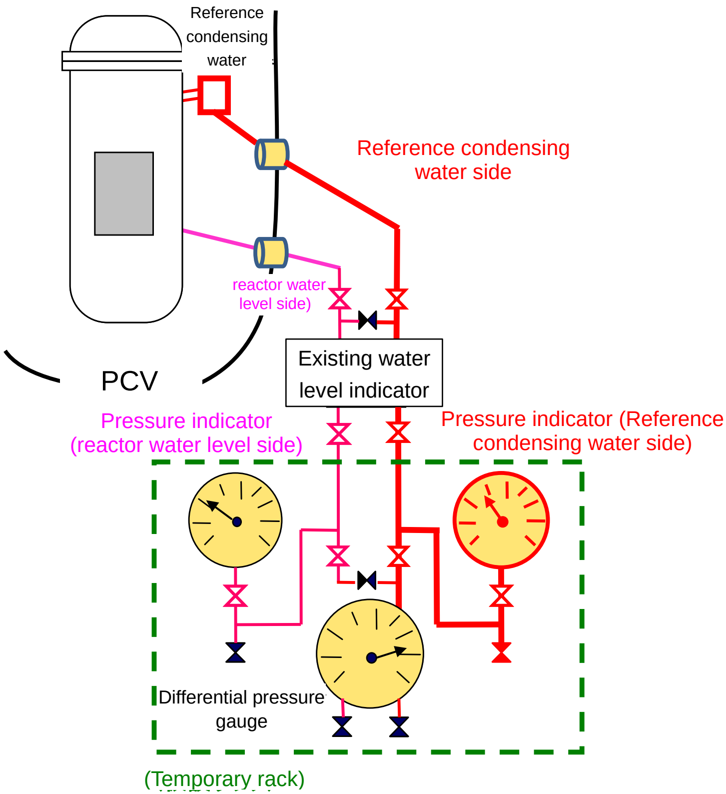

Figure 4　A schematic of temporary water level indictors for Unit-2

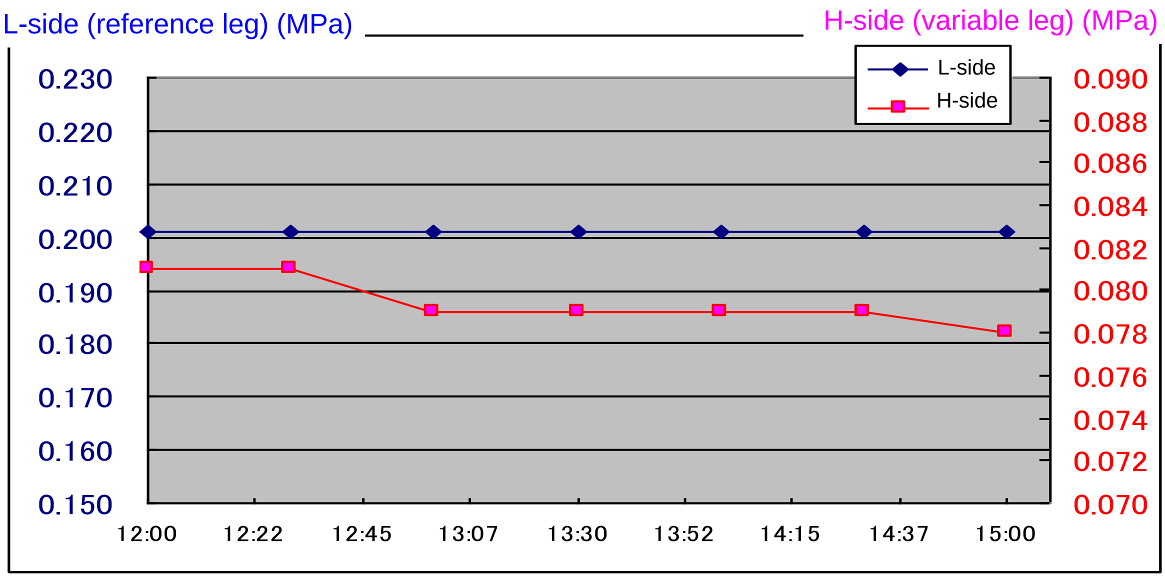

Figure 5　Changes of pressure indicator readings after water filling at Unit-2

Radioactivity concentrations in the atmosphere of the primary containment vessel

1. Outline

Gases in the Unit-1 primary containment vessel (PCV) were sampled on July 29, 2011 and again on September 14, 2011 for radioactivity concentration measurements, and the gases in the Unit-2 PCV were sampled on August 9, 2011.

2. Sampling methods

2.1. Sampling points of PCV gases

Figure 1 and Figure 2 show schematic drawings of the gas sampling systems. Both at Unit-1 and Unit-2, a temporary sampling rack was connected to the normal in-PCV oxygen analyzer rack, gases were sampled at the sampling point in the upper part of the PCV and returned to the sampling point in the middle.

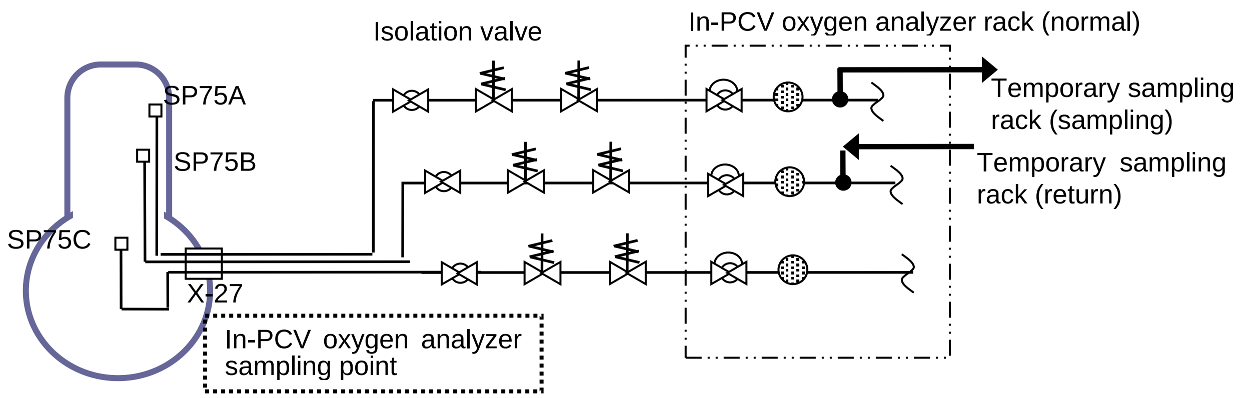

Figure 1 Unit-1 gas sampling system configuration for one-shot gas sampling

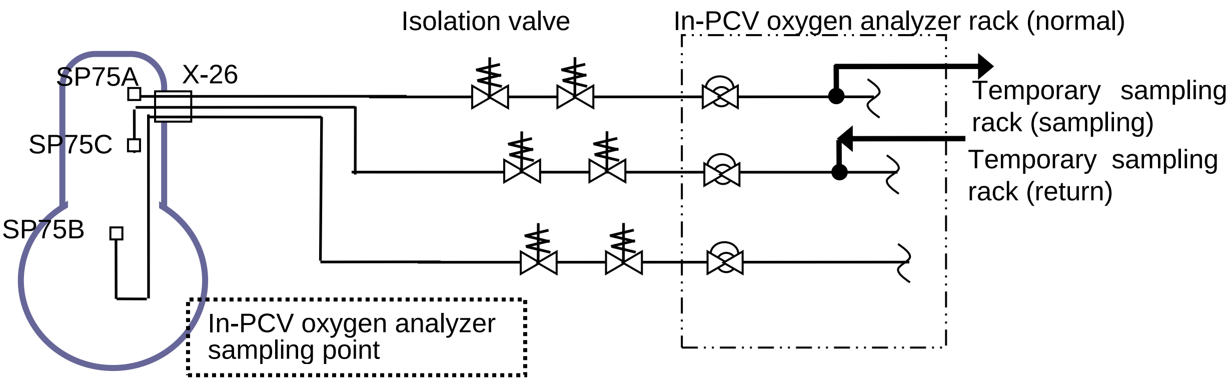

Figure 2 Unit-2 gas sampling system configuration for one-shot gas sampling

2.2. Temporary sampling rack

Figure 3 and Figure 4 show schematic drawings of the temporary gas sampling rack (Type 1 and Type 2). In Type 1 sampling rack, a sampling vessel (about 10 mL) mounted on the temporary sampling line is isolated with valves on both sides, removed after gas sampling, connected to a jig to transfer the sampled gas to a container while being stirred (diluted with air to 4 times larger volume). The sampled gas is then injected by a syringe into a gas vial for measurement by the Ge semiconductor detectors. The system operation procedures specify to purge the sampling line with nitrogen gas before and after sampling.

In Type 2 sampling rack, the sampled gas is led to two water-filled impingers (about 350 mL each) mounted on the temporary sampling line to capture water-soluble radioactive materials and collect condensate water. A gas vial can be connected to the sampling line for gas collection. The system operation procedures specify to purge the sampling line with nitrogen gas before sampling, conduct flow operations using a bypass line and purge the line with nitrogen gas again after sampling.

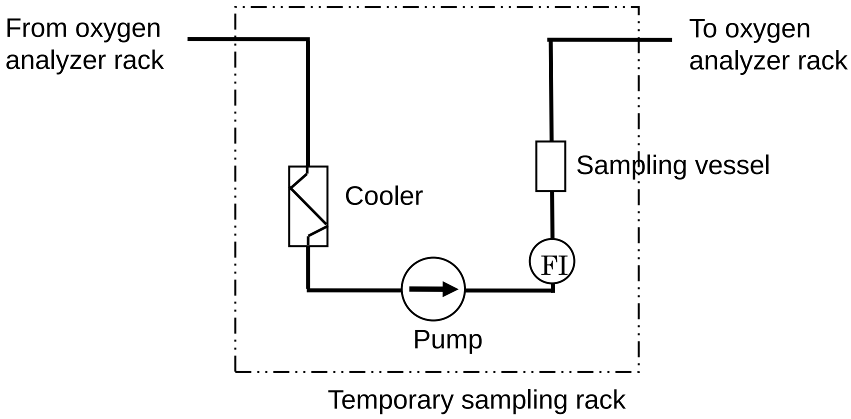

Figure 3　A schematic of the temporary sampling rack Type 1

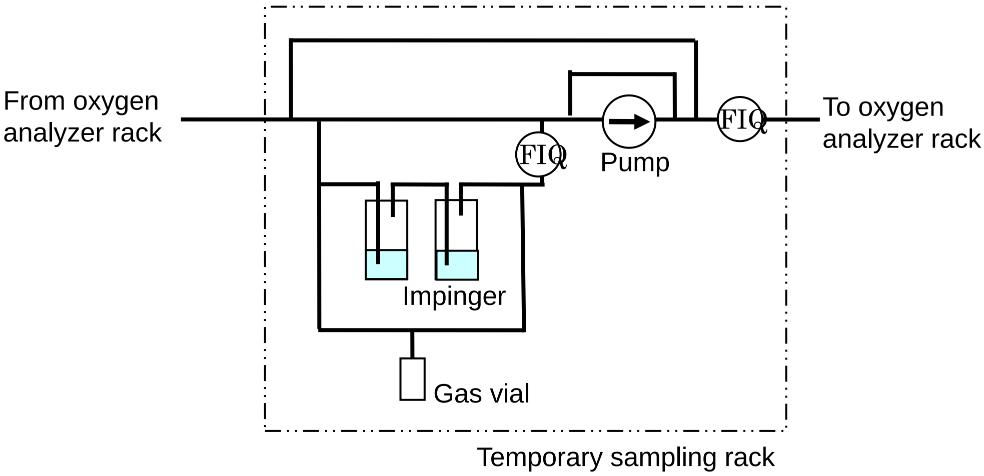

Figure 4　A schematic of the temporary sampling rack Type 2

2.3.　Gamma ray nuclide analysis

Sampled gas and condensate water are collected in a gas vial (about 14.1 mL) and a Marinelli beaker (about 500 mL) separately for gamma ray nuclide analysis by Ge semiconductor detectors. The energy range and resolutions of the semiconductor detectors are about 50 keV to 2.0 MeV, and about 1.8%, respectively and sufficient for the present measurement purposes.

3. Results

3.1. Collection of condensate water

Unit-1 in-PCV gas was sampled on July 29, 2011 using Type 1 temporary sampling rack, Unt-2 in-PCV gas was sampled on August 9, 2011 using Type 2 temporary sampling rack and Unit-1 in -PCV gas was sampled again on September 14, 2011 using Type 2 temporary sampling rack.

In the July 29 sampling (Unit-1, Rack Type 1), the gases flowed at the rate of 0.1 L/min for 2 hours and 1.0 L/min for about 30 min but no condensate water could be collected. This is believed to be because the pump capacity was too small to suction the condensate water-containing gases to the sampling point before the condensate water fell onto the lowest part of the piping.

In the August 9 sampling (Unit-2, Rack Type 2), the condensate water was confirmed to be flowing in the sampling device inlet line (a Teflon tube) when suctioned at the rate of 10 L/min (vapor components were fully condensed and remained in the piping in plug forms). By adjusting the flow rate, the condensate water was collected in the impingers and the gases were collected in the gas vial.

In the September 14 sampling (Unit-1, Rack Type 2), the rack used had a larger pump capacity for higher potential to collect condensate water. At the earliest sampling on July 29, 2011, the condensate water could not be collected using the Type 1 rack. By circulating the gases at the rate of about 10 to 40 L/min for several tens of minutes, the condensate water was confirmed to be flowing in the sampling device inlet line (hereafter the Teflon tube), the condensate water was collected in the impingers and the gases were collected in the gas vial.

3.2. Cs radioactivity concentration

Table 1 gives the measured radioactivity concentrations in the sampled condensate water, while Table 2 gives the measured radioactivity concentrations in the sampled gas. The results were used to derive the radioactivity concentrations in the PCV gases as given in Table 8 by the following conversion equations. Radioactivity concentrations in the condensate water and gas thus obtained were converted to the concentrations in the vapor and gases in the PCV, which are further converted to the in-PCV concentrations by the weighted average of the vapor fraction in the PCV.

[Conversion equations for in-PCV concentrations]

C1: Cs concentration in vapor	$C1 = \underline{C_{water}} \times \rho_{vapor}(T_{pcv}) / \rho_{water}(T_{sample})$	(Eq. 1)
C2: Cs concentration in gases	$C2 = \underline{C_{sampledgas}} \times T_{sample} / T_{pcv}$	(Eq. 2)
C_{pcv}: Cs concentration in the PCV gaseous phase	$C_{pcv} = \alpha \times C1 + (1-\alpha) \times C2$	(Eq. 3)

where

C_{water}: Cs concentration in the condensate water collected (measured) (Table 1)

$C_{sampledgas}$: Cs concentration in the sampled gas (measured) (Table 2)

T_{pcv}: Atmospheric temperature in the PCV (Table 3)

T_{sample}: Atmospheric temperature in the temporary sampling rack (Table 3)

ρ_{vapor} (T_{pcv}): Vapor density at temperature T_{pcv}

ρ_{water} (T_{sample}): Water density at temperature T_{sample} ($\fallingdotseq 1$)

α: Vapor fraction (Table 6, Table 7)

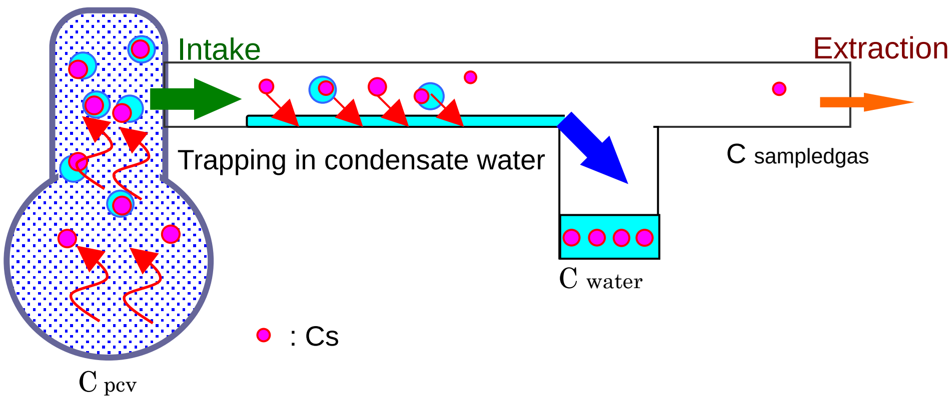

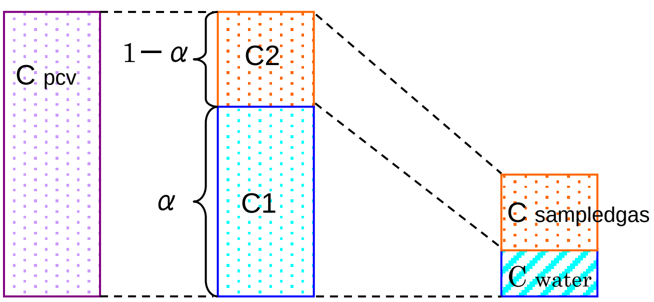

C1: Cs concentration in vapor

C2: Cs concentration in gases

C_{pcv}: Cs concentration in the PCV gaseous phase

C_{water}: Cs concentration in the condensate water collected

$C_{sampledgas}$: Cs concentration in the sampled gas

α: Vapor fraction

Figure 5　Conversion to in-PCV concentrations

Table 1　Concentrations in the condensate water collected (measured): C_{water}

		Radioactivity concentrations (Bq/mL)		
Nuclide (half-life)		Unit-1 Condensate water collected (9/14)	Unit-2 Condensate water collected (8/9)	Unit-1 Condensate water collected (7/29)
Cs-134 (about 2 years)	Set 1	3.8×10^2	6.9×10^2	
	Set 2	3.8×10^2	3.1×10^2	
	Set 3	3.4×10^2	4.9×10^2	
Cs-137 (about 30 years)	Set 1	4.2×10^2	7.3×10^2	
	Set 2	4.4×10^2	3.2×10^2	
	Set 3	4.2×10^2	5.1×10^2	
Note		—	—	Condensate water not confirmed, not collected

Table 2　Concentrations in the gas collected (measured): $C_{sampledgas}$

		Radioactivity concentrations (Bq/mL)		
Nuclide (half-life)		Unit-1 sampled gas collected (9/14)	Unit-2 sampled gas collected (8/9)	Unit-1 sampled gas collected (7/29)
Cs-134 (about 2 years)	Set 1	2.8	N.D.*	1.7×10^1
	Set 2	3.9	8.2×10^{-1}	
	Set 3	3.6	8.2×10^{-1}	
Cs-137 (about 30 years)	Set 1	3.4	7.0×10^{-1}	2.0×10^1
	Set 2	5.4	9.6×10^{-1}	
	Set 3	4.6	N.D.	

* N.D. means "Not detected,"

Table 3　Sampling temperatures

	Unit-1 sampled gas collected (9/14)	Unit-2 sampled gas collected (8/9)	Unit-1 sampled gas collected (7/29)
Temperatures of sampling environment: T_{sample}	25 deg C	26 deg C	26 deg C
D/W temperatures*: T_{pcv}	85 deg C	107 deg C	96 deg C

* Set as the vapor saturation temperature (at 127 kPaa of D/W pressure) for Unit-2, by assuming the D/W atmosphere was vapor.

For Unit-1, set as the seal bellows temperature, because the sampling point was high up in the RPV.

Table 4 Cs concentrations in vapor (converted from concentrations in the condensate water collected): C1 (from Eq. 1)

		Radioactivity concentrations (Bq/mL)		
Nuclide (half-life)		Unit-1 (9/14)	Unit-2 (8/9)	Unit-1 (7/29)
Cs-134 (about 2 years)	Set 1	1.4×10^{-1}	5.2×10^{-1}	
	Set 2	1.4×10^{-1}	2.3×10^{-1}	
	Set 3	1.2×10^{-1}	3.7×10^{-1}	
Cs-137 (about 30 years)	Set 1	1.5×10^{-1}	5.5×10^{-1}	
	Set 2	1.5×10^{-1}	2.4×10^{-1}	
	Set 3	1.5×10^{-1}	3.9×10^{-1}	

Table 5 Cs concentrations in gases (converted from concentrations in the gas collected): C2 (from Eq. 2)

		Radioactivity concentrations (Bq/mL)		
Nuclide (half-life)		Unit-1 (9/14)	Unit-2 (8/9)	Unit-1 (7/29)
Cs-134 (about 2 years)	Set 1	2.4	N.D.	1.4×10^{1}
	Set 2	3.2	6.4×10^{-1}	
	Set 3	3.0	6.4×10^{-1}	
Cs-137 (about 30 years)	Set 1	2.8	5.5×10^{-1}	1.6×10^{1}
	Set 2	4.5	7.6×10^{-1}	
	Set 3	3.9	N.D.	

Table 6 Vapor fractions estimated from total gas volume extracted and condensate water volume collected (Unit-1, September 2011)

	Total gas volume extracted	→ Temperature corrected	Condensate water collected	→ Converted to vapor volume	Vapor fraction: α
Set 1	490 L	587 L	25mL	7.07E4 mL	0.11
Set 2	396.3 L	475 L	30mL	8.48E4 mL	0.15
Set 3	348.7 L	418 L	95mL	2.69E5 mL	0.39

Table 7 Vapor fractions estimated from total gas volume extracted and condensate water volume collected (Unit-2, August 2011

	Total gas volume extracted	→ Temperature corrected	Condensate water collected	→ Converted to vapor volume	Vapor fraction: α
Set 1	9 L	11 L	550mL	7.32E5 mL	0.98
Set 2	0 L	0 L	160mL	2.13E5 mL	1.00
Set 3	87 L	111 L	150mL	2.00E5 mL	0.64

Table 8 Radioactivity concentrations in the PCV C_{pcv} (from Eq.3)

		Radioactivity concentrations (Bq/mL)		
Nuclide (half-life)		Unit-1 (9/14)	Unit-2 (8/9)	Unit-1 (7/29)
Cs-134 (about 2 years)	Total (weighted average) (*1)	1.6	0.44	4.7 to 6.0 (*2)
Cs-137 (about 30 years)	Total (weighted average) (*1)	2.0	0.46	5.5 to 6.9 (*2)
D/W temperatures		85 deg C	107 deg C	96 deg C
D/W pressures		124 kPa[abs]	127 kPa[abs]	133 kPa[abs]
Vapor fraction (*3)		About 47%	About 100%	About 66%

(*1) Three concentration measurement results of Unit-1 (9/14) and Unit-2 (8/9) were weight-averaged, that is the concentrations in the condensate water were weighted according to the amount of condensate water collected, and averaged. The concentrations in the gas were the simple average of measurements, because the amount collected in the gas vials was kept constant at all sampling times. The sample with radioactivity concentrations below the detection limits was excluded from the averaging.

(*2) Condensate water was not collected in Unit-1 (7/29). Values here were obtained by referring to the values of Unit-1 (9/14) and are the values when 40 to 4000 Bq/mL were assumed for Cs-134 and Cs-137 in the condensate water.

(*3) The vapor fraction was set as the ratio of the saturation pressure at the D/W temperature and the D/W pressure itself (Unit-1), and as just-saturated (Unit-2).

3.3. Estimation of the conditions in the RPV from the in-PCV gas analyses

Table 8 shows the radioactivity concentrations (Cs-134 and Cs-137) in the in-PCV gases are higher for Unit-1 than for Unit-2. Simple comparisons are not possible because of a potential difference in Cs discharge rates due to different vapor fractions and temperatures in the PCV gases; that said, the results are consistent with other evaluations suggesting larger damage to the RPV of Unit-1 than the Unit-2 PCV.

The scheme in Figure 6 points to the following. Cs discharged in the process of fuel melting in the early stage of the accident is considered to have mostly deposited on the RPV, PCV, in-RPV structures and other structures, or been transferred to the liquid phase. Cs in the PCV gases and in liquid is considered to have been released from the leaked gases, because significant leaks from PCV gases and liquid have been suggested by other evaluations. Therefore, the Cs in the PCV gases is considered to come mainly from additional releases from the reevaporated deposited materials.

According to the results of radioactivity analysis of sampled PCV gases, Cs concentrations in the Unit-1 PCV gases are higher than those in Unit-2 PCV gases. On the other hand, the temperature readings in the PCV are lower at Unit-1 at the time of sampling than those at Unit-2 at the time of sampling. This may indicate, as the reason for higher Cs concentrations in the PCV gases of Unit-1 than of Unit-2, that the amount of Cs discharged from fuel in the early stage of the accident is larger at Unit-1 than at Unit-2 and therefore the amount deposited, the main source of the current Cs release, is larger at Unit-1 than at Unit-2. The fraction of fuel being relocated to the PCV is larger for Unit-1 than for Unit-2 which also supports this estimation.

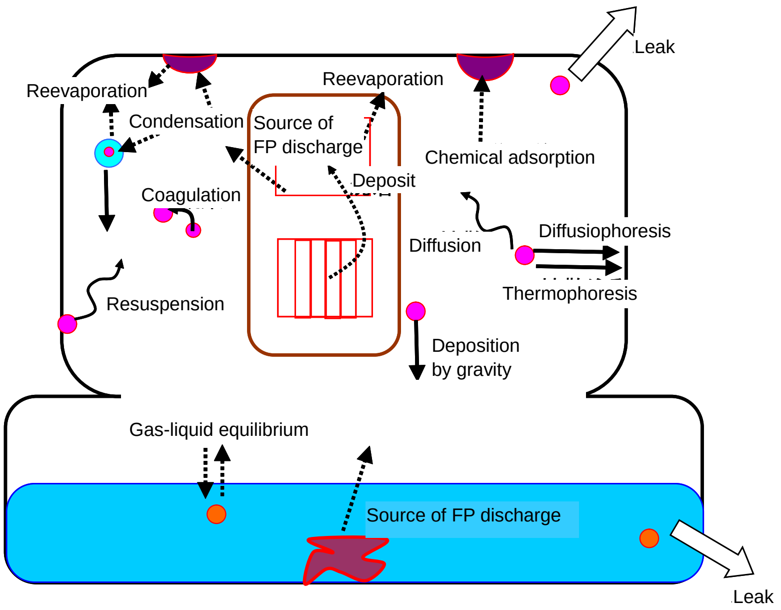

Figure 6　Scheme of the FP discharge mechanism

Attachment-7

Operability checks of local power range monitor (LPRM) detectors (Unit-2, Unit-3)
(Attempt to estimate core conditions from LPRM data)

1. Introduction

Time domain reflectometry (TDR) analyses of signal wave profiles of in-core instrumentation detectors (local power range monitor (LPRM), startup range neutron monitor (SRNM), source range monitor (SRM) may locate the position where the instrumentation lines were damaged (either short-circuited or disconnected). If the damage position is located in the core region, the damage can be considered to have indicated the fuel damage conditions. The information may be useful in estimating directly the damaged core conditions. The TDR analysis of Unit-2 and Unit-3 LPRM signals was conducted in October 2011.

The TDR analyses of Unit-1 detectors were not conducted and are not planned as of now (November 2011) from the following reasons: a superimposed voltage must be applied to the instrumentation lines to get signals for the TDR analysis but such a voltage cannot be applied where hydrogen is present at a concentration above its flammable limit; the hydrogen concentration in the Unit-1 reactor pressure vessel (RPV) would be relatively higher than those in Unit-2 and Unit-3 as of October 2011, because Unit-1 had been cooled to lower temperatures than Unit 2 and Unit-3 by that time; the TDR signal acquisition at Unit-1 had been suspended, until the advantages and disadvantages of TDR analysis were to be evaluated from the results of Unit-2 and Unit-3, but the results of Unit-2 and Unit-3 were found to be unsatisfactory.

2. Outline of TDR wave profile measurements

The TDR is a method to observe signal echo characteristics, when an instantaneous signal is sent to the in-core instrumentation detectors from the main control room and echoed back, by the measurement of characteristic impedances. The features of characteristic impedance may help locating the damage points of the instrumentation lines.

Figure 1 illustrates the layout of measurement devices from the main control room to the detectors and the TDR wave profiles expected to be observed. The instrumentation lines run from the main control room to the detectors via a containment vessel penetration and an LPRM connector at the bottom of the reactor vessel (RPV). These components in between return characteristic echo signals, which help in locating the damaged points of instrumentation lines.

In the TDR wave profile image diagram, the X-axis corresponds to the distance from the main control room, while the Y-axis corresponds to the impedance. If the line remains intact as far as to the detectors, a constriction can be identified at the position of the PCV penetration and the LPRM connector. If the line has a disconnected or short-circuited (lowered insulation) point in between, the impedance is known to change upward or downward at the point.

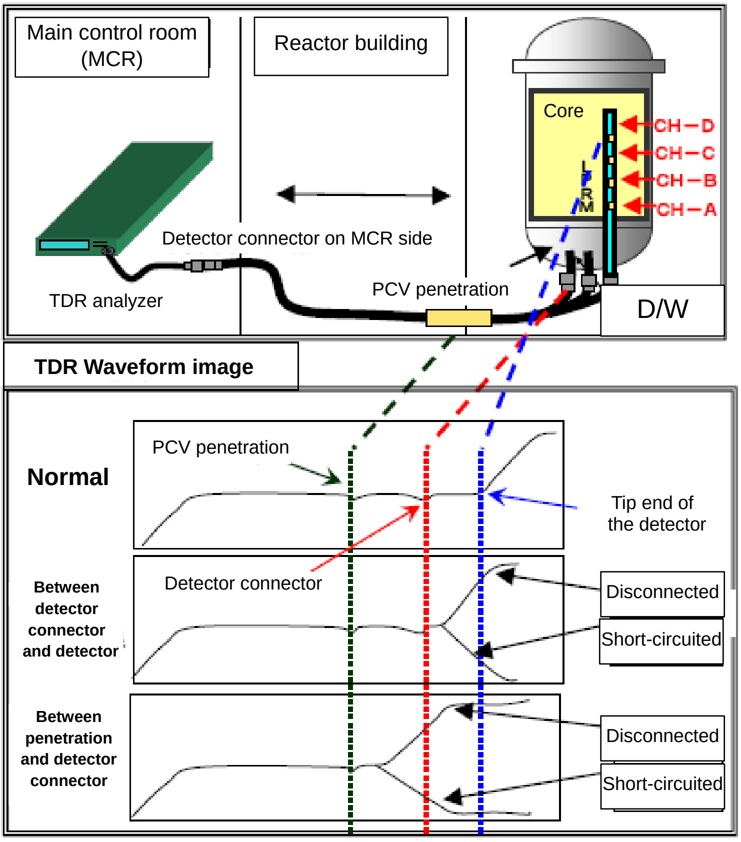

Figure 1　Layout of components from the main control room to detectors and TDR wave profiles expected to be observed (image)

3. Results of TDR wave profile measurements

3.1. Unit-2

Figure 2 is an image of the TDR wave profiles observed on the Unit-2 LPRM lines.

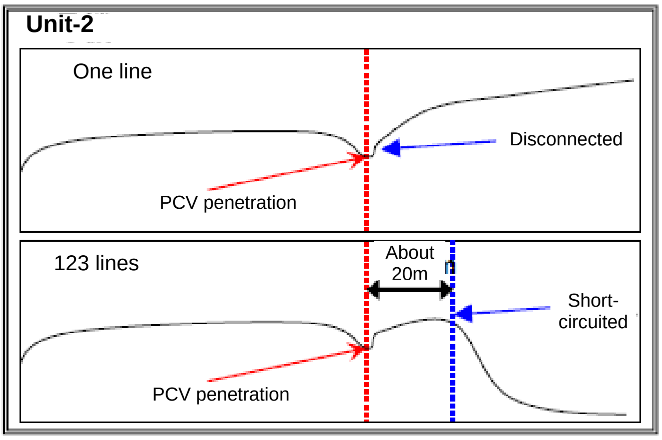

Figure 2　Unit-2 TDR profiles observed on LPRM lines (image)

The results indicated that one line had been disconnected and the remaining 123 lines had been short-circuited (lowered insulation). The disconnection point could be estimated to be near the PCV penetration by considering the distance from the main control room, while the short-circuited points could be estimated to be about 20 m beyond the PCV penetrations (near the pedestal, before the LPRM detector at the RPV bottom) (see Figure 3). No direct hints were obtained concerning the core conditions.

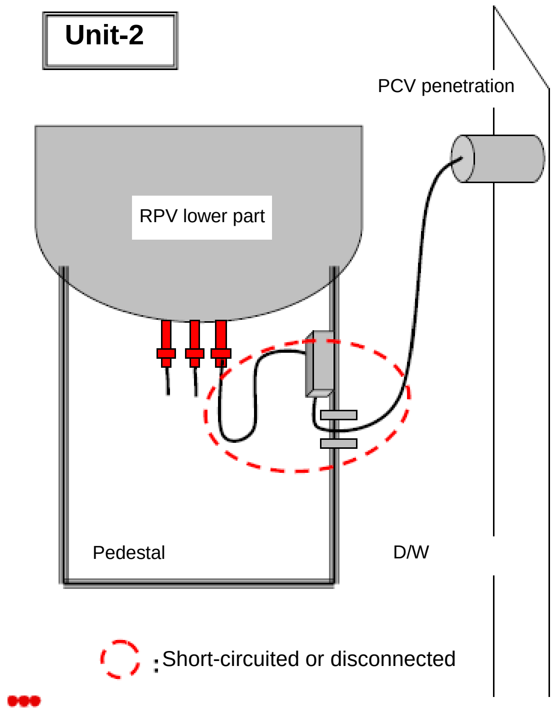

Figure 3　Estimation of short-circuited or disconnected points of Unit-2 from TDR analysis

3.2. Unit-3

Figure 3 is an image of the TDR wave profiles observed on the Unit-3 LPRM lines.

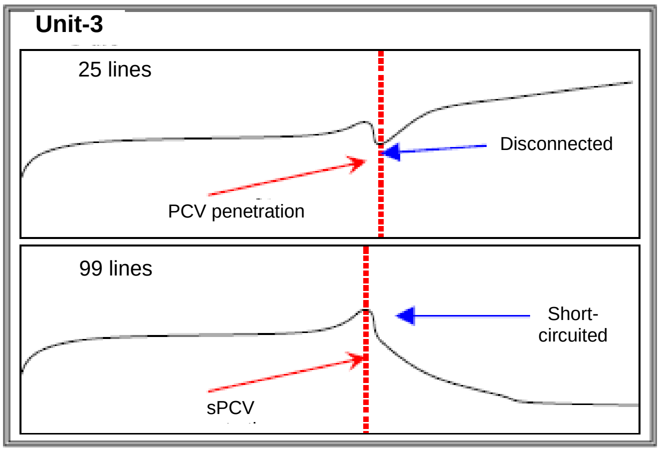

Figure 4 Unit-3 TDR profiles observed on LPRM lines (image)

The results indicated that 25 lines had been disconnected and the remaining 99 lines had been short-circuited (lowered insulation). All disconnected or short-circuited points could be estimated to be near the PCV penetrations by considering the distance from the main control room (Figure 5). No direct hints were obtained concerning the core conditions.

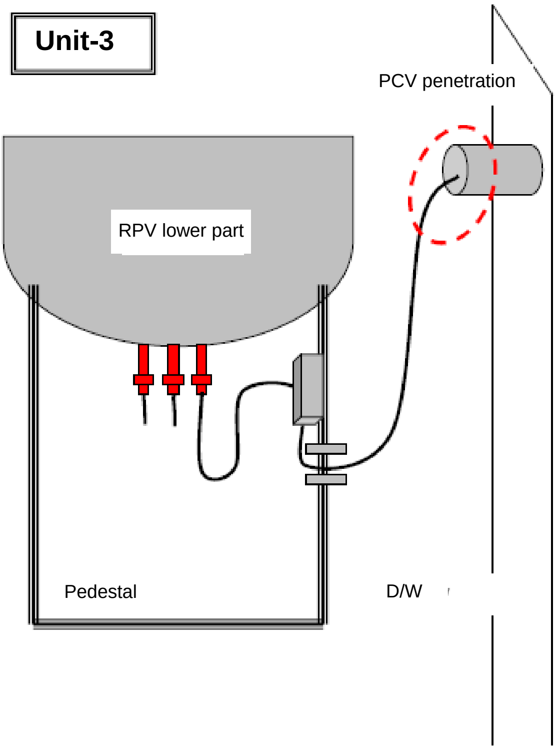

Figure 5 Estimation of short-circuited or disconnected points of Unit-3 from TDR analysis

4. Estimation of in-core conditions

The measurements were implemented with the anticipation that the information concerning the distribution of damaged points in the reactor (disconnected or short-circuited) of multiple in-core instrumentation lines might give some clues on the directional dependence of core damage and the integrity conditions of fuel remaining in the peripheral core region.

However, all instrumentation lines of Unit-2 and Unit-3 indicated their damage points (disconnected or short-circuited) were at points before the lines reached the core region. No useful information was obtained to evaluate the directional dependence of core damage or the estimated locations of integral fuel that remained.

The Unit-2 instrumentation cable, which assembled the instrumentation lines, was estimated to have been damaged near the pedestal, while the Unit-3 cable was estimated to have been damaged near the PCV penetrations. It is difficult to estimate the fuel conditions in the reactor. If the damaged fuel had been relocated, it might have damaged the cable in the RPV lower part. Elaboration is difficult as of now (November 2011) on the quantitative evaluation of the correlation between the fuel relocation and cable damage or of the relocated position of fuel.

5. Conclusions

TDR wave profiles of LPRM were measured at Unit-2 and Unit-3 with an objective of estimating core conditions.

The expectation was to estimate core conditions from the information of locations and other response signals of undamaged detectors. But the anticipated estimation was found to be quite difficult to achieve, because there were no intact detectors.

After the unsuccessful attempt using the LPRM detectors for this purpose, attempts with the SRNM or SRM also resulted in similar unsuccessful outcomes. As of now (November 2011), conducting additional attempts is considered not to be meaningful due to the increased radiation exposure for such work.

End

Condition checks of control rod position indicator probe (PIP) (Unit-1, Unit-3)
(Attempt to estimate core conditions from control rod position indicator probe (PIP) data)

1. Introduction

At boiling water reactors (BWRs) control rods are designed to be partly inserted in various profiles in the core during operation. Each control rod is equipped with a control rod position indicator probe (PIP) and its insertion depth is continually monitored during normal reactor operations. All control rods are known to have been fully inserted in a reactor scram immediately after the Great East Japan earthquake. In the accident progression process thereafter, the core was damaged, and part of the core fuel melted and was relocated downward. Some control rods and control rod drive mechanisms (CRDs) below them might have been damaged also. If a CRD was damaged, the PIP mounted on it would have been damaged, too. If a PIP indicates readings other than “fully-inserted” or unrealistic readings, it might hint at damage conditions at the bottom part of the reactor vessel (RPV). From this background, PIP conditions were checked at Unit-1 and Unit-3 in September 2011.

The condition check of Unit-2 PIPs was not conducted from the following reasons: Unit-2 PIPs needed to be operated from a local control panel, while Unit-1 and Unit-3 PIPs could be operated in the main control room; the Unit-2 PIP condition check had been suspended, until the advantages and disadvantages of Unit-1 and Unit-3 PIP condition checks were to be evaluated; but the results of Unit-1 and Unit-3 were found to be unsatisfactory. As of now (November 2011), the Unit-2 PIP condition check is not planned.

2. Outline of PIP condition checks

A PIP is located near the CRD at the RPV bottom (Figure 1). The control rod position (inserted depth) is detected upon the reaction of the permanent magnet mounted on the CRD and one of the lead switches vertically arranged on the PIP.

Normally, after the reactor is scrammed, lead switches “00 (Control rod No. 4 position indication unit at ‘fully inserted’)” and “51 (All control rod in-core position indication unit at ‘fully inserted’)” react to the permanent magnet, and other lead switches (for example, “48 (Control rod No. 4 position indication unit at ‘fully withdrawn’)” or “20 (Control rod No. 4 position indication unit at ‘partly inserted’)” should not react. If conduction states different from such normal states can be recognized, clues might be obtained to estimate conditions in the reactor or the RPV bottom.

In the current check work, conduction states were checked on lead switches “00,” “51,” and “48,” which should have indicated unique positions, and on the lead switch “20” as a position indicator unit representing other lead switches arranged at mid-positions.

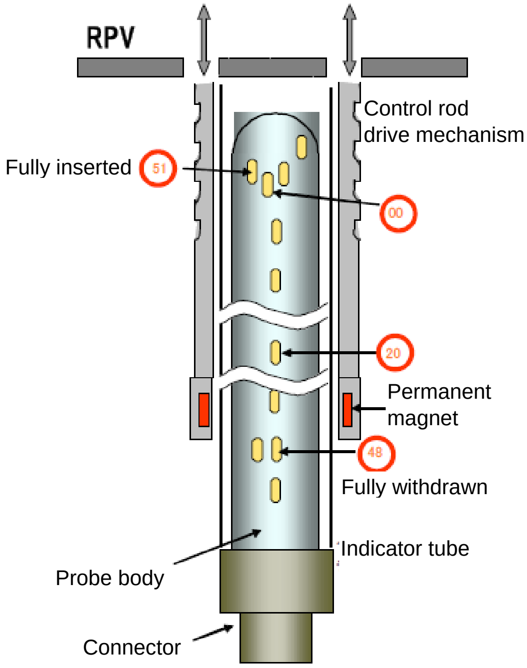

Figure 1 Illustrated structures of control rod drive mechanism (CRD) and control rod position indicator probe (PIP)

3. Results of PIP condition checks

Conduction states of lead switch contact points of each control rod were checked, which confirmed conductions at several contact points. The results were categorized into the following.

A: Conductions at 4 contact points

C: Conductions at 2 contact points only at the fully inserted position

D: No conductions at all 4 contact points

In: Conduction only at the inserted position

Dr: Conduction only at the withdrawn position

20: Conduction only at Position 20

00: Conduction only at Position 00

?: Conductions at more than 2 contact points other than the fully inserted position

3.1. Unit-1

Figure 2 shows the PIP condition check results of all control rods of Unit-1.

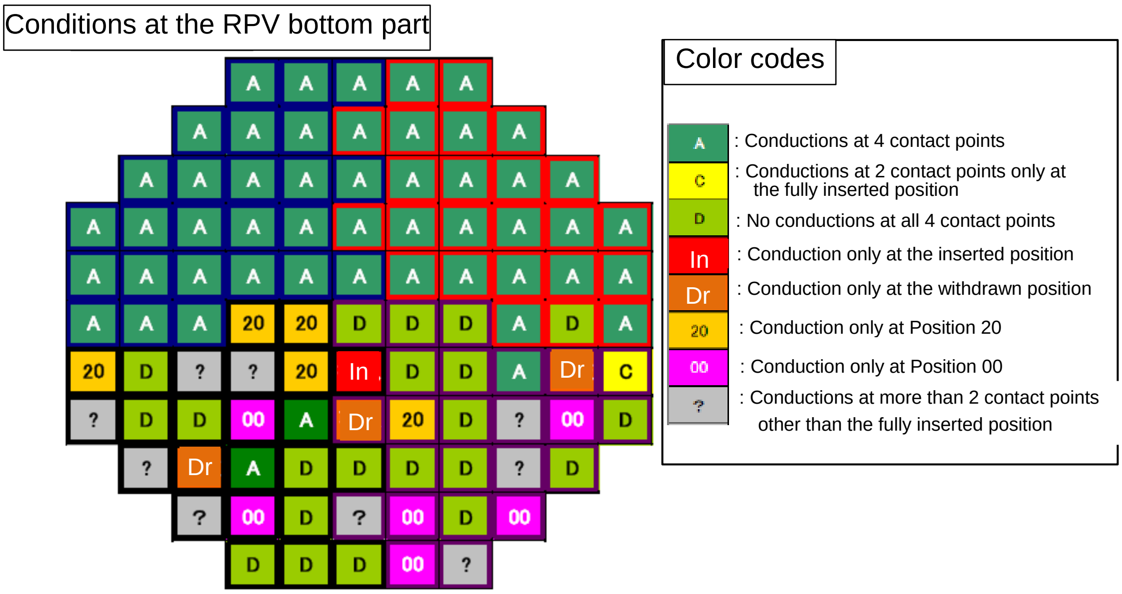

Figure 2 PIP conduction states check results (Unit-1)

One PIP marked as “C” on the right side of the figure indicated “normal.” But all other PIPs were categorized as “unusual.” Several PIP cables penetrated the containment vessel (PCV) in a bundle (PIP cables penetrating the PCV at a particular penetration are colored as either red, blue, violet or black boxes in the figure). PIPs penetrating the same PCV penetration seemed to show a similar tendency. For example, all control rods in red boxes in the upper right were “A,” and all control rods in blue boxes in the upper left were “A,” too. Control rods in violet boxes in the lower right were randomly categorized, so were the control rods in black boxes in the lower left. From this observation, the information obtained from the measurement of PIP conditions is more likely to have indicated the conditions at the position of the PCV penetrations, rather than at the RPV lower part.

3.2. Unit-3

Figure 3 shows the PIP condition check results of all control rods of Unit-3.

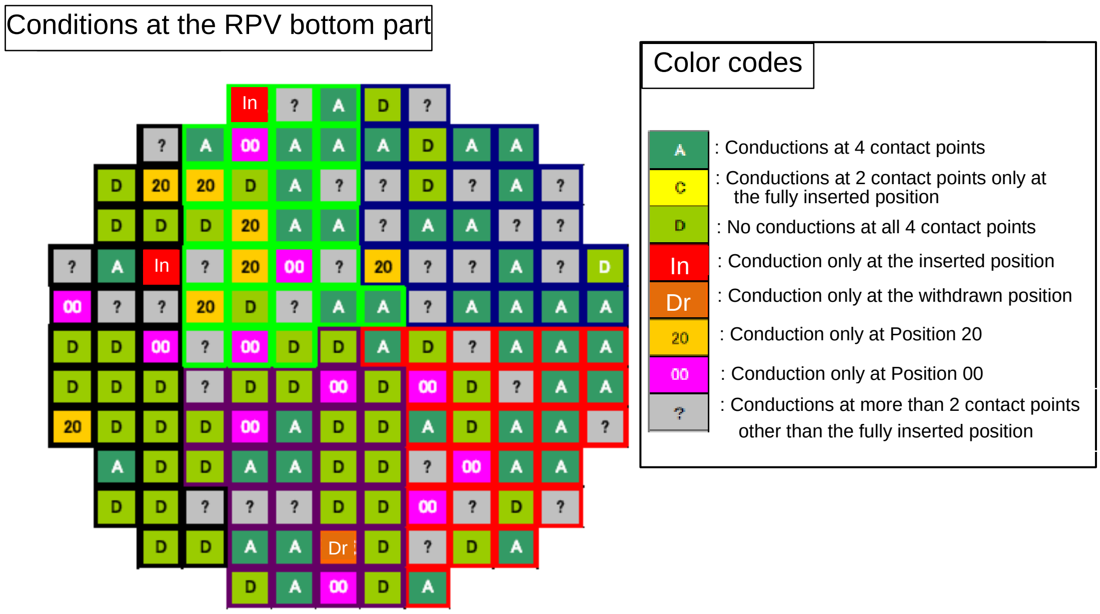

Figure 3 PIP conduction states check results (Unit-3)

No PIP was marked as "C," i.e., all control rods were categorized as "unusual." No correlation was identified, either, between PIP cables penetrating the PCV at the same penetration (represented in either red, blue, violet, yellow-green or black boxes in the figure), as had been observed at Unit-1 (See 3.1).

4. Estimation of in-core conditions

The overall view of the upper right and upper left of Figure 2 for Unit-1 indicated the high likelihood of PIP cable damage near the point where the cables were bundled (near the PCV penetration). This information was not helpful to estimate the conditions at the upper right or upper left region of the RPV bottom part or the conditions in the reactor. On the other hand, no meaningful features were recognized in the lower half of Figure 2, either, and the damage conditions at the RPV bottom part could not be estimated. One "normal" PIP could be confirmed but was not helpful to estimate in-reactor conditions, because no correlation with the states of PIPs around it was confirmed.

The overall view of Unit-3 reactor in Figure 3 indicated that the right half tended to be short-circuited, while the left half tended to be disconnected, although these tendencies were not clearly noticeable. Some PIPs in the right half could be estimated to be disconnected, and some PIPs in the left half could be estimated to be short-circuited. It is difficult as of now (November 2011) to estimate conditions in the reactor and RPV bottom part from the information at this stage. PIPs transfer their signals outside the PCV through one of five PCV penetrations. A similar tendency was recognized among PIPs penetrating the PCV at one penetration, but the tendency was not clear enough to draw conclusive estimations.

5. Conclusions

PIP conditions of Unit-1 and Unit-3 were checked in order to estimate conditions in the reactor and the RPV bottom.

Attempts were made to estimate the conditions in the reactor and the RPV bottom from PIP conduction states but they were unsuccessful.

Similar attempts at Unit-2 will result in outcomes similar to those of Unit-1 and Unit-3. It is considered as of now (November 2011) that the benefit of additional investigation work at Unit-2 would not be able to overcome the disadvantage of exposure dose for the work.

End

Results of condition checks and behavior of drywell (D/W) sump thermometers

1. Conditions checked

(1) Unit-1 (checked on September 23, 2011)

Tag No.	Average line resistance (A)	Average line resistance at the time of periodic maintenance (B)	A/B	Result of direct current resistance (*)	TE temperatures
TE-2001-412	60.5Ω	76.1Ω	0.795	Insulation resistance decrease	36.6℃

(2) Unit-2 (checked on November 15, 2011)

Tag No.	Average line resistance (A)	Average line resistance at the time of periodic maintenance (B)	A/B	Result of direct current resistance (*)	TE temperatures
TE-20-362	∞	144.6Ω	—	Disconnected	—

(3) Unit-3 (checked on November 15, 2011)

Tag No.	Average line resistance (A)	Average line resistance at the time of periodic maintenance (B)	A/B	Result of direct current resistance (*)	TE temperatures
TE-20-362	54.3Ω	60.9Ω	0.892	Insulation resistance dropped	39.9℃

(*) Criteria for evaluating direct current resistance

Good: 1.1≧R≧0.9, where R=A/B=Resistance measured/Normal resistance

Insulation resistance dropped: R<0.9

Disconnected: R>1.1

2. Thermometer readings behavior

(1) Unit-1

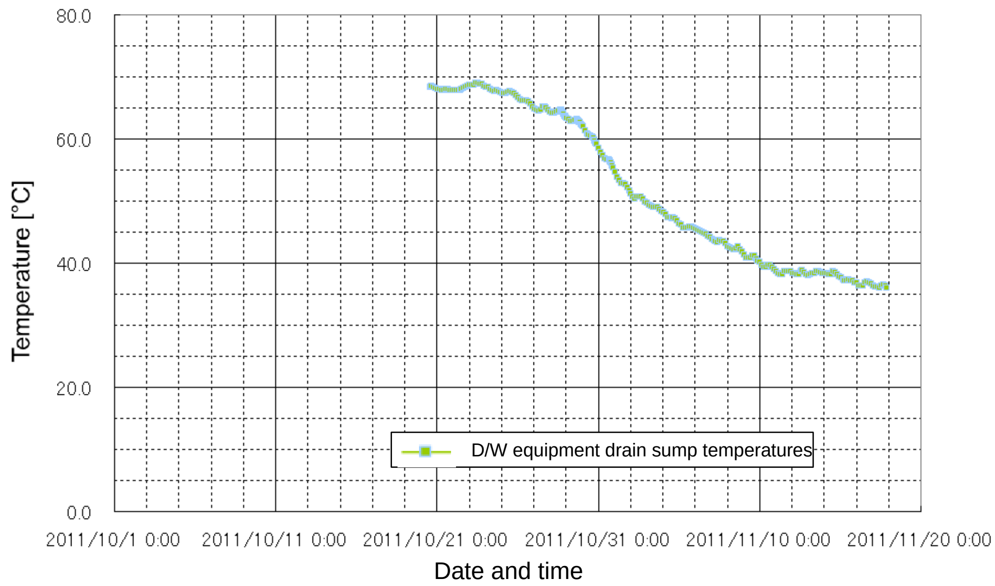

Figure 1 D/W equipment drain sump temperature behavior (Unit-1)

(Data acquisition started on October 20, 2011 with a digital recorder)

(2) Unit-2

Data acquisition failed due to the instrumentation line disconnection.

(3) Unit-3

Reporting is omitted because data have not yet been sufficiently accumulated since the start of their collection.

End

Results of condition checks and behavior of PLR pump inlet thermometers

1. Conditions checked

1.1. Unit-1 (checked on November 22, 2011)

Tag No.	Average line resistance (A)	Average line resistance at the time of periodic maintenance (B)	A/B	Result of direct current resistance (*)	TE temperatures
TE-261-8A	43.5Ω	56.0Ω	0.78	Insulation resistance decrease	39.2℃
TE-261-8B	43.4Ω	52.7Ω	0.82	Insulation resistance dropped	41.4℃

1.2. Unit-2 (checked on November 22, 2011)

Tag No.	Average line resistance (A)	Average line resistance at the time of periodic maintenance (B)	A/B	Result of direct current resistance (*)	TE temperatures
TE-2-145A	95.5Ω	96.6Ω	0.99	Good	44.7 to 52.8℃
TE-2-145B	93.0Ω	92.4Ω	1.01	Good	50.6℃

1.3. Unit-3 (checked on November 22, 2011)

Tag No.	Average line resistance (A)	Average line resistance at the time of periodic maintenance (B)	A/B	Result of direct current resistance (*)	TE temperatures
TE-2-145A	59.2Ω	74.2Ω	0.80	Insulation resistance decrease	40.8℃
TE-2-145B	58.5Ω	66.4Ω	0.88	Insulation resistance decrease	52.1℃

(*) Criteria for evaluating direct current resistance

Good: 1.1≧R≧0.9, where R=A/B=Resistance measured/Normal resistance

Insulation resistance dropped: R<0.9

Disconnected: R>1.1

2. Behavior of thermometer readings

2.1. Unit-1

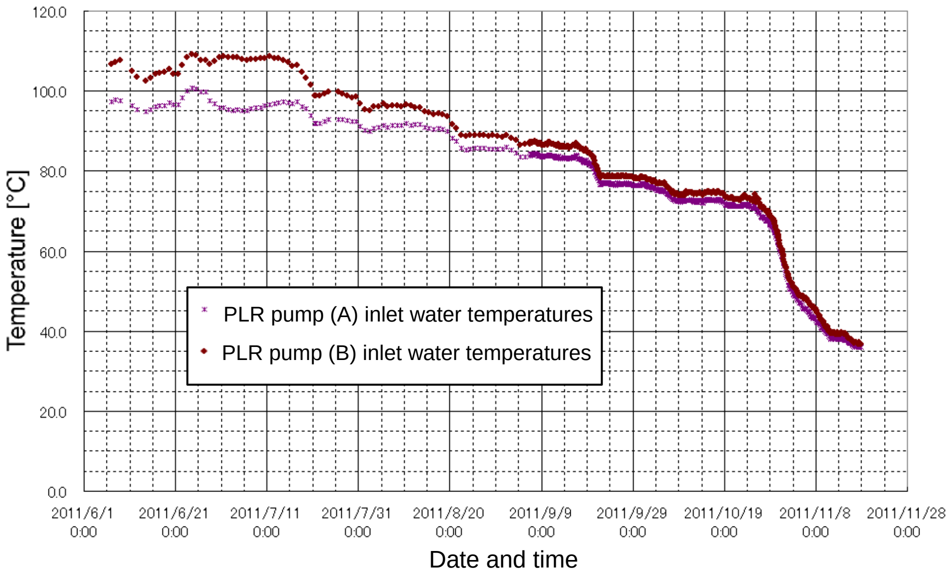

Figure 1 PLR inlet water temperature behavior (Unit-1)

2.2. Unit-2

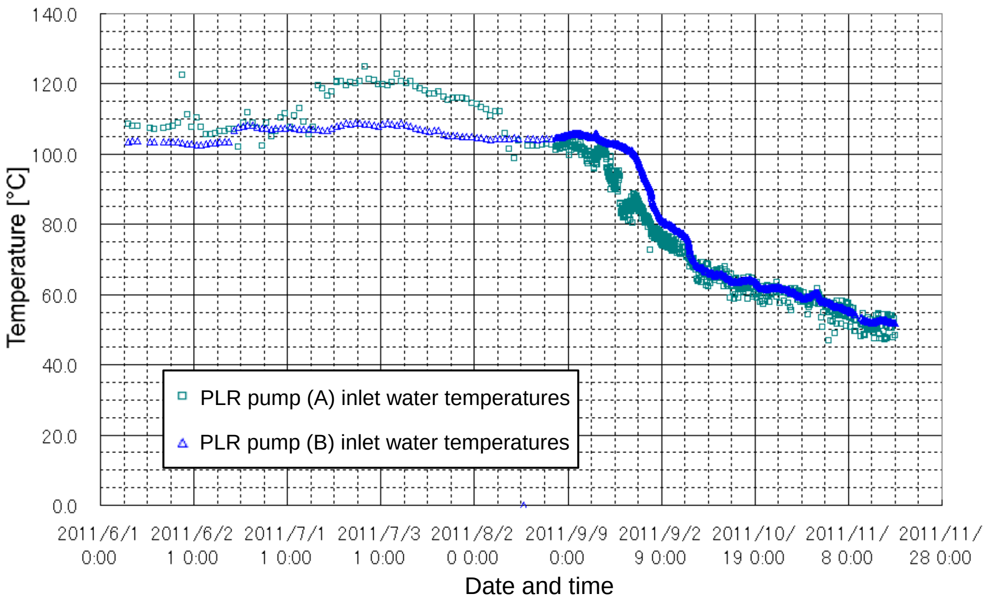

Figure 2 PLR inlet water temperature behavior (Unit-2)

2.3. Unit-3

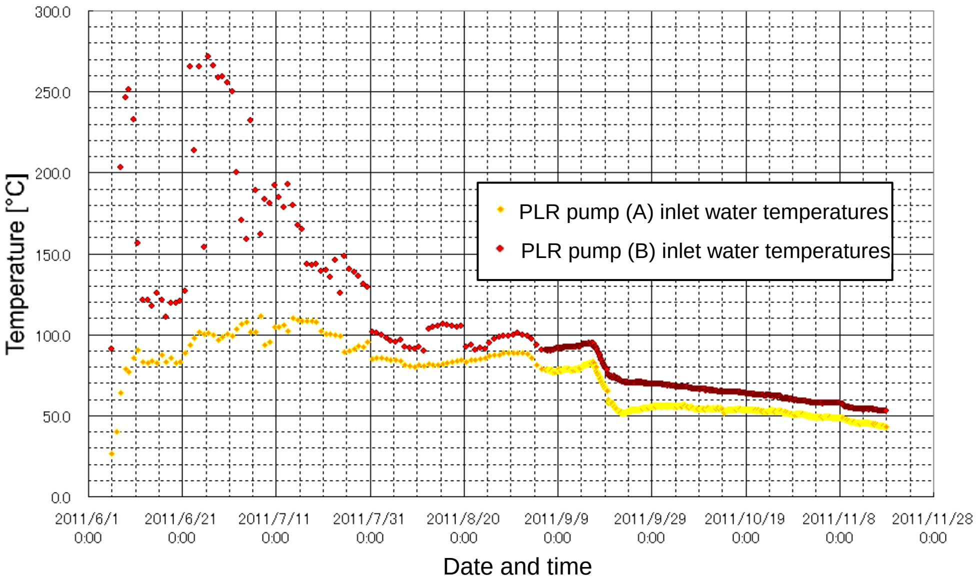

Figure 3 PLR inlet water temperature behavior (Unit-3)

End

Contamination of the reactor building closed cooling water (RCW) system

1. Unit-1 reactor building closed cooling water (RCW) system

Radiation distributions measured on May 9, 2011, at various spots in the Unit-1 reactor building (R/B) showed high dose rates on the RCW system lines (Figure 1). The RCW is a closed loop for cooling auxiliary equipment and it is unlikely to be contaminated as high as several hundreds of mSv/h in normal situations. But the RCW lines were laid widely throughout the R/B and they cooled the equipment in the containment vessel (PCV), too. As seen in Figure 2, the RCW line for drain cooling was laid in the equipment drain pit in the lower part of the PCV. Therefore, it was highly possible in Unit-1 that the molten fuel was relocated to the equipment drain pit and damaged the RCW piping and this caused the high RCW line contamination. Upon damage of the RCW piping, high dose steam and/or water is considered to have transferred to the RCW secondary system piping, accompanying radioactive materials.

Subsequent measurements of radiation doses were conducted thereafter in the R/B (Figure 3 to Figure 6). High dose rates over 1000 mSv were obtained on Unit-1 R/B Floor 2. The area of interest was where the RCW heat exchanger had been installed. Extremely high dose rates in the area were considered to have been caused by the large amount of radioactive materials deposited in the heat exchanger. A heat exchanger is the equipment to exchange heat between the primary side and the secondary side, and therefore the surface temperatures of RCW primary piping are considered to be lower than those at other parts of the primary side piping. Volatile radioactive materials such as Iodine and cesium might have deposited on the piping surfaces. This might lead to a possibility that the RCW piping damage at Unit-2 and Unit-3 could be diagnosed by comparing radiation doses in the RCW heat exchanger installation areas.

2. Unit-2 and Unit-3 RCW heat exchangers

Figure 7 to Figure 13 show radiation dose rate distributions in the Unit-2 R/B and Unit-3 R/B (where measurements were made). The RCW heat exchangers of Unit -2 and Unit-3 were both installed on Floor 2 of each R/B. Figure 10 shows the dose rate distribution on the Unit-2 R/B Floor 2, while Figure 12 shows that on the Unit-3 R/B Floor 2. The dose rates around the heat exchangers were both in the range of several tens of mSv/h, not extremely high dose rates as had been observed at Unit-1. The RCW piping in the Unit-2 PCV and Unit-3 PCV were likely not to have been damaged.

Unit-1 R/B survey results

May 14, 2011
Tokyo Electric Power Company

Survey date: 16:01 to 17:39 on May 13, 2011 (Dose rates shown in green)
11:32 to 11:58 on May 5, 2011 (Dose rates shown in blue)
04:18 to 04:47 on May 9, 2011 (Dose rates shown in red)

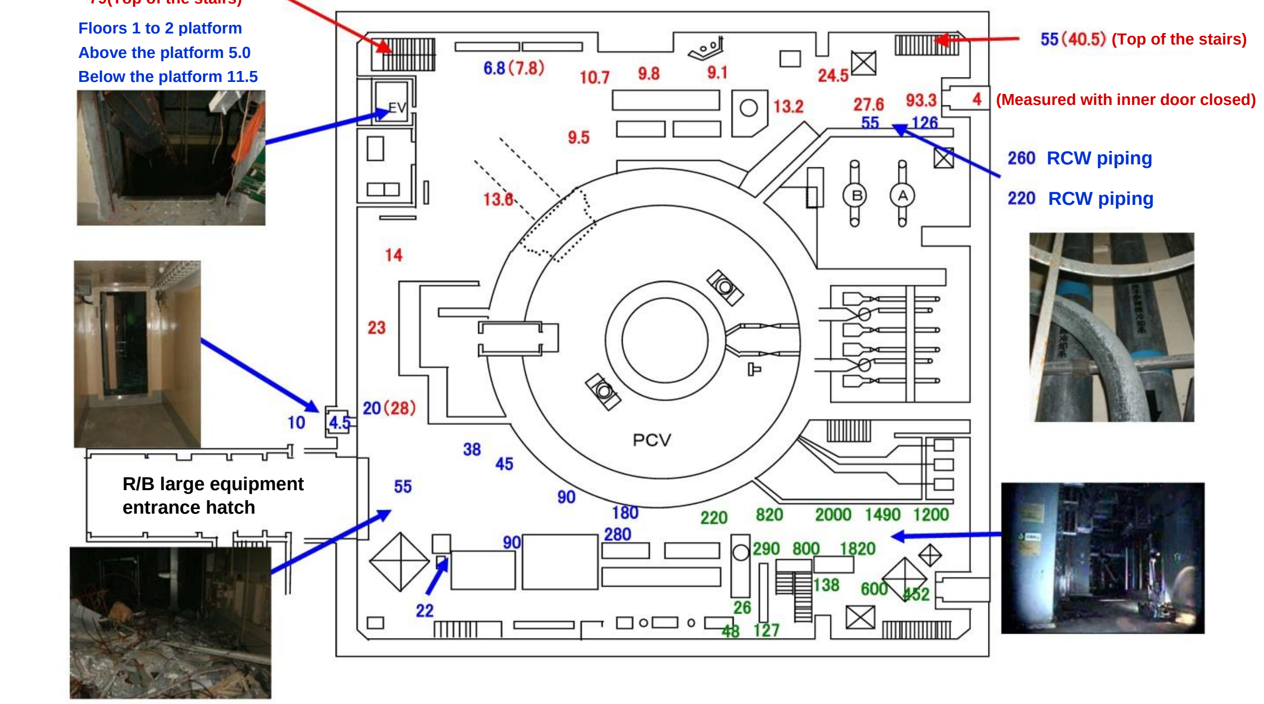

Figure 1　Unit-1 R/B dose rate survey results

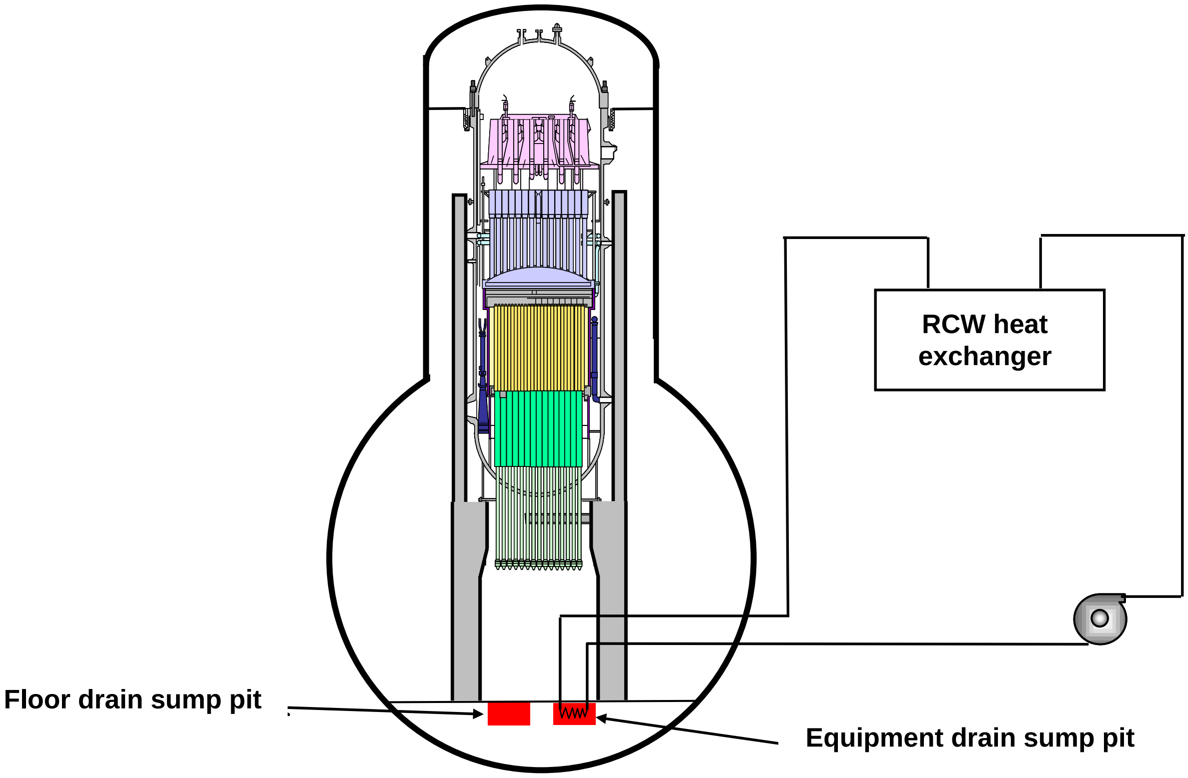

Figure 2　Schematic of interface between RCW and equipment drain pit

Unit-1 R/B Floor 4

Unit: mSv/h

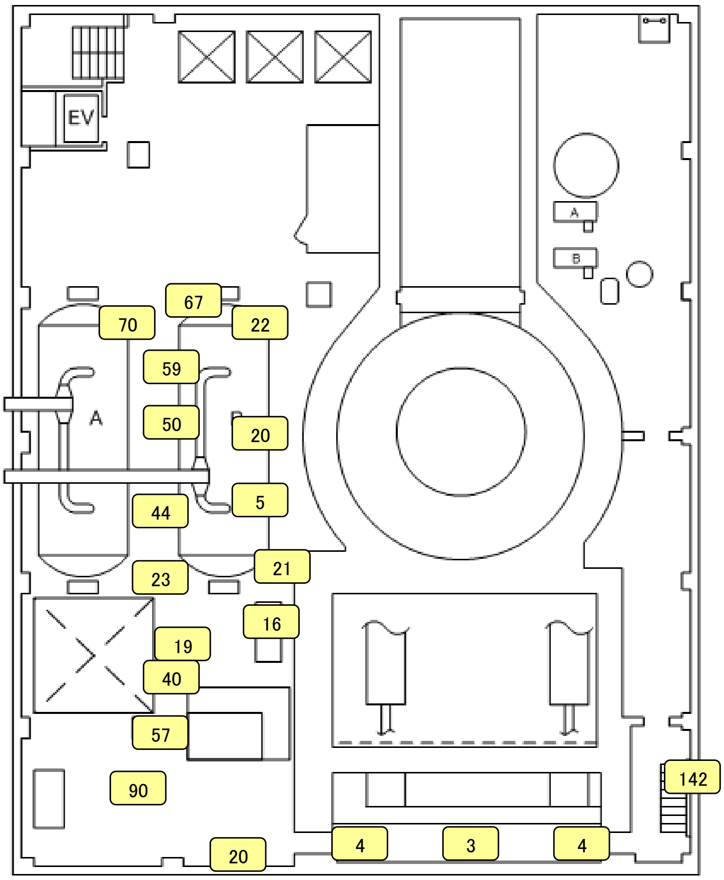

Unit-1 R/B Floor 4

Figure 3　Dose rate distribution on Unit-1 R/B Floor 4

Unit-1 R/B Floor 3

Unit: mSv/h

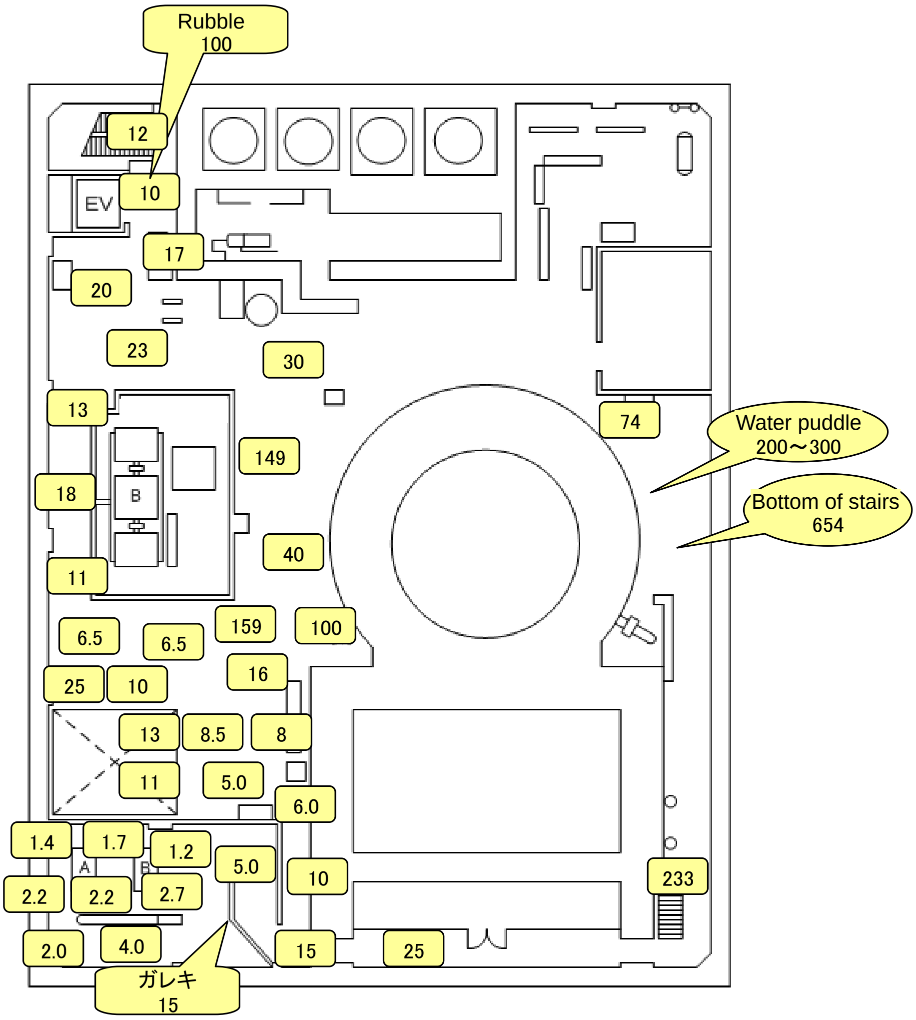

Unit-1 R/B Floor 3

Figure 4 Dose rate distribution on Unit-1 R/B Floor 3

Unit-1 R/B Floor 2

Unit: mSv/h

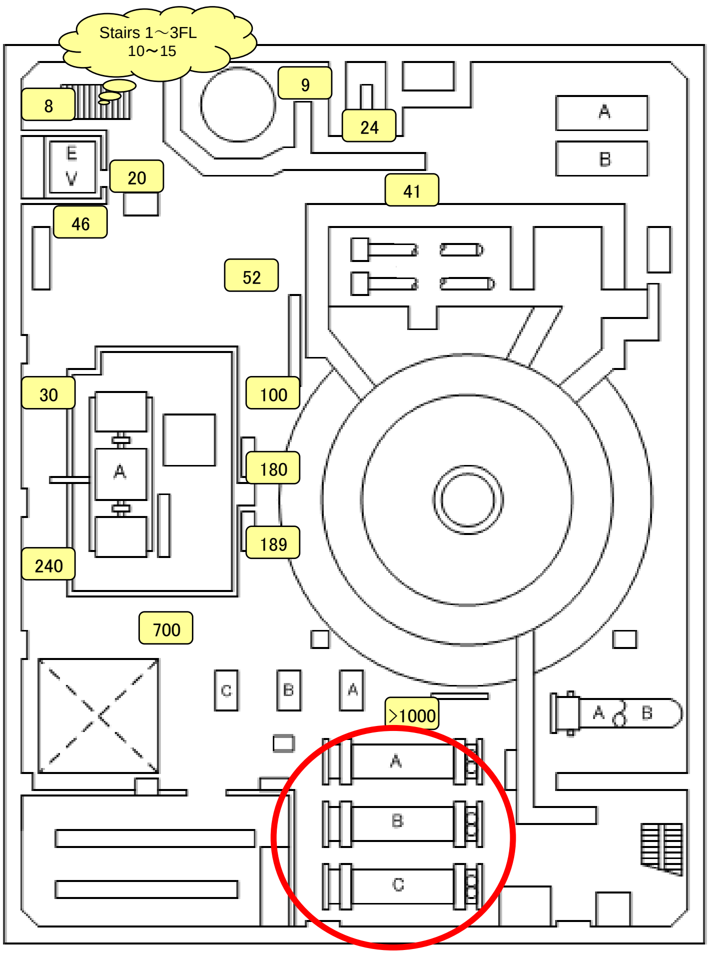

Unit-1 R/B Floor 2

RCW heat exchangers installed

Figure 5　Dose rate distribution on Unit-1 R/B Floor 2

Unit-1 R/B Floor 1

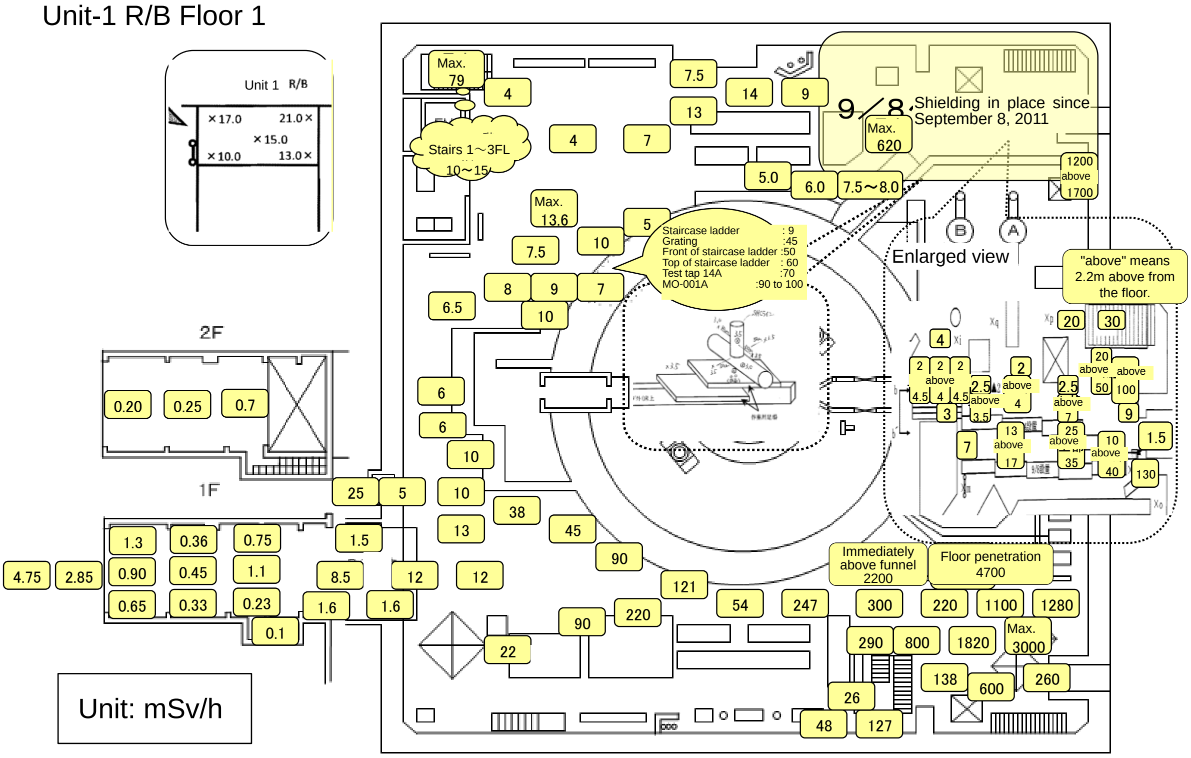

Unit: mSv/h

Unit-1 R/B Floor 1

Figure 6　Dose rate distribution on Unit-1 R/B Floor 1

Unit-2 R/B Floor 5

Unit: mSv/h

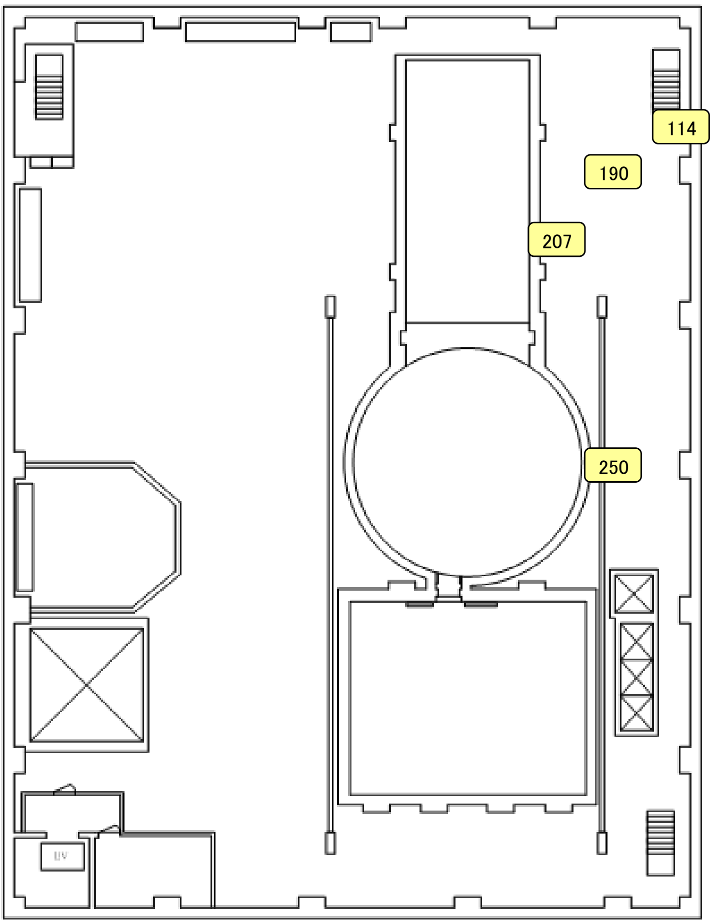

Unit-2 R/B Floor 5

Figure 7　Dose rate distribution on Unit-2 R/B Floor 5

Unit-2 R/B Floor 4

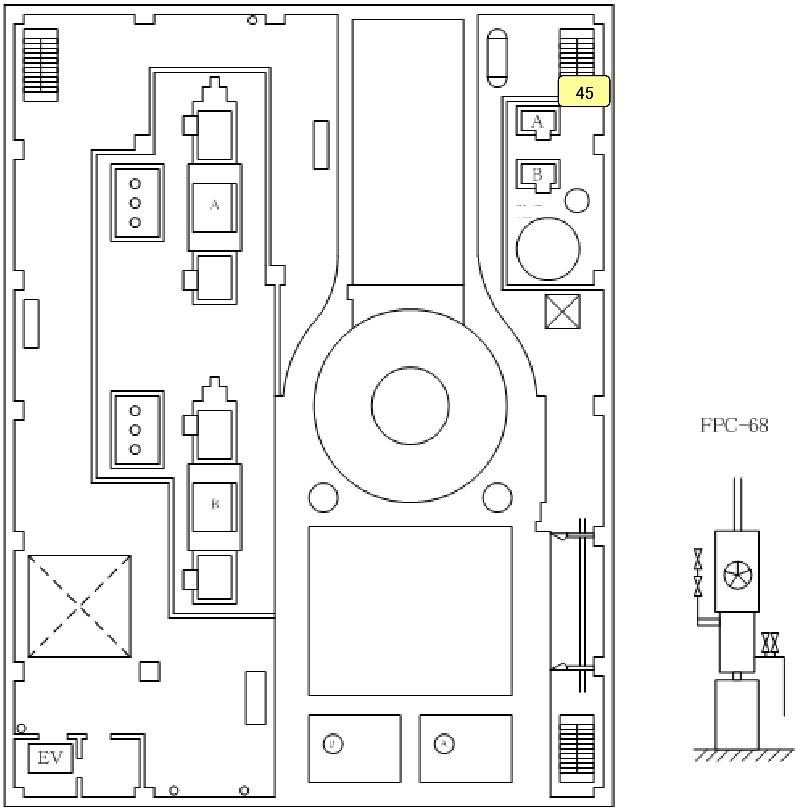

Unit: mSv/h

Unit-2 R/B Floor 4

Figure 8　Dose rate distribution on Unit-2 R/B Floor 4

Unit-2 R/B Floor 3

Unit: mSv/h

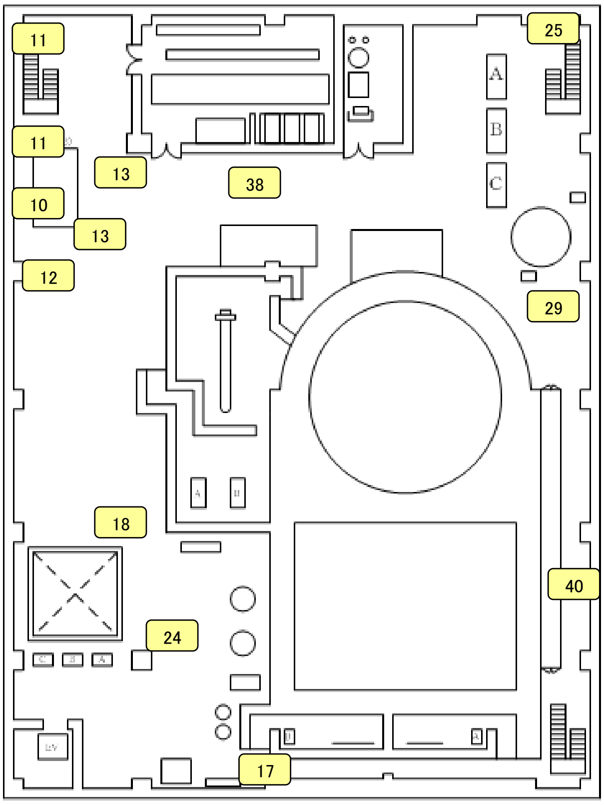

Unit-2 R/B Floor 3

Figure 9　Dose rate distribution on Unit-2 R/B Floor 3

Unit-2 R/B Floor 2

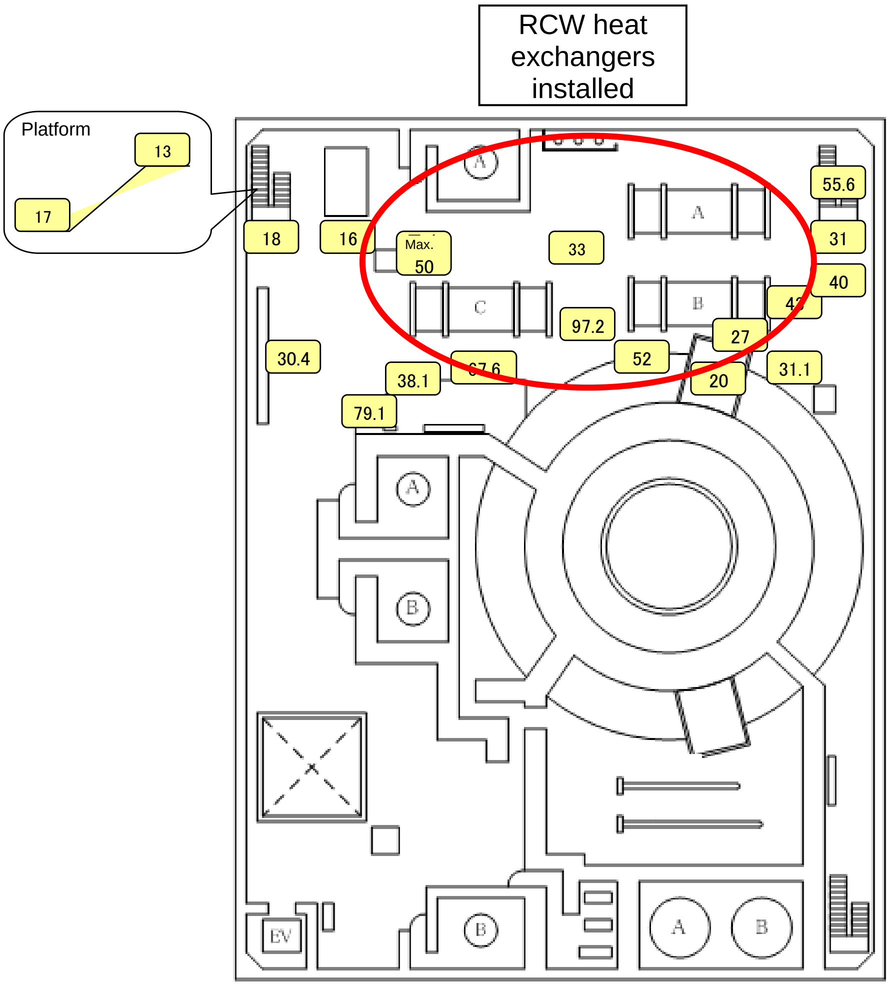

Unit: mSv/h

Unit-2 R/B Floor 2

Figure 10　Dose rate distribution on Unit-2 R/B Floor 2

Unit-2 R/B Floor 1

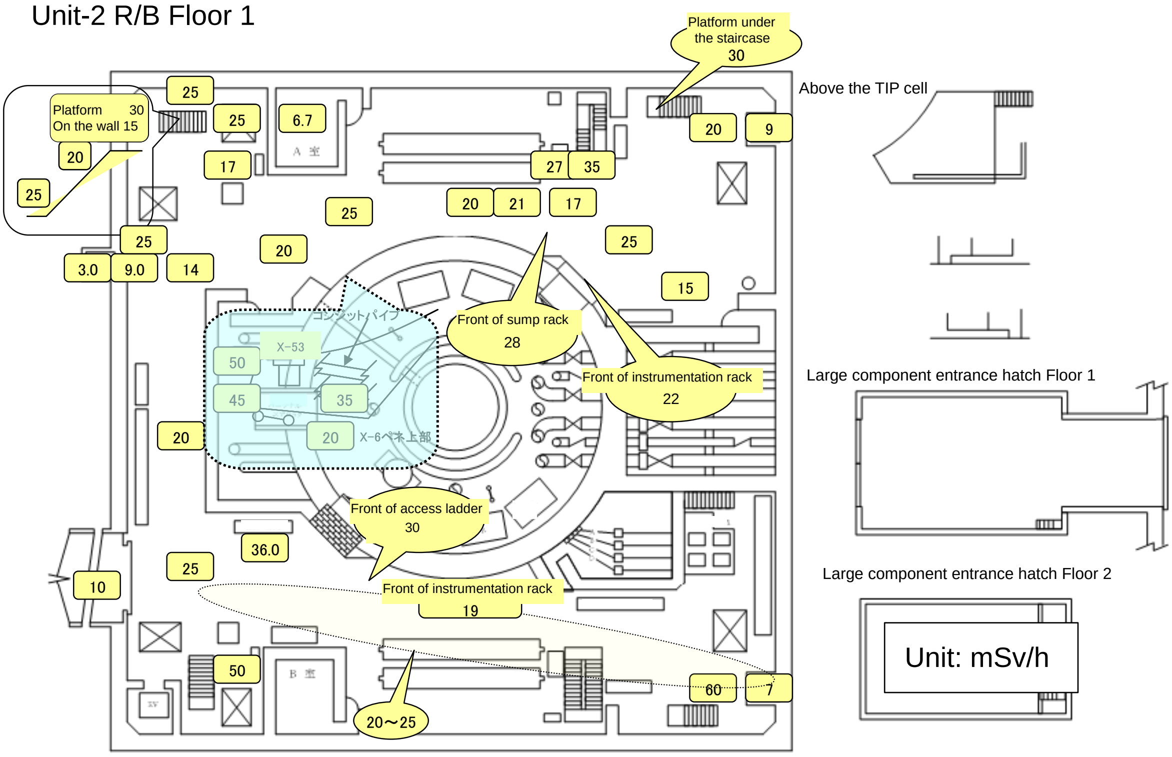

Unit-2 R/B Floor 1

Figure 11 Dose rate distribution on Unit-2 R/B Floor 1

Unit-3 R/B Floor 2

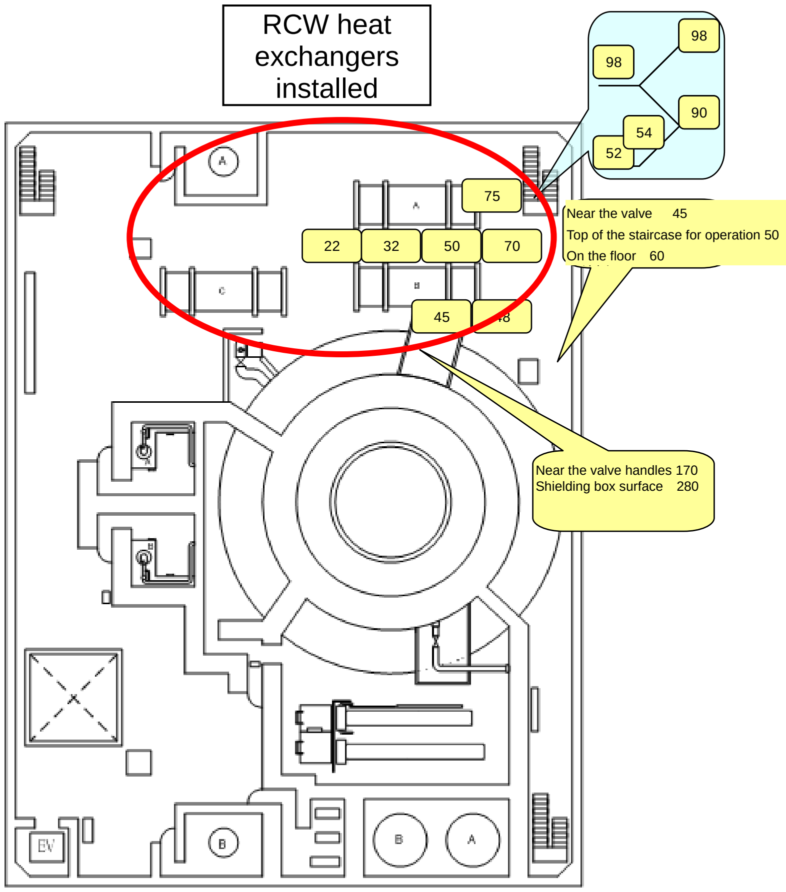

Unit: mSv/h

Unit-3 R/B Floor 2

Figure 12 Dose rate distribution on Unit-3 R/B Floor 2

Unit-3 R/B Floor 1

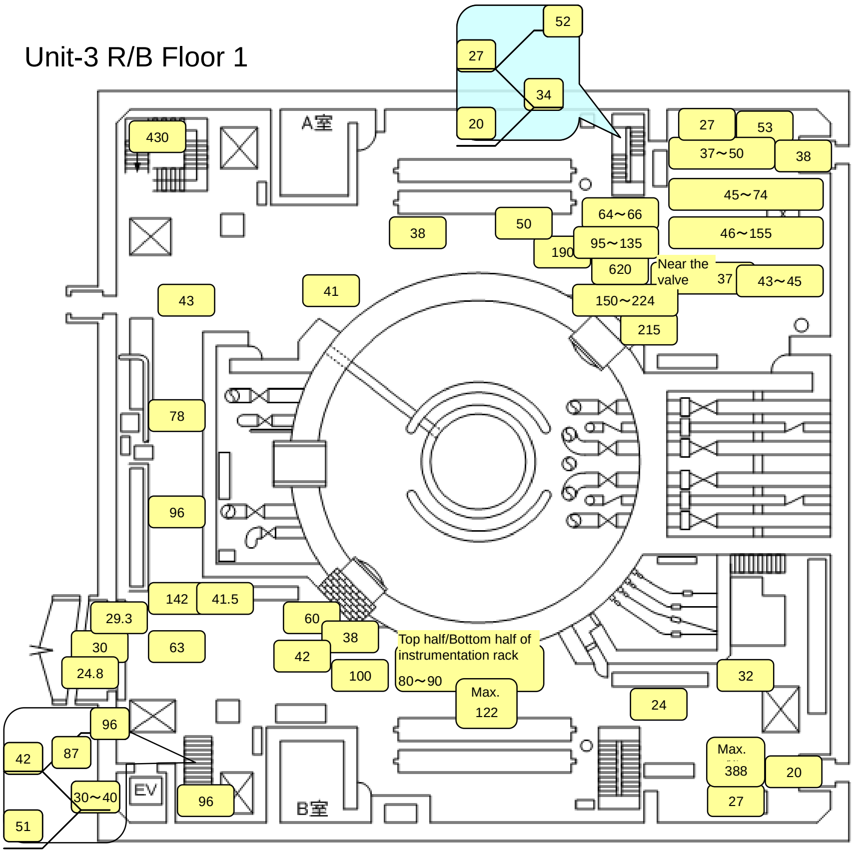

Unit: mSv/h

Unit-3 R/B Floor 1

Figure 13　Dose rate distribution on Unit-3 R/B Floor 1

End

Impacts of core-concrete reactions on the reactor containment vessel

When the damaged core melts core internal structures, melt stacks on the RPV bottom as fuel debris, and it is relocated to the reactor containment vessel (PCV) pedestal, the pedestal can be damaged due to the so-called molten core-concrete reactions (MCCI), in which the fuel debris reacts with the pedestal concrete.

This document presents review results of the impacts of MCCI on the PCV at each of Unit-1 to Unit-3.

1. Molten core-concrete reactions (MCCI)

(1) Outline of a core-concrete reaction

A core-concrete reaction is a chemical reaction in which concrete is decomposed when heated up above its melting point upon contact with high temperature fuel debris. When decomposed, the concrete generates hydrogen, carbon dioxide and other gases, while the fuel debris dissolves the residual concrete and erodes the concrete. When the fuel debris is not sufficiently cooled, and the decay heat exceeds the amount of heat to be released from its surface, the excess heat is absorbed by the concrete. When the concrete temperatures exceed its melting point, the erosion starts.

The reactions decline with time and eventually cease in a limited time in a limited erosion volume as the decay heat decreases with time and the core-concrete contact area increases in inverse proportion to the progress of erosion.

(2) Phases of core-concrete reactions development

Upon relocation of molten fuel to the reactor containment vessel (PCV), it will spread on the pedestal floor if the fluidity is maintained, part of the molten fuel further will leak out through pedestal slits and solidify as flat lumps with a large surface (Figure 1).

If there are openings on the pedestal floor, such as an equipment drain sump pit, the fuel debris may clog them heavily (Figure 2).

If water is retained on the bottom of the PCV, the molten fuel will solidify, being cooled upon contact with water, into many small lumps. Thus, there are large uncertainties in configurations and distributions of fuel debris, once the molten fuel is relocated to the PCV.

Large uncertainties also exist in the heat transfer from the fuel debris to water. Shortly after relocation, the fuel debris is considered to contact water with a solidified crust in between (Figure 3). Carbon dioxide and other gases would be generated during the concrete erosions, and these gases would build up and would crush the crust. The molten fuel underneath can erupt above the crusts and form fine grains in the water pool. Part of the coolant water may flow downward through the crushed crust and cool the fuel debris (Figure 4).

Various assumptions are thus needed, and therefore large uncertainties would be inevitable, in estimating the erosion conditions in the PCV pedestal.

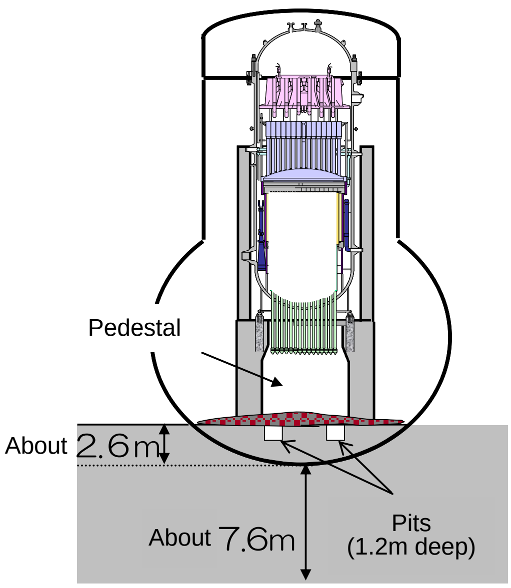

Figure 1 Estimated configuration of fuel debris relocated to the PCV pedestal (fluid fuel debris spreads widely)

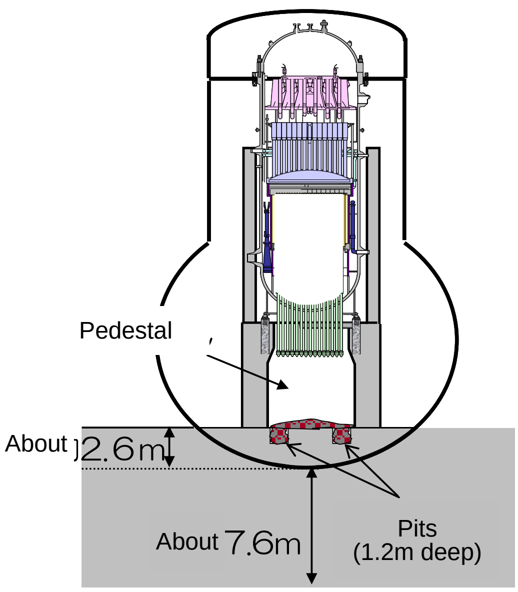

Figure 2 Estimated configuration of fuel debris relocated to the PCV pedestal (fuel debris clogs the pits)

- Debris configuration
  - In a spread fuel debris geometry, the surface area per unit decay heat enlarges and the core-concrete reactions cease earlier.
  - In a stacked fuel debris geometry at one place, the surface area per unit decay heat decreases and the core-concrete reactions cease slowly.

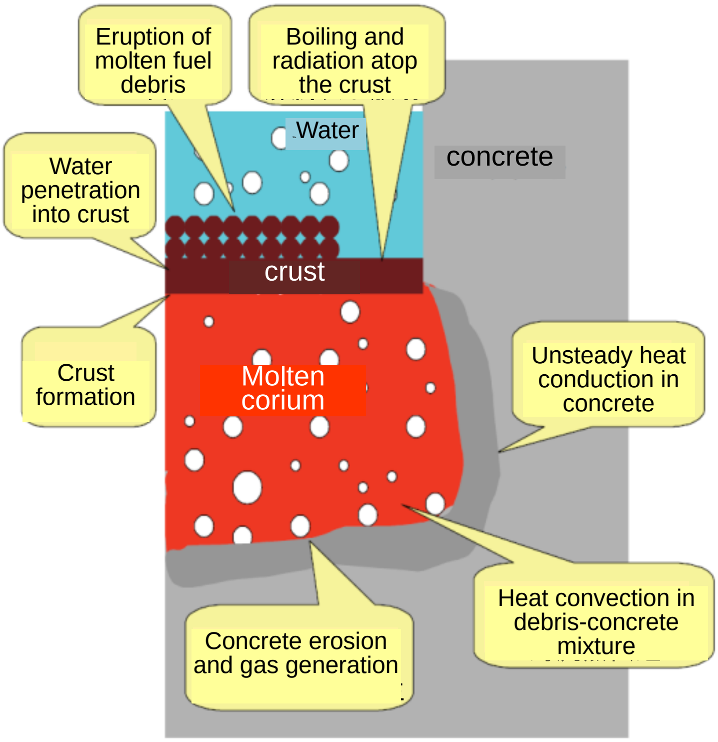

Figure 3 Geometrical configuration of fuel debris – concrete – coolant water (image)

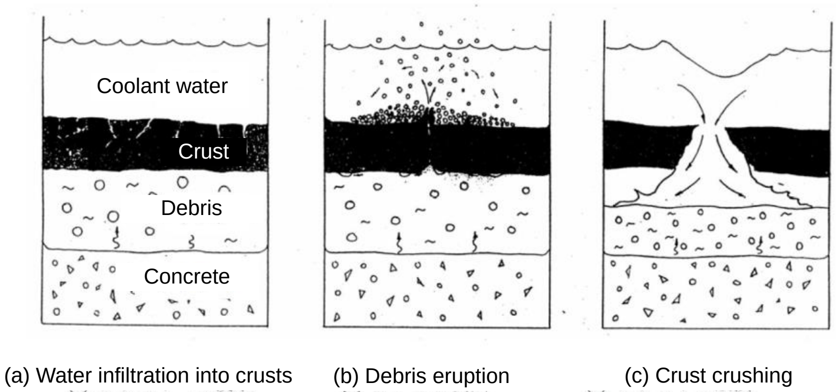

Figure 4 Heat transfer from fuel debris to cooling water (image)

– Heat transfer

- Coolant water from above may solidify the top part of the fuel debris into crust, which may inhibit heat transfer and limit heat removal.
- Internal pressures due to gases generated in core-concrete reactions may enhance heat transfer in the debris and at the boundaries.

2. Evaluation of MCCI impacts

(1) Conditions for evaluating concrete erosion depths

Several assumptions are inevitable in evaluating concrete erosion depths because of unknown debris configurations and cooling environment uncertainties as described in the previous section. The analysis results can vary significantly depending upon these assumptions.

The following are the model and conditions set for the analysis.

① Outline of analysis model

A MAAP built-in sub-program “DECOMP” for core-concrete reaction analyses was used in evaluating concrete erosion depths. The analysis model is outlined below.

- Debris compositions (those of molten fuel and in-core structures dissolved by the fuel debris) were taken from the MAAP results.
- The ORIGEN2* model was used for the fuel debris decay heat. The MCCI was set to have started at the time when the reactor vessel (RPV) had been damaged in the MAAP analysis and the decay heat attenuation thereafter was considered.

  * Revised version in 1980 of the original nuclear fuel burn up calculation model ORIGEN that was developed in 1970 by the US Oak Ridge National Laboratory.
- Heat generated when the zirconium was oxidized, which the fuel debris had dissolved before it was relocated to the pedestal, was taken into account.
- The fuel debris was assumed to spread uniformly on the pedestal floor, but part of the fuel debris was assumed to flow out to the drywell floor through slits. The fuel debris also flowed into the equipment drain sump pits as well as the floor drain sump pits and piled up. Figure 5 illustrates the analytical model of the configuration of fuel debris that had been piled up in the drain sump pits.
- The fuel debris piled up in the drain sump pits was assumed to be always covered with the coolant water, and the heat removal (heat flux) by the water was assumed to be constant at 125 kW/m^2, by referring to the MCCI test data (debris cooling tests under the condition of atmospheric pressure and silicic acid base concrete), which had been obtained by the OECD.
- The fuel debris layer in the drain sump pits
  - The fuel debris was assumed to form a homogenous pool.
  - Crust layers were assumed to be formed on the top and bottom (side) of the fuel debris pool.
- The crust layers in the drain sump pits

   - The changing rates of crust layer thicknesses were estimated from the energy balance of the crusts (heat transfers from the fuel debris pool and to the coolant water or concrete).
- The concrete erosion in the drain sump pits
   - Temperature distributions from the concrete surface into its depth direction were calculated in a one-dimensional heat convection model.
   - Erosion was assumed to start as soon as the concrete temperatures exceed its melting point at 1500 deg K.
   - The erosion depths were estimated from the heat balance between the inflows from the fuel debris and losses by the latent heats of concrete decomposition and dissolving.
   - The interface area of fuel debris and concrete was assumed to increase (Figure 6).
- Heat conduction model
   - Between the top crusts and coolant water: heat removal from the fuel debris (constant heat flux), constant heat transfer area (the drain sump pit cross-section)
   - In the crust: a parabolic temperature distribution assumed
   - Between the fuel debris pool and crust: heat transfer by convection
   - Between the fuel debris pool and concrete: the total of heat convection from the fuel debris pool to the crust layer and the decay heat within the crust

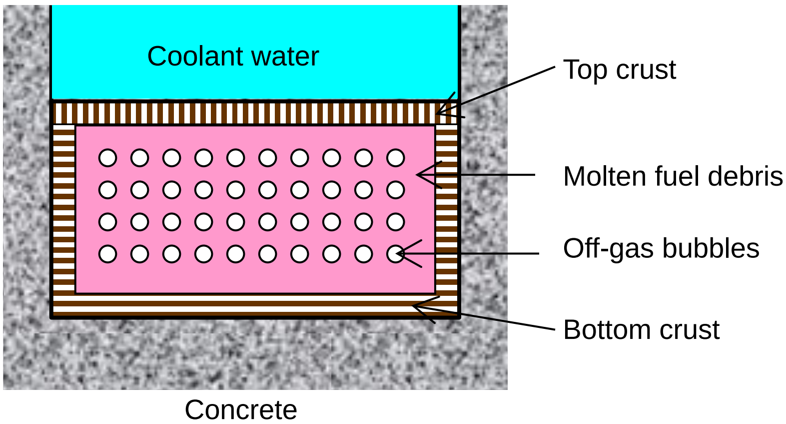

Figure 5　A schematic of fuel debris configuration in the analysis model

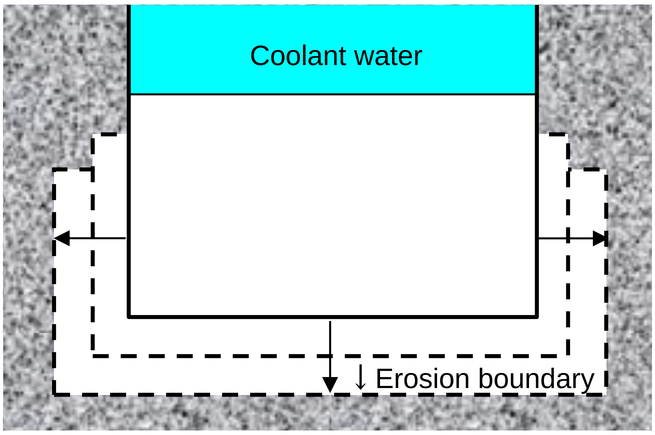

Concrete

Figure 6　A schematic of concrete erosion in the analysis model

② Condition settings for analysis

－ Fraction of core fuel having been relocated to the PCV pedestal

The amount of relocated fuel debris is not certain as of now (November 2011). In the analysis, the following values were assumed based on the maximum fractions that have been obtained in the MAAP analysis. Therefore, the evaluation should lead to conservative results.

- Unit-1: 100%
- Unit-2: 57%
- Unit-3: 63%

－ Decay heat

An assumption was made that the volatile fission products (volatile FPs) had been discharged from the fuel debris before the fuel debris had been relocated from the RPV to PCV pedestal and that, therefore, the decay heat of volatile FPs had not contributed to MCCI (i.e., 20% of the decay heat was assumed to have attenuated before the fuel debris relocation).

－ Initial water inventory in the pedestal before fuel relocation

Seal water was supplied to the mechanical seal component of reactor coolant recirculation pumps to protect reactor water from flowing out. This seal water was supplied by the control rod drive mechanism system (CRD system). Upon the station blackout, the CRD system stopped its functions and part of the reactor water was considered to have flowed out via the mechanical seal components.

The reactor water, which flowed out from the mechanical seal component, traveled to the equipment drain sump pit in the PCV pedestal via the drain line. Excessive water over the equipment drain sump pit capacity was accumulated in the pedestal, part of which might have further traveled to the drywell floor though slits until the water level reached the lower end of vent tube to the suppression chamber.

If a sufficient amount of water was accumulated by the time of fuel debris relocation to the pedestal, part of the fuel debris would be formed into fine grains when contacted with the water, by which the fuel debris cooling would advance. The following assumptions were made to evaluate the advanced cooling by fine grain formation. (There are other cooling processes for the fuel debris, but only the cooling effect by fine grain formation of fuel debris was considered in the current evaluation for conservative results.)

- Unit-1: the amount of water was assumed to be insufficiently accumulated in the pedestal to form fine grains of fuel debris, because the MAAP analysis had predicted a relatively short time for the fuel debris to be relocated to the pedestal. The situation would change little even if the amount of water that had been accumulated in the equipment drain sump pit during the normal operations was taken into account.
- Unit-2: the amount of water was assumed to be sufficiently accumulated to reach the level at the bottom end of the vent tube to the suppression chamber, because the MAAP analysis had predicted a relatively long time for the fuel debris to be relocated to the pedestal. Two paths of fuel debris relocation were assumed to evaluate the degree of fine grain formation of fuel debris. One was a path for the fuel debris to be relocated through the instrumentation line penetrations, and the other path was through the CRD penetrations. The degree of fine grain formation was evaluated by using the Ricou-Spalding correlation equation and other relevant equations*. The fuel debris not having been formed into fine grains was used to evaluate concrete erosions.

*The fuel debris was assumed to be relocated in a cylindrical jet form in the diameter of either the instrumentation penetration or CRD penetration. Part of the jet would disperse into fine grains upon rushing into the pedestal water surface. The equivalent jet diameter would decrease thereafter. The fraction of fine grain formation was estimated from the different jet diameters at the time of entry into the pedestal water and at the time of arriving at the pedestal floor. Specifically, the fractions of fine grain formation per unit surface area were obtained by the Ricou-Spalding correlation equation (F.B. Ricou and D.B. Spalding, "Measurements of Entrainment by Axisymmetrical Turbulent Jets," *Journal of*

Fluid Mechanics, Vol.11, 1961). The jet diameter on arriving at the pedestal floor was estimated by integrating the results of fractions of fine grain formation along the relocation path of the fuel debris to the floor. Figure 7 illustrates an image of fine grain formation in the water.

- Unit-3: same as in Unit-2.

– Fuel debris sediment

Certain uncertainties are considered to be inevitable in estimating the situation of relocation development of fuel debris from the RPV bottom to the PCV and the configuration of fuel debris sediment.

In the current evaluation, the configuration of sediment on the pedestal floor and the drywell floor was assumed as follows on a prerequisite that the fuel debris would have been relocated from the RPV bottom (Figure 8).

The fuel debris was assumed to maintain its fluidity due to its high temperatures while being relocated down in the pedestal water, but to lose its fluidity gradually by heat radiation while spreading from the pedestal floor to the drywell floor. The fuel debris fluidity would have been further lost by the injected water for cooling.

- The fuel debris would spread isotropically upon relocation on the pedestal floor.
- Part of the fuel debris that had been relocated to the pedestal floor would further flow out to the drywell floor through slits. The fuel debris could have damaged the PCV steel plates (the so-called PCV shell attack) depending on the fuel debris spillage conditions to the drywell. But no plant parameters of Unit-1 to Unit-3 indicated until now (November 2011) have hinted at changes due to the PCV shell attack.
- The fuel debris that had spilled to the drywell was assumed to spread radially with an angle of 130 degrees. This assumption was based on research results.
- The fuel debris would melt the metallic covers of the equipment drain sump pit and floor drain sump pit in the pedestal and flow into these pits. For conservative evaluation, not only the fuel debris sedimented on the pit covers, but the part of fuel debris sedimented on the pedestal floor within the fan-shaped 90-degree area around the pit was assumed to have flowed into the pits, too.
- The sediment thickness of fuel debris in the drain sump pits should be larger than that spread uniformly on the pedestal floor or drywell floor. The concrete erosion depths were evaluated, therefore, on the concrete around the fuel debris sediment in the drain sump pits.

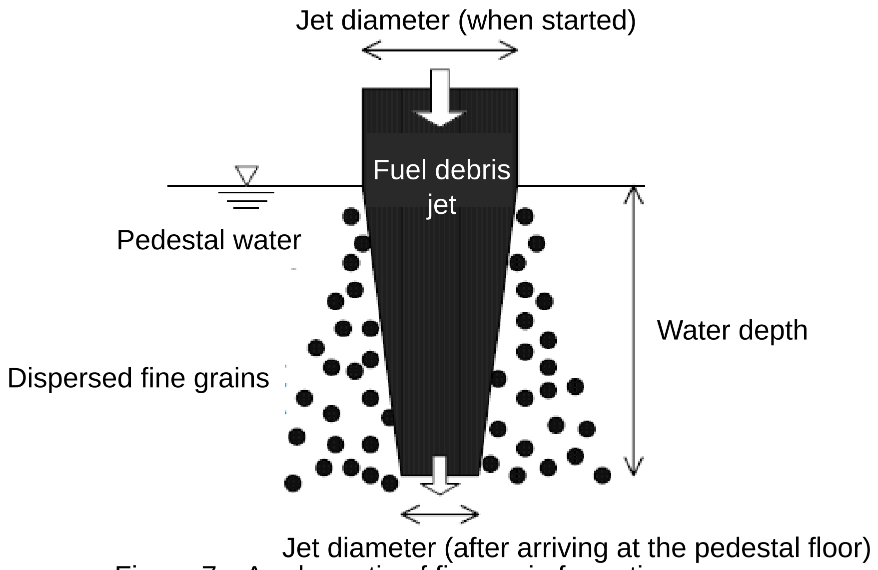

Figure 7　A schematic of fine grain formation

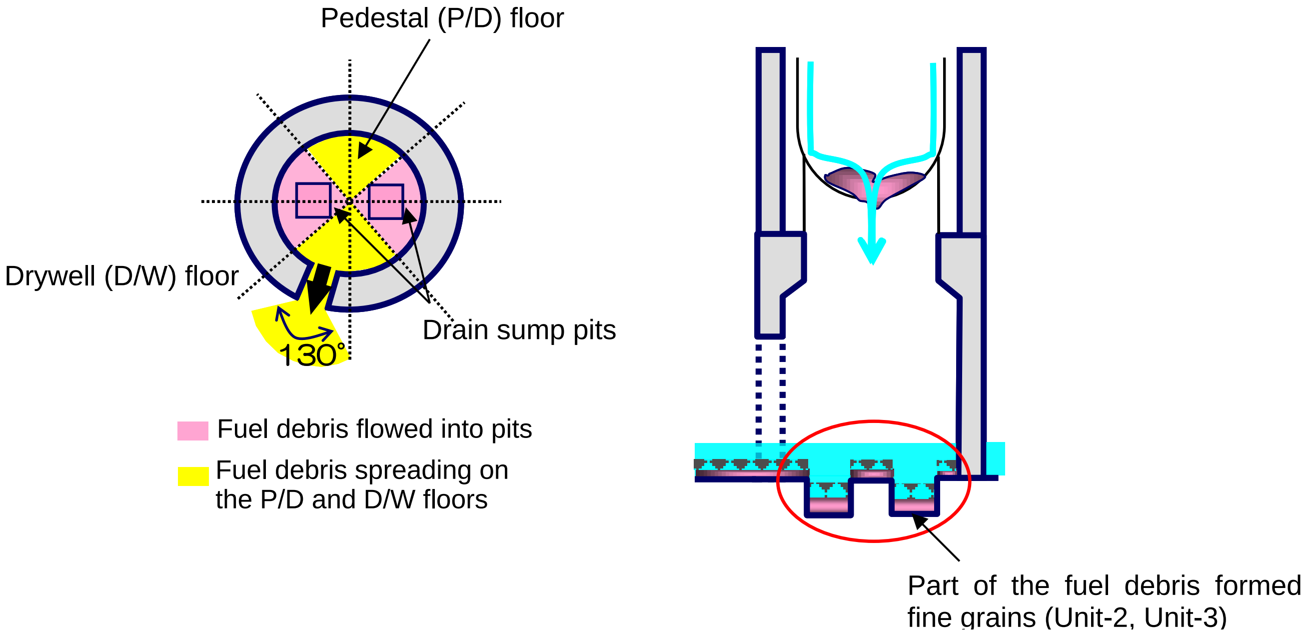

Figure 8 Fuel debris sediment configuration (image)

(2) Results of erosion depth evaluation

– Unit-1

The results of erosion depth estimation are shown in Table 1, Figure 9 and Figure 10 and Figure 11.

Fraction of fuel relocation	100 %
Fuel debris sediment thickness	0.81 m
Erosion depths	0.65 m

Table 1 Unit-1 concrete erosion depth evaluation results

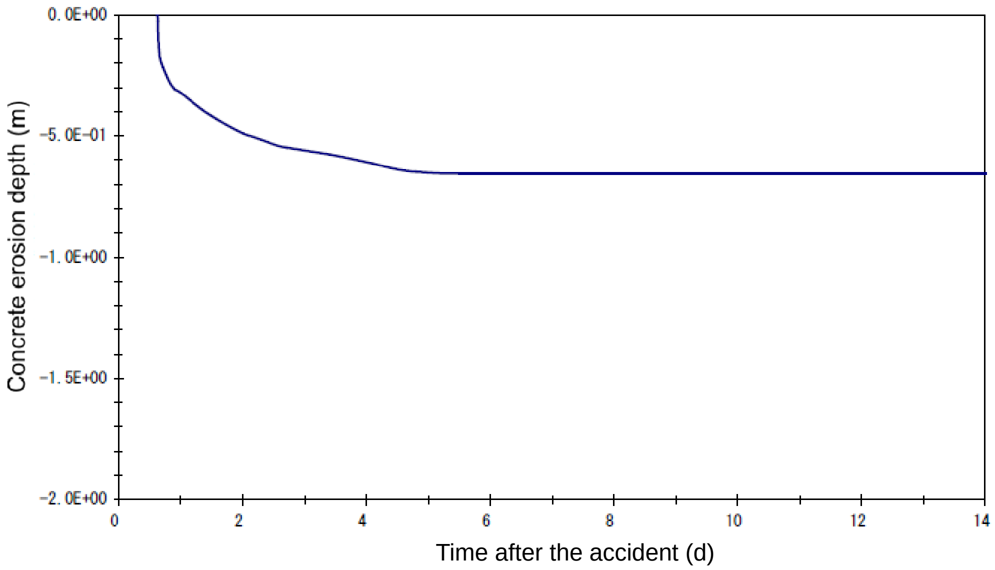

Figure 9 Progression of concrete erosion with time (Unit-1)

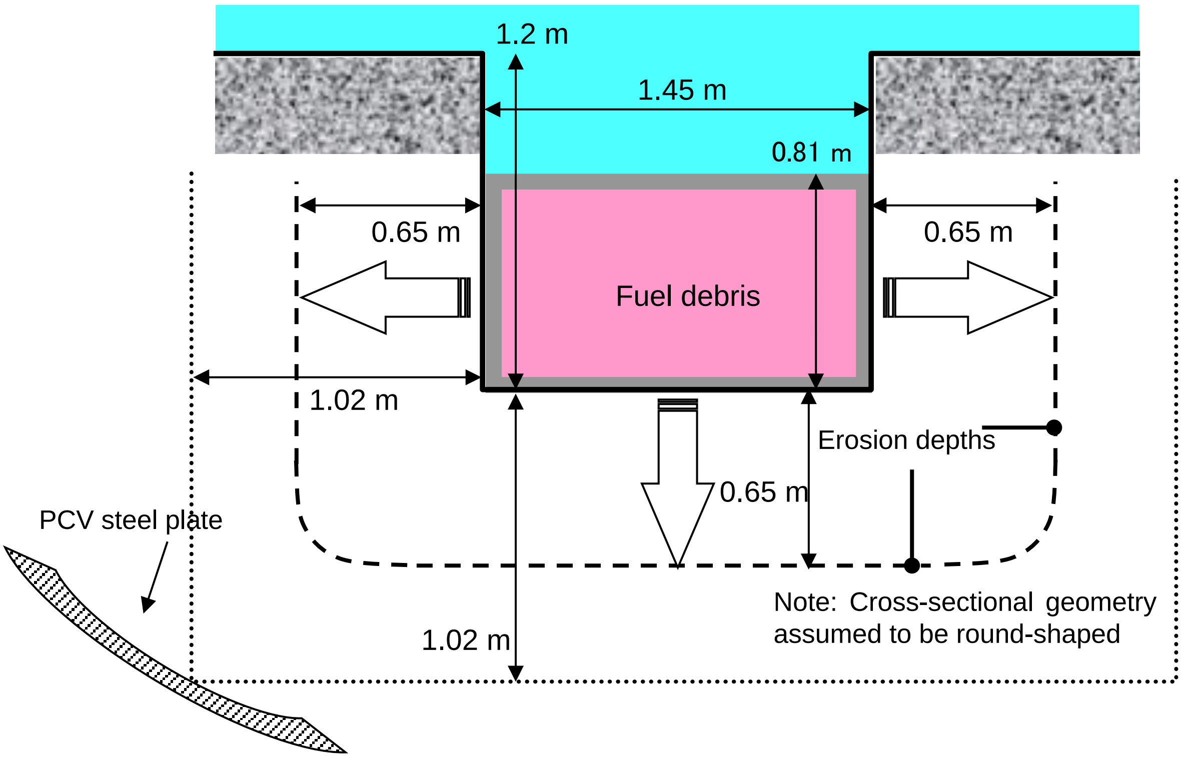

Figure 10 A schematic of concrete erosion (vertical view) (Unit-1, Fuel relocation 100%)

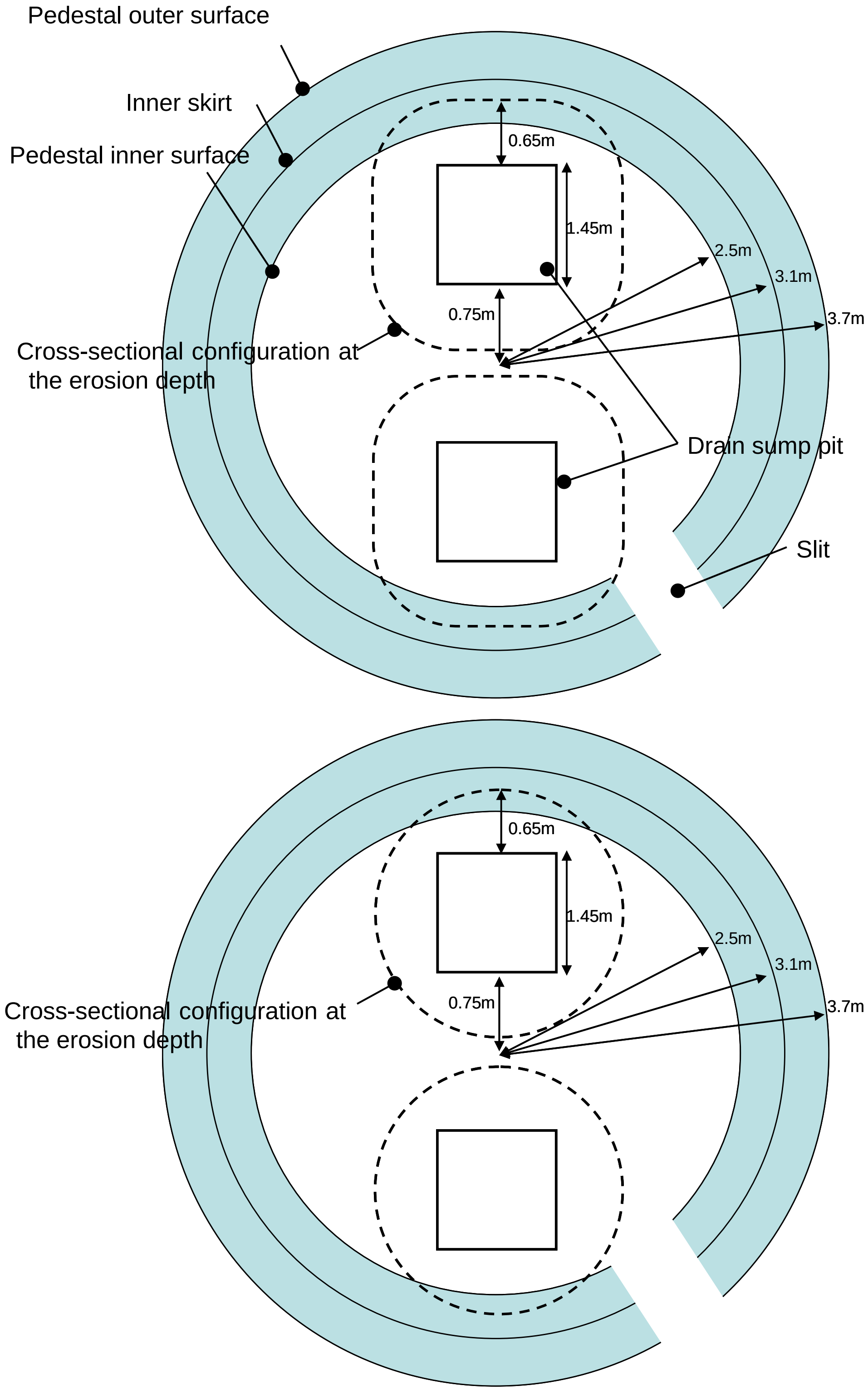

The erosion volume surface is considered to become round-shaped as the sump pit walls became eroded by the fuel debris sediment in the drain sump pits.
The actual cross-sectional configuration of the erosion volume will be a geometry between the top and bottom figures.

Figure 11 Schematic of concrete erosion (plane view) (Unit-1, Fuel relocation 100%)

－ Unit-2

Table 2, Figure 12 and Figure 13 show the results of erosion depth estimation.

Fraction of fuel relocation	57%	57%
Relocation path	Instrumentation line penetration	CRD penetration
Fraction of fine grain formation	0.62	0.27
Debris sediment thickness	0.20 m	0.40 m
Erosion depth	0.07 m	0.12 m

Table 2　Unit-2 concrete erosion depth evaluation results

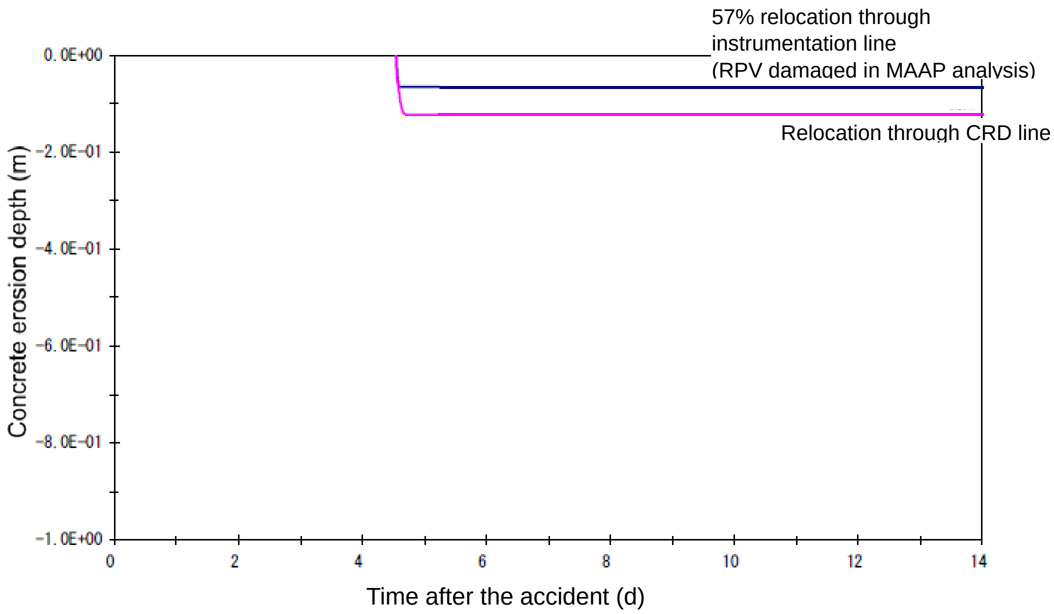

Figure 12　Progression of concrete erosion with time (Unit-2)

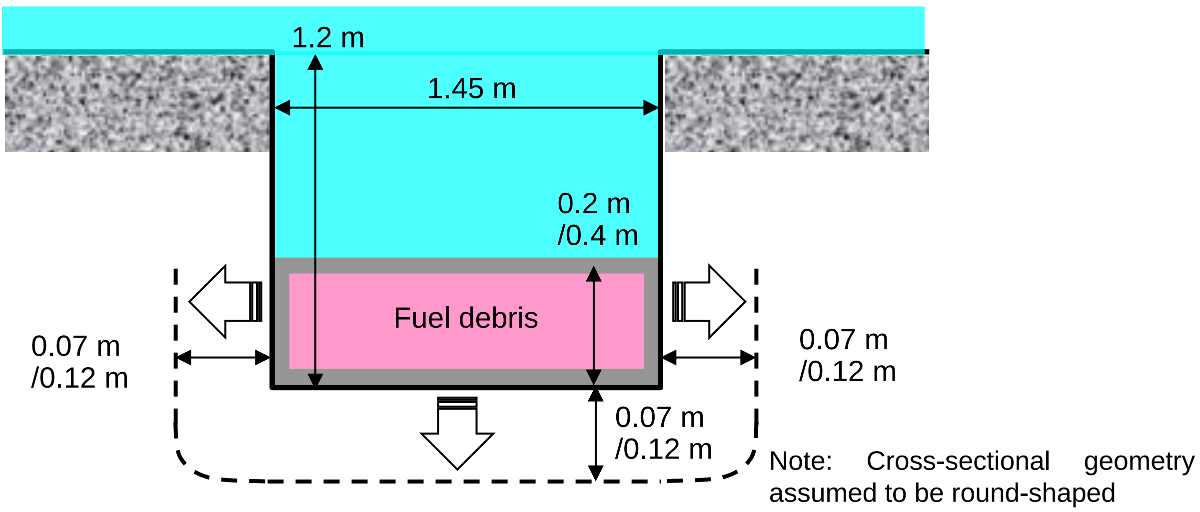

Figure 13　A schematic of concrete erosion (Unit-2, Fuel relocation 57%)

－　Unit-3

Table 3, Figure 14 and Figure 15 show the results of erosion depth estimation.

Fraction of fuel relocation	63 %	63 %
Relocation path	Instrumentation line penetration	CRD penetration
Fraction of fine grain formation	0.56	0.25
Debris sediment thickness	0.31 m	0.53 m
Erosion depth	0.13 m	0.20 m

Table 3　Unit-3 concrete erosion depth evaluation results

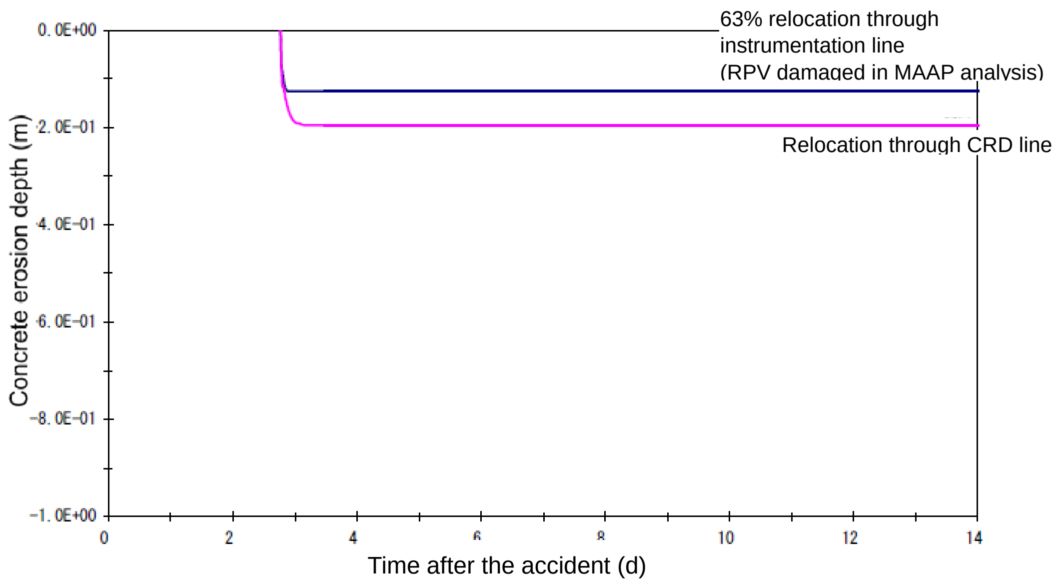

Figure 14　Progression of concrete erosion with time (Unit-3)

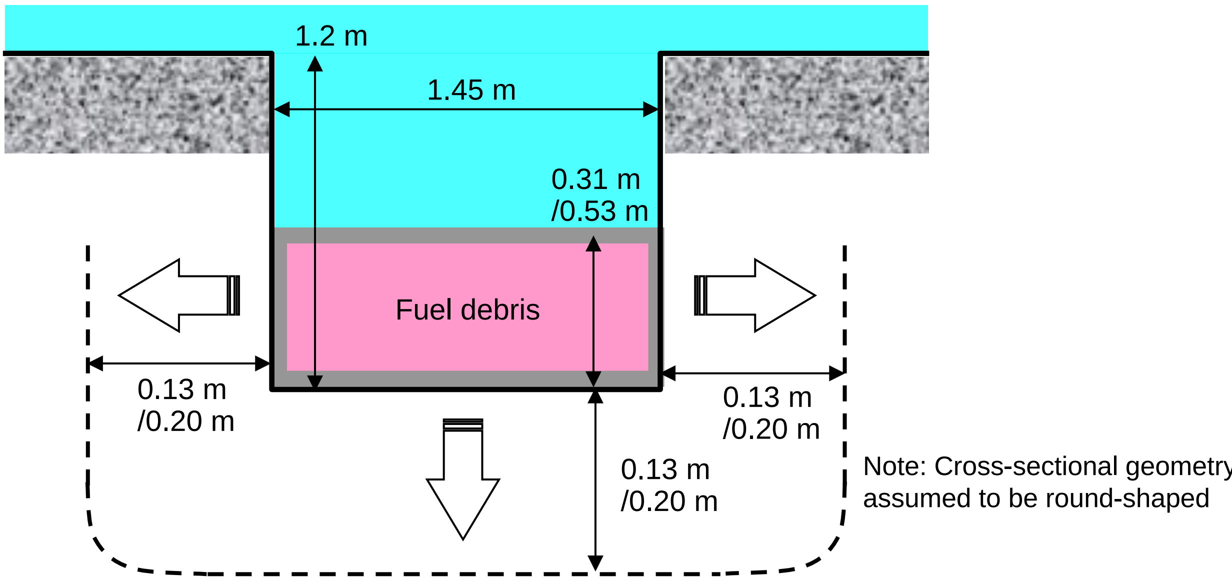

Figure 15　A schematic of concrete erosion (Unit-3, Fuel relocation 63%)

3. Conclusion

The erosion depths of pedestal concrete due to core-concrete reactions were evaluated for Unit-1 to Unit-3. The deepest erosion depths under the assumptions set in the current study were 0.65 m at Unit-1, 0.12 m at Unit-2 and 0.20 m at Unit-3.

Current results indicate that the largest erosion occurred at Unit-1 but its erosion depth was still less than the depth to reach the PCV steel plate (1.02 m), i.e., the fuel debris eroded the pedestal floor but could remain inside the PCV.

There were other possible development processes in fuel debris behavior when it is relocated, which were not dealt with in the current quantitative evaluation. For example, a model (*) was not assumed, in which the crust was crushed by the gases generated in the fuel debris while being cooled and the molten fuel debris erupted above the crust. In this case, the cooling effects would be significant. The consequences of concrete erosion would be milder than the results in the current evaluation, i.e., the current evaluation results would be conservative.

Other forms of development which may affect the fuel debris cooling, or the debris sediment depths include: fuel debris cooling by the water having been present in the equipment and floor drain sump pits at the beginning of accident; debris sediment thickness decrease by possible debris leaks to drain pump pits via a connection pipe from the equipment and floor drain sump pits; heat removal by the melting of CRD mechanisms and other components in the pedestal or fuel debris heat density decrease, etc.

(*) The fuel debris when erupted solidifies in crushed stone forms. Because of their uneven surfaces, the solidified fuel debris is well cooled. In parallel, coolant water infiltrates the crust through the crushed gaps and contact fuel debris, advancing cooling.

The Japan Nuclear Energy Safety Organization (JNES) earlier also evaluated the impacts of MCCI on the PCV. These results concluded, despite different assumptions set in the analysis such as the debris configuration when sedimentation occurred, that the fuel debris had remained in the PCV, although it eroded the pedestal floor. (See the Annex to this document for major differences in analysis conditions.)

End

Annex 1

Comparison of the current IAE evaluation results of impacts of core-concrete reactions on the reactor containment vessel with the JNES evaluation results

JNES issued the following evaluation reports concerning the erosions of PCV (pedestal) by the fuel debris.

- Report (1): Issue No.6 to be investigated, Core-concrete interactions (CCI), March 25, 2011
- Report (2): Possibility of core-concrete reactions (MCCI) and their impacts, April 6, 2011
- Report (3): Possibility of core-concrete reactions (MCCI) and their impacts (Part 2), April 7, 2011
- Report (4): Possibility of core-concrete reactions (MCCI) and their impacts (Part 3), April 13, 2011

Key conditions for analysis are compared below between the current IAE analysis and the JNES analysis by referring to these published reports.

○ Fraction of fuel relocation

IAE set the fraction of core damage, based on the MAAP analysis, as the maximum amount of fuel debris (100% core at Unit-1, 57% core at Unit-2 and 63% core at Unit-3) assumed in the case of the RPV being damaged.

JNES set 100% core for all units, Unit-1 to Unit-3, as the amount of fuel debris except in Report (2). (In Report (2), 70% core for Unit-1, and 30% core for Unit-2 and Unit-3 were assumed).)

⇨ JNES estimated larger erosion depths for Unit-2 and Unit-3.

○ Conditions of fuel debris sediment on the pedestal floor

IAE set the fuel debris sediment thickness by assuming that the fuel debris having been relocated from the RPV bottom would uniformly spread on the pedestal floor and thereafter partly further spread out to the drywell floor through pedestal slits or partly flow into the equipment and floor drain sump pits on the pedestal floor.

JNES set the fuel debris sediment thickness by assuming that the fuel debris having been relocated from the RPV bottom would uniformly spread on the pedestal floor (drain sump pits were not considered).

⇨ JNES assumed thicker debris sediments on the pedestal floor, while IAE assumed sediments in the drain sump pits. Both assumptions are conservative in evaluating erosion depths.

○ Configuration of fuel debris

IAE assumed that, at Unit-2 and Unit-3, part of the molten fuel debris would be formed into fine grains, before it reached the pedestal floor, in the water layer in the pedestal, which had been accumulated with the water having leaked out from the reactor through the recirculation pump mechanical seal component. The MCCI was evaluated by using the fuel debris which had not been formed into fine grains. As for Unit-1, the amount of water was assumed to be insufficiently accumulated in the pedestal to form fine grains of fuel debris, because the MAAP analysis had predicted a relatively short time for the fuel debris to be relocated to the pedestal.

In the JNES evaluation, the molten fuel debris was assumed to form a pool on the pedestal floor, although JNES acknowledged the cooling effect of crushed debris in the coolant water.

⇨ The JNES assumption was more conservative for evaluating the erosion depths at Unit-2 and Unit-3.

○ Decay heat

Both IAE and JNES assumed the attenuation of the volatile FP contribution to the decay heat as 20% (the volatile FP decay heat was subtracted from the fuel debris decay heat as the heat source for the MCCI, assuming that the volatile FPs had volatilized prior to the MCCI).

IAE used ORIGEN2 in evaluating decay heat. The MCCI was set to have started at the beginning of the accident (when the RPV was damaged). The heat generated in the zirconium oxidation was also added, in addition to the decay heat, to the heat source for the MCCI.

JNES used the ANSI/ANS5.1-1979 or May Witt data for evaluation. The MCCI was assumed to start 20 days after the accident. The heat generated in zirconium oxidation was not taken into account (i.e., the zirconium was assumed to have been oxidized completely before the core-concrete reaction started).

⇨ IAE assumed core-concrete reactions to have started earlier after the accident. IAE added the heat generated by the zirconium oxidation to the heat source for core-concrete reactions. For these reasons, IAE assumptions are more conservative for erosion depths evaluation than the JNES assumptions.

○ Cooling model

Both IAE and JNES assumed that the molten fuel debris contacted coolant water at its top and heat was removed via the crust having been formed on the boundary and contacted concrete at its bottom and heat was discharged for concrete erosion via the crust having been formed on the boundary.

JNES assumed a model, trying a realistic modelling, in which the upper crust would be crushed by gas pressures having been generated in the course of MCCI and the fuel debris would erupt above the coolant water.

⇨ IAE did not assume the fuel debris would erupt. This should have resulted in more conservative concrete erosion.

○ Erosion depths

JNES Reports (1) to (4) do not specify the difference in concrete erosion depths depending upon different analysis conditions, but Report (4) specifically concluded the erosion depth as “about 1 m” and the fuel debris would remain in the PCV. The IAE result in the current study predicted the erosion depth at Unit-1 was about 0.65 m and that the fuel debris would remain in the PCV.

Comparisons of analysis conditions are summarized below.

Table 4　Comparison of analysis conditions in the IAE and JNES evaluations

	JNES Report (1) March 25, 2011	JNES Report (2) April 6, 2011	JNES Report (3) April 7, 2011	JNES Report (4) April 13, 2011	IAE	Remarks
Fraction of fuel relocation	100%	1F1: 70% 1F2,3: 30%	100%	100%	1F1: 100% 1F2: 57% 1F3: 63%	
Debris sediment	P/D floor only	P/D floor only	P/D floor only	P/D floor only	P/D and D/W floor	
Debris configuration	Fine grains not formed	Fine grains not formed	Fine grains not formed	Fine grains not formed	Fine grains formed in 1F2 and 1F3	
Decay heat (source)	Not specified	ANSI/ANS5.1 -1979	May Witt	Not specified	ORIGEN2	
Volatile FP decay heat attenuation	Considered	Not considered	Considered	Considered	Considered	
Timing of MCCI initiation	Immediately after RVP damage	20 days after the accident	27 days after the accident	27 days after the accident	Immediately after RVP damage	
Heat of Zr oxidation	Not considered	Not specified	Not specified	Not considered	Considered	
Erosion depths (Cooling effect of erupted fuel debris not considered)	1F1 to 1F3: Fuel debris is cooled and solidifies before erosion starts.	1F1: 0.92m 1F2: 0.07m 1F3: 0.07m	1F1: 1.8 m 1F2: Not ceased by day 10 1F3: Same as 1F2	1F1 to 1F3: about 1m (No specific values reported for respective units)	1F1: 0.65m 1F2: 0.07m*1 0.12m*2 1F3: 0.13m*1 0.20m*2	*1: Fuel relocated via instrumentation line *2: Fuel relocated via CRD penetration
Erosion depths (Cooling effect of erupted fuel debris considered)	—	—	1F1: 0.48m*3 0.63m*4 1F2: 0.7 m*3 1.1 m*4 1F3: Same as 1F2		—	*3: Debris eruption coefficient E=0.12 assumed *4: E=0.08 assumed

Note: 1F1, 1F2 and 1F3 are named as Unit-1, Unit-2 and Unit-3, respectively, in other places in the report.

Estimation of the conditions of structural materials in the Unit-1 containment vessel

1. Outline

A significant amount of fuel debris is estimated as highly possible to have been relocated in Unit-1 and eroded the concrete surrounded by the RPV pedestal. This document investigates the conditions of structural materials in the containment vessel (PCV) in such a situation.

2. Structural configuration in the Unit-1 containment vessel

Figure 1 shows the structural configuration in the Unit-1 PCV. The RPV loads (dead weights, seismic loads and other loads) are transferred first to the RPV pedestal made of reinforced concrete and eventually to the base mat made of reinforced concrete via steel inner skirts.

3. Part of concrete eroded by the fuel debris

The fuel debris is estimated currently (November 2011) to have been relocated to the position shown in Figure 1 and to have eroded the concrete as shown in Figure 2. Drain sump pits were located where the fuel debris is estimated to have been relocated, and the fuel debris sedimented in the pits was assumed to have eroded the concrete around. This concrete was not a stiff member of the structure and had no rebars to bear any loads (it had several exceptional steel bars but they were to prevent cracking). The concrete eroded by the fuel debris would be difficult to bear loads, but it is of no significance because the part currently estimated to have been eroded was not designed originally to bear any loads.

Thus, as long as the fuel debris is assumed to remain where it is currently estimated to be present, it has no direct impacts on the structural members to support heavy structures in the PCV such as the RPV and therefore, the structural integrity can be considered to be ensured.

Structures in Unit-1 PCV

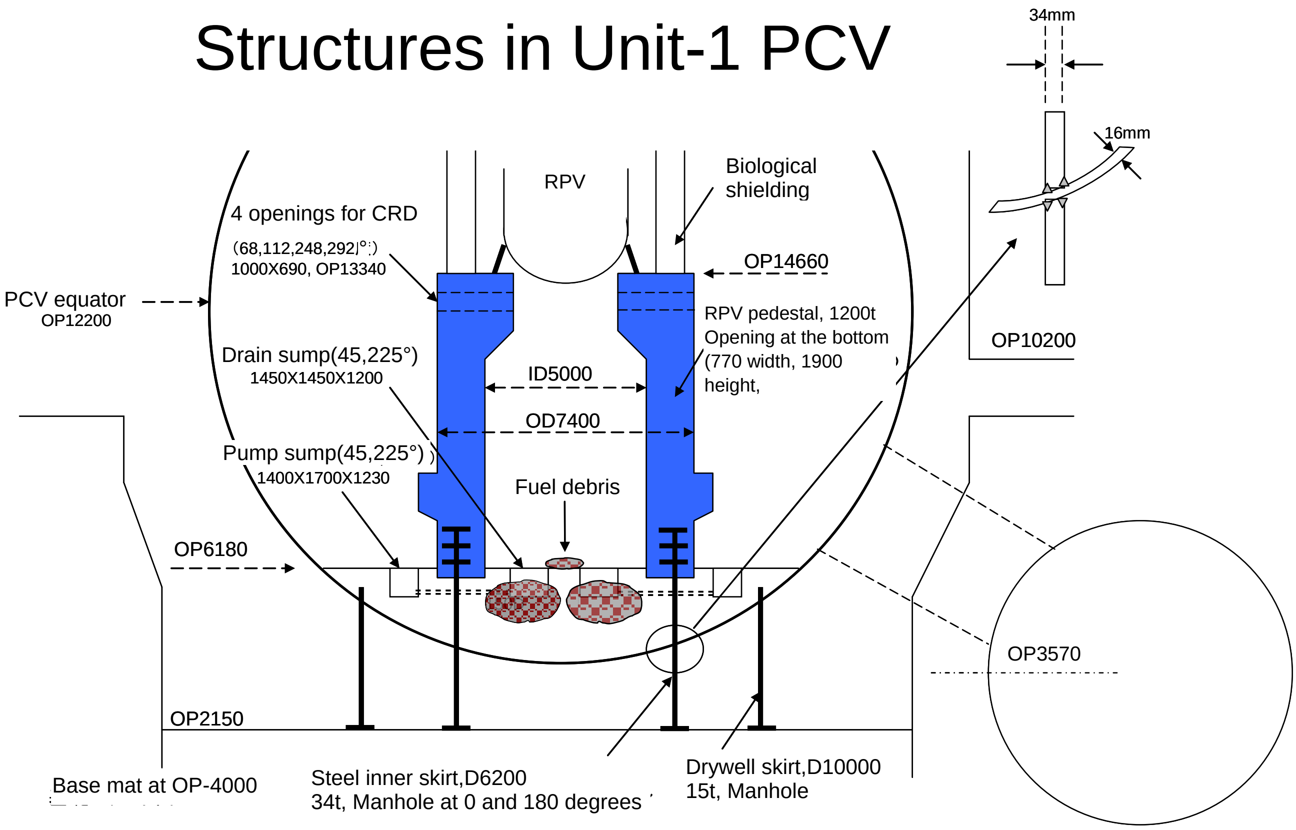

Figure 1　Structures in Unit-1 PCV

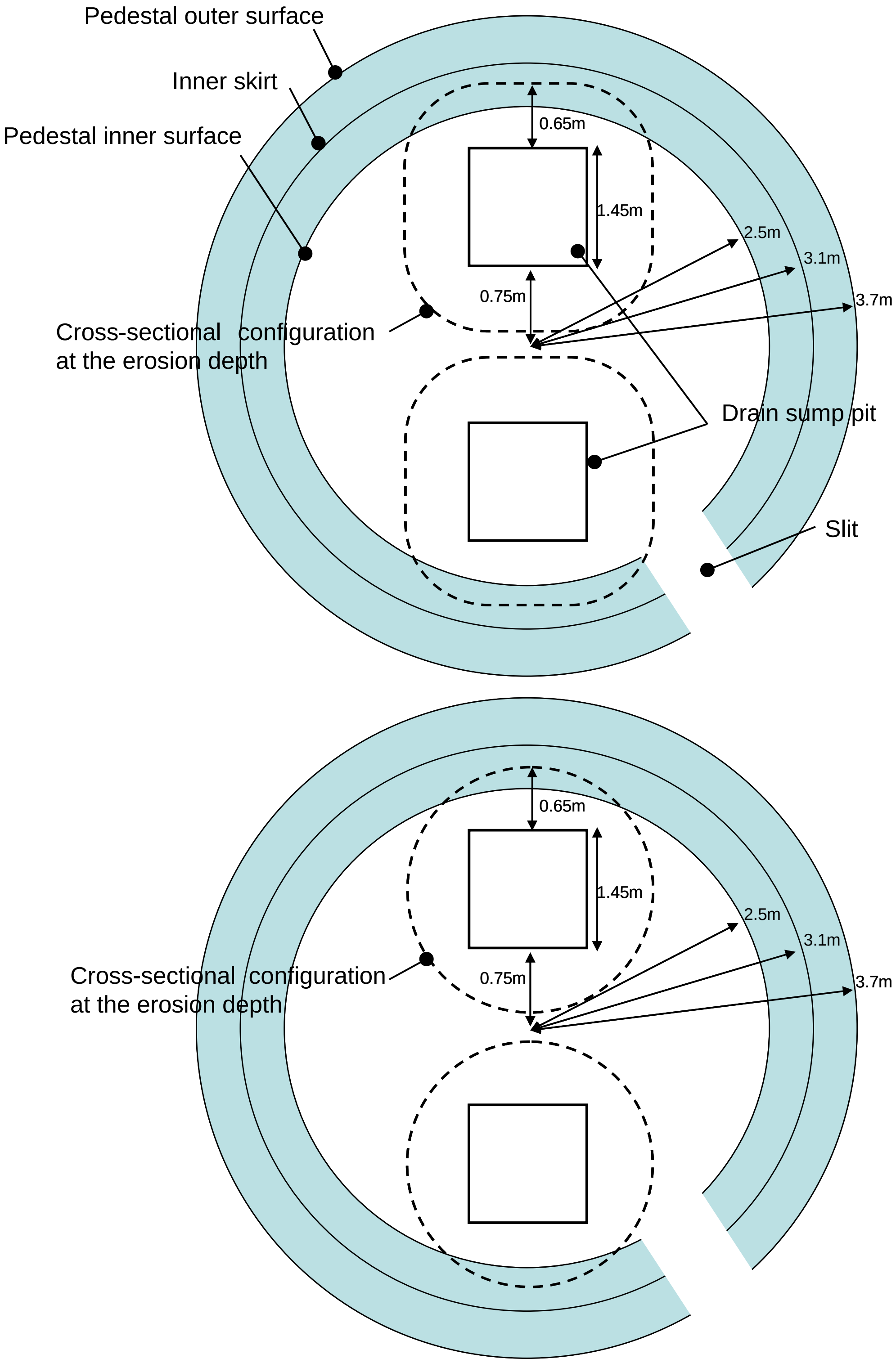

The erosion volume surface is considered to become round-shaped as the sump pit walls became eroded by the fuel debris sediment in the drain sump pits.
The actual cross-sectional configuration of the erosion volume will be a geometry between the top and bottom figures.

Figure 2　Schematic of concrete erosion

Results of in-containment gas composition analysis

1. Outline

Gas samples were collected from the Unit-1 and Unit-2 containment vessels (PCVs) on July 29, August 9 and September 14, 2011, to measure concentrations of radioactive materials in the PCV (Figure 1, Figure 2). The collected samples were analyzed to obtain gas compositions of hydrogen, carbon monoxide and carbon dioxide. PCV gas samples analyzed were the following nine lots.

- Lot Nos. 1 to 3: Unit -1 PCV gas samples (collected on July 29, 2011), three lots
- Lot Nos. 4 to 6: Unit -2 PCV gas samples (collected on August 9, 2011), three lots
- Lot Nos. 7 to 9: Unit -1 PCV gas samples (collected on September 14, 2011), three lots

Lot Nos. 1 to No. 3 were collected on July 29, 2011. Lot No. 1 is the gas vial containing the gas sample collected on July 29, 2011, and Lot Nos. 2 and 3 are two gas vials containing the samples redistributed on October 3, 2011, from the lot having been stored after collection (collected on July 29, 2011).

Lot Nos. 4 to No. 6 were three lots collected on August 9, 2011, from the Unit-2 PCV.

Lot Nos. 7 to No. 9 were three lots collected on September 14, 2011, from the Unit-1 PCV.

Table 1 shows the results of analysis. The results are the gas concentrations in the gas vials. Hydrogen was detected in both Unit-1 and Unit-2 samples. Carbon monoxide was detected in Unit-2 sample (at the level of the detection limit), but not in Unit-1 sample. Carbon dioxide was detected in both Unit-1 and Unit-2 samples.

Figure 1　Temporary PCV gas sampling rack (Unit-1, July 2011)

Figure 2　Temporary PCV gas sampling rack (Unit-2 in August 2011 and Unit-1 in September 2011)

Table 1　Results of gas analyses (concentrations in vials)

(unit: vol %)

Lot No.	Sample	H	CO	CO_2
1	Unit-1 (July) ①	<0.001	<0.01	0.139*[1]
2	Unit-1 (July) ②	<0.001	<0.01	0.133*[1]
3	Unit-1 (July) ③	<0.001	<0.01	0.112*[1]
4	Unit-2 (August) ①	0.507	0.014	0.145
5	Unit-2 (August) ②	0.964	0.015	0.143
6	Unit-2 (August) ③	<0.001	<0.01	0.145
7	Unit-1 (September) ①	0.14	<0.01	0.114
8	Unit-1 (September) ②	0.092	<0.01	0.189
9	Unit-1 (September) ③	0.072	<0.01	0.124
10	Air (outdoors)	<0.001	<0.01	0.074
Information	Detection limit	0.001	0.01	0.01

*1 Information only because of the high dilution in air and the influence of CO_2 concentration in the air.

2. Concentrations of gas compositions in the containment vessel (PCV)

Lot Nos. 1 to No. 3 (collected in July 2011, from Unit-1 PCV) were diluted in the sampling tools with air into 4.32 times by volume, and then the 6 mL diluted gas was injected with a syringe into vacuumed vials of 14.1 mL. Before filling, the vials contained the indoor atmosphere (in the analysis room), unlike Lot Nos. 4 to No. 9. Consequently, the PCV gas volume in the vial was calculated to be 1.4 mL, the rest being the air. The PCV gas concentrations (concentrations in the non-condensable gas) can be obtained by Eq. 1 below.

$$A = \frac{14.1C - 12.7B}{1.4} \qquad \text{Eq. 1}$$

Here, A is the concentration in the non-condensable gas, B is the concentration in air and C is the concentration in in the vial.

From Lot Nos. 4 to No. 9 (collected in August 2011 from Unit-2 and in September 2011 from Unit-1), the sample gas was directly extracted from the sampling tools, and then the 12.8 ml sample gas was injected into vacuumed vials of 14.1 mL. Before filling, the vials contained the outdoor atmosphere. Consequently, the PCV gas concentrations (concentrations in the non-condensable gas) can be calculated by Eq. 2 below.

$$A = \frac{14.1C - 1.3B}{12.8} \qquad \text{Eq. 2}$$

Table 2 shows the gas concentrations derived from the analysis results and corrected for dilution by air. The concentrations in Lot No. 10 was used as concentrations in the air, as needed for corrections. Concentrations of hydrogen and carbon monoxide were set at the value of detection limits.

It should be noted that the estimation of the in-PCV gas carbon dioxide concentration was concluded to be not possible from the Lot Nos. 1 to No. 3 for the following reasons: these samples collected in Unit-1 (July 2011) were diluted with air in a high dilution ratio and about 90% of the diluted gas samples were indoor air with higher carbon dioxide contents as compared with the outdoor air. Consequently, most carbon dioxide detected in Lot Nos. 1 to No. 3 was considered to have originated in the diluted indoor air; Table 3 shows the results of sensitivity analysis of in-PCV gas carbon dioxide concentrations derived by Eq. 1 when the in-air carbon dioxide concentration was parametrically changed between 0.038 % and 0.20 %. If the in-air carbon dioxide concentration was low, the in-PCV gas carbon dioxide concentration should become very high, while if it was high, the in-PCV gas carbon dioxide concentration should become negative; the in-air carbon dioxide concentration predominates the estimation results of the in-PCV gas carbon dioxide concentration, but the carbon dioxide concentration in the diluted air in the vial was not accurately known.

Table 2　Concentrations in the PCV non-condensable gases (Corrected for dilution by air)

(unit: vol %)

Lot No.	Sample	H	CO	CO_2
1	Unit-1 (July) ①	<0.001	<0.01	See Table 6
2	Unit-1 (July) ②	<0.001	<0.01	See Table 6
3	Unit-1 (July) ③	<0.001	<0.01	See Table 6
4	Unit-2 (August) ①	0.558	0.014	0.152
5	Unit-2 (August) ②	1.062	0.016	0.150
6	Unit-2 (August) ③	<0.001	<0.01	0.152
7	Unit-1 (September) ①	0.154	<0.01	0.118
8	Unit-1 (September) ②	0.101	<0.01	0.201
9	Unit-1 (September) ③	0.079	<0.01	0.129

Table 3　In-PCV gas CO_2 concentrations estimated from the in-air CO_2 concentration (sensitivity analysis, Sample 1 collected in July 2011)

(unit: vol %)

Lot No.	Sample	In-air CO_2 concentrations assumed		
		0.038%	0.074%	0.20%
1	Unit-1 (July) ①	1.055	0.729	−0.414
2	Unit-1 (July) ②	0.995	0.668	−0.475
3	Unit-1 (July) ③	0.783	0.457	−0.686

3. Situation of core-concrete reactions estimated from CO and CO_2 concentrations

Gas concentrations of carbon monoxide and carbon dioxide in the Unit-1 and Unit-2 PCVs were estimated in a situation if core-concrete reactions had been ongoing when the gas samples had been collected. The DECOMP, a MAAP built-in sub-program for core-concrete reaction evaluation, was used to evaluate the core-concrete reactions. Table 4 shows the generation rate and concentration of carbon monoxide and carbon dioxide gases when the fuel debris having been relocated to the pedestal reacted with concrete. The non-condensable gas concentrations in the PCV were evaluated in terms of the ratio $(CO+CO_2)/(N_2+CO+CO_2)$. If the core-concrete reactions had been ongoing at the time of gas sampling, the concentration of $CO+CO_2$ should be more than 10%, but the concentration observed in the gas composition analysis was significantly lower (Table 1 and Table 2). Gas compositions observed (Table 1 and Table 2) are different from the gas compositions due to core-concrete reactions by computational analysis (Table 5), too. It is unlikely that the core-concrete reactions are in progress now (November 2011).

Table 4 Estimation of the amount of CO and CO_2 production and concentration due to core-concrete reactions (computational analysis) *1

		Unit-1	Unit-2	
Fraction of fuel relocation to PCV (%)		100%	57% (via instrumentation line penetration)	57% (via CRD penetration)
Amount of production (kmol) (accumulated)	Steam	75.8	1.18	4.3
	H_2	37.8	2.06	4.1
	CO	5.2	0.04	0.1
	CO_2	8	0.12	0.46
Gas production rate (Nm^3/h) (average) *2	Steam	15.4	19.8	24.6
	H_2	7.6	34.8	23.4
	CO	1.0	0.8	0.6
	CO_2	1.6	2.0	2.6
$CO+CO_2$ concentration in non-condensable gas (%)	$CO+CO_2/N_2+CO+CO_2$	8.5	17.7	19.8

*1 Gas production in the pedestal sump pits only.

*2 The accumulated amount divided by the time duration of core-concrete reactions.

Table 5 Gas compositions in core-concrete reactions (DECOMP)

		Unit-1	Unit-2	
Fraction of fuel relocation to PCV (%)		100%	57% (via instrumentation line penetration)	57% (via CRD penetration)
Compositions of Non-condensable gas generated	H_2	75%	93%	88%
	CO	10%	2%	2%
	CO_2	16%	5%	10%

– Supplement (1) Discharge of carbon dioxide dissolved in the injected water to PCV and RPV

The water that had been injected to the reactor at the time of gas sampling (July to September 2011) is considered to have contained a certain degree of carbon dioxide (free carbonic acid). The properties of the water can be considered to be close to those of surface water or dam water. Table 6 shows the estimated carbon dioxide concentration discharged in the PCV, when the free carbonic acid concentration was 2 to 10 mg/L (Water Statics 2000, MLFW), which is close to the value in the surface water or dam water.

Depending on its concentration in the injection water, the free carbonic acid dissolved in the injection water can influence the carbon dioxide concentration of about 0.01% to 0.16%. The carbon dioxide concentration observed in the PCV gas samples may have been significantly influenced by the free carbonic acid dissolved in the injection water.

Table 6 CO_2 amount contained in the injection water and estimated CO_2 concentration in the PCV non-condensable gases

	Unit-1		Unit-2	
Amount of water injection [m^3/h]	4	4	4	4
Amount of N_2 gas injection [Nm^3/h]	28		13	
CO_2 concentration in water [mg/L]	2	10	2	10
Estimated CO_2 concentration (in non-condensable gases) [%]	0.01	0.07	0.03	0.16

– Supplement (2) Thermal decomposition of polymer compounds used for electric cables and others

Polymer compounds in the PCV such as electric cable covering materials generate carbon monoxide and carbon dioxide when heated up. But the current PCV temperatures have been below the level of polymer thermal decompositions (for example, about 200 deg C for vinyl chloride resins) from the time of sample collection till now (November 2011). Therefore, it is unlikely that carbon monoxide or carbon dioxide were and are now being generated during this time period.

Gas residues from the early phase of core-concrete reactions

1. Summary

A large amount of steam was being generated in the reactor after the accident by water injection for fuel cooling. Gases in the containment vessel (PCV) could leak out at the time of interest, and therefore non-condensable gases generated in the early phase of the accident have unlikely remained till now (November 2011) in significant amounts. On the other hand, a small amount of rare gas (Kr-85) was detected in the gas samples of Unit-2, indicating that part of the non-condensable gases generated in the early phase of the accident could have remained locally.

2. PCV gas replacement due to steam production

A large amount of steam was being generated in the reactor after the accident by water injection for fuel cooling. Figure 2 shows the amount of water injection which could remove the fuel decay heat of Unit-2 by the latent heat for boiling (equivalent to the decay heat). If the amount of steam generated is assumed to be the amount of water injected equivalent to the decay heat, the total amount of steam generated between April 1, 2011 and June 28, 2011, when nitrogen gas filling started is about 6300 t, which is equivalent to about $1.1x10^7$ m^3 of steam at atmospherical pressure and 100 deg C. Assuming the Unit-2 PCV open volume as about 3500 m^3 (with no water accumulation), the total amount of steam generated is about 2400 times the PCV open volume. As the gases in the reactor pressure vessel (RPV) and PCV could leak out at the time of interest, the PCV gases could have been replaced about 2400 times. Consequently, non-condensable gases can be considered unlikely to have remained in a significant amount in the PCV.

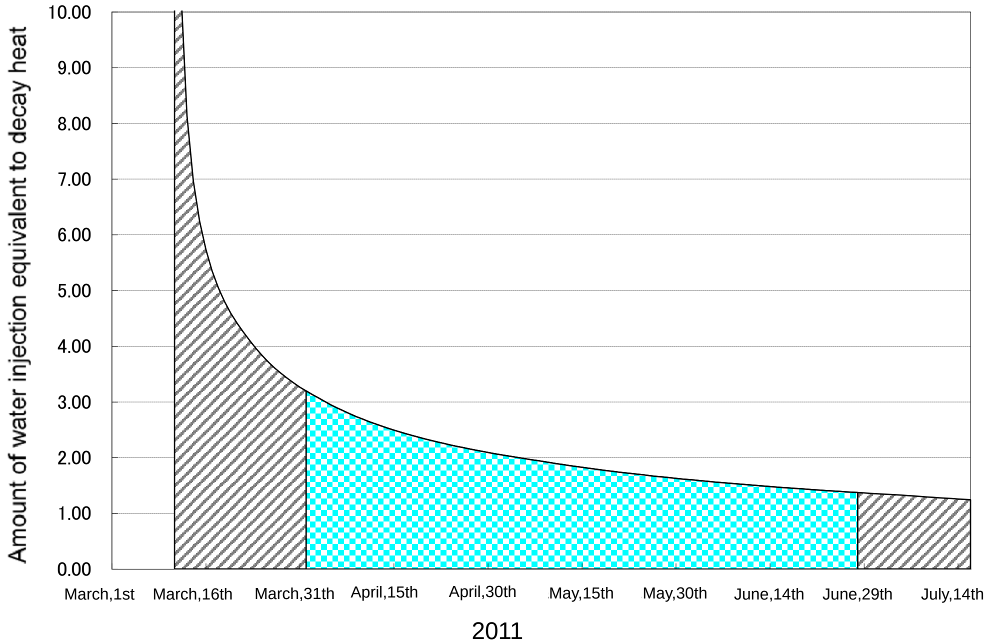

Figure 1 Amount of water injection equivalent to decay heat of Unit-2

3. Residue fractions in the Unit-2 PCV gases

A small amount of rare gases (Kr-85 and others) was detected in August 2011 upon PCV gas sampling and gamma analysis of sampled gases of Unit-2. Kr-85 has a long half-life and its yield from spontaneous fissions is negligibly small. Therefore, the detected Kr-85 is considered to have originated and been accumulated during normal plant operations. The residue fraction of Kr-85 can be obtained as the ratio between the initial inventory and in-PCV inventory (to be estimated from the detected concentration of Kr-85).

$$\alpha = \frac{A_{Kr85} \times (1 - \beta) \times V_{PCV}}{M_{Kr85}} \qquad \text{Eq. 1}$$

α: residue fraction, β: steam fraction, V_{PCV}: PCV volume

A_{Kr85}: Kr-85 concentration in non-condensable gases

M_{kr85}: Kr-85 initial inventory

If this residue fraction is applied to other non-condensable gas components, the initial inventories of each gas component can be inversely calculated.

$$M_{GAS} = \frac{A_{GAS} \times (1 - \beta) \times V_{PCV}}{\alpha}$$

$$= \frac{A_{GAS}}{A_{Kr85}} M_{Kr85} \qquad \text{Eq. 2}$$

A_{GAS}: Gas concentrations in the non-condensable gases,

M_{GAS}: Gas initial inventories

The Kr-85 initial inventory was set as the inventory 150 days after reactor shutdown, by taking the attenuation by decay into account. If the carbon dioxide detected in the samples collected in August 2011 (see Attachment-14) is assumed to be the residue of carbon dioxide which had been generated at an early phase of the accident only, the carbon dioxide initial inventory at the early phase of the accident can be estimated by Eq. 2 and the results are shown in Table 1.

Table 1 Carbon dioxide initial inventory at Unit-2 estimated from Kr-85 residue ratio

Kr-85 concentration in the non-condensable gases [Bq/cm^3]	74.5
Kr-85 initial inventory (150 days after reactor shutdown by ORIGEN [Bq]	2.20E+16
CO_2 concentration in the non-condensable gases [%]	0.151
CO_2 concentration in the non-condensable gases [mol/cm^3]	6.76E-08
CO_2 initial inventory [mol]	2.00E+07

4. Residue ratios in the Unit-1 containment vessel

It is considered to be unlikely that the non-condensable gases generated at an early phase of the accident remain in the PCV. But, the residue ratios at Unit-1 were also examined in the following three cases, by considering that a small amount of rare gas was detected at Unit-2. At Unit-1, too, the gamma ray nuclei analysis (using germanium detectors) recorded signals which could have come from Kr-85 of the sample collected in July 2011, although the rare gases were as a whole below the detection limits.

Case 1: The same Kr-85 residue ratio as that of Unit-2 was assumed.

Case 2: The estimated amount of Kr-85 in the July 2011 sample (below detection limit) was used to estimate the residue ratio.

Case 3: The residue ratio was estimated by exponentially relating the ratio (of the Kr-85 amount) between the July sample and the September sample.

4.1. Case 1

Gas leak paths from the PCV are unknown and nitrogen gas filling started in early April at Unit-1. The residue ratio will be different in Unit-1 and Unit-2. It will overestimate the initial inventories to assume the same residue fraction in Unit-1 as that in Unit-2. If the residue fraction were assumed to be equal, and if the carbon dioxide detected came from only the carbon dioxide having been generated in the early phase of the accident, the initial inventories will be such as given in Table 2.

Table 2 (Case 1) CO_2 initial inventory of Unit-1 estimated from the residue ratio of Unit-2

Case 1	July 2011 *	September 2011
CO_2 concentration in the non-condensable gases [%]	6.18E-01	1.49E-01
CO_2 concentration in the non-condensable gases [mol/cm^3]	2.76E-07	6.66E-08
CO_2 initial inventory [mol]	8.15E+07	1.97E+07

* Information only due to high dilution with air and the in-air CO_2 concentration dominates the results.

4.2. Case 2

At Unit-1, the gamma ray nuclei analysis (using germanium detectors) recorded energy peaks which could have come from Kr-85 from the sample collected in July 2011, although the amount was below the detection limit. If this peak were really from Kr-85, the amount should have been 4.67×10^2 Bq/mL (the detection limit was about 5.31×10^2 Bq/mL*). Table 3 shows the initial inventories derived by Eq. 2 using this measured value. Numerically, the results are in the same order with the results in Case 1, but the value from the Unit-1 July sample should be regarded as information only, because the sample was diluted with air in a high dilution ratio and the in-air CO_2 concentration dominates the results.

*The actual detection limit is about 1.23×10^2 Bq/mL. The value of 5.31×10^2 Bq/mL is the non-condensable gas concentration equivalent to the detection limit when the effect of dilution by 4.32 times is taken into account.

Table 3 (Case 2) CO_2 initial inventory of Unit-1 estimated from the Kr-85 residue ratio

	July 2011 *
CO_2 concentration in the non-condensable gases [%]	6.18E-01
CO_2 concentration in the non-condensable gases [mol/cm^3]	2.76E-07
CO_2 initial inventory [mol]	1.01E+07

* Information only due to high dilution with air and the in-air CO_2 concentration dominates the results.

4.3. Case 3

If the non-condensable gas concentrations in the PCV can be assumed to decrease exponentially, the residue fraction can be estimated from the ratio of concentrations in the samples collected in July 2011 and in September 2011. Table 4 shows the residue fractions and carbon dioxide initial inventory thus estimated. By using the residue fractions, the amount of Kr-85 can be inversely calculated at any time points. The results are shown in Table 5. The amount of Kr-85 residue as of July 2011, the timing of sample collection, far exceeds the detection limit (about $5.31\text{x}10^2$ Bq/mL*), which is inconsistent with the result of gamma ray nuclei analysis (using germanium detectors). Case 3 can be concluded as “not applicable.”

*The actual detection limit is about 1.23x102 Bq/mL. The value of $5.31\text{x}10^2$ Bq/mL is the non-condensable gas concentration equivalent to the detection limit when the effect of dilution by 4.32 times is taken into account.

Table 4 CO_2 initial inventory estimated from the concentration ratio in July and September 2011

Unit-1 Average CO_2 concentration in July 2011 [%] *	0.618
Unit-1 Average CO_2 concentration in September 2011 [%]	0.149
Attenuation ratio (September/July)	2.42E-01
Attenuation rate per day	9.70E-01
Initial CO_2 Inventory [mol]	2.84E+06

* Information only due to high dilution with air and the in-air CO_2 concentration dominates the results.

Table 5 Kr-85 residue amount estimated from Case 3 residue fraction

	July 2011	September 2011
Kr-85 initial inventory	1.70E+16	
Inventory in PCV	2.47E+14	5.97E+13
PCV open volume [m^3]	2800	2800
Steam fraction in PCV	0.65	0.46
Estimated radioactivity concentration in PCV [Bq/cm^3]	8.82E+04	2.13E+04
Estimated radioactivity concentration in non-condensable gases [Bq/cm^3]	2.52E+05	3.95E+04

5. Gas residues from the early phase of the accident estimated from the gas residue fractions

Table 6 gives the initial inventories of carbon monoxide and carbon dioxide estimated by DECOMP, the MAAP built-in sub-program for core-concrete reaction evaluation. They are at most 1.4×10^4 mol, about 3 orders of magnitude less than the values given in Table 1 to Table 3, which are in the order of 10 to the 7th power. In estimating residue fractions, the initial inventories tend to be overestimated if an additional amount flows in from outside during the process. It is estimated, therefore, that the carbon dioxide detected in the sampled PCV gases had flowed in by unknown reasons to the PCV from outside. Even if large scale core-concrete reactions had occurred at an early phase of the accident, hardly any of the gases generated at the time would have remained till now and the gases that flowed in during the process would be currently dominant.

Table 6 Amount of CO and CO_2 at the time of core-concrete reactions (analysis by DECOMP)

		Unit-1	Unit-2	
Fraction of fuel relocation to PCV (%)		100%	57% Instrumentation line penetration	57% CRD penetration
Integrated amount of gas generated (by analysis) (kmol)	Steam	75.8	1.18	4.3
	H_2	37.8	2.06	4.1
	CO	5.2	0.04	0.1
	CO_2	8	0.12	0.46
	CO+ CO_2	13.2	0.16	0.56

Note: Gases generated in the pedestal sump pits only

Paint stripping-off incidents of Unit-2 reactor building ceiling cranes

1. Outline of the incident

In a photo taken on September 17, 2011, a white gas, probably steam, was observed to be blowing out from immediately above the reactor. About one month later, on October 20, 2011, no gas blowout was observed in the photo but some stripping-off was recognized on part of the ceiling crane coatings. This stripping-off is considered to have occurred after the steam blowout ceased.

2. Stripping-off mechanism

Defects of coating such as stripping-off or cracking are generally considered to be attributed to the internal stresses generated in the coatings. When the internal stresses exceed the coating adhesion strengths, the coatings strip off. Coatings bear contraction stresses ever since they were constructed at the beginning. The stresses repeat ups and downs in response to ambient temperature changes. It is known that the internal stresses gradually decrease with time in a higher humidity environment. The stresses mitigated by moisture absorption increase again when dehydrated [1].

Therefore, the mechanism of ceiling crane coating stripping-off at Unit-2 can be considered as follows:

① The coatings were deteriorated by the heat and steam at the time of the accident and their adhesion strengths decreased.

② Water injection to the reactor for fuel cooling suppressed steam production and the ambient temperatures decreased. As the result, the coatings were dehydrated, and the internal stresses recovered to higher values.

③ The coatings stripped off when the recovered internal stresses exceeded the lowered adhesive strengths of the coatings.

Reference

[1] Kozo Sato, *Adhesion of coatings, its theory of, and commentary to, the mechanism*, RIKO Publishing Corporation, 1981 (in Japanese).

End